Hybrid Welding of Thermoset and Thermoplastic Composites: Adhesion Improvement

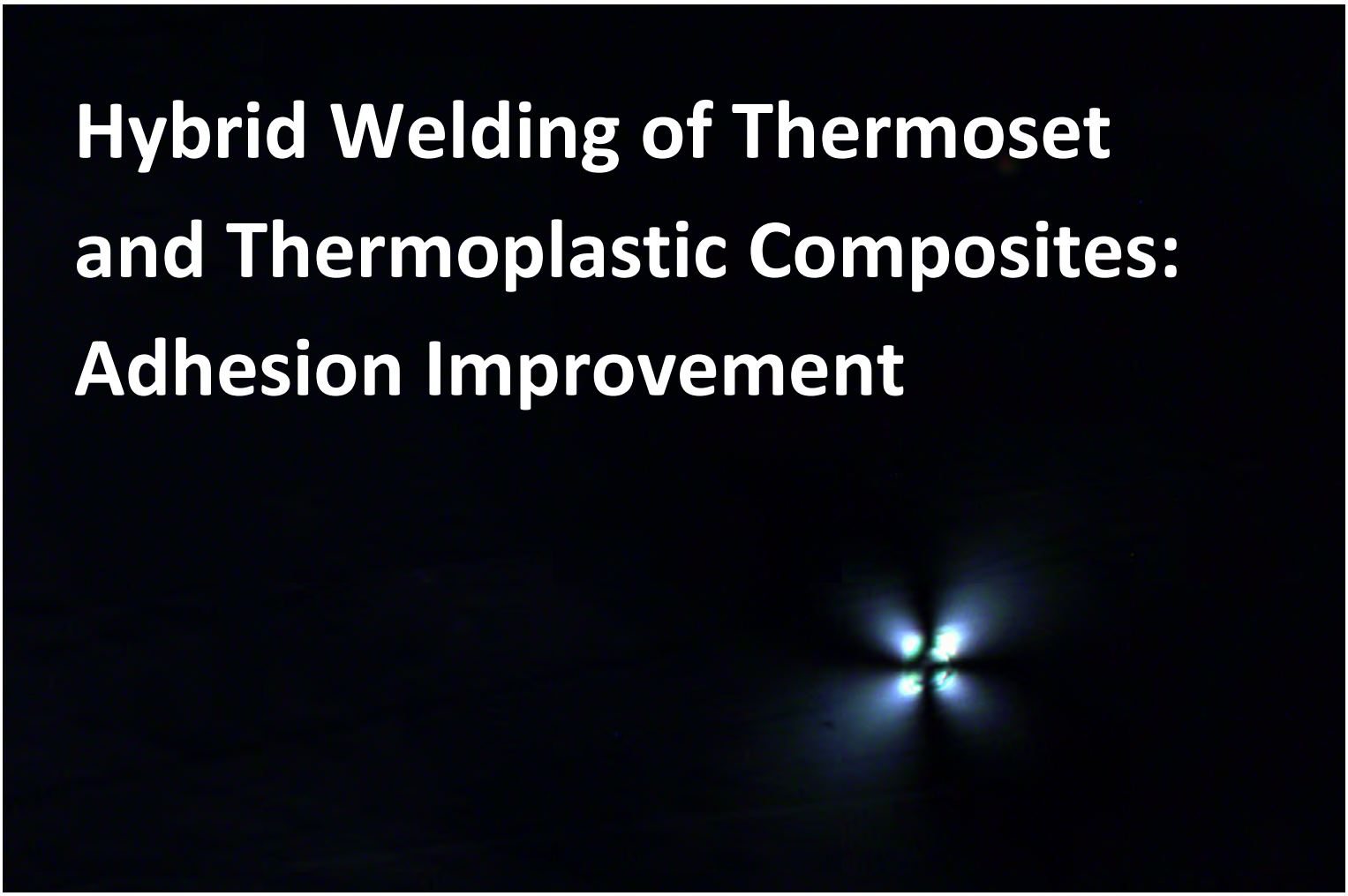

Universidad Carlos III de Madrid and Delft University of Technology

Bachelor Thesis by María de Nicolás Morillas

Bachelor in Aerospace Engineering

Supervisors: Dr. Irene Fernández Villegas and Dr. José Manuel Torralba Castelló

July 2015

Hybrid Welding of Thermoset and Thermoplastic Composites: Adhesion Improvement

by

María De Nicolás Morillas

In partial fulfilment of the requirements for the **Bachelor's Degree in**

Aerospace Engineering.

At the **Universidad Carlos III de Madrid**,

at the Department of Materials Science and Engineering and Chemical Engineering,

in collaboration with **Delft University of Technology**.

Supervisors:

Dr. Irene Fernández Villegas (Technical University of Delft)

Dr. José Manuel Torralba Castelló (Carlos III University of Madrid)

Thesis committee:

Manuel Fernando Soler Arnedo

Beatriz Velasco Núñez

Daniel González Arribas

July 2015

Cover image: *Crystal surrounded by amorphous region in semi-crystalline PPS film, cross-polarized optical microscope picture.*

A mi abuela Chelo,

por su fuerza. Y por sus "papas con choco".

Agradecimientos

En primer lugar, quería dar las gracias a mi supervisora en la Universidad Técnica de Delft, Irene Fernánez Villegas, por haberme hecho parte de su equipo y por todo. Lo que he aprendido bajo su tutela tiene un valor incalculable, además de haberme inspirado a dedicarme a esta potente e innovadora rama de la ingeniería aeroespacial. Sabe exactamente cómo guiar al alumno en una investigación para que llegue a buen puerto, pero siempre haciendo que él mismo se haga con su trabajo. Es una profesional de los pies a la cabeza, y mejor persona.

Quiero agradecer también a mi tutor y antiguo profesor en la Universidad Carlos III de Madrid, José Manuel Torralba Castelló, el haberme puesto en contacto con Irene y dado esta oportunidad, su ayuda, y que nos hizo comprender el importante papel de los materiales en el mundo de la aviación; razón no le falta en absoluto.

A Pablo, el predecesor de esta tesis, por todo su apoyo, ánimo y consejos. Volarás muy alto.

A Genevieve, Mladen, Hari y Régis, por la ayuda prestada durante este proyecto. A Rubén por haber ejercido de profesor a distancia de Mecánica de Vuelo Avanzada. A José Daniel, por su amistad y su asistencia.

Mis *gracias* van también para los peces del "Fish Tank", esta experiencia no habría sido lo mismo sin vosotros. Espero y deseo que lo que ha unido Holanda no lo separen los kilómetros.

A mis amigos de España, por estar siempre ahí, por quererme tal y como soy desde hace años.

A mi familia por estar tan unidos a pesar de la distancia, por vuestro apoyo incondicional, por hacer de Sevilla, Ceuta y Las Palmas otro hogar.

A mi hermana, por ser la prueba de que la Teoría de la Evolución de Darwin funciona en la misma generación. Como dijo Ernest Legouvé: "Un hermano es un amigo dado por la naturaleza".

Y gracias a mis padres, porque sin ellos nada de esto hubiera sido posible. Son un ejemplo a seguir, cuesta expresar con palabras lo mucho que los quiero y agradezco todo lo que hacen por mi, cada día. Su cariño y confianza son mi motor, y su alegría con mis pequeños éxitos hace que todo esfuerzo merezca la pena.

Index

List of Figures

List of Tables

Abbreviations

AFM	Atomic Force Microscopy
CFRP	Carbon Fibre Reinforced Plastic
DASML	Delft Aerospace Structures and Materials Lab
DCB	Double Cantilever Beam
DPSS	Diode-pumped, solid-state
ED	Energy Director
FTIR	Fourier Transform Infrared Spectroscopy
HAZ	Heat Affected Zone
IPN	Interpenetration network
LSS	Lap Shear Strength
NT	Not Treated
OM	Optical Microscopy
PEEK	Polyetheretherketone
PEI	Polyether imide
PEKK	Polyetherketoneketone
PPS	Polyphenylene sulphide
SEM	Scanning Electron Microscope
SIPN	Semi-interpenetration network
SLS	Single-Lap Shear
TP	Thermoplastic
TPC	Thermoplastic composite
TS	Thermoset
TSC	Thermoset composite
TU Delft	Technical University of Delft
UC3M	Carlos III University of Madrid
UD	Unidirectional
UV	Ultraviolet

INTRODUCTION

Chapter 1

Introduction

This chapter will be devoted to the discussion of the reason of this study: the importance of composite materials and polymers, highlighting their ease of use in the aerospace industry, their characteristics, joining techniques, and remarkable experiments other researchers have carried out in this field. Then, the experiments and goals of this bachelor thesis will be presented in the 'Project Plan' section.

1.1. MOTIVATION AND STATE OF THE ART

1.1.1. Motivation

Airplanes are the man-made birds of the sky. Their efficiency for travelling, humanitarian aid, war and transport are self-evident. They have demonstrated to be safe and fast, with a constant increase in the number of users and passengers throughout the years. Intense research is carried out in this field, and the aerodynamics, electronics and materials of the aircrafts have been continuously evolving.

The aerospace and automotive industries have been replacing heavy materials, such as steel or aluminium, by lighter and tougher alternatives such as composite materials, which play nowadays a dramatic role in aircraft's composition. For example, aluminium is being replaced by GLARE ("Glass Laminate Aluminium Reinforced Epoxy"), a structure that interlays aluminium films with glass fibre prepreg laminates, with better damage tolerance, corrosion and fire resistance, and lower specific weight than conventional aluminium. Boeing 787 is made by a 50% of composite materials, including them in its fuselage, wings, tail, doors and interior. Airbus 380, the world's largest passenger airliner, is made by a 25% of composite materials [1].

Composites used in the aerospace engineering are made of a resin, generally a polymer, and a reinforcement, such as carbon or glass fibres. In particular, according to F. Fischer et al. [2]: "The use of carbon-fibre reinforced plastics (CFRP) is increasing in all areas where weight reduction enables an improvement, either in an economic or ecological way or as regards performance". Polymers can be, essentially, of three kinds: thermoplastics, thermosets and elastomers. Polymers count with the benefits of excellent bulk and surface properties, low cost and good mechanical

properties. As stated by M. Hou [3]: “There is not one ideal engineering material for every application”. Regarding the properties of each material, and the cost-efficiency in their manufacturing, they are devoted to different structural parts.

Thermoplastics and thermosets are currently being used for aerospace applications, the second ones usage in aircrafts being predominant over thermoplastics, which are used only in a few applications nowadays. Thermoplastics present high ductility, fracture toughness and impact resistance; moreover, thermoplastic composites (TPCs) can be cost-effectively joined and manufactured. Thermosets, on the other hand, do not count with these properties, but they have good compression, fatigue resistance and creep resistance. Regarding their characteristics, for some applications, thermoplastics may be used, and for others, thermosets are the answer: Thermoplastics are preferably used in small to medium-sized parts, and thermosets are more economical to be used in large parts. Their combination, in order to take advantage of the benefits of both materials for each application, is a fact in current aircraft structures. Here is where the main challenge of using these new materials arises: the joining of thermoplastics and thermosets. Mechanical fastening is the conventional method to join these materials. For example, in the fuselage of A350, the structural frame is joined to the thermoset composite skin through thermoplastic clips and cleats [4]. Apart from the extra weight and stress concentrations they imply – lightweight potential of the composite material is lost due to the need of reinforcement in the areas where the rivets and screws are inserted – when insufficient economical investment is devoted to their insertion, in order to assure the correct performance of the joining procedure, several problems may occur, such as delamination, water intrusion, galvanic corrosion and intensive labour they induce, among others. Then, in order to avoid the damage of the composite materials, and to save weight and economical resources, other joining alternatives are being taken into account [5].

Aerospace industry has been investigating adhesives and the associated adhesion mechanisms for more than 50 years [6]. Nevertheless, the use of adhesives is not the most reliable joining technique for composite materials, and they are prone to be environmentally degraded, as it will be explained hereinafter. The need for a joining technique that lead to strong, cost-effective and reliable joints gave birth to the idea of welding. Thermoplastics can be welded, due to their ability to melt and be re-processed, whereas thermosets cannot be re-melted once they are cured.

Bearing in mind that direct welding of thermoset and thermoplastic materials is not possible, different methods are being investigated, such as hybrid welding, a combination of bonding and welding were the a reinforced thermoset is co-cured with a layer of thermoplastic, and later welded to a thermoplastic composite.

One of the problems of welding thermosets and thermoplastics is that the first ones cannot be reprocessed, which, combined with their relative low melting temperatures, probably explain the fact that temperature and welding time degrade them. Among all the possible welding techniques, ultrasonic welding counts with the shortest processing times, the ability to monitor and control the process and the lack of foreign, non-polymeric materials at the interface. In this process, force and amplitude are applied to the composites to be joined, using a thermoplastic energy director (ED) at the interface. By choosing large values of force and amplitude (without compromising the available power of the welder machine), short welding times are achieved, on the order of 4 to 6 seconds. Bearing in mind that direct welding of thermoset and thermoplastic materials is not possible, or

results in very weak welds were the thermoset is damaged [4], different methods are being investigated, such as hybrid or indirect welding, were a reinforced thermoset is co-cured with a layer of thermoplastic, and later welded to a thermoplastic composite. This has proven to improve the strength value of the joint with respect to direct welding in a 680%, as proved by P. Vizcaíno Rubio in the investigation he carried at TU Delft University, under the supervision of Dr. I. Fernández Villegas.

In the investigation carried by P. Vizcaíno [4], direct and hybrid ultrasonic welding were studied. This thesis was born with the objective of continuing the potential and promising ultrasonic hybrid welding technique and, in particular, focusing on the improvement of the adhesion between thermoset and thermoplastic materials. Also, an alternative procedure for improving direct welding will be investigated.

1.1.2. State of the Art

Materials Background

Composites are made by combining two or more materials, which will have unique and better properties than when the materials are used alone. Nevertheless, each material retains its physical, chemical and mechanical properties, as opposed to metal alloys. Usually, composite materials are made of two components: a resin[1] or binder, that constitutes the matrix of the union and that can be metallic polymeric or ceramic, and a reinforcement, the fibres that the resin holds together, for example, carbon or glass fibres. The advantage of composite materials is the freedom to create light and strong parts, with complex shapes, meeting the needs of the application it is used for. A drawback is the high price of the raw materials and of their processing [7], [8], [9]. For the purpose of this investigation, a unique focus on polymers will be done.

The term "polymer' stands for "many units": polymers are composed of long chains of molecular units or monomers. There are five important temperatures or states that define a polymer: the **freezing point**, the temperature at which the molecules remain static and the material becomes a solid; the **glass transition temperature (T_g)**, which occurs in the solid phase and transforms a rigid polymer into a more pliable one; the **heat distortion temperature (HDT)**, that is the deflection temperature under load test at which the polymer deforms, a way to measure the maximum use temperature of a polymer; and **degradation**, when the polymer is sufficiently heated, atoms start to vibrate and translate, breaking the primary bonds of the monomer, so the polymer breaks apart and degrades [10].

Artificial polymers are classified in the following categories: elastomers, thermoplastics and thermosets. Thermoplastics and thermosets are plastics, whereas elastomers are rubbers [10]. For the purpose of this thesis, focus will be made on thermoplastic and thermoset materials, which will be the ones used in the experiments.

- THERMOPLASTICS

Thermoplastics are fully reacted, high-molecular-weight, high-viscosity resins – meaning they count with long polymer chains – which are usually solid at room temperature. Thermoplastics do not cure, which means they do not undergo chemical reactions when heated – they are fully reacted,

[1] A resin is a soft solid or highly viscous substance, usually containing pre-polymers with reactive groups [11].

as just mentioned – so they can be *consolidated*. They have the simplest plastic-polymers molecular structure, with chemically independent macromolecules: linear/chain-like or branched structures, shown in Figure 1.

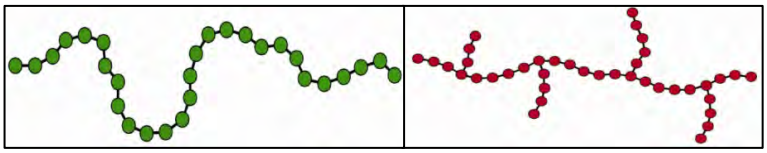

Figure 1: Linear (left) and branched (right) thermoplastic structures [10].

Thermoplastics count with an additional characteristic temperature: the **melting point**, at which they become liquid and which is strongly dependent on the molecular weight, related to the length of the chains that form the polymer. They can be heated and reheated without severe damage, so reprocessing and recycling are allowed. Nevertheless, there is actually a limit in the number of heating and cooling cycles polymers can be subjected to: as their processing temperatures are very high (260-450°C) and close to the polymer degradation temperatures, multiple reprocessing can degrade and make the thermoplastic structure change to a cross-linked one, which cannot be reprocessed and is very sensitive to thermal degradation.

This re-processing characteristic allows the repair of thermoplastic-made parts, for example, when a crack appears on the surface. They can be handled by simply heating them above their melting temperature. When cooled, they can be shaped, formed, welded or solidified, so complex geometries can be achieved.

Some additives are often added to the thermoplastics in order to improve their properties, for example, thermal stability or UV resistance. It is worth to mention that some thermoplastics are able to cross-link and form, then, a thermoset, as shall be seen in the "Thermoset" section. Examples of this type of thermoplastics are polyethylenes [10], [12], [8].

Thermoplastics can be amorphous or semi-crystalline (see Figure 2): amorphous thermoplastics contain a massive random array of entangled molecular chains; they exhibit good elongation, toughness and impact resistance. Semi-crystalline structures contain areas of crystallites (tightly folded chains) connected together with amorphous regions. They reveal a sharp melting point when the crystallites start dissolving, opposed to amorphous structures, which gradually soften while heated above their T_g [8]. Semi-crystalline thermoplastics exhibit better chemical resistance than amorphous ones, which is the reason why they are used in principal aerospace structures, such as wings, which may be in contact with chemical substances.

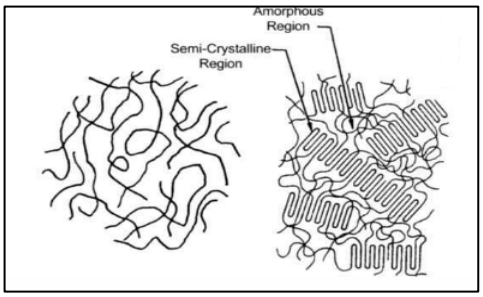

Figure 2: Amorphous (left) and semi-crystalline (right) thermoplastic structures [8].

Some of the most common thermoplastics are: polyethylene, polypropylene, nylon, polycarbonate, etc. In this project, four high-performance thermoplastics will be used: PEEK (polyetheretherketone), PEKK (polyetherketoneketone), PEI (polyether imide) and PPS (polyphenylene sulphide), both in reinforced and resin film forms, which will be explained hereinafter.

- THERMOSETS

Thermosets are low-molecular-weight, low-viscosity monomers that are converted into 3D tightly cross-linked structures when cured (see Figure 3), becoming infusible and insoluble. These resins are liquid or easily-melted solids at room temperature. Cross-linking results from chemical reactions when heat is either applied or generated by the chemical reactions themselves, since all thermosetting reactions are exothermic: This is the curing process of a thermoset, in which monomers form polymers that cross-link forming the characteristic thermoset net. They can also be cured with suitable radiation. The cross-linking rate highly depends on the mass of the thermoset, temperature and time.

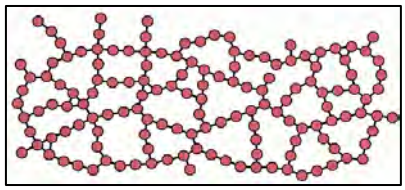

Figure 3: Tightly cross-link structure of a thermoset [10].

Examples of thermoset composite matrices are polyesters, vinyl esters, epoxies, bismaleimides, cyanate esters, and polyimides, among others. Epoxies are the dominant material for resin or matrix of high-performance composites and adhesives. Among their advantageous properties are strength, adhesion, low shrinkage and versatile processing. Their matrices are normally composed blends of mayor epoxies, the principal constituents, and minor epoxies, which are added for viscosity control, lower moisture, or improve toughness and high-temperature properties, combined with curing agents. Thermosets toughening can be improved by adding thermoplastics to the resin [8].

Figure 4 shows the curing process of a thermoset. The stages are: (a) polymer and curing agent prior to reaction, (b) curing initiated with size of molecules increasing, (c) gelation with full network formed, and (d) fully cured and cross-linked [8].

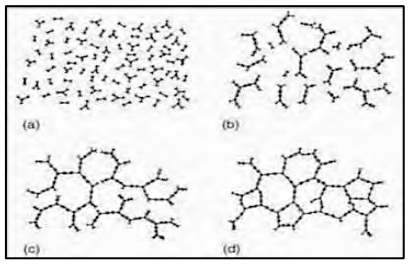

Figure 4: Thermoset curing stages [8].

A practical production control for thermosets is the staging: the “A-stage” corresponds to the mixing of the thermoset formula, where crosslinking has not begun yet; as time and crosslinking

progress, the thermoset enters in the “B-stage”; the “C-stage” refers to the cured state [13]. Figure 5 shows these three stages.

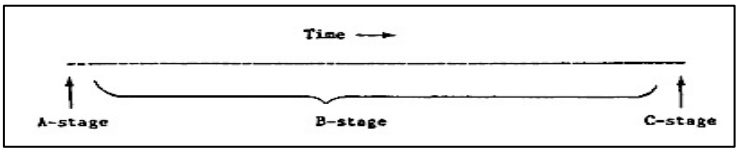

Figure 5: Thermosets staging process [13].

In view of the growing use of composite materials in aircrafts, the different characteristics of thermosets and thermoplastics, and the fact that they are currently joined by mechanical fastening, it is clear that a method for effectively connecting them in a chemical way must be used.

Composites Joining Techniques

The two most common ways of joining thermoplastics and thermosets are mechanical fastening and adhesive/solvent bonding. For joining thermoplastics among them, welding is used. Thermosets can be joined using co-curing and co-bonding concepts. In another section, a new method for joining thermoplastics and thermosets will be presented: hybrid welding.

- MECHANICAL FASTENING

Mechanical fastening is a joining method traditionally used to connect metals, but which can also be employed to join composites. The elements used for this purpose are generally screws, nuts, inserts, washers, pins, snap-fits and rivets, which can be metallic or plastic.

Fasteners can be separate parts – also called non-integral attachments – or integral parts, where the attachment feature is directly moulded into the part. Non-integral attachments require materials able to bear the strain and stress the fastener induces. They add cost to the process and product because they are more labour-intensive, increase the assembly time and require additional material. Integral attachments require strong plastics that can withstand strain, the service load and repeated use. The process can be easily automated and the assembly is fast. Nevertheless, they are prone to break before the assembly and some of them may require a more expensive mould design.

Mechanical fastening has the advantages of requiring no surface preparation, the pieces can be disassembled, there are no thickness limitations (although thin parts are preferred), the manufacturing and inspection are relatively simple, and it provides through-the-thickness reinforcement. Nevertheless, this joining technique also implies the appearance of some problems: Fasteners introduce considerable stress concentrations and add undesired weight to the structure; when not sufficient investment is devoted to this manufacturing process, additional problems arise: Drilling can cause localised wear that produces delamination, there can be differential thermal expansion of the fasteners relative to the materials to be joined, galvanic corrosion can develop at fastened joints, hole drilling extends the time and labour required to manufacture the part, there may be water intrusion between the fasteners and the materials to be joined, and, if the fasteners are metallic, electrical conductance and arching may appear. These drawbacks made clear that the ideal structure would be one without joints, so other joining techniques arose [14], [15], [16].

➢ SOLVENT AND ADHESIVE BONDING

In adhesive and solvent bonding, or cementing, two surfaces are joined by a different material. It is the most general joining technique and can be used to join plastics together or to dissimilar materials, such as wood, ceramics or metals.

Solvent bonding implies application of a solvent that softens the parts to be bonded, thus increasing the movement of the polymer chains. If the polymer is cross-linked, the chains cannot move but more spacing between them is created; if the polymer is not cross-linked, the solvent separates the polymer chains as if they were in a solution. When the softened parts come in contact, Van der Waals attractive forces[2] appear between the molecules, so polymer chains from both surfaces cross the interface, intermingle and entangle. As the solvent evaporates, polymer chains restrict their movement, and when the solvent has completely evaporated, polymer motion stops: the amount of entanglement across the bond interface determines the bond strength. This solvent evaporation can last hours or even days. A good interaction between the solvent and the polymer must be accomplished and the quantity of solvent applied must be correctly controlled in order to achieve a strong joint [14].

Adhesive bonding comprises two types of elements: the adhesive, that is the "glue" that connects the parts together, and the adherends, which are the parts to be joined. Adsorptive, electrostatic and diffusive forces develop between the adhesive and the adherends at the interface. When the adhesive forces are stronger than the cohesive forces of the adherend or the adhesive, joint failure occurs at the adhesive or the adherend, but not at the adhesion interface between the adherent and the adhesive [14]. The most common adhesives used in aerospace engineering are: epoxies, bismaleimide, cyanate ester and hybrids [17].

Regarding adhesive bonding, surface treatment plays an important role. Intimate contact and wetting are ensured when there is strong attraction between the liquid adhesive and the polymer. Wetting is the spreading of a liquid on a solid surface, and it is related to the surface tension of both the liquid and the surface: It is achieved when the surface tension of the liquid adhesive is lower than that of the adherends. Liquids are prone to adopt shapes that minimize their surface area: as the surface tension of the liquid rises, the liquid will tend to adopt a more spherical shape. Therefore, an adhesive which droplet tends to flatten is wanted for good surface wettability, this will mean that its surface tension is lower than that of the solid surface. A way to measure this is the contact angle: if it is less than 60°, good surface wettability will be achieved; on the contrary, poor surface wettability is attained when the contact angle is greater than 90°. Surface preparation can improve wettability, attraction and joint strength. This treatment implies the cleaning of the adherent surface and/or the introduction of chemical substances [14].

Moreover, adherends' surfaces should be rough, to promote keying of the adhesive and the adherend and increase the wet surface. According to the boundary layer theory of adhesive joint strength, macromolecules of adsorbed adhesive, the one that penetrates across the adherend interface, form an interfacial layer which ability to withstand external stresses determines the strength of the joint [14].

[2] Van der Waals forces are the sum of the attraction or repulsion forces between molecules.

Bonded joints comprise the following advantages: small stress concentrations in the adherends, stiff connection, excellent fatigue properties, lightweight structures, good damage tolerance, and no corrosion nor fretting. For composite structures, it also avoids the damage of the fibres that inevitably occurs in mechanical fastening. Nevertheless, there are also some drawbacks when using this joining technique: there is a thickness limit, inspection and quality control are difficult, the joints are likely to be environmentally degraded and contaminated, the assemblies are sensitive to through-the-thickness and peel stresses, parts cannot be disassembled, and the process is not cost-effective as compared to other joining techniques (for example, mechanical fastening) [15]. Occasionally, the surfaces of the bonds are in intimate contact but little or no adhesion occurs, called "kissing bonds", which are difficult to detect because there is no evident separation between the adhesive and the adherends [18].

As mentioned previously, surface preparation of the substrate enhances the bond strength and durability. Generally, these treatments can be mechanical, chemical or electrical. Laser and UV light are new methods being used for this purpose that will also be used in this investigation.

Failure modes in adhesive bonds

- Adhesive failure: Failure between the adhesive and the substrate, primarily due to lack of adhesion between them. It can be caused by poor surface preparation or contamination, or by incorrect adhesive selection for the used substrates. Figure 6 shows a sketch of this type of failure.

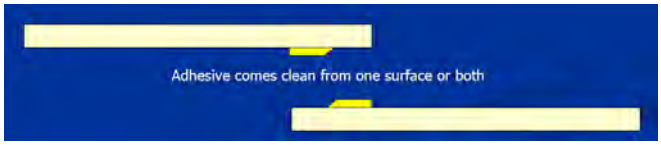

Figure 6: Adhesive failure [17].

- Cohesive failure: Failure that occurs in the adhesive layer (see Figure 7). It is the optimum type of failure in adhesive bonded joints when failure occurs at the predicted loads; if failure occurs at lower loads than the expected, the adhesive may be poorly cured or contaminants might be present in the sample.

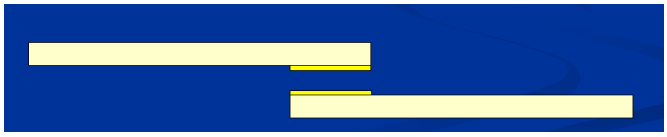

Figure 7: Cohesive failure [17].

- Substrate failure: It is an interlaminar fracture in the composite material, generally between the first and second layers from the bondline, a common failure in brittle epoxy composites [25]. Figure 8 shows a sketch of this type of failure.

Figure 8: Substrate failure [17].

The concept of adhesion

For the sake of this investigation, the concept of adhesion and the mechanisms used to promote it will be now further discussed.

According to F. Awaja *et al.* (2009, see reference 6): '*Adhesion is the interatomic and intermolecular interaction in the interface of two surfaces*'. This phenomenon strongly depends on the surface characteristics of the materials to be joined.

There are three mayor adhesion mechanisms in polymer systems:

-*Mechanical coupling or interlocking*, where the adhesion mechanism relies on the adhesive keying or anchoring of the substrate surface. Figure 9 shows this mechanical coupling between the substrates:

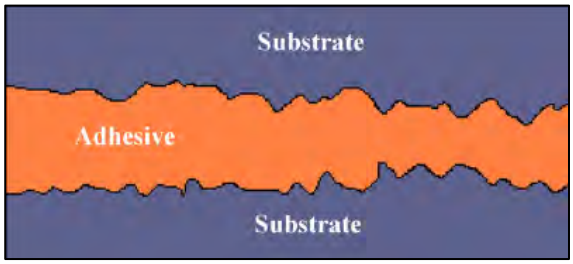

Figure 9: Mechanical locking between substrates [6].

Regarding this adhesion mechanism, there exists controversy: some researchers believe that mechanical interlocking improves the adhesion strength. The other side of the argument states that the roughening of the surface simply increases the surface area, enabling more molecular bonding interactions to occur, so that adhesion strength is improved in combination with van der Waals forces.

-*Molecular bonding*, which explains the adhesion between two surfaces by the intermolecular forces between the substrates and the adhesive, such as dipole-dipole interactions, van der Waals forces and chemical interactions (ionic, covalent and metallic bonding), and by the presence of polar groups[3]. This mechanism requires intimate contact between the substrates. For polymer-polymer joints, the architecture of the substrates and the stresses at the interface control the adhesion mechanism. It was found that adhesion was governed by the molecular weight, interface crystalline structure, annealing and molecular architecture of the polymer. Figure 10 shows a scheme of the molecular bonding between the substrates:

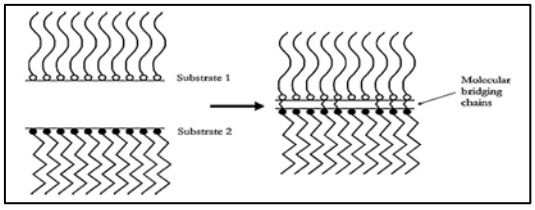

Figure 10: Molecular bonding of the substrates [6].

[3] The attraction between molecules in the liquid state is determined by their polarity. Opposite-charge molecules are attracted to each other [19].

-*Thermodynamic mechanism of adhesion,* which only requires an equilibrium process at the interface for good adhesion, not molecular interaction. Here, the surface tension of the adhesive and the substrates plays a dramatic role: The surface tension of the adhesive must be smaller than that of the substrates.

There are other adhesion mechanisms such as the electrical or the rheological adhesion mechanism. The latter focuses on polymer-polymer adhesions, and occurs due to the interpenetration of molecules across an interface. To increase the polymer chain mobility, the substrates are heated above the T_g, allowing the formation of a strong adhesive bond [6].

In order to promote adhesion in polymer surfaces, chemical and plasma treatments – among other possibilities– can be done in the surfaces to be joined. Chemical treatments seek to create chemical/functional groups at the joining interface. Increasing the surface polarity increases molecular force between the substrates, leading to an increase in adhesion strength. Plasma treatments are a fast and effective way to enhance the adhesive properties of the substrates. This environmentally friendly technique changes the properties of the adherends surfaces without modifying the polymer overall bulk properties. A drawback of this treatment is that surface properties degrade through ageing. There are other techniques used for the cleaning and preparation of CFRP parts prior to adhesive bonding, such as mechanical abrading, blasting processes and the removal of peel-plies. The latter have demonstrated to be not so efficient: among other disadvantages, they induce thickness variation in the composite resin layer and transfer residues to it. On the other hand, mechanical abrading processes are normally wet, which need further rinsing and drying, and are difficult to automatize [20]. For the sake of this investigation, UV/ozone and laser surface treatments will be commented:

The *ultraviolet-ozone (UV-O_3) treatment* has also reported good adhesion results. It is a dry process where the surface is cleaned by UV-irradiation decomposition of contaminants and ozone chemical action, increasing its surface energy and enhancing adhesion [21]. The most common way to apply this surface treatment is with a UV lamp. In one of the experiments carried out by P. Vizcaino at TU Delft**,** where the mechanical strength of a weld was improved by using this technique, will be commented in the ultrasonic welding section [4].

Laser surface treatment has also proved good adhesion results, and it is particularly of high interest nowadays. One of the lines of investigation of this thesis is to study the improvement of adhesion when using laser treatment. There are various types of laser treatments, differing in the cost, material removal mechanisms, operating and application; the most common ones are: carbon dioxide (CO_2) lasers, diode-pumped, solid-state (DPSS) lasers, frequency multiplied DPSS lasers, and excimer lasers.

Laser treatments have the ability to effectively remove all contaminant residues from the CFRP surface and also to prepare the surface for bonding. It is a dry process that may not require previous or further surface cleaning, and that does not damage the composite fibres if the correct parameters are selected. Moreover, this technique can be easily automated, so it is compatible with the manufacturing of big production lots.

A study carried out by F. Fischer et al. [22], comparing the atmospheric-pressure plasma and laser-based treatments, showed that both methods led to cohesive failure, but that the atmospheric-

pressure plasma technique could not assure the elimination of contamination and the release agent. In another article written F. Fischer et al. [20], excimer laser-based surface cleaning is studied and proposed as an alternative and advantageous surface treatment for bonding CFRPs (carbon fibre reinforced plastics). Excimer lasers have demonstrated to be a precise, reliable, ideal-for-high-volume, cost-effective cleaning technique of CFRPs. Their output stability levels permit achieving accuracy and repeatability for industrial mass manufacturing [3]. They produce UV light, so they can remove CFRP material without producing a HAZ (Heat Affected Zone): UV lasers perform photoablation, a process that removes material by breaking molecular or atomic bonds rather than by bulk heating of the composite. Moreover, CFRPs absorb UV light, avoiding it to further penetrate into the material. The laser beam is flexible and permits to shape it as best for the geometry of the parts to be bonded. By increasing the intensity, the process can be controlled to remove the surface contaminant and leave the bulk material unchanged, to exposure of the underlying fibres through material removal [20], [2].

- FUSION BONDING OR WELDING

Fusion bonding or welding is a joining technique to connect thermoplastics together, where the efficiency of the welded joint can approach the properties of the adherends. It is well suited and applied for the joining of thermoplastics, which soften above a certain temperature when heat is applied, and maintain the desired shape when they cool down. The two parts are joined by melting plus consolidation when applying pressure to their interface. As the bulk laminates are consolidated prior to the welding operation, consolidation in fusion bonding is mainly characterised by a polymer-polymer healing process, which can be reduced to the steps of intimate contact and autohesion. Intimate contact refers to the surface approach and wetting; the autohesion or inter-diffusion stage stands for the process that takes place when intimate contact is achieved and inhomogeneities at the interface have disappeared, so that the molecular chains of the polymers are free to move across the interface. Autohesion model relies on DeGennes theory of reptation, where polymer chains are confined into tubes, symbolizing the constraints of adjacent tubes, and can move up and down inside the tube, but not laterally (Brownian motion). Over a period of time, the end segments move outside the tube until the motion propagates to the centre of mass of the tube; finally, the whole chain moves out of the first tube and a new tube forms [16], [23], [24]. Figure 11 shows this chain flow and entanglement concept.

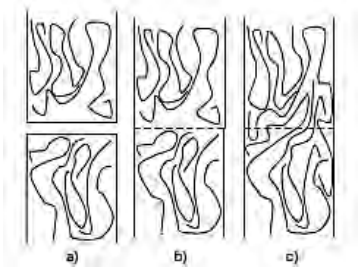

Figure 11: Healing of a polymer-polymer interface: (a) two distinct interfaces, (b) achievement of intimate contact, (c) collapse of the interface through inter-diffusion (autohesion) [16].

Fusion bonding techniques classify according to the way heat is introduced into the process. According to C. Ageorges *et al.*, there are four classes: bulk heating, frictional heating, electromagnetic heating and two-stage techniques.

The three most promising techniques, especially for continuous fibre reinforced thermoplastic composites (CFRTPCs) are induction welding, resistance welding and ultrasonic welding, which will be now explained in detail. In particular, the latter is the welding process that will be used in this thesis experiments due to its advantages, which shall be pointed out hereinafter. Although fusion bonding may induce residual stresses, uneven heating, delamination or distortion of the laminates, it eliminates the stress concentrations of holes, and reduces processing times and surface preparation [16], [23].

Induction welding

In induction welding, electrically conductive and/or magnetic materials are heated under an alternating magnetic field produced by an induction coil. It belongs to the electromagnetic heating type of welding. The electrically conductive materials heat due to the Joule[4] and dielectric[5] effects, and the magnetics ones, due to hysteresis[6] losses. Figure 12 shows an induction welding process [25]. Voltage drops in the eddy currents, flowing along conductive loops in the composite, are responsible for the heating and welding.

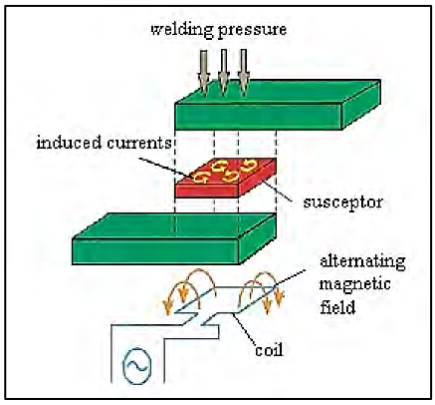

Figure 12: Induction welding process [25].

In this process, a bonding agent consisting on ferromagnetic particles (susceptors), embedded in the thermoplastic matrix at the joint, is placed before welding. Slight pressure is applied to the parts and high frequency current passed through the coil. The heat generated at the susceptors, due to hysteresis and eddy current losses melts the thermoplastic, which fills the joint line, flowing into voids and surface irregularities and forming a weld when cooled. Welding can be accomplished in 1 or 2 seconds for a part of 6.4 mm thickness, approximately. Bond strength is proportional to the surface area of contact [14].

The internal heat generated is 'volumetric', and depends on the properties of the composite material. This effect introduces the advantage of high volumetric heating rates, velocities and throughputs, compared to other conventional manufacturing processes. Moreover, induction is a

[4] **Joule effect** refers to Joule's first law, that states that the passage of an electric current through a conductor releases heat, which is stated by: $Q \propto I^2 \cdot R$. Faraday's Law states that a time-varying magnetic field will produce an electric field, thus producing the electric current that will make the temperature rise.
[5] The **dielectric effect** is the polarization of a material when an electric field is applied.
[6] **Hysteresis** stands for the dependence of the actual state of a system on the history of past and current inputs. To predict its future outputs, its internal state or history must be known. In this case, it refers to the change in direction of the dipoles.

multi-ply process, which also reduces the cycle times. However, the magnetic field generated by an induction coil is not uniform and generates non-uniform heating.

This joining technique is more suitable for long/thin parts, due to the coil geometry. In order to create a closed loop, fabric or UD cross-plied composites should be used. The main advantage of this process is the ability to make continuous joints by moving the coil along the joint [16], [26].

Resistance welding

Resistance welding, also called resistive implant welding, electrical-resistance fusion or electrofusion, is a joining process in which current is applied to a conductive heating element or implant (a metal mesh, for example) placed between the two parts to be joined. It is another type of electromagnetic heating welding. By making electrical current flow in the insert, its temperature rises (Joule heating), melting the plastics to be joined and creating a weld. This method was formerly introduced to join CFR thermoplastics, but is currently being used to join thermosets and metals, previously coated with a thermoplastic surface layer, where the strength of the joint can be superior to that of adhesive bonding. Figure 13 shows the steps of the process:

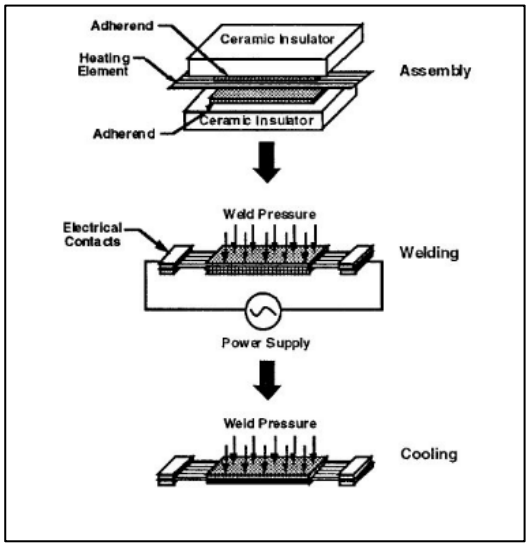

Figure 13: Resistance welding process [14].

A problem with resistance welding when using fibre reinforcement is the current leakage due to their conductive nature. To solve this issue, it is necessary to insulate the resistance heating-element with neat resin films, which apart from providing thermal and electrical insulation to the laminates to be joined, creates a resin-rich region by which diffusion process is enhanced.

As it can be appreciated in Figure 13, the weld assembly consists of the two adherends that sandwich the heating element; resin films such as thermoplastic layers can be placed between the heating element and the adherend for the insulation purpose mentioned above. Insulators, such as ceramic plates, are placed on top of the upper adherend and below the lower one, mainly to avoid the heating of those parts of the substrates, and maintaining it concentrated at the interface. When power is supplied, temperature of the heating element is raised and melts the plastics in contact with it. Pressure is applied throughout the welding and cooling of the element [14], [16].

Resistance welding is a joining technique broadly used in the automotive industry. Its promising advantages are that it is a fast, simple, cheap and clean process, which requires simple tooling and little or no surface treatment; moreover, the combination of sequential plus impulsive resistance welding as one welding system, is able to provide high-quality welds for large aerospace structures. Nevertheless, as every manufacturing process, it is not infallible; the most common failing modes are: failure at the interface (where the laminate and the heating element are separated due to lack of consolidation at the joint area), tearing or cohesive failure of the heating element, or tearing of the laminates. The fact that the heating element remains trapped in the joint implies the drawback of a metal element with undesired possible corrosion and extra weight but, on the other hand, it permits reprocessing if inspection shows flaws or incomplete bonding [27], [25].

According to an investigation carried out by T. J. Ahmed, D. Stavrov and H. Bersee, resistance welding produced more repeatable and consistent welds compared to those produced by induction welding. The latter showed more data scatter, but stronger welds [25].

Ultrasonic welding

Ultrasonic welding is the joining technique selected for this investigation. It is the most commonly used welding technique for thermoplastics, and the fastest one, with welding times of the order of 0.1-1.0 seconds, and 4-6 seconds of total welding time (taking into account the building-up of the force and the cooling of the weld while force in being held). In this process, the parts to be joined, two substrates that are generally reinforced thermoplastics, are held together under pressure and subjected to high-frequency (10-70 kHz), low-amplitude (10-250 µm) ultrasonic vibrations perpendicular to the area of contact. To concentrate the heat at the interface, thermoplastic-resin energy directors are inserted between the substrates, due to their low stiffness compared to the substrates one. Typically, the energy director uses the same thermoplastic as the matrix of the composite substrates to be welded; however, other combinations will be studied in this thesis.

Figure 14 shows the configuration and different parts of the ultrasonic welding device: it consists of a power supply, a horn or sonotrode that transfers the mechanical vibrations to the parts, a converter (piezoelectric transducer) with booster attachment to vary the vibration amplitude, fixtures to hold and align the welding parts, and an actuator which contains the converter, booster, horn and pneumatic controls [14]. The pneumatic press allows vertical movement and provides the welding and solidification force [28].

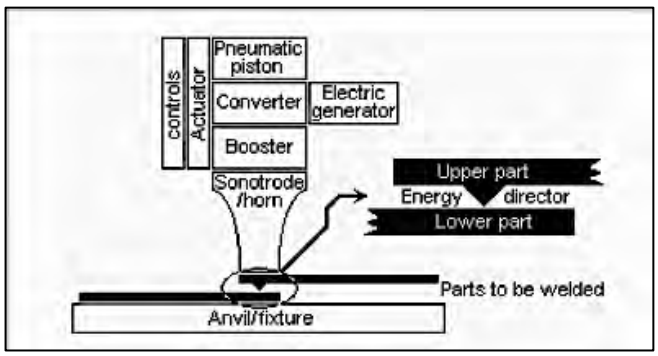

Figure 14: Ultrasonic welding device [29].

Ultrasonic welding is a type of frictional heating welding technique: Heat is generated by a combination of surface and intermolecular friction in the material, as a result of the sinusoidal standing waves produced by the ultrasonic vibrations that generate in the material to be joined. In other words, temperature rise is due to volumetric heating (viscoelastic heating), influenced by the amplitude of the vibration, and localized heating at the interface, governed by the amplitude and the welding force [14], [16], [27]. The most driving parameters of ultrasonic welding are: the **frequency of the vibration**; the **vibration time**, which is the duration of the horn vibration per cycle; the **amplitude of the vibration**, proportional to the applied strain; the **weld pressure or force**, that couples the welding horn to the parts to be vibrated and holds the parts together when cooling and solidification take place; and the **solidification time** [14], [28].

In a more general view, ultrasonic welding consists of a vibration plus a solidification phase; in the latter one, the weld is cooled down below the T_g (glass transition temperature) of the thermoplastic material to achieve consolidation [14], [28]. Being more specific, these two phases can be broken down into five: Mechanics and vibrations, viscoelastic heating of the thermoplastic, heat transfer, flow and wetting, and intermolecular diffusion.

There are two types of ultrasonic welding depending on the distance of the source of vibrations and the joint – the closer they are, the less energy that is lost through absorption: Near-field welding, where the distance between the source and the joint is less than 6.4 mm, is used for crystalline and low stiffness materials due to their characteristic high-energy absorption; far-field welding, where the distance is greater than 6.4 mm. It is employed for amorphous and high stiffness materials, which have low-energy absorption.

The energy directors or susceptors are generally man-made asperities moulded onto the part to initiate melting, with a triangular or rectangular cross-section. However, they can also be manufactured separately in the form of welding tapes for the ease of sample preparation and to avoid an additional cycle to the manufacturing of the composite laminates, as done in I. F. Villegas, L. Moser, A. Yousefpour, P. Mitschang and H. E. N. Bersee investigation [23]. Melting of the energy directors is due to the ultrasonic vibration and the pressure applied to them. Their shape and configuration has great influence on the weld quality.

In one of the investigations carried out by I. F. Villegas [30], flat thermoplastic resin films were used as energy directors, which heated up preferentially due to their lower stiffness and higher deformation under vibration compared to the substrates. The experiments carried out showed that these energy directors provided fully welded areas without the intense research of defining a suitable shape and configuration for the energy directors of each welding scenario [28].

One of the drawbacks of ultrasonic welding, as in other welding techniques, is the difficulty to monitor and assure a good quality of the weld, without the use of intensive inspection tests that are time-consuming. The quality of the weld is driven by the frequency, amplitude, welding force, vibration time, and solidification force and time; welding time and pressure values are intimately correlated, as demonstrated by E. C. Eveno, B. K. Harras, H. M. Lu and A. Benatar among others. All these parameters, together with the different types of possible welds, make each welding unique and difficult to inspect and quality-assure for airworthiness certification authorities: each heat transfer scenario at the welding interface imposes different optimal processing parameters. Nevertheless, a research carried out by I. F. Villegas (see reference 30), demonstrating the findings of

A. Benatar and T. G. Gutowski (see reference 24), showed that monitoring of ultrasonic processes can be controlled with the dissipated power and the acceleration of the fixture, using flat energy directors that covered the whole overlap area. It is worth to mention that, if other energy directors were used, the process can also be monitored, but the shape of the curves will slightly change. In the Power, Sonotrode displacement vs. Time graphs, and five stages could be clearly distinguished for every case, as shown in Figure 15 [14], [30]:

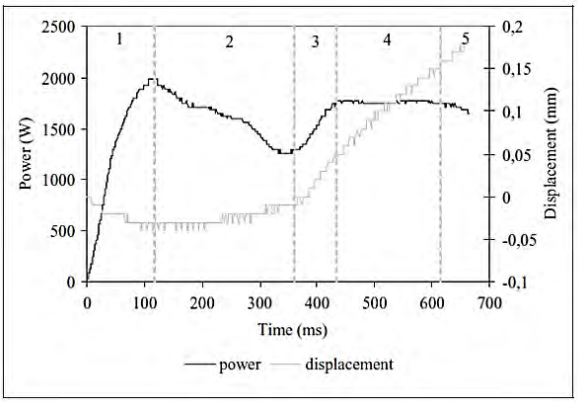

Figure 15: Dissipated power and displacement of the sonotrode during the vibration phase of ultrasonic welding (positive values indicate downward displacement) [30].

Stage I outstanding characteristic is ramping power and a retraction of the sonotrode to accommodate the vibration. At the end of this stage, power increase rate reduces and power reaches a peak: increasing the amplitude of the vibration or the welding force, increased the magnitude of the power peak, as already pointed out by A. Benatar, T. G. Gutowski, E. C. Eveno and J. W. Gillespie Jr. Moreover, the power peak happened earlier for higher amplitude vibrations, but increasing the welding force did not produce that effect. Both interfacial and viscoelastic heating are involved in the occurrence of this power peak.

Stage II is characterised by a step-like fashion power decrease, due to the progressive reduction in the solid area of the energy director. The step-like shape of the power graph is due to the melting and re-solidification of the resin as heat is transferred to the colder areas. This stage is more sensitive to welding force than to the amplitude of the vibrations.

In Stage III, downward displacement of the sonotrode starts, due to the squeeze of the flow of the energy director; thus, the thickness of the weld line starts to decrease. Dissipated power increases due to the mechanical-impedance increase at the interface when the melt fronts meet.

Stage IV is characterized by the continuation of the squeezing of the molten energy director flow until the thickness of the weld line is almost dropped to zero. Local melting of the resin from the substrates starts to occur, due to the heat transferred from the interface; this phenomenon makes the power diminish which, compensated by the power increase due to the molten energy director presence at the interface, leads to a power plateau. Increasing the welding force reduces the duration of this step.

In Stage V, practically no resin remains at the interface. Here, the melting of the composite substrates governs. Heat generation and flow squeezing lower their rates.

The conclusions of the study were that power and displacement data provided by ultrasonic welders can be used for in situ monitoring of the process and the weld quality: there was a clear correlation between the data provided by the welder and the physical changes at the joint interface. Also, this data can be experimentally used to define the optimum processing parameters for each material, set-up and welding scenario [30].

Ultrasonic welding can be controlled in three ways: By time, by energy or by displacement of the sonotrode, as a percentage of the thickness of the energy directors. The later one has proven to lead to strong and controllable welds, as shown in several investigations carried out by Irene Fernández Villegas: As compared to displacement-controlled welding processes, time-controlled ones were seen to have larger scatter in the weld strength. Energy-controlled welding processes introduce the drawback that the energy computed by the welder not only includes the energy to create the weld but also the one dissipated by the adherends, welding fixture and base, so changing the welding configuration would also imply a redefinition of the optimum welding energy that produces the maximum weld strength. In displacement-controlled welding, the vibration duration can be chosen, indirectly controlled by the sonotrode displacement, based on the power and displacement data for the combination of force and amplitude. As it only focuses on the physical changes happening at the interface, no redefinition is needed when the welding configuration is changed. The displacement-controlled welding is able to weld in the same stage of the process for a fixed set of force, amplitude and travel conditions, enabling to control and monitor the process.

In a further investigation carried out by I. F. Villegas (see reference 28), the correlation between the data given by the welder and the weld characteristics was studied. It was demonstrated that the strongest welds with minimum fibre deformation are obtained in Stage IV, so it constitutes a target for optimum welding conditions, specifically at the end of the power plateau, that coincides with a change in slope of the displacement rising curve. Then, as virtually the same shape of curves for power-displacement as function of time, regardless of the type of materials used, are obtained, for each welding scenario, ultrasonic welding process can be controlled and monitored to produce good-quality and repeatable welds for a fixed combination of force and amplitude by selecting this optimum travel value, when flat energy directors are used [28]. This will be the type of energy directors and ultrasonic process that will be used in this thesis.

It was also discovered that increasing the amplitude or the force increases the dissipated power and the heating rate, decreasing the vibration duration for a given travel value. A high force and amplitude leads to a faster welding, but imposes a higher power demand. Moreover, a high force and amplitude combination led to the smallest HAZ, but no significant drop in maximum LSS was observed [28].

As pointed out, ultrasonic welding is mainly applied to thermoplastics; however, dissimilar materials can be also ultrasonically welded, but they must be chemically compatible materials containing similar molecular groups, and their melting temperature difference should not exceed 22°C. Nevertheless, in an investigation carried out by P. Vizcaino Rubio and I. F. Villegas at TU Delft, a carbon-fibre reinforced thermoset substrate was welded using this technique to a carbon-fibre reinforced thermoplastic one, leading to consistent and strong welds, and demonstrating that welding of these two dissimilar materials can be performed [4]. The short-time ultrasonic welding avoids the degradation of the thermoset substrate, thus making this process the preferable and most

promising one for the joining of thermosets and thermoplastics. More discussion on their results and deeper explanation on hybrid welding will be done hereinafter. This thesis will continue this hybrid-welding line of study, in particular, seeking for adhesion improvement at the thermoset-thermoplastic interface.

Ultrasonic welding using UV-Ozone surface treatment

As stated before, UV/ozone is a surface cleaning technique that combines the ultraviolet radiation with ozone particles to clean and increase the surface energy of the treated surface. Nevertheless, this method is not able to remove contaminants such as dust or skin oils, so the surfaces need to be previously cleaned with a solvent, such as PF-QD, a quick-drying cleaning and degreasing solvent, or ethanol.

The principle of UV/ozone cleaning relies in the conversion of organic compounds into volatile substances due to the decomposition of UV rays with varying wavelength and the formation and decomposition of O_3, being removed from the contaminated surface. An ultraviolet ray with a wavelength of 184.9 nm irradiates atmospheric oxygen (O_2); then, oxygen absorbs this radiation and forms ozone (O_3). When ozone absorbs UV rays with a wavelength of 253.7 nm, it decomposes, generating atomic oxygen (O) with a strong oxidizing ability. Then, the contaminant organic compounds, which are irradiated with UV rays with stronger energy than their bond energy, absorb them causing photolysis and generating: ions, free radicals, excited molecules and neutral molecules. These excited contaminants react with atomic oxygen to form CO_2, H_2O, and atmospheric oxygen, which are removed from the surface [21].

In one of the experiments carried out by P. Vizcaíno Rubio, in the investigation carried out at TU Delft under the supervision of I. Fernández Villegas, five thermoset samples were treated with UV/ozone, exposing them to 3 minutes of UV radiation at 5 cm from the UV lamp. To measure the increase of surface energy, a CAM 200 Contact Angle Goniometre was used to take the contact angle measurements (it is worth to remind that lower contact angles indicate a higher surface energy). The UV/ozone treatment led to satisfactory results, lowering the contact angle and increasing the surface energy. Afterwards, the treated thermoset samples were ultrasonic-welded and single lap shear tests were performed. It could be proved that the UV/ozone treatment clearly improved the LSS results with respect to untreated surfaces: Mean LSS value of 8 MPa for UV-treated samples, with respect to the 4.3 MPa mean value for non-treated epoxy (which had large scatter) [4].

Ultrasonic welding has the advantages of being a fast, economical, easily automated technique. No foreign materials are needed at the welding interface. Up to 60 parts per minute can be welded using it, creating consistent, high-strength joints in the lowest time for a welding method. Tooling can be quickly changed, and no ventilation system is needed to remove fumes or heat. Nevertheless, it has also got limitations, such as the impossibility to weld large parts with the current technology, being a good option for welding of small parts or spot welding. Research is being done in this field to overcome such problem, and sequential ultrasonic welding of larger areas is regarded as a future option.

➢ JOINING OF THERMOSETS

As mentioned previously, thermoset components can be joined by mechanical fastening. Nevertheless, to overcome the problems this technique introduces, two alternative processes are used:

- ***Co-curing:*** This term stands for the process were the composite laminate is simultaneously cured and bonded to another uncured material. Note that both materials are uncured prior to bonding [25]. The resins must be compatible; otherwise, lower mechanical properties can develop at the interface. This technique is currently being used in the A400M cargo door.
- ***Co-bonding:*** In this process, two materials are cured together, but one of them is already fully cured and the other one is uncured. It requires conscious surface preparation of the previously cured material, and additional adhesive might be also required at the interface [17]. This method is also being applied in the aerospace industry: a plate reinforced with an S-frame in the A380 airplane [31].

➢ HYBRID WELDING

This is the state of the art technique for joining thermoplastic and thermoset materials together. Knowing that for a number of applications, thermoplastics cannot substitute thermosets, it is clear that a method for effectively joining both materials must be used – it is worth to remember that direct welding of thermoplastics and thermoset materials is not possible. Here arises the concept of hybrid welding: a process where adhesive bonding and welding are combined to join thermosets with thermoplastics. In this method, the thermoset is coated with a layer of thermoplastic, and then the stack is welded to a thermoplastic composite. Ultrasonic welding is a preferred option in this field: Thermal degradation requires time to occur, but as ultrasonic welding is a very fast process, degradation of the thermoset can be avoided when it takes part in the welding process. Also, the co-cured layer of thermoplastic shields the thermoset from the high temperatures that are reached during the welding. There are two remarkable procedures:

- ***Co-cure concept:*** In this method, a TP layer is cured with the TSC laminate; the TP must be chemically compatible with the TS matrix. Bond strength relies in the inter-diffusion of the macromolecular chains of the TS resin and the TP. Also, a third polymer, compatible with the TP and the TS, can be added to the TP during the process, so an IPN (interpenetrating network) can be created when cured with the TS, as Roderic C. Don *et al.* patented to promote the adhesion between thermoplastics and thermosets [32]. Then, the stack can be welded to a TPC laminate. The main constraint of this technique is the thermal degradation of the thermoset that arises due to high welding temperatures of the thermoplastic [16].

M. Hou, from the University of Queensland, Australia, did great advances in this topic. In particular, he carried a study where a thermoplastic film was co-cured with a thermosetting epoxy composite, forming a SIPN (semi-interpenetrating network, more discussion about this phenomenon will be done in the following section). Then, two samples of the thermoset co-cured with the thermoplastic were thermally welded, and the bond created was of equal or superior characteristics – LSS, high temperature, low temperature and anti-chemical resistance – to that obtained by adhesive bonding of the thermosets using Cytec FM300K adhesive.

For the experiment, a carbon fabric epoxy prepreg was used as the thermoset composite. It was co-cured with a thermoplastic film, and the samples were welded to other samples by different heating methods, such as co-consolidation in an oven and localized heating in a hot press. Prior to welding, the surfaces were cleaned with isopropyl alcohol. The process is shown in Figure 16:

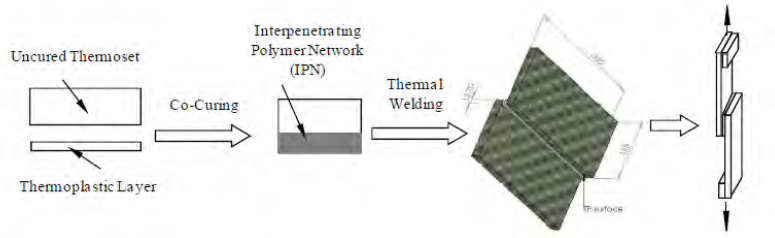

Figure 16: M. Hou's experimental procedure [3].

At the epoxy-thermoplastic interface, a SIPN is created: during curing, molecules of epoxy diffuse into the thermoplastic and cures in the polymer, creating an entanglement of molecular chains and a SIPN when cured. The result is an extreme quality bond between the thermoplastic and the thermoset: the SIPN enhances the strength of the thermoplastic-thermoset interface.

Welding of the samples, apart from improving the characteristics of the bond with respect to the FM300K adhesive bonding procedure, also proved that increasing the thermal-welding temperatures, higher strength was achieved.

The advantage of co-curing the thermoset composite with a thermoplastic film and then welding them to a thermoplastic composite, instead of using adhesive bonding, is the speed of assembling the joints. Moreover, it is an environmentally friendly technique and eliminates the need of surface preparation [3].

In one of the experiments P. Vizcaíno's investigation at TU Delft, great advances were achieved in this field too: CF/Epoxy prepreg was co-cured with two PEEK films of different thickness, 50 µm and 250 µm, and ultrasonically welded to CF/PEEK. Slightly higher mean lap shear strength mean value with less scatter was obtained for the thicker co-cured layer welds, and showing that co-curing the thermoplastic layer with the thermoset dramatically increased the LSS value of the weldings [4].

Interpenetrating networks

The concept of interpenetrating network is of high interest and will be also studied in this thesis. It is defined as a combination of two or more polymers in a network form, synthesized in a juxtaposed way. There are several ways this "interpenetration" can be accomplished, among them, interpenetrating and semi-interpenetrating networks are of special interest for this investigation.

Interpenetrating networks (IPN) consist of a gel composed of two interpenetrating polymer networks by cross linking a polymer into a pre-existing highly cross-linked polymer network of a different kind, such that elastic and mechanical properties are enhanced. The network cannot be separated unless chemical bonds are broken. This type of entanglement can only be achieved between polymers that are able to cross link, mainly thermosets or elastomers, but not thermoplastics.

Our study on interpenetrating networks is focused on the entanglement formed between thermosets and thermoplastics, and to improve their adhesion. Then, the type of polymer combination we aim to study is the SIPN (semi-interpenetrating polymer network). They consist of one or more networks or branched polymers: some of the linear or branched macromolecules must penetrate in a molecular scale in at least one the networks. The linear macromolecules correspond to the thermoplastic chains, and the network into which they penetrate, is the thermoset molecular structure. The branched or linear polymers can be separated from the polymer network without breaking the chemical bonds because they are polymer blends, a fact that distinguishes them from IPN. Figure 17 shows another illustration of a SIPN. This is the type of union constitutes the ideal interface when co-curing thermosets and thermoplastics together. Not all thermoplastics are able to form SIPNs with a thermoset [33], [34].

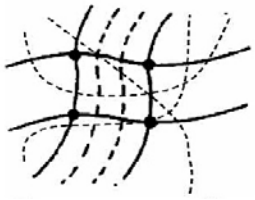

Figure 17: SIPN [34].

In a study performed by L. J. Vandi, M. Hou *et al.* [35] – following the study carried out by M.T. Heitzmann *et al.* [36] – uncured (A-stage) epoxy was poured onto thermoplastic films, PEI, PSU and PES, and the mixtures were cured for 2 hours at 180°C under atmospheric pressure. Observations performed by Scanning Electron Microscope (SEM), optical microscopy (Figure 18) and AFM showed that there was an actual diffusion layer between the epoxy and the thermoplastics, a semi-interpenetrating network, showing the feasibility of its formation between epoxy and these thermoplastic materials [36].

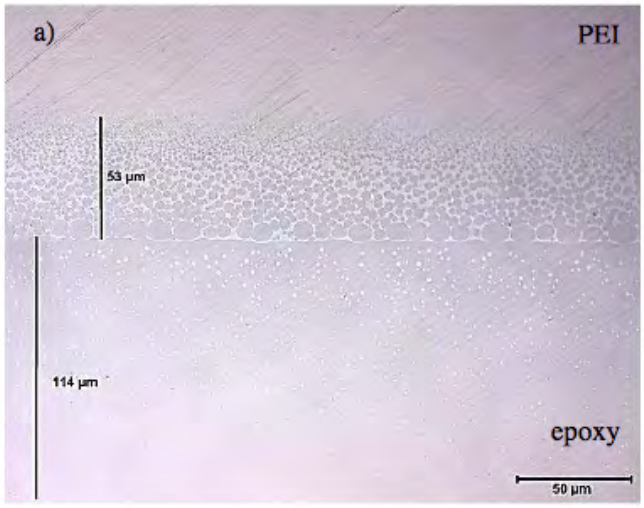

Figure 18: Optical microscope image of the SIPN formed between PEI and epoxy resin [36].

- ***TP hybrid interlayer:*** It consists of a woven roving fibre prepregged with a TP polymer that is later cured with a TSC laminate. The prepregging process is controlled such that only half of the fabric is impregnated with the thermoplastic layer, and half of it remains free. Then, the hybrid layer is placed with the uncured and wet TSC laminate and cured all together. The thermoset resin flows

and impregnates the free half of the woven fabric, so that the fabric promotes mechanical interlocking between the thermoplastic and the thermoset. The viscosity of the thermoset during curing should be kept high, so that the thermoplastic conserves its penetration in the fabric. An advantage of this method is that no chemical compatibility between the thermoplastic and the thermoset is needed (as opposed to the co-curing process). Figure 19 shows this process [16]. Then, the assembly can be welded to a TPC laminate if desired.

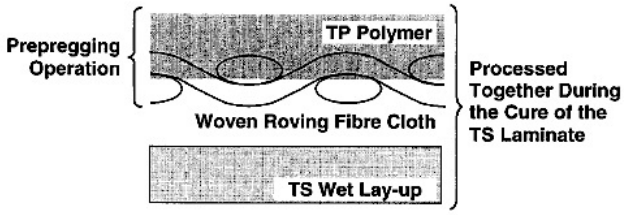

Figure 19: TP hybrid interlayer process [16].

1.2. PROJECT PLAN

This bachelor thesis will specifically study the adhesion between thermoplastics and thermosets for ultrasonic welding of these dissimilar materials, and will follow two main lines of investigation:

A. DIRECT WELDING: *Macro-Interlocking. Adhesion phenomenon: Fibre-resin interlocking between the TP and the fibres:* As already commented, thermoset matrix cannot re-melt when welded due to its nature. This line of the thesis will study direct welding, with a main focus on physical mechanical interlocking.

A.1. Degradation study: A reinforced thermoset substrate will be directly welded to a reinforced thermoplastic one. The purpose of this section is to check that the epoxy is not degraded when not co-cured with a thermoplastic film – for hybrid welding – with the chosen set of welding parameters.

A.2. **Laser treatment:** Second, the laser surface treatment will be applied to the thermoset prior to welding it to the thermoplastic composite (CF/PEEK). The aim of applying the laser cleaning is to uncover the outermost fibres of the thermoset, without damaging them, to promote mechanical interlocking between the fibres and the thermoplastic when direct welding, like the TP hybrid interlayer concept but without adding any external woven fabric elements. Dr. Fabian Fischer, head of the Department of Adhesive Bonding and Composite Technologies at the Institute of Joining and Welding at the Technical University of Braunschweig, will perform three different types of laser treatments.

B. INDIRECT OR HYBRID WELDING: *Micro-interlocking.* Molecule interlocking in thermoplastic-thermoset co-curing: Study of the mechanical interlocking of the molecules of both materials for optimum bond strength and the generation of a SIPN (semi-interpenetrating network) when possible – among the four thermoplastic materials available for this investigation (PEI, PPS, PEEK and PEKK), SIPN are possible between epoxy and PEI [45], but not for the other three thermoplastic materials available. The interface between the thermoset and the co-cured thermoplastic layer will be studied before and after the performance of ultrasonic welding.

There will be two welding studies:

B.1. Standard Hybrid Welding: With the help of M. F. Motovilin, where thermoset prepreg will be co-cured in the autoclave, using the fabricant's recommended cycle, with different thermoplastic films non-treated and treated with different surface modification procedures. The three types of thermoplastic materials used were: PEEK, PEKK and PPS. The same thermoplastic resin for the matrix of the TPC substrate, the energy director and the co-cured TP film, will be used in each sample.

B.2. Multi-Material Hybrid Welding: An experiment using the provided thermoset laminate, a PEI film and a PEEK laminate will be carried out: CF/Epoxy (carbon-fibre reinforced epoxy) prepreg will be co-cured with the PEI film, and the assembly will be ultrasonic-welded with a CF/PEEK. It was given this name to differentiate this study from the "Standard Hybrid Welding" one. The aim of this composition is to study the compatibility between the thermosetting epoxy and PEI, and between PEI and PEEK. PEI and PEEK energy directors will be used, in order to check their characteristics and

differences. Moreover, a SIPN formed between the thermoset and the PEI will be sought, as previous studies have demonstrated its feasibility [45]. The strongest connection between thermosets and thermoplastics are SIPNs; nevertheless PEI is amorphous and not as chemically stable as semi-crystalline PEEK, so PEI is not used in important aircraft structural parts that can be in contact with chemicals, as opposed to PEEK. Then, proving the compatibility of PEI and PEEK, creating a strong connection and possible SIPN between the thermoset and the PEI, and achieving a strong weld, would prove a new welding combination of thermoplastic and thermoset materials, that combines strong and chemically stable composite materials, and a welding interface with good compatibility and entanglement among the different thermoplastic materials and the thermoset.

There were additional experiments and tests performed that were decided to be performed during the development of the investigation, so they could not be included *a priori* in the "Project Plan". They will be explained in their corresponding sections.

All of the experiments described in this thesis were executed at the 'Delft Aerospace Structures and Materials Lab', in the Aerospace Engineering faculty of the Technical University of Delft, under the supervision of Dr. Irene Fernández Villegas.

Chapters' Summary

A brief overview of the contents of each chapter will be now presented, with the purpose of giving the reader an idea of the organisation of the thesis contents now that the general lines of investigation have been explained:

INTRODUCTION

- **Chapter 1: Introduction.** Already presented, with a theoretical background on the materials and techniques used, and the thesis project plan.

EXPERIMENTAL

- **Chapter 2: Experimental.** This section will be divided in four categories:
  - Materials: Brief explanation of the specific characteristics of the thermoplastic and thermoset materials used.
  - Manufacturing: Manufacturing procedures of the samples used in the experiments explained in the 'Project Plan'.
  - Welding process: Explanation of the ultrasonic welding process, configuration and definition of welding parameters.
  - Analysis techniques: The description of the main methods to analyse the weld quality and characteristics will be explained here: Single-lap shear tests, optical microscopy and Fourier Transform Infrared Spectroscopy (FTIR).

EXPERIMENTS and RESULTS

The welding experiments and results of the thesis will be divided in two parts:

PART I: Standard Hybrid Welding (SHW). This part will be divided into three chapters, each one explaining one of the thermoplastic materials used in this line of the investigation: PEKK, PEEK and PPS.

- **Chapter 3: SHW – PEKK.** CF/epoxy to CF/PEKK welds, using a PEKK ED.
- **Chapter 4: SHW – PEEK.** CF/epoxy to CF/PEEK welds, using a PEEK ED.
- **Chapter 5: SHW – PPS.** CF/epoxy to CF/PPS welds, using a PPS ED.
- **Chapter 6: SHW additional studies**
- **Chapter 7: New experiments and SHW conclusions.**

PART II: Other types of welds

- **Chapter 8: Multi-Material Hybrid Welding** (PEI coating).
- **Chapter 9: Direct welding.** In this chapter, the degradation study and laser welds will be explained.
- **Chapter 10: Thermoset to Thermoset Welding.** This section will be devoted to a study not included in the project plan because the materials arrived in a time window not compliant with the time planning: Thermoset to thermoset ultrasonic welding, co-cured with two thermoplastic

films of different thicknesses, in order to study the feasibility of ultrasonic welding without the use of an energy director when the co-cured thermoplastic layer is thick enough. The materials were provided by Professor Alfonso Maffezzoli, from Salento University (Italy).

CONCLUSIONS AND FUTURE WORK

- **Chapter 11: Conclusions and Future work.** This last chapter will present the conclusions of this thesis, and future work that can be performed in the investigated areas.

EXPERIMENTAL

Chapter 2

Experimental

This chapter is devoted to the description of the materials, manufacturing and welding processes, as well as analysis techniques used in this research.

2.1. MATERIALS

The aim of this section is to describe the different types of materials used in this research.

Thermoplastic Materials

For this project, four thermoplastic materials will be used: PEEK, PEKK, PPS and PEI.

- PEKK

PEKK stands for "polyetherketoneketone". Its molecular structure is shown in Figure 20. It is a high-performance, semi-crystalline thermoplastic, with high toughness and damage tolerance. It has outstanding flame, toxicity and smoke performance [37].

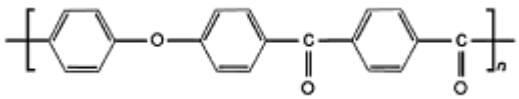

Figure 20: PEKK molecular structure.

The type of PEKK film used in this project is provided by Cytec, 40-45 µm-thick, with a melting temperature of 304–366°C, a specific density of 1.27–1.3 g/ml, a decomposition temperature of 410°C, and a glass transition temperature of 159°C. It was rough/mate on one side and shiny on the other.

The PEKK substrates were provided for this investigation in two batches, both of carbon-fibre reinforcement type: The first batch, supplied by Fokker and provided by Cytec, consisted of samples already consolidated and cut into 25.4 x 101.6 mm^2 dimensions, with a thickness of 1.7 mm; the second one was provided by Ten Cate in a consolidated 480 x 485 mm^2 panel, 2 mm-thick. Both of them had unidirectional reinforcement; the samples from Fokker had its layers with the zero-

direction of the fibres aligned with the longest side of the sample, and the Ten Cate panel had its layers perpendicularly stacked ([0/90]).

- PEEK

PEEK material, which stands for “polyetheretherketone”, belongs to the polyaryletherketone polymers family (PAEKs). The PAEK family consists of high-performance thermoplastic polymers, with an aromatic backbone molecular chain interconnected by ether and ketone functional groups. More precisely, PEEK belongs to PEKs sub-family (polyetherketones or polyketones).

PEEK is used in a wide range of applications, from biomedical purposes to aerospace industry. It is a linear homopolymer, meaning that the monomers that repeat to form the polymer are of the same type and are disposed in the shape of non-branched chains (see Figure 21). More precisely, PEEK is a linear chain of 100 monomer units with a molecular weight (related to the length of the chain) of 80,000–120,000 g/mol. The length and composition of the molecular chain determines the temperature and rate of the deformations; PEEK is stable at temperatures above 300°C, has good chemical and radiation resistance, bears glass and carbon fibres reinforcements, and has great strength.

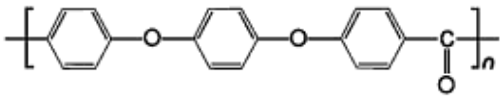

Figure 21: PEEK molecular structure.

The molecular chain of PEEK vibrates and rotates when force or heat is applied to the material. When cooled from its molten state, PEEK eventually forms a two-phase microstructure, where crystal and amorphous regions coexist (semi-crystalline structure). The content or extension of the crystal fase depends on the thermal processing history of the material. In PEEK film formation, adjustment of the cooling rate can lead to completely amorphous films. Its glass transition temperature (T_g) is 143°C, below this temperature, polymers behave like a brittle glass, responding to mechanical stresses with the rupture of the covalent bonds; nevertheless, PEEK behaves in a ductile way. Above the glass transition temperature, amorphous regions gain mobility and van der Waals forces (secondary intermolecular forces) govern the flow movement. For PEEK, there exists a recrystallization temperature, T_c or T_r, related to the formation of crystals, which may be around 150°C, depending on the type of PEEK used. The melting temperature T_m, at which most of the crystalline zones have melted, is around 343°C; it is worth to mention that thicker and more perfect PEEK crystals tend to melt at higher temperatures. Its flow transition temperature, T_f (when it becomes liquid), is around 390°C [38].

The PEEK film being used in this project is provided by Victrex, 250 µm-thick, with a melting point of 343°C, an auto-ignition temperature of 595°C and a density of 1.3 g/ml. The film was shiny/smooth on both sides.

For the manufacturing of the PEEK substrates, a carbon fibre reinforced PEEK prepeg will be used, continuous-fibre woven fabric of 5 Harness Satin, provided by Ten Cate.

- PEI

PEI stands for “polyether imide”, a high-performance thermoplastic with ether links and imide groups in its polymer chain (see Figure 22). It exhibits high tensile strength, flame resistance and low smoke emission. It has a wide range of processing temperatures due to its high stability.

PEI’s peculiarity is that it can behave either as a thermoplastic or as a thermoset. As a thermoplastic, it has a linear structure and it is solid at room temperature. When used as a thermoset, it is branched and is liquid at room temperature. It has been used in space applications in its both available types. Thermoplastic PEI has a glass transition temperature of 216°C [39].

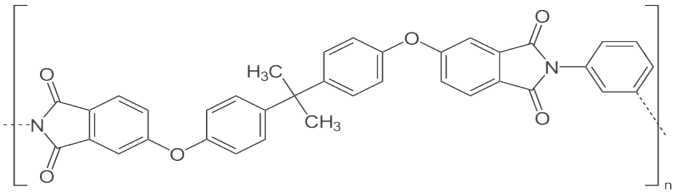

Figure 22: PEI molecular structure.

The PEI used in this project was of thermoplastic type, with a linear structure and solid at room temperature. The available PEI was provided by SABIC, 50 µm-thick, rough/mate on one side and shiny on the other.

No PEI substrates were used in this thesis.

- PPS

PPS stands for “polyphenylene sulphide”, a high-performance thermoplastic material that alternates sulphur atoms and phenylene rings (see Figure 23). It is very stable, bearing chemical and thermal degradation up to 350°C. PPS is a semi-crystalline polymer, with a crystalline melting point of 285°C. It can be easily mixed with glass fibres and other fillers. The glass transition temperature for this thermoplastic is 85-90°C [40].

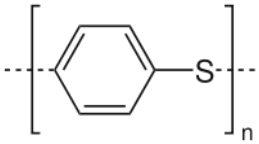

Figure 23: PPS molecular structure.

The PPS available film for this investigation was provided by Fortron, with a thickness of 75 µm.

The PPS substrates were manufactured using a CF/PPS prepeg, continuous-fibre woven fabric of 5 Harness Satin, provided by Ten Cate.

Thermoset Materials

The thermoset composite that will be used in this project was a carbon fibre reinforced epoxy used for most of this thesis was Hexply 8552 epoxy, provided by Hexcel, in its prepreg (pre-

impregnated) tape form. Its characteristics are: UD tape (unidirectional reinforcement), Hand-Lay Up (HLU), AS4 fibre type, 37% Resin Content prepreg.

For the additional experiments, two other thermosetting epoxies were used: A woven carbon-fibre reinforced one, provided by Professor A. Maffezzoli of Salento University, and Hexply M21, this last one provided also by Hexcel.

2.2. MANUFACTURING

2.2.1. Epoxy composites

For the manufacturing of the thermoset substrates, the cited CF/Epoxy prepeg mainly used in this investigation, Hexply 8552, was cured in three autoclave processes, which will be described hereinafter. Stacks of 11 unidirectional layers where done by hand lay-up, aligned in the zero-direction ($[0°]_{11}$). The prepreg was cut using the Shear Cutter available at the DASML. Specimens of this material will be used as substrates in the ultrasonic welding and for the study of epoxy degradation – 25.4 x 101.6 mm^2 in order to meet ASTM D1002 standard dimensions, for the later welding and testing – with the zero-direction of the fibres aligned with the longest side of the welding specimen.

Two types of samples were manufactured: the first type were composed only by CF/Epoxy, and the second type, composed by CF/Epoxy and a thermoplastic film, intended for 'Standard Hybrid Welding' and 'Multi-Material Hybrid Welding'. The thermoplastic film was added or not depending on the type of specimen that was desired to be obtained. These thermoplastic films were cut with a pair of scissors and cleaned with ethanol before co-curing them with the epoxy. The panels were cured in the Scholtz Autoclave available at the DASML of TU Delft, which applies the necessary pressure and temperature for the thermoset to cure. The curing cycle for the used thermoset prepreg curing was: 110°C for 60 minutes, then 180°C for 120 minutes, 7 bars of pressure, shown in Figure 24. This was the cycle used for monolithic structures, as recommended by the manufacturer.

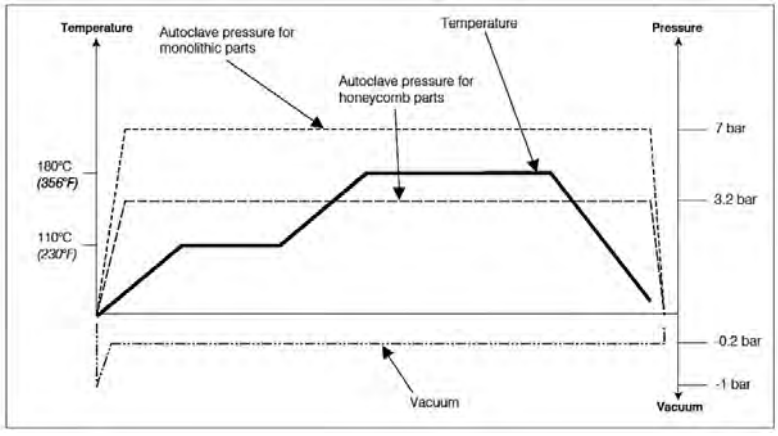

Figure 24: Hexply 8552 epoxy manufacturer's recommended cycle for honeycomb and monolithic components [41].

In the three autoclave processes, the same vacuum bag layup was used, mounted on an aluminium plate able to withstand a temperature of 200°C. The layers, from bottom to top, are the following [41]:

1) **Aluminium plate (200°C):** The base of the vacuum-bag layup
2) **Reinforced Teflon film:** Instead of coating the aluminium plate with a release agent, a reinforcement Teflon film was placed to release the cured prepreg once cured from the plate and assure a smooth surface.
3) **Tacky tape (204°C)** on the edges of the aluminium plate, reinforcing the corners, which ensures a sealed bag from which to extract the air to provide vacuum conditions.
4) **FEP Foil red A400 film (260°C)**, which does not adhere to the panels when they are cured.
5) **Panels** to be cured.
6) Another layer of **FEP Foil red A400 film (260°C)**.
7) **Peel Ply white/red tracer Stitch Ply A film (232°C):** Prevents further flow of epoxy matrix and permits air and volatiles to pass to the bleeder blanket on top.
8) **Breather Blanket Air Weave N10 film (204°C):** Removes air and volatiles from the whole layup and enables the appliance of vacuum.
9) **Vacuum bagging foil Green Roll WL7400 (204°C)**, on top of the tacky tape, to seal the bag.
10) **Vacuum valve** attached to the green bagging foil and on top on the breather blanket, which removes the air and volatiles and enables the vacuum conditions inside the bag.

Figure 25 shows a scheme of the vacuum bag layup:

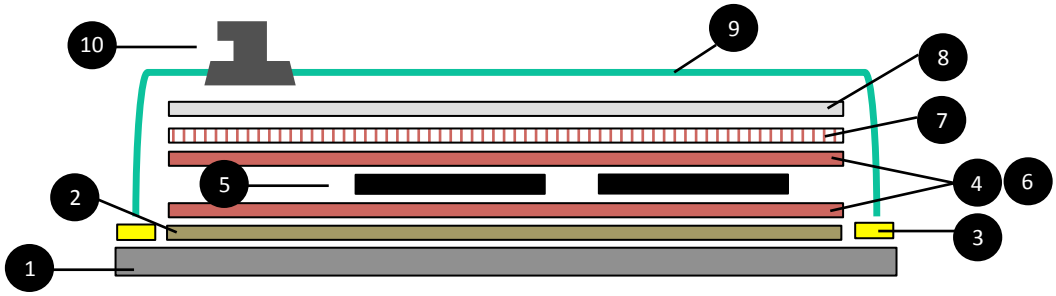

Figure 25: Vacuum bag layup used in all the performed autoclave processes. The numbers correspond to each layer previously cited.

For the three the autoclave curing cycles, the panels were prepared and formed according to aerospace standards and requirements. The first two autoclave processes were performed with the help of Mladen Motovilin, who collaborated with the 'Standard Hybrid Welding' part of the investigation.

In the first autoclave process, three types of thermoplastic films were co-cured with the epoxy: PPS, with a thickness of 75 µm; PEKK, with a thickness of 65 µm; and PEEK, with a thickness of 100 µm; they were property of M. Motovilin. Some were left untreated, and the rest were treated with different procedures, depending on the type of thermoplastic: UV-O_3[7], acetic acid, chloroform and long-chain amine formula, all procedures performed by M. Motovilin. Also, two unidirectional carbon-fibre reinforced PEEK prepreg layers were used for co-curing with the CF/Epoxy in two of the stacks.

[7] The UV-ozone (UV-O_3) treatment consisted of exposure of the film to a UV lamp, available at the Physical Lab of the DASML at TU Delft. The lamp was positioned 3-5 cm from the film. One side of the film was treated for 30 minutes, and the other one for 2-3 minutes. The side treated for 30 minutes was the one in contact with the CF/Epoxy prepreg for the co-curing in the autoclave.

In the second and third autoclave processes, CF/Epoxy panels, using a co-cured PEI thermoplastic layer, 45-50 µm-thick, and no thermoplastic co-cured layer, were obtained. The second autoclave process also used the PEEK film of the first cycle (100 µm-thick) in two of the panels.

In Table 1, the characteristics of all the autoclave-cured panels will be summarized. All of them used 11 layers of Hexply 8552 epoxy prepeg, with a $[0]_{11}$ stacking sequence, as the base material.

Panel Reference [a]	Thermoplastic co-cured film	Thickness of the TP film (µm)	Panel observations	Cycle observations
Panel 1-1	PEEK NT (Not Treated)	100	Detached thermoplastic layer after curing.	In the first curing cycle, panels had 165 x 310 mm^2 dimensions. The thermoplastic films were placed below the CF/Epoxy prepeg stack for the curing. This led to a rough and textile-pattern on the upper part of the panels – induced by the peel ply white/red tracer and bleeder blanket layers – and a smooth bottom part, because the Teflon and red foil used were flat and had a smooth surface. As the thermoplastic film was placed below the prepreg stack, the surface devoted to welding remained smooth.
Panel 1-2	PPS NT	75	-	
Panel 1-3	PEEK UV-treated	100	-	
Panel 1-4	PEKK UV-treated	65	-	
Panel 1-5	PEKK NT	65	-	
Panel 1-6	UD CF/PEEK layer [0/90]	- [b]	Curved panel after curing, indicating delamination and failure. It was discarded.	
Panel 1-7	UD CF/PEEK layer [0/0] + PEEK film	-	The PEEK film used had a shiny and a rough surface. The shiny surface was scratched and in contact with the CF/PEEK layer, which was in contact with the CF/Epoxy prepeg. After curing, partially detached co-cured films were observed.	
Panel 1-8	PPS UV-treated	75	After curing, partially detached PPS film was observed.	
Panel 1-9	PPS treated with acetic acid	75		
Panel 1-10	PEKK treated with chloroform and long chain amine	65	-	
Panel 1-11	UD CF/PEEK layer [0/0]	-	-	
Panel 1-12	PEEK treated with acetic acid + UV-O_3 (5minutes)	100	-	
Panel 2-1	PEEK NT	100	The same PEEK film as in the first cycle was used. Here, the mate/rough part was co-cured facing the CF/Epoxy prepreg [c].	Panels 2-1 and 2-2 were cured with the thermoplastic film on top of the epoxy prepeg stack, and an aluminium plate wrapped in release foil (so that the epoxy would not
Panel 2-2	PEEK NT	100	Using the same PEEK film as in the first cycle, this panel	

			was co-cured with the shiny parts facing the epoxy prepeg. After the curing, the film was completely detached [c].	stick during the curing) to assure a smooth surface. Their dimensions were 165 x 310 mm^2.
Panel 2-3	-	-	This panel was co-cured with no TP layer, in order to obtain CF/Epoxy samples.	Panels 2-3 and 2-4 did not have an aluminium plate on top, so their top surfaces had a woven pattern (as in the first autoclave cycle). Their dimensions were 300 x 380 mm^2. Panel 2-4 was cured with the PEI film on top, this was the surface where the textile pattern remained [d].
Panel 2-4	PEI NT	45-50	The PEI film had a shiny and a rough face. The rough face was in contact with the epoxy during the co-curing, seeking for mechanical interlocking.	
Panel 3-1	-	-	No TP co-cured layer.	The dimensions of the four panels were 300 x 380 mm^2. An aluminium plate wrapped in release foil was placed on top of the four of them, in order to assure a smooth top surface [e].
Panel 3-2	-	-		
Panel 3-3	PEI NT	45-50	The rough side of the PEI film was in contact with the epoxy prepeg during the curing cycle.	
Panel 3-4	PEI NT	45-50		

Table 1: Hexply 8552 CF/Epoxy panels cured in the three autoclave cycles.

[a] Panel Reference: # curing cycle - # panel.
[b] Reliable measurements of the thicknesses of the CF/PEEK prepegs used could not be obtained.
[c] The aim of panels 2-1 and 2-2 was to seek and prove the mechanical interlocking between the thermoplastic and the thermoset due to the characteristics of their surface: Co-curing the mate surface in contact with the epoxy lead to an attached thermoplastic film when the process had finished, enhancing their adhesion.
[d] The surface of panel 2-4 showed that, in some areas, the PEI had perfectly sunk in the epoxy, and in other areas, the film seemed to be un-sunk and with a soft-shiny appearance. The cross-section of these areas was studied with microscopy, and the results will be presented in Chapter 7 ('Multi-Material Hybrid Welding').
[e] PEI film had perfectly sunk in the CF/Epoxy, and that the sample had a smooth and uniform surface. The observation of the cross section of the sample with the microscope will confirm these positive results.

There was a fourth autoclave process performed, whose purpose and characteristics will be explained in the 'Standard Hybrid Welding' part.

The panels, with a thickness of 1.7-1.8 mm, were sent to Van Nobelen Delft VB company to be water-jet cut into 25.4 x 101.6 mm^2 (1 x 4 $inch^2$) samples, in order to meet ASTM D1002 standards. It is worth to mention that, when the samples of panel 2-1 were cut, the PEEK film detached, showing that although some mechanical interlocking was attained by co-curing its rough surface in contact with the epoxy, untreated PEEK does not effectively adhere to it.

Fifteen samples of CF/Epoxy, not co-cured with a thermoplastic film, were sent to Dr. Fabian Fischer to be laser treated; this experiment will be presented in Chapter 8.

M. Motovilin donated three samples of a Cytec UD carbon-fibre reinforced epoxy, which used the same curing cycle as Hexcel 8552, co-cured with the same PEKK film used in the first cycle (65 µm-thick), treated with another formula of chloroform and amine. From now on, this new formula will be called "second formula", and the one used in the first cycle, "first formula".

Figure 26 shows the vacuum bag coming out of the autoclave after the first curing cycle was performed.

Figure 26: Vacuum bag lay-up being extracted from the autoclave after curing.

2.2.2. Thermoplastic composites

Three types of carbon-fibre reinforced materials will be used in this project: CF/PEKK, CF/PPS and CF/PEEK. The specimens made of these materials will be used as substrates for ultrasonic welding.

As mentioned in section 2.1, carbon-fibre reinforced PEKK (CF/PEKK) was provided in two batches: the first one, supplied by Fokker and provided by Cytec, was already cut into samples with the desired dimensions to meet the ASTM D1002 standard (25.4 x 101.6 mm^2); the second one, provided by Ten Cate in a consolidated panel, was taken to Van Nobelen Delft VB company to be water-jet cut into 25.4 x 101.6 mm^2 samples. Due to the perpendicular stacking of the panel, one of the faces had the carbon fibres aligned with the long side of the samples (101.6 mm) – the chosen one for the welding contact surface – and the other face had the fibres aligned with the short side of the sample (25.4 mm).

CF/PEEK was available in its pre-impregnated form, as described in section 2.1. The roll was cut using the Gerber Cutting Machine, available at the DASML of TU Delft, in six layers of 580 x 580 mm^2. They were stacked using the sequence $[0/90]_{3S}$, that is, three layers with the weft side[8] upwards, and three other layer on top with the warp side upwards, such that the warp directions remain on the two outside faces of the stack. They were joined to maintain position until consolidation with a Rinco handheld ultrasonic welder, providing 6 plunges per welding of 2 layers. Then, the stack edges were covered with aluminium tape, such that the resin could flow in it when heated to consolidate. The consolidation of the prepreg was done in the Joos Press available at the DASML of TU Delft. For this process, Figure 27 shows the stack of layers was inserted between the plates of the press.

[8] It is worth to explain that the weave thermoplastic prpegs used in this thesis had a warp face or side and a weft one, showing perpendicular main apparent orientation of the fibres to one another.

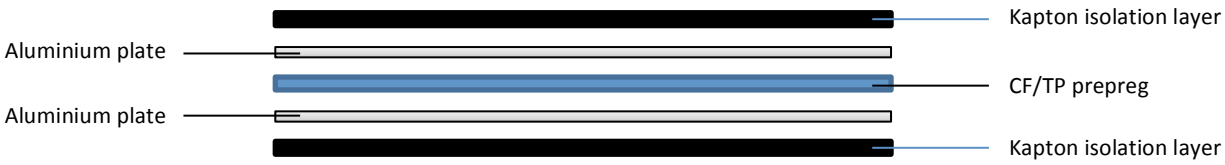

Figure 27: Layers for the press consolidation process of the reinforced-thermoplastic prepegs.

The Kapton isolation layer ensures uniform temperature distribution at the material to be consolidated. The aluminium plates provide a smooth surface to the consolidated specimen and permit the unmoulding of the sample once consolidated. This last function is achieved through covering the aluminium plate with Marbocote 227CEE release agent (3 layers, waiting 15, 10 and 5 minutes between layers). The consolidation cycle for CF/PEEK was: 385°C for 20 min at 10 bar, 10°C/min heating/cooling rate. The consolidated panel had a thickness of 1.8-1.9 mm, approximately. A total of two panels were manufactured. Also, 49 cured CF/PEEK samples with the 25.4 x 101.6 mm^2 dimensions, using the same prepeg material as the one for the Joos Press re-consolidation, were available for the use of this project.

CF/PPS was also available as a prepreg, as described in section 2.1. The same procedure as the used for the CF/PEEK was followed to manufacture the 580 x 580 mm^2 stack to be consolidated at the Joos Press. The consolidation cycle for CF/PPS was: 320°C for 20 min at 10 bar, 10°C/min heating/cooling rate. One panel was consolidated, with a thickness of 1.9 mm.

The Joos Press consolidated woven panels were taken to Van Nobelen Delft VB company to be water-jet cut into samples of 25.4 x 101.6 mm^2, in order to meet ASTM D1002 standard. The main apparent orientation of the fibres was directed along the longest side of the samples (101.6 mm).

2.2.3. Energy directors:

For the manufacturing of the energy directors (EDs) that will be used in the ultrasonic welding, four materials were used: PEKK, PEEK, PEI and PPS films, whose precedence and characteristics were explained in section 2.1. The aim was to manufacture energy directors with a thickness of 0.25 mm, a value that lead to positive results in previous investigations, as already highlighted in the first chapter of this project. As each available thermoplastic film had a different thickness, different processes were used for each material to manufacture the desired EDs. The films with less thickness than the desired one had to be stacked and reconsolidated in the Joos Press, with the same stacking of Kapton and aluminium layers as in the CF/TP manufacturing. All of them were cleaned with ethanol prior to re-consolidation. The overlap area for the ultrasonic welding of this project is of 12.7 x 25.4 mm^2, so a surface of 26 x 26 mm^2 for the energy directors, cut from a bigger film with a pair of scissors, was chosen in order to be conservative, to cover the whole overlap area and leave some margin. The four procedures will be explained in Table 2:

ED thermoplastic material	Film thickness (µm)	Press re-consolidation?	Cycle	Number of layers
PEKK	40-45	Yes	325°C, 20 bar	6
PEEK	250 (0.25 mm)	No	-	-

PPS	45-50	Yes	260°C, 20 bar	5
PEI	75	Yes	270°C, 20 bar	4

Table 2: PEKK, PEEK, PPS and PEI energy directors manufacturing.

PPS EDs turned out to slightly thicker, around 0.3 mm thick, but this value was inside the margin of 0.25-0.4 mm thickness for the flat-ED welding monitoring process with which the optimum welding parameters for each material will be determined (following section).

2.3. WELDING PROCESS

In this section, the process determine the parameters for optimum weld achievement – which will be called "optimum parameters" – for each material type will be described. The welding conditions depend on the type of energy director and TP substrate chosen. It is worth to remind that the ultrasonic welding has three main parameters that characterize the process: Force, amplitude, and travel. The best conditions will be the ones that ensure that no epoxy degradation is occurring, and that the power available in the ultrasonic welder is not exceeded. In this investigation, and throughput this whole thesis, the process was controlled with the travel of the sonotrode, proportional to the ED thickness. The degradation of the epoxy resin is avoided by decreasing the welding time, and this can be achieved by selecting a high force-amplitude combination, within the power limit of the welder. The Rinco Dynamic ultrasonic welder machine will be used, with a maximum power output of 3000 W, available at the DASML of TU Delft. For the welding, 25.4 x 101.6 mm^2 samples were used, with a 12.7 mm overlap, according to the dimensions of the jig used to clamp the samples in the welder, in accordance with standard ASTM D1002. The energy directors were attached to the lower substrate using adhesive tape, not in contact with the welding area. A 40 mm-diameter circular sonotrode was used.

Optimum Parameters Determination

The process for the determination of the parameters for each material is the following:

- First, CF/TP to CF/TP are welded, using the same material of the energy director as the matrix. Cytec CF/PEKK samples, and the CF/PEEK, CF/PPS and energy directors previously manufactured were used in this section. The selected travel at this stage is 100%, that is 0.25 mm (the thickness of the energy director). Various combinations of force and amplitude are selected. Then, the Power, Travel vs. Time curves are used to check the optimum travel for the selected material and each force-amplitude combination. As explained in Chapter 1, the optimum travel is the one corresponding to end of power plateau (Stage IV) of the power curve; Figure 28 shows an example of a typical Power, Travel vs. Time curve obtained for 100% travel, using a flat ED, and the point of optimum travel for the force-amplitude combination. It coincides with a change in slope of the travel curve, that is, the displacement of the sonotrode. Figure 29 shows an example of the welding configuration for CF/TP to CF/TP weldings, using PPS:

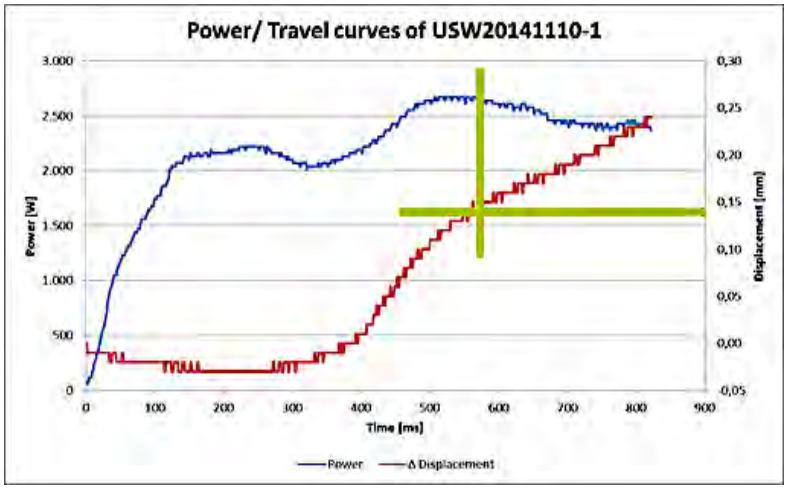

Figure 28: Example of a Power, Travel vs. Time curves for ultrasonic welding. Vertical green line represents the end of power plateau (end on Stage IV), and horizontal green line relates this value to the optimum travel of the sonotrode, which matches a change in slope in the travel curve.

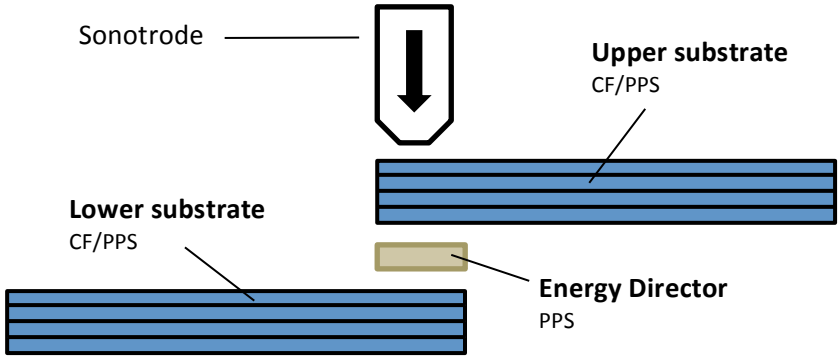

Figure 29: Sketch of the welding configuration for CF/PPS to CF/PPS ultrasonic welding.

- Once the optimum conditions for each TP material were chosen, degradation on the epoxy with those conditions must be studied. For this, PEKK was chosen, as it is the material among the four used ones that leads to higher welding times (the main driver of epoxy degradation). A substrate of CF/PEKK (Ten Cate) and another one of CF/Epoxy, both of 25.4 x 101.6 mm^2, were welded using a PEKK energy director of 0.25 mm thickness. The assembly could be broken simply with the hands, since no special treatment was given to the CF/Epoxy substrate, and the degradation on the epoxy could be determined by visual inspection, checking if the fibres of the top layer of the epoxy were exposed and burnt, and FTIR (Fourier Transform Infrared Spectroscopy) analysis, results that will be presented in Chapter 8.

After trying the previous combinations of force and amplitude, two of them were selected for deeper study, because they were the ones that produced no or less epoxy degradation without compromising the available power of the welder:

A) 1500 N (500 N/s rise force), A9 amplitude (86.2 µm).
B) 2000 N (1000 N/s rise force), A6 amplitude (73.4 µm).

It is worth to mention that both sets of parameters led to approximately the same optimum travel for the thermoplastic materials used in this thesis. As PEKK and PEEK have similar characteristics and welding behaviour, 'A' conditions were selected for both of them. For PPS, 'B'

conditions were chosen, because its welding time is shorter (300-400 s), and the fracture surfaces of the CF/PPS to CF/PPS weldings for these conditions with the optimum travel, had a better appearance. Then the optimum parameters for each material are presented in Table 3:

Thermoplastic material	Optimum welding parameters		
	Force (N)	Amplitude	Travel (mm)
PEKK	2000	A6 (73.4 µm)	0.17
PEEK	2000	A6 (73.4 µm)	0.15
PPS	1500	A9 (86.2 µm)	0.25

Table 3: Optimum welding parameters for the welds using PEKK, PEEK and PPS substrates and energy directors.

2.4. ANALYSIS TECHNIQUES

The principal methods to assess weld quality and characteristics used in this thesis will be now explained.

2.4.1 Mechanical Testing: Single-Lap Shear Tests

A way to measure the weld quality by mechanical testing, specifically with the Single-Lap Shear Test, where the maximum force, maximum shear stress and failure mode are obtained after applying a tensile load to the specimen. The welds and test were performed in accordance with the ASTM D1002 standard, with 25.4 x 101.6 mm^2 samples and an overlap area of 12.7 x 25.4 mm^2. Figure 30 shows a scheme of this test configuration:

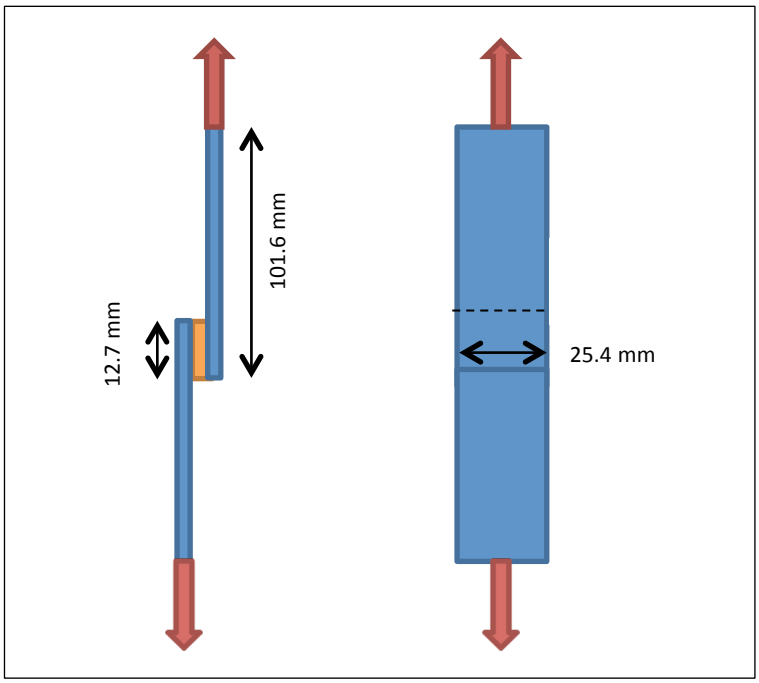

Figure 30: Lap Shear Test scheme for ASTM D1002 standard. Red arrows indicate the direction of the tensile load.

In order to carry out this process, a tensile testing machine, software/electronic to operate it and obtain the results, and grips to hold the piece and perform the test are needed. Tensile load is

applied at the grips that hold the piece; as results, the maximum force, maximum shear stress –the division of the maximum force by the shear or overlap area – and strain are reported [42].

The machine used was the Zwick 250 kN, available at the DASML of TU Delft, and hydraulic grips were used to clamp the specimens, which were offset to minimize the bending of the sample. A grip to grip separation of 60 mm was chosen.

2.4.2 Optical microscopy

Another way to characterize the welding interface is by optical microscopy. To do so, the welds were cut using a diamond blade cutter, embedded in resin – two types where used, transparent and green – and polished with the Rotopol-2 (Struers) machine, all of the equipment available at the DASML of TU Delft. For the polishing, there were two parts: The 'sanding', where water was used as lubricant, and the 'fine-polishing', where ethanol was used for lubricating the sample; different sand papers and cloths were used, from larger to smaller grain size. The samples were cleaned with ethanol and compressed air between the steps of each part. Figure 31 shows the polishing Rotopol machine (left) and two samples using the two different resins (right)

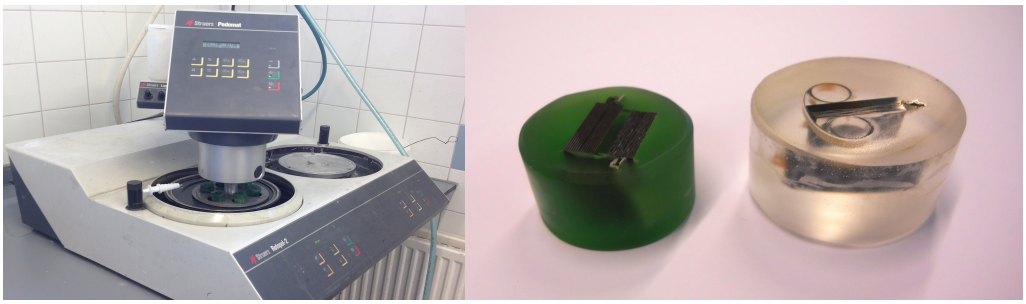

Figure 31: Rotopol-2 (Struers) polishing machine (left) and two polished samples using the two different resins (right).

Figure 32 shows the part of the cross-section that could be seen in the embedded samples (the sample shown is just an example), so that one of the edges of the embedded sample corresponds to the centre of the cross section of the weld, and the other one, to the edge of the cross-section:

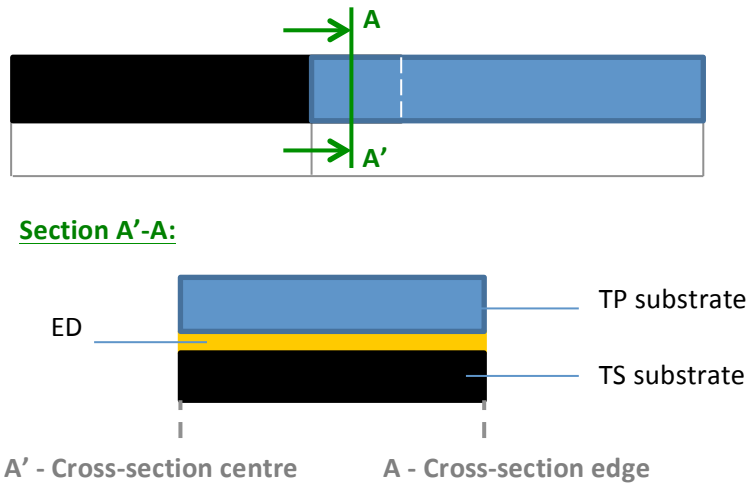

Figure 32: Scheme of the welds cutting pattern and cross-section area embedded in resin for optical microscope observation.

2.4.3 FTIR analysis

FTIR (Fourier Transform Infrared Spectroscopy) test consists in the analysis of a flat surface by collecting its infrared spectrum of absorption or transmittance (in this thesis, absorption results will be presented), that is, the ability of the material to absorb or transmit light at each wavelength, measuring the vibrations of the chemical bonds in the materials, based on the infrared radiation absorption. The spectrometer device measures the wavelengths and the intensity of the absorption. The wavelengths are characteristic of the chemical groups present in the material, and the intensity of absorption denotes the concentration of this chemical groups. A spectrum is created using a Fourier Transform.

This technique will be used to check if the thermoset has degraded, measuring the fracture surfaces of the welded samples after mechanical testing has been performed: It measures, in a non-destructive way, the vibrations of the chemical bonds in the materials, based on the infrared radiation absorption. The spectra of the non-welded and welded epoxy samples, which fracture surface reveals a flat epoxy resin surface, will be compared in order to check if degradation has occurred.

To do so, a Spectrum 100 Spectrometer (Perkin Elmer), available at the DASML of TU Delft, will be used. It takes effectively reliable data from 550 to 4500 cm^{-1} wavelengths.

EXPERIMENTS AND RESULTS

Part I: Standard Hybrid Welding

This first part of the thesis will focus on the 'Standard Hybrid Welding' (SHW) welds, where thermoplastic composite substrates were ultrasonic welded to thermoset ones, which were co-cured with a thermoplastic film. This co-cured thermoplastic film will strengthen the joint and shield the thermoset from degradation during the welding process, as demonstrated in P. Vizcaíno's investigation [4]. The matrix of the reinforced thermoplastic substrate, the energy director, and the co-cured thermoset film, will use the same thermoplastic material. The thermoplastics that will be used in this part will be PEEK, PEKK and PPS, which do not form SIPN with the epoxy, but micro-interlocking is attained between their molecules by the improvement of adhesion. Figure 33 shows a sketch of the welding configuration for this part of the thesis:

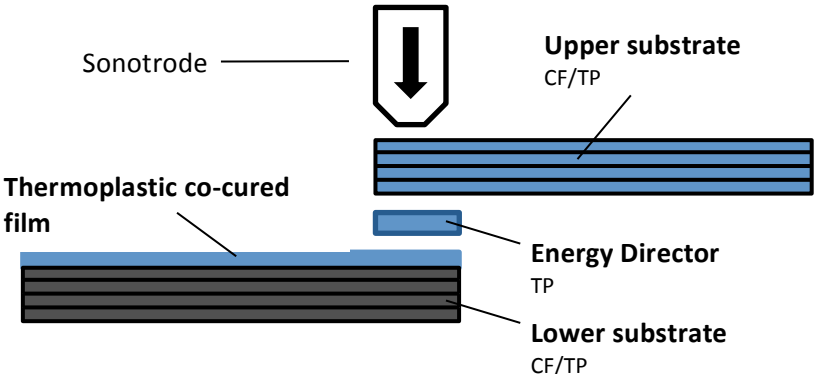

Figure 33: Sketch of the welding configuration for 'Standard Hybrid Welding' welds.

Thermoplastic films were treated and co-cured to a thermoset prepreg in the autoclave. Then, the cured samples were ultrasonically welded to a thermoplastic composite. The quality of the weld and the degradation of the thermoset will be studied using different techniques.

The treatments to the thermoplastic films and the co-curing in the autoclave were performed with the collaboration of M. Motovilin. One of them will be the exposure of the films to UV-O_3: It was proven that this technique improved the LSS value in direct welding of thermoset to thermoplastic composites [28], where the thermoset substrate was not co-cured with a thermoplastic film, so this adhesion improvement will be tried for the case of hybrid or indirect welding.

Chapter 3

Standard Hybrid Welding – PEKK

This chapter will explain the CF/Epoxy to CF/PEKK hybrid welds.

3.1. PROCEDURE

Table 4 summarizes the welds performed with the samples and energy directors explained in Chapter 2.

Sample reference	Bottom substrate	Top substrate	Thermoplastic coating	Observations
REF-PEKK	CF/PEKK (Ten Cate)	CF/PEKK (Ten Cate)	-	Reference welds. Six welds performed: -5 samples for mechanical (LSS) testing. -1 sample for optical microscopy (OM).
SHW-PEKK-1	CF/Epoxy (Hexcel 8552)	CF/PEKK (Cytec)	PEKK NT	Two welds performed, one for LSS testing and another one for OM.
SHW-PEKK-2	CF/Epoxy (Hexcel 8552)	CF/PEKK (Cytec)	PEKK UV-O_3	Two welds performed, one for LSS testing and another one for OM.
SHW-PEKK-3	CF/Epoxy (Hexcel 8552)	CF/PEKK (Cytec)	PEKK chloroform + amine (1st formula)	Two welds performed, one for LSS testing and another one for OM.
SHW-PEKK-4	CF/Epoxy (Cytec)	CF/PEKK (Ten Cate)	PEKK chloroform + amine (2nd formula)	Two welds performed, one for LSS testing and another one for OM. The energy director slipped in both welds, a possible reason being the high stiffness of the epoxy substrate.

Table 4: PEKK reference and hybrid welds.

The aim of the reference welds is to have a reference value for the LSS and the ED-TPC interface of the hybrid welds.

In Table 5, the welding conditions and welder outputs for each welding combination are collected:

Sample reference	Welding parameters			Average welding time (ms)	Average consumed power (%)	Average welding distance (mm)
	Force (N)	Amplitude	Travel (mm)			
REF-PEKK [a]	1500	A9 (86.2 µm)	0.17	515	110	0.25

SHW-PEKK-1	2000	A6 (73.4 µm)	0.17	517	93	0.24
SHW-PEKK-2				524	90	0.25
SHW-PEKK-3				482	91	0.25
SHW-PEKK-4 [b]				360	62	0.20

Table 5: Welding conditions and outputs for PEKK welds.

[a] PEKK reference welds used these set of parameters, because the welder seemed to have some difficulties when the 2000N force was commanded, so in order to overload it with numerous welds using these parameters. Moreover, they produced no significant difference in the cross-section and LSS values with respect to the other parameters.

[b] The energy director moved in the two welds of this welding type.

3.2. MECHANICAL TESTING

The results for the single-lap shear tests performed on the reference and the PEKK hybrid welds are presented in the chart of Figure 34.

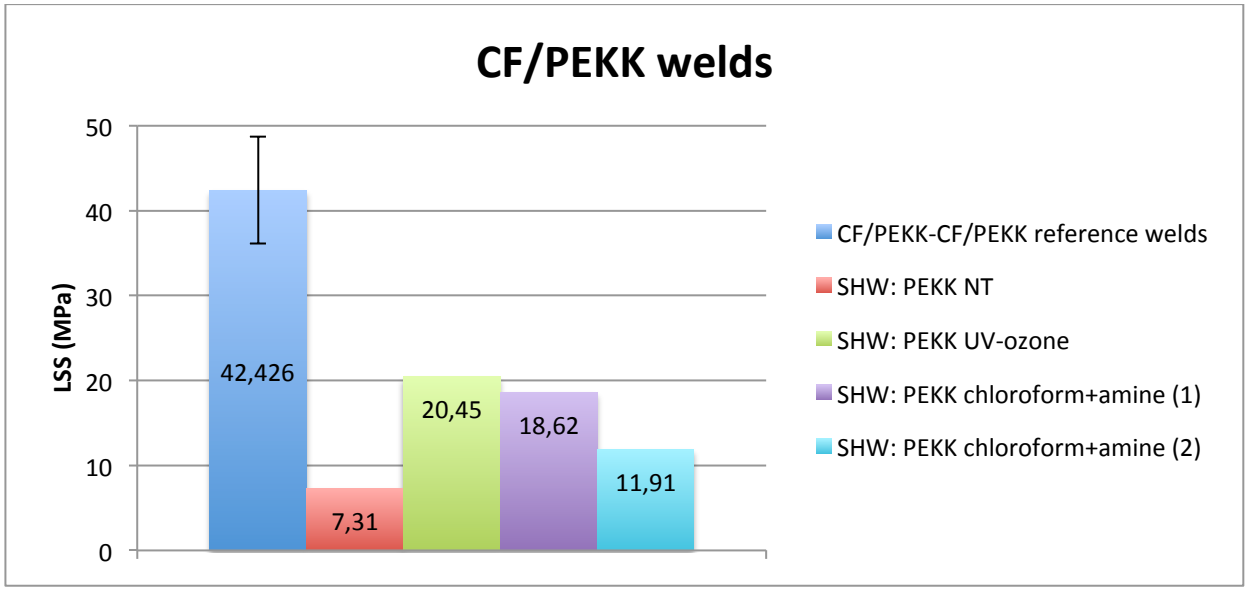

Figure 34: LSS values for PEKK welds. The vertical black line in the reference welds bar indicates the scatter of the results.

Five samples were tested for the reference welds, with a medium LSS value of 42.43 MPa and a standard deviation of 6.30. For PEKK hybrid welds, one sample per treatment was tested.

From the results presented, it could be appreciated that treating chemically the PEKK co-cured film prior to welding, greatly improved the mechanical behaviour of the weld, specially for UV-O_3 and chloroform + amine (1st formula) treatments. Nevertheless, these lap-shear results were found to be lower than expected. According to ultrasonic hybrid welds performed with CF/PEEK and using another epoxy (Hexply 913), with a co-cured layer of PEEK treated with UV-O_3 for 5 minutes, performed by Pablo Vizcaino, strengths up to 30 MPa can be achieved in this type of hybrid joints [28]. Observation of the fracture surface and cross-section of the samples will bring more light to the reason of this drop in the lap-shear strength.

Hereinafter, the reference CF/PEKK-CF/PEKK weld and each PEKK treatment results and characteristics, from higher LSS obtained to lower, will be analysed separately. Cross-section and

fracture surface studies will be mainly performed. An FTIR test could be carried out in PEKK NT weld, where flat epoxy fracture surfaces were found and reliable measurements were obtained.

3.3. CF/PEKK-CF/PEKK REFERENCE WELD

3.3.1 Cross section analysis

Figure 35 shows the cross-section of the CF/PEKK-CF/PEKK reference weld, with arrows pointing to the interface location.

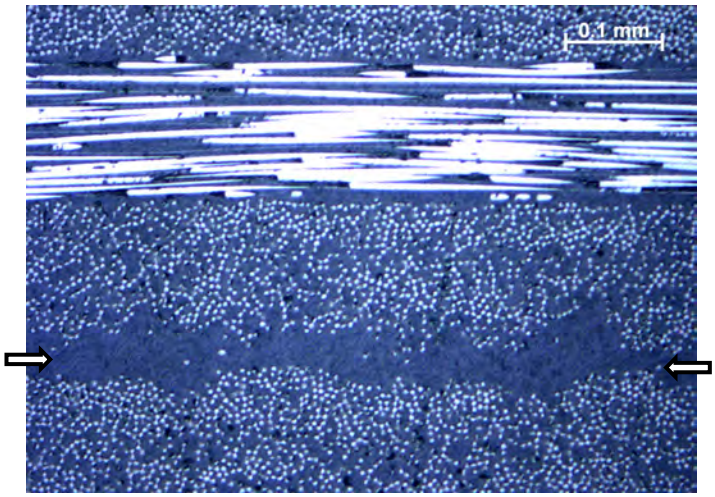

Figure 35: Zeiss optical microscope picture (x20 magnification) of CF/PEKK-CF/PEKK reference weld cross-section. Arrows point to the location of the interface.

The cross-section shows to be uniform, with no notable defects and good merging of the energy director and PEKK matrix. Carbon fibre diffusion from he substrates towards the thermoplastic-rich interface can be appreciated.

3.3.2. Fractography

Figure 36 shows the fracture surface, after mechanical testing was performed, of the PEKK reference weld. Slight fibre distortion at the edges of the weld is observed. Failure occurs at the interface and at the inner layers of both substrates.

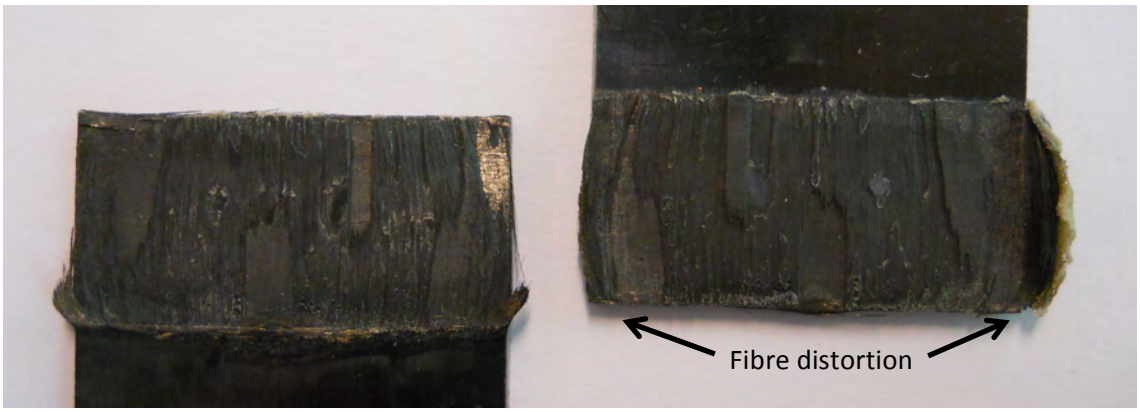

Figure 36: CF/PEKK-CF/PEKK reference weld fracture surface. Slight fibre distortion on the edges could be observed.

3.4. SHW: PEKK UV-O_3

3.4.1. Cross section analysis

Figure 37 shows an optical microscope picture that shows the cross-section of the CF/Epoxy co-cured with PEKK UV-O_3 substrate. It can be appreciated that there is excellent adhesion between the thermoset and the thermoplastic (micro-interlocking). Apart from the good adhesion observed between them, physical of macro-interlocking occurs, with carbon fibres from the epoxy diffusing into the PEKK film, and merging and keying of the two resins at their interface.

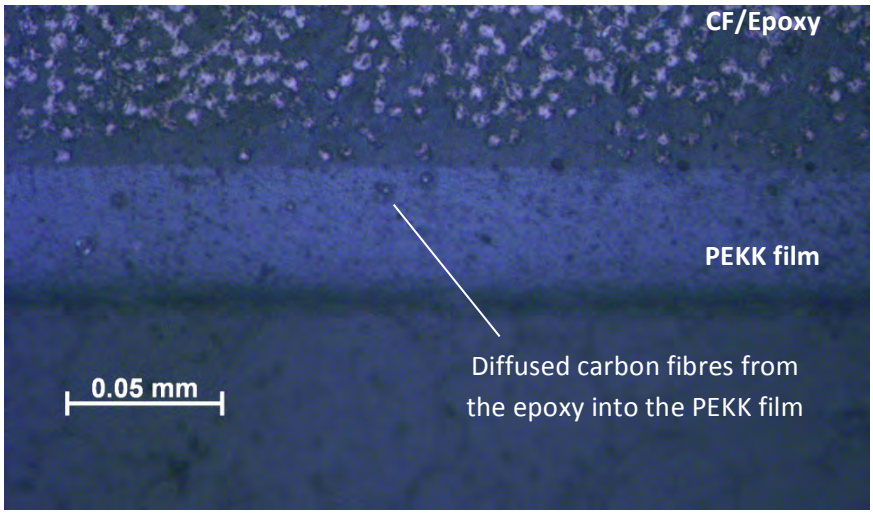

Figure 37: Zeiss optical microscope picture (x50 magnification) of the CF/Epoxy and co-cured UV-treated PEKK film substrate. Really well adhesion, with macro and micro-interlocking between both materials can be appreciated.

Figure 38 shows two optical microscope pictures of the cross section of the ultrasonic weld. It revealed to be uniform, with an excellent merging of the PEKK resins and adhesion between the thermoset and the thermoplastic.

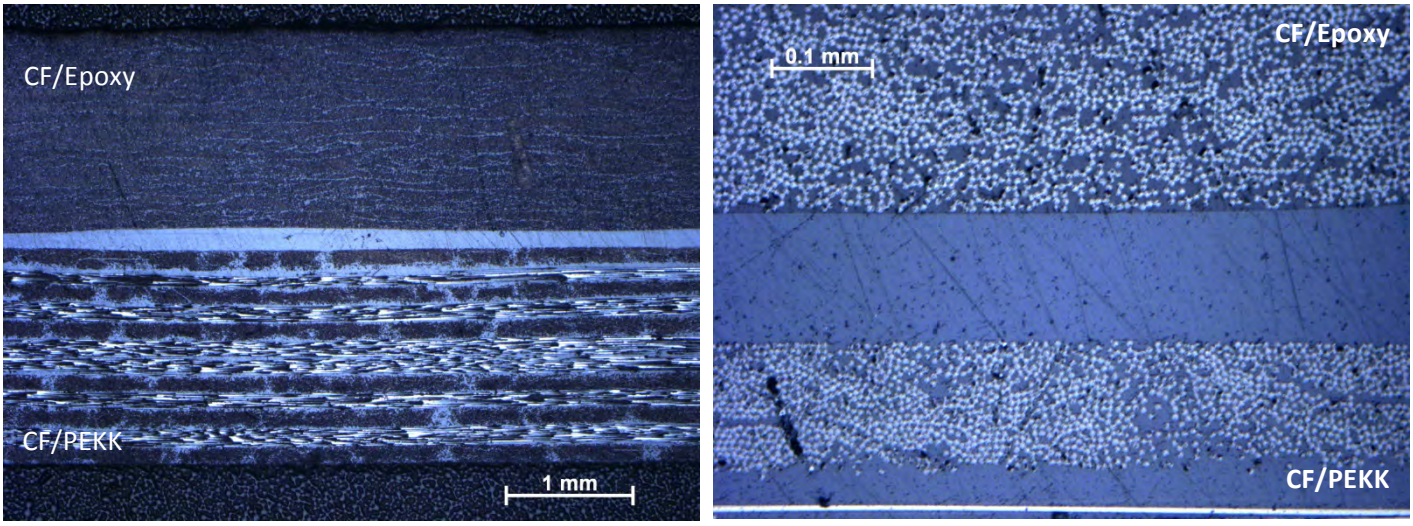

Figure 38: Zeiss optical microscope pictures (left: x2.5 magnification, right: x20 magnification) of the CF/Epoxy co-cured with UV-treated PEKK film and CF/PEKK weld, using a PEKK ED. A uniform interface can be appreciated, with no remarkable defects, a good merging of the PEKK resins and an excellent adhesion with the thermoplastic.

3.4.2. Fractography

Figure 39 shows the fracture surface of the studied weld, after performing the LSS test. This fracture reveals mainly what is believed to be failure in the internal layers of the epoxy, leaving plenty of carbon fibres from this substrate attached to the CF/PEKK one, and exposing dry carbon epoxy fibres, with burnt epoxy resin on the corners of the edge of the weld. Some small zones with PEKK and epoxy resin can be spotted on the CF/Epoxy surface too. On the CF/PEKK substrate, PEKK that outflowed from the interface appears to be burnt. It can be concluded from this fracture surface is that good adhesion between the PEKK film and the epoxy occurred. Also, the PEKK-rich spots on the CF/PEKK substrate, mainly composed of energy director resin, are seen. These thermoplastic-rich spots are due the travel value selected, which is the optimum; by not selecting 100% travel, not of the thermoplastic is squeezed out of the interface, and there are some areas where it tends to concentrate, as it can be seen in this fracture surface and in all of the rest ones that will be studied, where thermoplastic-rich areas, of higher or lower extent depending on the weld, can be seen on the reinforced thermoplastic substrate. They will appear in virtually all the welds performed in this thesis.

Some bubbles were spotted on the edge of the edge of the CF/Epoxy fracture surface, which coincide with burnt PEKK resin that outflowed from the welding interface and remained attached to the CF/PEKK substrate. These bubbles are normal to be seen in the cross section of most welds, on the edges, where the high-temperature thermoplastic outflows from the interface and is in contact with the air.

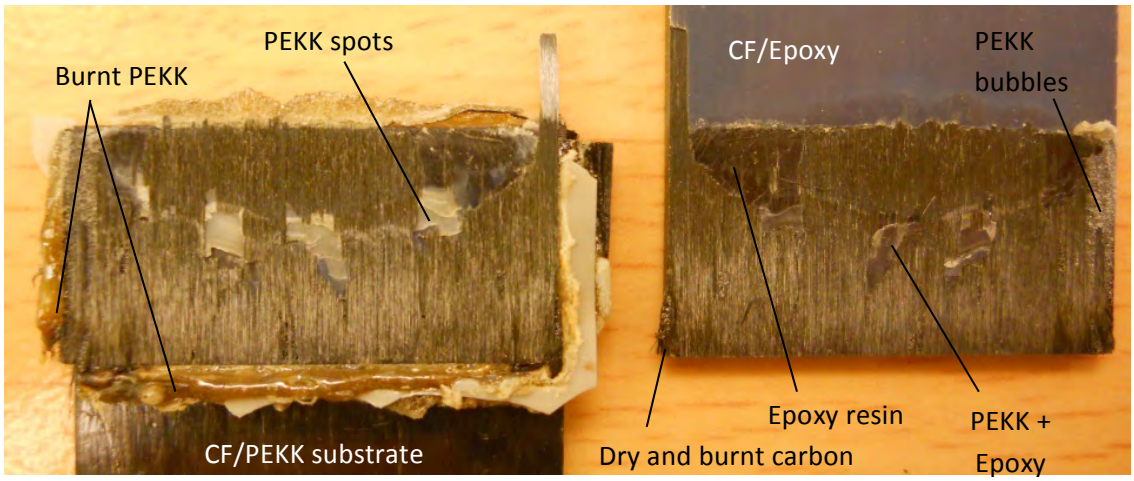

Figure 39: Fracture surface after LSS test of CF/Epoxy co-cured with a PEKK film treated with acetic acid and UV-light, and ultrasonically welded to CF/PEKK using a PEKK ED. Dry carbon fibres, burnt on the corners of the weld, and some spots with epoxy resin and PEKK can be seen of the CF/Epoxy-substrate fracture surface; on the CF/PEKK one, stuck carbon fibres from the epoxy substrate and burnt PEKK resin that outflowed out of the interface can be appreciated, apart from some spots of concentrated PEKK.

The lap shear strength of this sample was high (20.45 MPa), but not as much as expected (around 30 MPa). The "low" LSS value, combined with the odd dry-exposed epoxy fibres of the fracture surface, gave the idea that something was not right with the epoxy.

3.4.3. Interlaminar properties of Hexply 8552

The fracture surface revealed that failure was occurring mainly in the internal layers of the epoxy, what is believed to be interlaminar failure of the epoxy. This fact gives the idea that the strength of the weld, and the union of the epoxy to the co-cured PEKK film, is higher than the one of the epoxy material used, and that the LSS values obtained in the mechanical testing are actually characteristic of the epoxy. A deeper study of this type of failure and what is causing it will be performed in Chapter 6. Figure 40 shows a sketch of the fracture location at the welding interface.

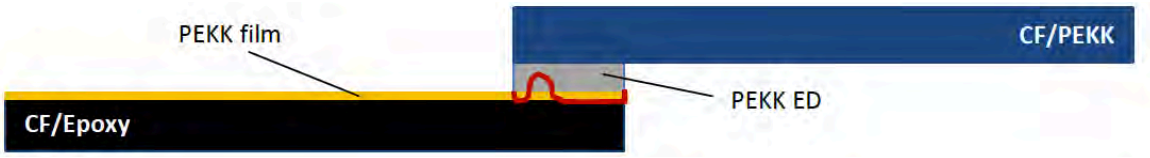

Figure 40: Sketch of the fracture location (red line) in the studied weld. Most of the failure occurs in the epoxy.

3.4.4. FTIR analysis

An FTIR analysis was tried on the small exposed epoxy resin surface of the CF/Epoxy substrate, but the results obtained were not reliable, probably due to a rough surface.

3.5. SHW: PEKK CHLOROFORM + AMINE (1ST FORMULA)

3.5.1. Cross section analysis

Figure 41 shows the optical microscope picture of the cross section of CF/Epoxy co-cured with the treated PEKK substrate. Well adhesion and merging between the thermoset and the thermoplastic is confirmed, which lead to the relatively high LSS value obtained for this weld.

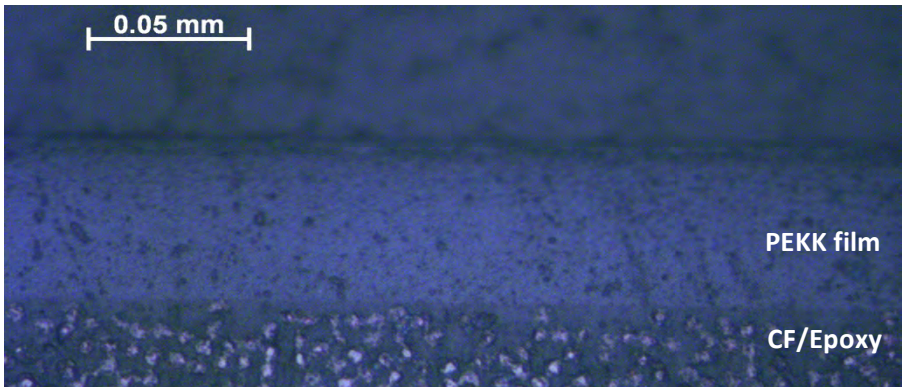

Figure 41: Zeiss optical microscope picture (x50 magnification) of the cross-section of CF/Epoxy co-cured with PEKK film (treated with chloroform and long chain amine, first formula) substrate, before welding. Good merging and adhesion between both materials can be appreciated.

Figure 42 shows two pictures of the cross section of the CF/Epoxy co-cured with PEKK treated film (with chloroform and amine, first formula). The welding interface appears to be uniform, although some cracks and holes appeared in the CF/Epoxy substrate close to the edge of the cross section, probably due to high pressure.

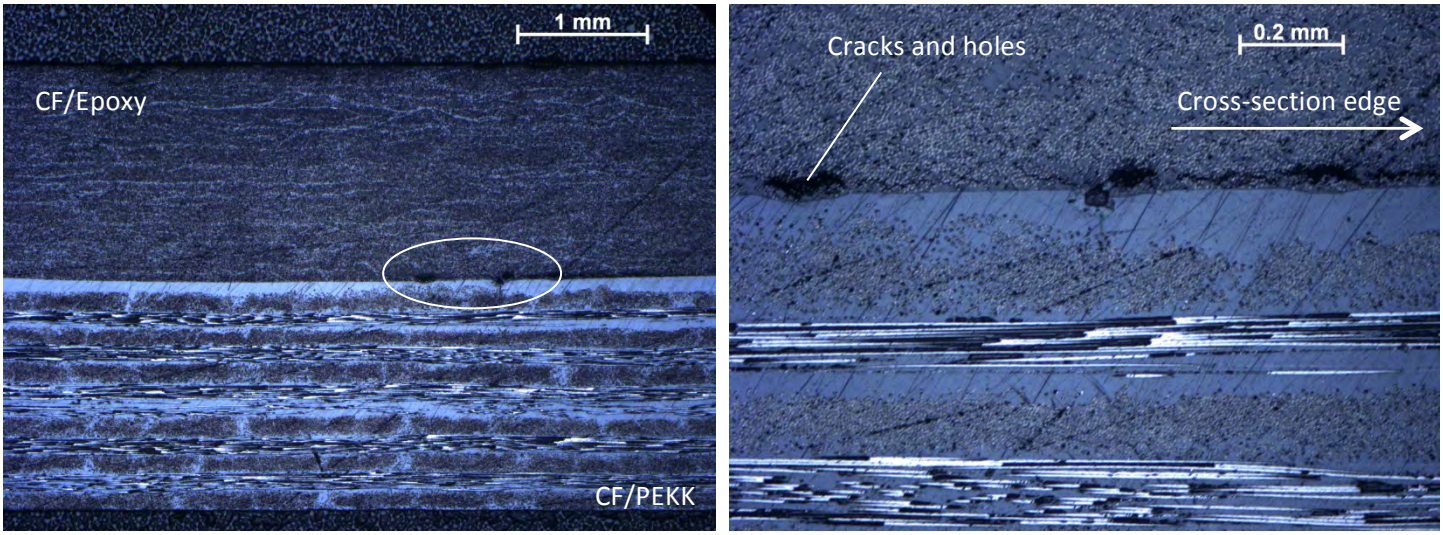

Figure 42: Zeiss optical microscope pictures (left: x2.5 magnificcation, right: x20 magnification) of the weld formed by CF/Epoxy co-cured with chloroform and amine-treated PEKK (first formula) and CF/PEKK substrates, using a PEKK ED. Cracks and holes appeared in the CF/Epoxy substrate near the welding interface near the edge of the cross-section. Image on the right represents a closer look of the area enclosed in the elipse of the picture on the left.

3.5.2. Fractography

The fracture surface of the studied weld (Figure 43) revealed also what seems to be interlaminar failure of the epoxy – because failure occurred in the internal layers of the epoxy – in the CF/Epoxy substrate part, although there are also some regions where epoxy resin or PEKK remained. One of the edge corners shows to have dry carbon fibres and burnt epoxy resin. On the CF/PEKK fracture surface, burnt PEKK resin that had outflowed from the welding interface and stuck carbon fibres from the epoxy substrate could be appreciated. Some PEKK bubbles are spotted on one of the sides of the epoxy fracture surface, coinciding with burnt PEKK resin that outflowed from the welding interface. PEKK-rich areas of the CF/Epoxy substrate are appreciated too.

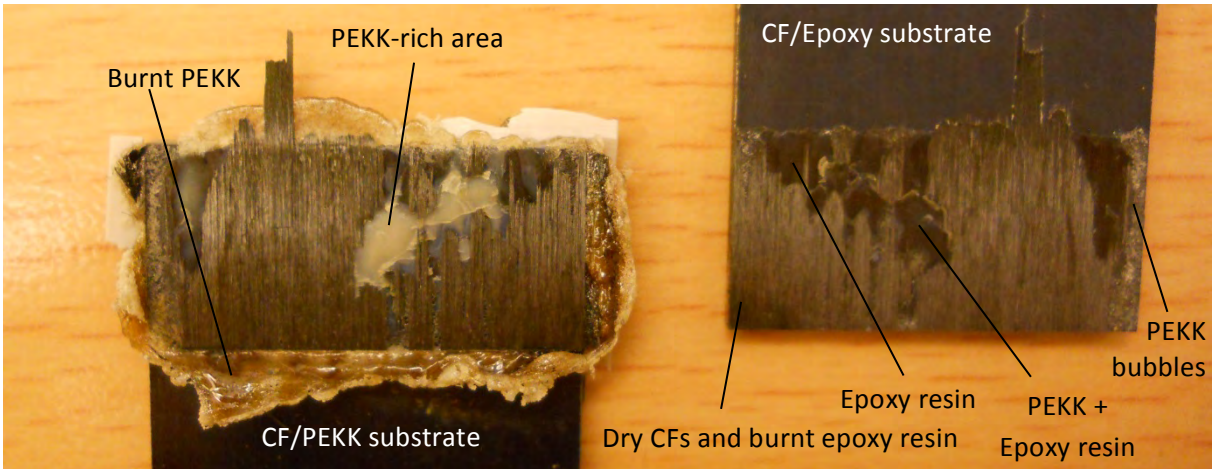

Figure 43: Fracture surface of the ultrasonic weld of CF/Epoxy, co-cured with a chloroform and amine-treated PEKK film (1st formula), and CF/PEKK substrates, using a PEKK ED, after the lap-shear test was performed. In the CF/PEKK fracture surface, burnt outflowed PEKK and a PEKK-rich area in the centre of the weld can be seen; in the CF/Epoxy one, interlaminar failure of the epoxy, with some areas where epoxy and PEKK could be spotted, occurred, and some PEKK bubbles, dry exposed carbon fibres and burnt epoxy resin on the edges can be appreciated.

The LSS value for this type of weld was relatively high (18.62 MPa) and shows that the treatment greatly improves the welding characteristics with respect to non-treated co-cured PEKK film, as shall be seen in section 3.7,but not as much as the UV-light treatment.

3.6. SHW: PEKK CHLOROFORM + AMINE (2ND FORMULA)

3.6.1. Cross section analysis

Figure 44 shows the cross section of the CF/Epoxy co-cured with the treated PEKK film substrate. The adhesion is greatly enhanced with this treatment with respect to non-treated PEKK (section 3.7), and both materials seem to merge perfectly. Nevertheless, when being welded to the corresponding CF/PEKK substrate, using a PEKK ED, as Figure 45 shows, the treatment turns out to be incompatible for the desired process: When applying temperature and pressure to the remaining chemical substances in the PEKK film, they burn and create voids along the whole interface of the effective weld, most likely inducing the epoxy to burn too. This burnt interface and the smaller welding area, due to the displacement of the energy director, are likely the reasons for the low LSS value obtained (11.91 MPa), with respect to the previous chloroform + amine formula and UV-treated films.

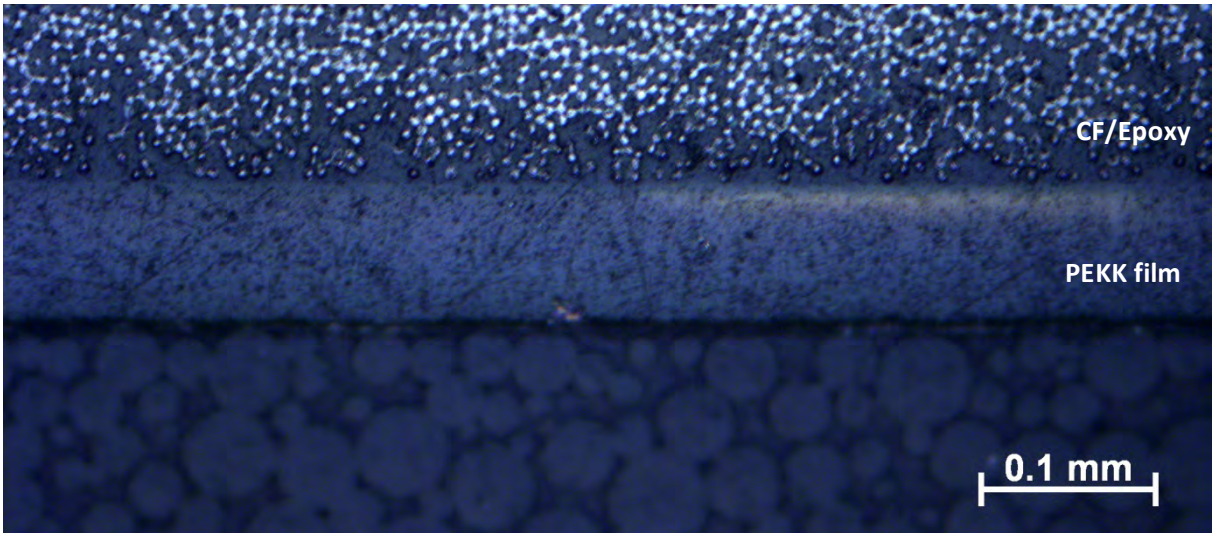

Figure 44: Zeiss optical microscope picture (x20 magnification) of the cross-section of the CF/Epoxy co-cured with treated PEKK film (with chloroform and long chain amine, second formula) substrate. The adhesion of both materials is excellent.

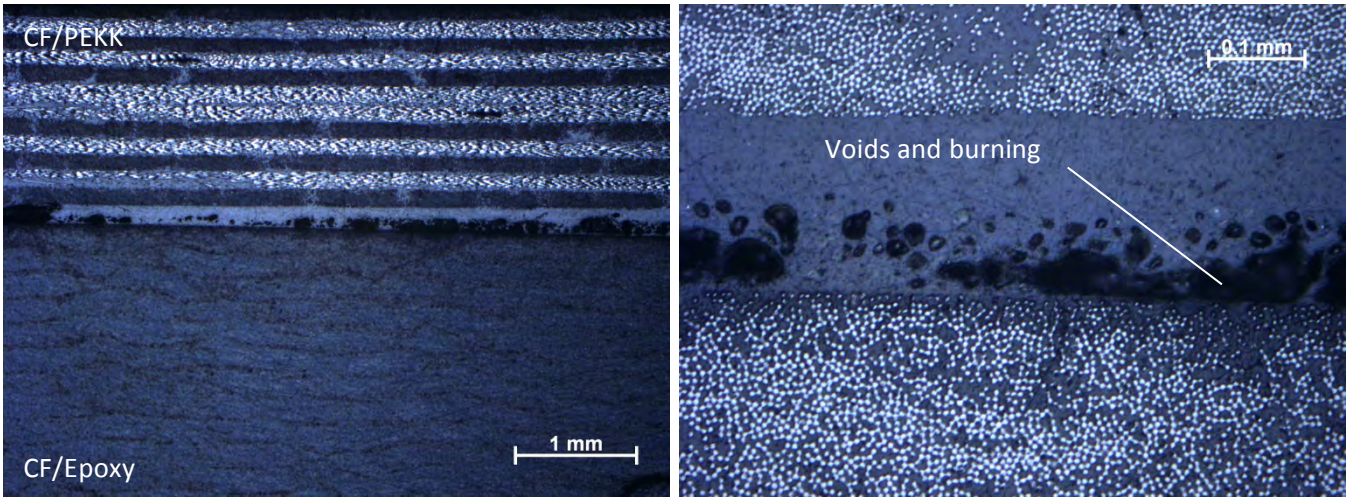

Figure 45: Zeiss microscope pictures (left: x2.5 magnification, right: x20 magnification) of the cross section of the weld formed by CF/Epoxy co-cured with chloroform and amine-treated PEKK (second formula) and CF/PEKK substrates, using a PEKK ED. Voids from burning of the chemical substances in the PEKK co-cured film appear accros the whole welding interface. Picture on the right is a closer look to the welding interface shown in the left image.

This weld is the perfect example for showing that, although some treatments greatly enhance the adhesion of the epoxy and the co-cured thermoplastic film, they are incompatible for the performance of ultrasonic welding, due to their response to the application of heat and pressure to join the materials. A good film treatment is the one that provides good adhesion and does not develop secondary effects when the samples are welded.

3.6.2. Fractography

Figure 46 shows the fracture surface of the studied weld. Mladen Motovilin donated three samples of this CF/Epoxy (Cytec) co-cured with treated PEKK (chloroform and long chain amine, 2nd formula). The ED was displaced during the welding process in the two welds performed for this treatment, even though it was correctly tapped to the CF/Epoxy substrate. Apart from this, it showed to not have completely melted. These behaviours may be due to the high stiffness of the PEKK co-cured film and the CF/Epoxy itself, due to the treatment that was applied to the PEKK film. Then, the effective welding area is less than 12.7 x 25.4 mm^2, a fact that influenced in the LSS obtained (11.91 MPa). In the area where the ED could melt (the only effective welding area), failure seems to occur mainly in the PEKK co-cured film (with some epoxy surface being exposed too), leaving a hole on the CF/Epoxy substrate and remaining attached and burnt to the CF/PEKK one after the LSS was performed. No failure occurring in the internal layers of this Cytec epoxy substrate was observed.

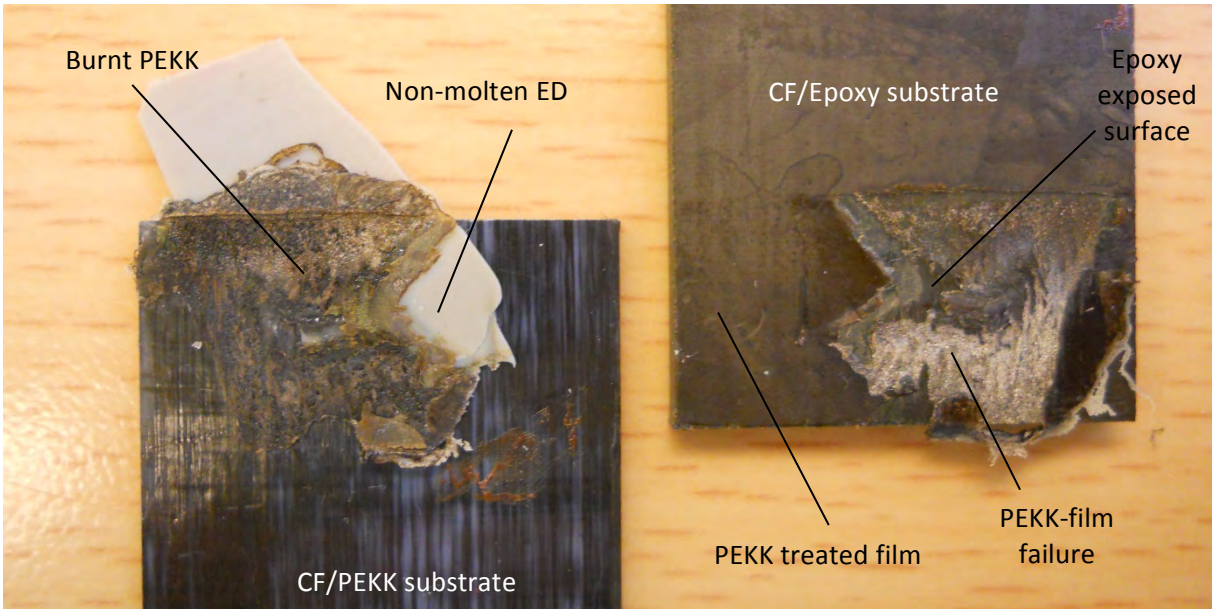

Figure 46: Fracture surface, after LSS test was performed, of the weld formed by CF/Epoxy, co-cured with a PEKK film treated with chloroform and long-chain amine (2nd formula), and CF/PEKK, ultrasonically welded using a PEKK ED. The ED was moved during the welding and it did not completely melt; burnt PEKK was found in the effective welding area.

3.7. SHW: PEKK NT

3.7.1. Cross section analysis

Figure 47 shows the cross section of the Hexcel 8552 CF/Epoxy substrate co-cured with the non-treated PEKK film before being welded. It shows apparent good adhesion between the thermoset and the thermoplastic film.

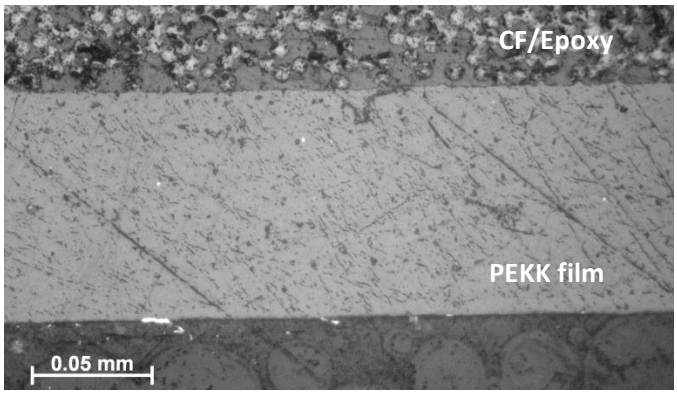

Figure 47: Zeiss optical microscope picture (x50 magnification) of the cross-section of the substrate formed by CF/Epoxy co-cured with a non-treated PEKK film before being welded.

Figure 48 shows the cross-section of the weld of the previously observed specimen to a CF/PEKK substrate, using a PEKK ED. A line dividing the matrix of the PEKK plus energy director merge, and the PEKK co-cured layer can be appreciated. Some remarkable defects are the cracks that appear in the CF/Epoxy substrate near the welding interface and a gap between the PEKK substrate, in the area where the PEKK matrix meets the PEKK energy director, appearing in some regions of the cross section. These defects, due to a high pressure at the interface that eventually cracks the epoxy

and breaks the not-well-adhered thermoplastic interface, are believed to be responsible for the extremely low shear strength obtained (7.31 MPa).

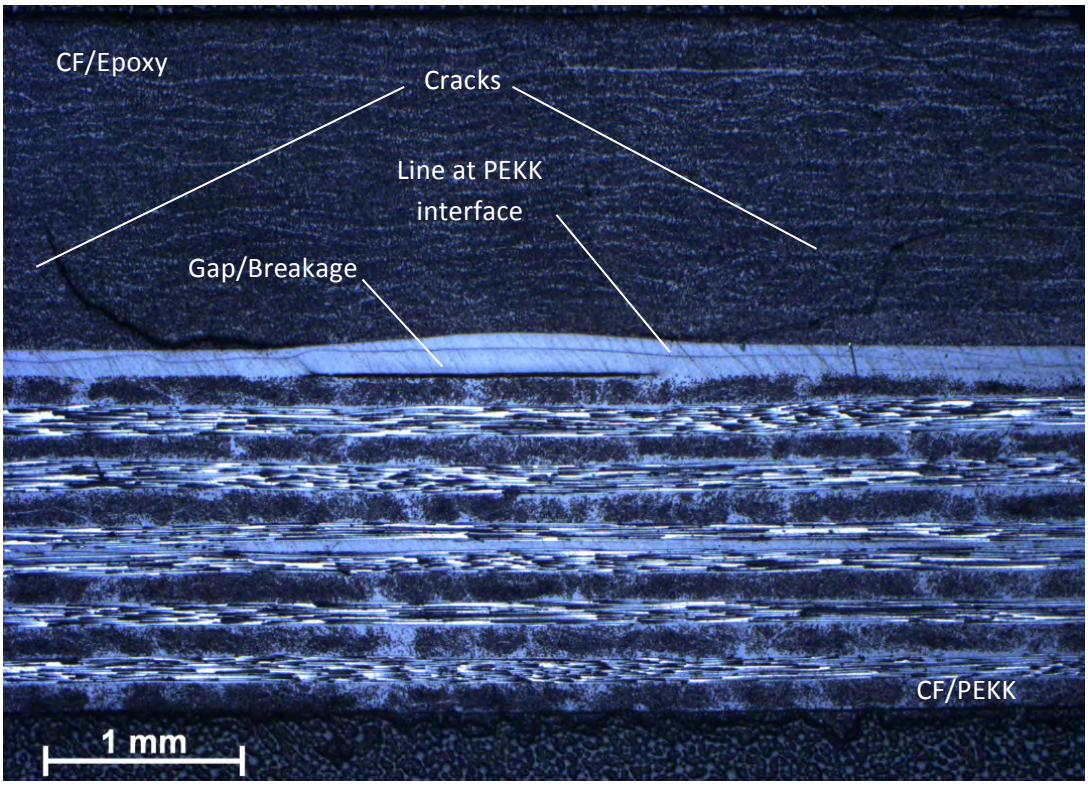

Figure 48: Zeiss optical microscope image (x2.5 magnification) of the cross section of the ultrasonic weld formed by CF/Epoxy co-cured with a non-treated PEKK film and CF/PEKK substrates, using a PEKK ED. Cracks on the CF/Epoxy substrate, the line between the PEKK film and the PEKK ED, and the gap/breakage in the CF/PEKK substrate can be appreciated.

3.7.2. Fractography

Figure 49 shows the fracture surface of this weld after the LSS test was performed. Some brown and burnt PEKK resin, mainly from the ED and film co-cured with the epoxy, can be seen to have been squeezed out of the overlap area and remained stuck to the CF/PEKK substrate. Moreover, PEKK-rich areas can be appreciated the centre of the welding area in the CF/PEKK substrate.

Some carbon fibres from the epoxy substrate remained fixed to the CF/PEKK substrate, showing failure in the epoxy, but this is not the main failure type in this weld: Main failure type occurred between the co-cured PEKK film and the epoxy, although a little top part of the epoxy matrix remained stuck to the CF/PEKK substrate. The fact that the fracture surface shows little epoxy resin stuck on the CF/PEKK substrate, and a mainly shiny surface on the CF/Epoxy part, indicates that the entanglement or adhesion between the thermoset and the thermoplastic co-cured film was not as good as the pre-welded cross-section of this substrate revealed.

Some bubbles of PEKK were found on the edges of the CF/Epoxy substrate, coinciding with the regions of burnt PEKK resin.

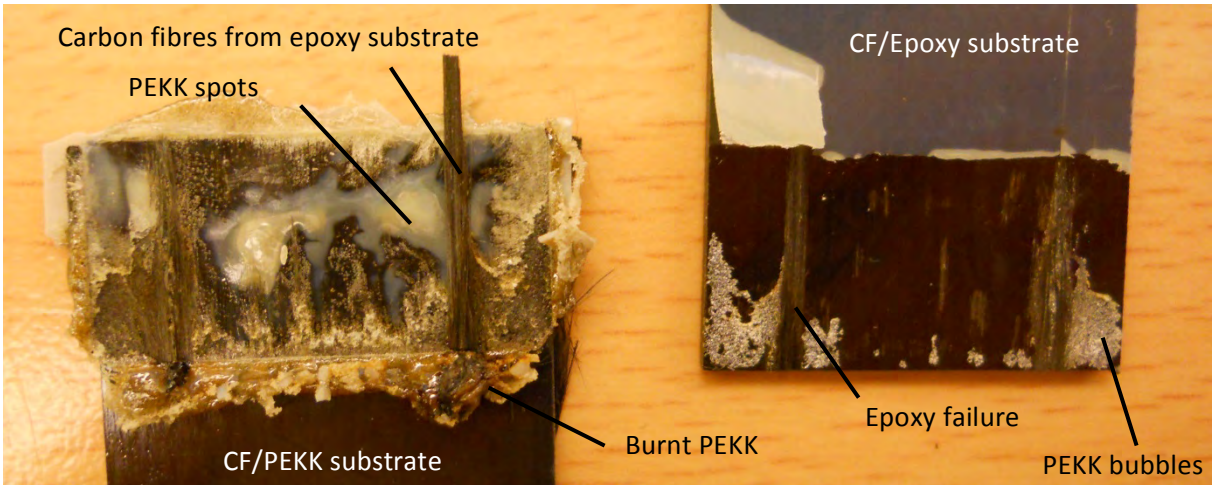

Figure 49: Fracture surface after LSS test of CF/Epoxy co-cured with a non-treated PEKK film and ultrasonically welded to CF/PEKK using a PEKK ED. The interlaminar failure and PEKK bubbles on the edge of the CF/Epoxy substrate, and burnt PEKK outflow, PEKK-rich area and stuck epoxy-reinforcement carbon fibres can be appreciated.

3.7.3. FTIR analysis

After mechanical testing, the CF/Epoxy of the weld that used PEKK NT film was analysed with FTIR testing in order to check for degradation of the epoxy. The flat epoxy resin rich fracture surface of the CF/Epoxy, after mechanical testing, made possible to perform this analysis. The aim is to check if degradation occurred and the effect of the PEKK film on the epoxy due to co-curing and welding. Figure 50 shows the spectra for a reference non-welded CF/Epoxy sample, CF/Epoxy after the weld and LSS test were performed, and PEKK film.

This shown range covers from 1550 to 3700 cm^{-1} wavelengths. It can be appreciated that "CF/Epoxy after welding" spectra is equal to the reference sample except for two peaks: One at 1650 cm^{-1} wavelength, which is an effect of the PEKK film that presents a high-intensity peak at that wavelength, and another small peak at 1727 cm^{-1} whose precedence may also come from the high-intensity PEKK peak at 1650 cm^{-1}; it may also be to slight degradation, because this hybrid welding time was on the order of 0.2 seconds higher than the time for direct welding of CF/PEKK and CF/Epoxy substrates, which results will be explained in Chapter 8. The spectra from 550 to 1550 cm^{-1} wavelengths were identical for the welded and non-welded CF/Epoxy samples. It is interesting that the only effects of PEKK film on the welded samples occur in the C=0 bond region of the epoxy.

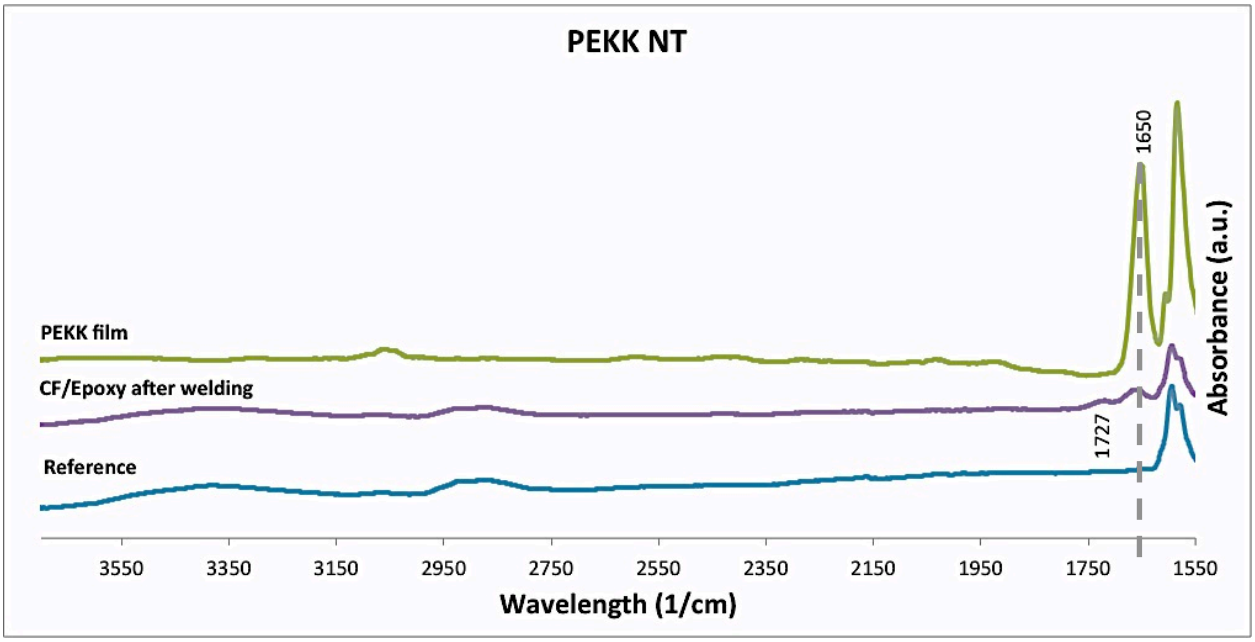

Figure 50: FTIR spectra for a CF/Epoxy reference weld, CF/Epoxy from PEKK NT weld after the welding was performed, and PEKK film. The term 'a.u.', in the absorbance y-axis title, stands for "arbitrary units".

3.8. COMPARATIVE EVALUATION

PEKK hybrid welds have been performed in this chapter. Treating the PEKK co-cured epoxy film has demonstrated to enhance the adhesion between the thermoplastic and thermoset materials with respect to the non-treated film, improving also the strength of the welds.

In the chemically treated films, main failure was found in the internal layers of the epoxy, exposing its dry carbon fibres. This is believed to be interlaminar failure, and a deeper study carried in Chapter 6 will bring more light to this issue.

The weld using non-treated PEKK co-cured film lead to a fracture surface that enabled the performance of an FTIR study, which revealed no apparent epoxy degradation and influence of the PEKK co-cured film.

Chapter 4

Standard Hybrid Welding – PEEK

This chapter will be devoted to the CF/Epoxy to CF/PEEK hybrid welds.

4.1. PROCEDURE

Table 6 summarizes the welds performed, using the samples and energy directors presented in Chapter 2.

Sample reference	Bottom substrate	Top substrate	Thermoplastic coating	Observations
REF-PEEK	CF/PEEK (Ten Cate)	CF/PEEK (Ten Cate)	-	Reference welds. Six welds performed: -5 samples for mechanical (LSS) testing. -1 sample for optical microscopy (OM).
SHW-PEEK-1	CF/Epoxy (Hexcel 8552)	CF/PEEK (Ten Cate)	PEEK UV-O_3	Two welds performed, one for LSS testing and another one for OM.
SHW-PEEK-2	CF/Epoxy (Hexcel 8552)	CF/PEEK (Ten Cate)	UD CF/PEEK layer [0/0]	Two welds performed, one for LSS testing and another one for OM.
SHW-PEEK-3	CF/Epoxy (Hexcel 8552)	CF/PEEK (Ten Cate)	UD CF/PEEK layer [0/0] + PEEK film	Two welds performed, one for LSS testing and another one for OM.
SHW-PEEK-4	CF/Epoxy (Hexcel 8552)	CF/PEEK (Ten Cate)	PEEK acetic acid + UV (5 minutes)	Two welds performed, one for LSS testing and another one for OM.

Table 6: PEEK reference and hybrid welds.

In Table 7, the welding conditions and welder outputs for each welding combination are collected:

Sample reference	Welding parameters			Average welding time (ms)	Average consumed power (%)	Average welding distance (mm)
	Force (N)	Amplitude	Travel (mm)			
REF-PEEK [a]	2000	A6 (73.4 µm)	0.15	500	79	0.23
SHW-PEEK-1				558	72	0.23
SHW-PEEK-2				686	75	0.23
SHW-PEEK-3				752	86	0.24
SHW-PEEK-4				568	79	0.23

Table 7: Welding conditions and outputs for PEEK welds.

4.2. MECHANICAL TESTING

The results for the single-lap shear tests performed on the reference and the PEKK hybrid welds are presented in the chart of Figure 51. SHW-PEEK-3 weld, which used UD CF/PEEK layer [0/0] + PEEK film as the co-cured epoxy layers, could be broken simply with the hands, so no lap-shear test could be performed.

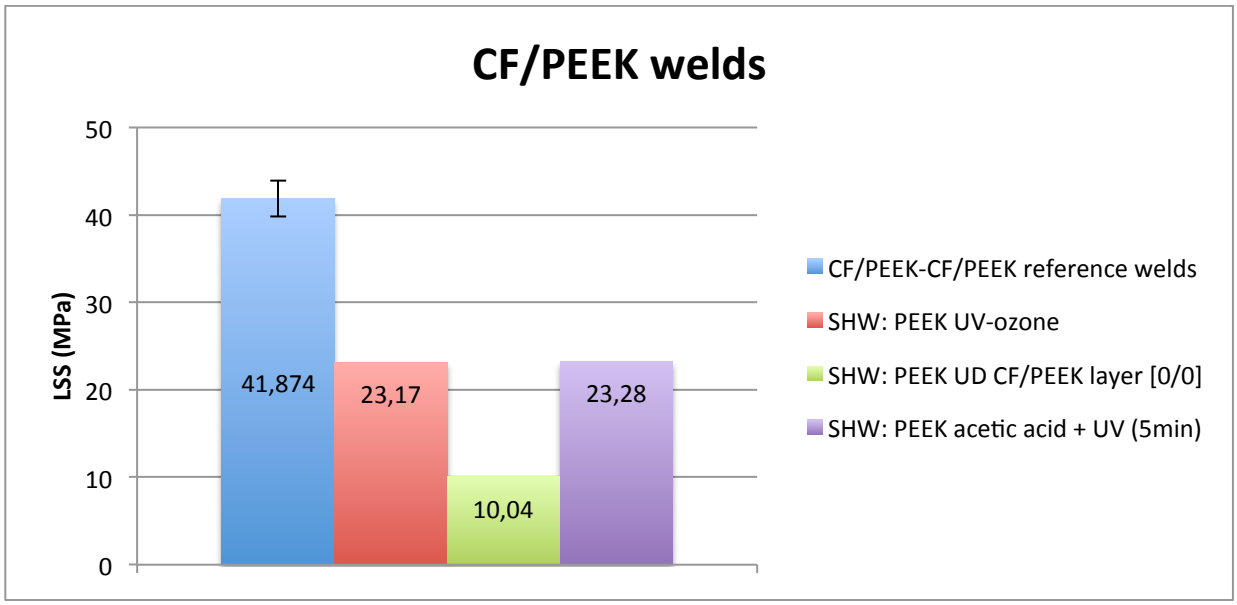

Figure 51: LSS values for PEEK welds.

Five samples were tested for the reference welds, with a medium LSS value of 41.87 MPa and a standard deviation of 2.07. For PEEK hybrid welds, one sample per treatment was tested.

These results also showed lower LSS results than the ones obtained by P. Vizcaíno in his investigation, as commented in Chapter 3 [28].

The reference CF/PEEK-CF/PEEK weld and each PEEK treatment results and characteristics, from higher LSS obtained to lower, will be analysed separately. As in Chapter 3, analyses of the cross-sections and fracture surfaces will be mainly performed.

4.3. CF/PEEK-CF/PEEK REFERENCE WELD

4.3.1. Cross section analysis

Figure 52 shows an optical microscope picture of PEEK reference weld interface. Good merging of the energy director and substrate matrices can be appreciated, as well as carbon fibres diffusion towards the thermoplastic-rich area of the interface.

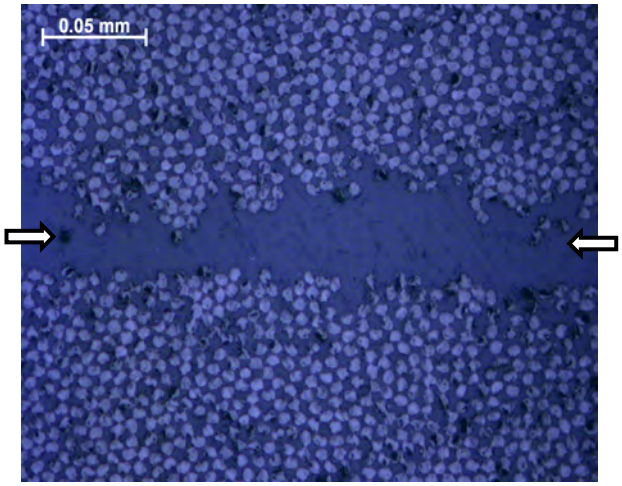

Figure 52: Zeiss optical microscope picture (x50 magnification) of CF/PEEK-CF/PEEK reference weld cross-section. Arrows point to the location of the interface.

4.3.2. Fractography

Figure 53 shows the fracture surface of the CF/PEEK-CF/PEEK reference weld. Cohesive failure occurred, with a thermoplastic rich interface and some exposed carbon fibres. Two PEEK-rich spots, mainly non-molten energy director, can be appreciated in both substrates. One of the weld edges was slightly burnt, showing also some fibre distortion.

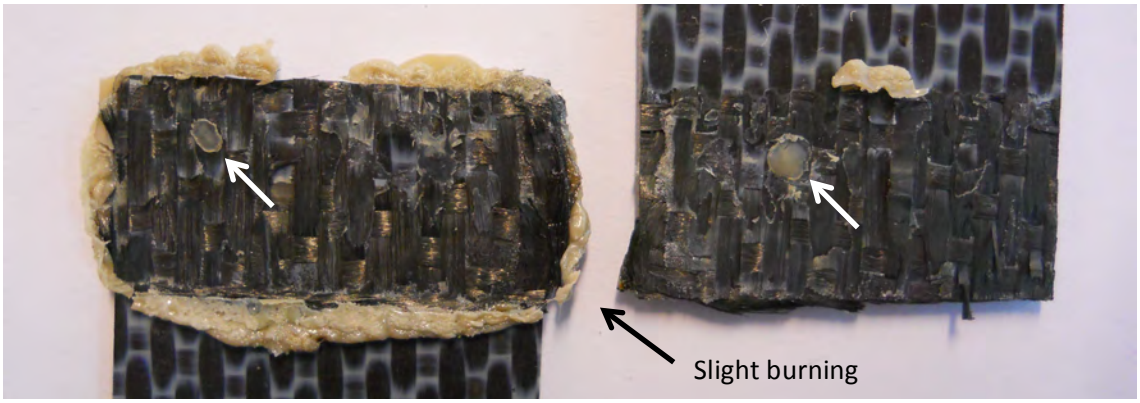

Figure 53: CF/PEEK-CF/PEEK reference weld fracture surface. White arrows point to PEEK-rich spots found in both substrates. In one of the edges of the slight burning and fibre distortion occurred.

4.4. SHW: PEEK ACETIC ACID + UV-O_3 (5 min)

4.4.1. Cross section analysis

Figure 54 shows the cross section of the studied weld: CF/Epoxy co-cured with PEEK film, treated with acetic acid and UV-light for 5 minutes, and welded to a CF/PEEK substrate using a PEEK energy director. Good adhesion of the thermoplastic and thermoset material is observed. When the ultrasonic weld with the CF/PEEK substrate was performed, the interface was uniform and good compatibility among the difference materials could be stated, as the cross section of Figure 55 shows. Some voids were observed on the bottom part of a group of carbon fibres in the PEEK substrate, close to the interface. Nevertheless, it is a punctual and not important defect, and no special attention should be taken to them. The lap shear of this weld was the highest achieved with

the used epoxy (23.28 MPa), showing that the applied treatment worked, improving the thermoset-thermoplastic interface and being suitable for the temperatures and pressures acquired during the welding process.

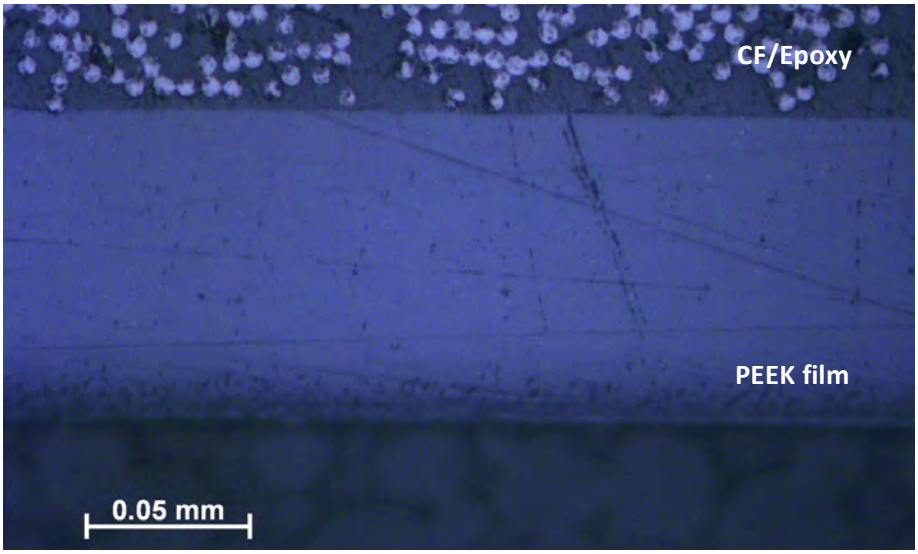

Figure 54: Zeiss optical microscope picture (x50 magnification) of the cross-section of the substrate formed by CF/Epoxy co-cured with PEEK film, treated with acetic acid and UV (5 minutes). Good adhesion of both materials is observed.

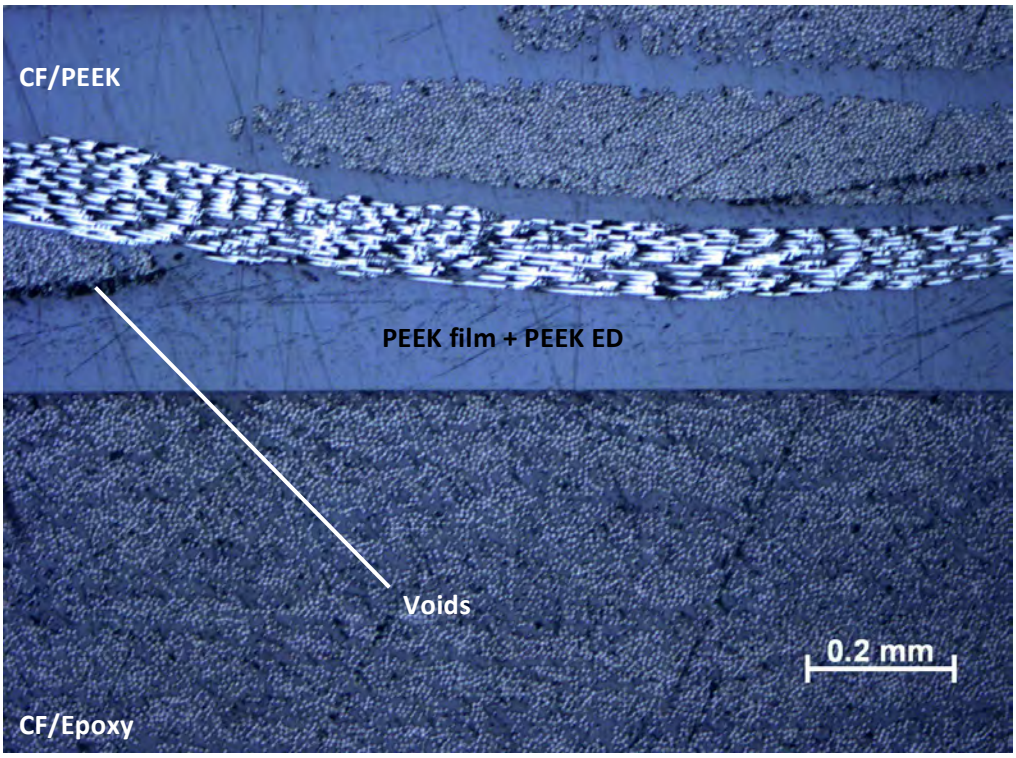

Figure 55: Zeiss optical microscope image (x10 magnification) of the weld composed by CF/Epoxy (co-cured with acetic acid/UV treated PEEK film) and CF/PEEK substrates, and a PEEK ED. Good compatibility among the different materials was observed. Some voids on the bottom part of a group of carbon fibres in the PEEK substrate where spotted.

4.4.2. Fractography

Figure 56 shows the fracture surface of the studied weld. In the picture, failure in the epoxy shows to be the main breakage type, exposing dry internal carbon fibres from the epoxy. Also, some areas with PEEK acetic/UV film and epoxy resin were found on the CF/Epoxy substrate, with a bubbly appearance. The two corners of the weld edge are greatly burnt, and so are the epoxy resin and PEEK resin in these areas; PEEK-rich spots are also seen.

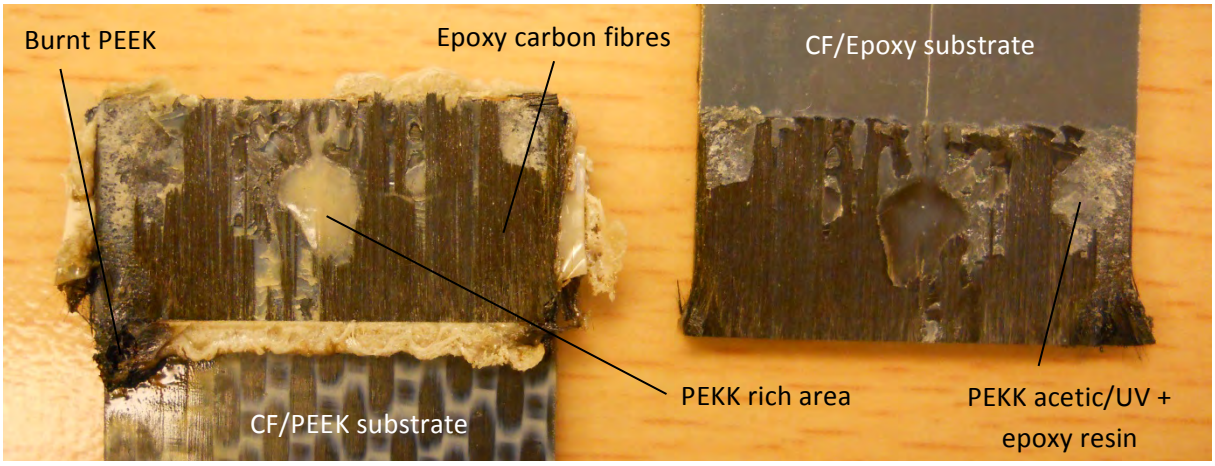

Figure 56: Fracture surface, after lap-shear test was performed, of the weld formed by CF/Epoxy, co-cured with PEEK film treated with acetic acid and UV-light for 5 minutes, and CF/PEEK substrates, using a PEEK ED. Burnt corners, PEEK rich areas and failure in the epoxy can be appreciated.

4.5. SHW: PEEK UV-O_3

4.5.1. Cross section analysis

Figure 57 shows the cross section of the CF/Epoxy substrate, which was co-cured with a UV-treated PEEK film. Both materials seem to have good adhesion, which was due to the applied UV treatment because, as it may be remembered, untreated PEEK was unable to remain stuck to the CF/Epoxy after being cut into 25.4 x 101.6 mm^2 samples.

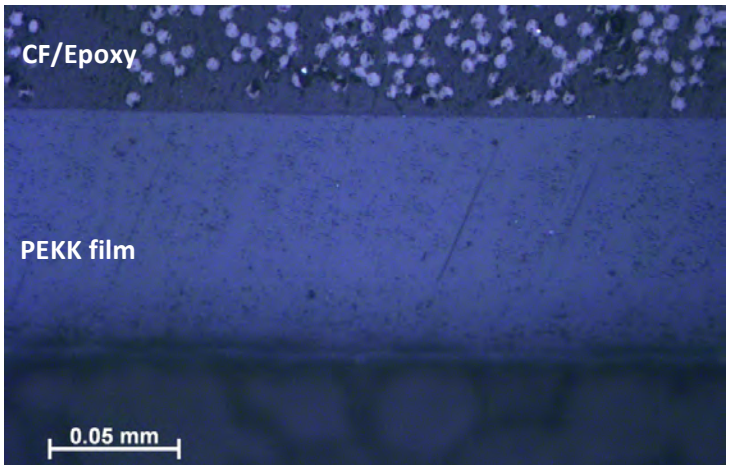

Figure 57: Zeiss optical microscope picture (x50 magnification) of the cross section of CF/Epoxy co-cured with UV-treated PEEK film substrate. Good adhesion between both materials can be appreciated; there were no areas with detached thermoplastic film.

Figure 58 shows the cross-section of the studied weld: CF/Epoxy, co-cured to a UV-treated PEEK film, and ultrasonically welded to CF/PEEK, using a PEEK ED. The interface of this weld showed to be uniform, with good merging of the PEEK resins and no detachment between the PEEK film and the epoxy after the performance of the welding. There were two punctual defects observed: a little crack on the epoxy substrate near the interface and a void in the PEEK one, but they were not repeated along the interface, so they are assumed to be isolated defects.

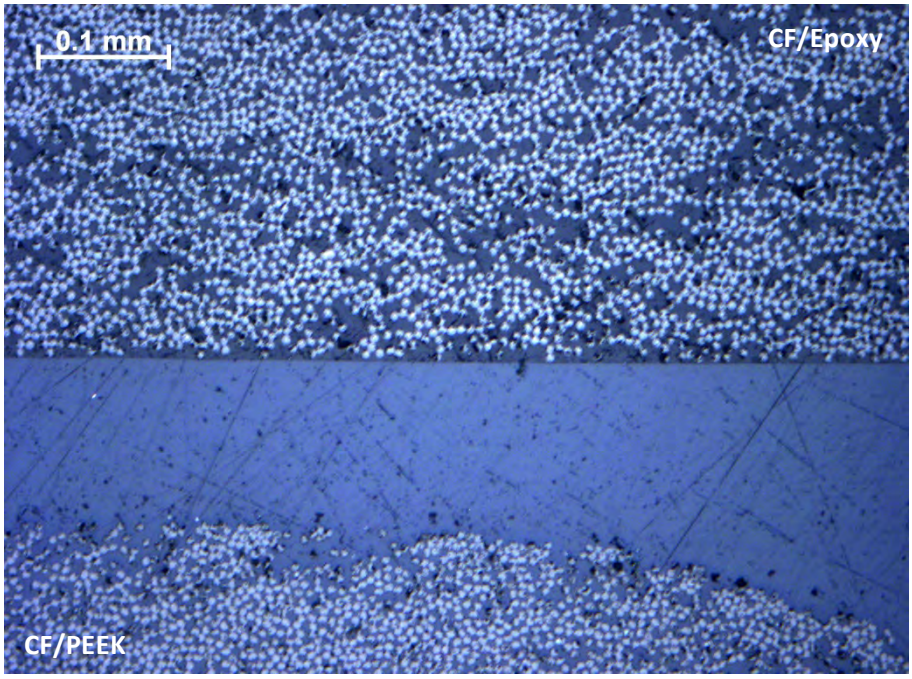

Figure 58: Zeiss optical microscope picture (x20 magnification) of the cross section of the weld formed by CF/Epoxy, co-cured with a UV-treated PEEK film, and CF/PEEK substrates, ultrasonically welded using a PEEK ED. A uniform cross section and good merging of the PEEK resins was achieved.

4.5.2. Fractography

For this weld, the fracture surface obtained after performing the LSS test is shown in Figure 59, where it can be appreciated that mainly failure in the epoxy (most likely interlaminar failure) occurred, exposing dry carbon fibres from its reinforcement internal layers, and leaving some of these fibres attached to the CF/PEEK substrate. There are some areas with PEEK-rich spots, noticeable in both substrates. In the CF/Epoxy one, dry fibres and burnt epoxy resin can be appreciated in one of the corners; there are also some small areas where the top epoxy resin layer is un-covered, so that here the failure occurred between the thermoplastic co-cured film and the CF/Epoxy. The PEEK that outflowed from the interface seems to be not burnt except in the corner that coincides with the burnt epoxy fibres. As occurred with PEKK, this fracture surface matches the relatively high LSS value (23.17 MPa) that resulted from the lap-shear test.

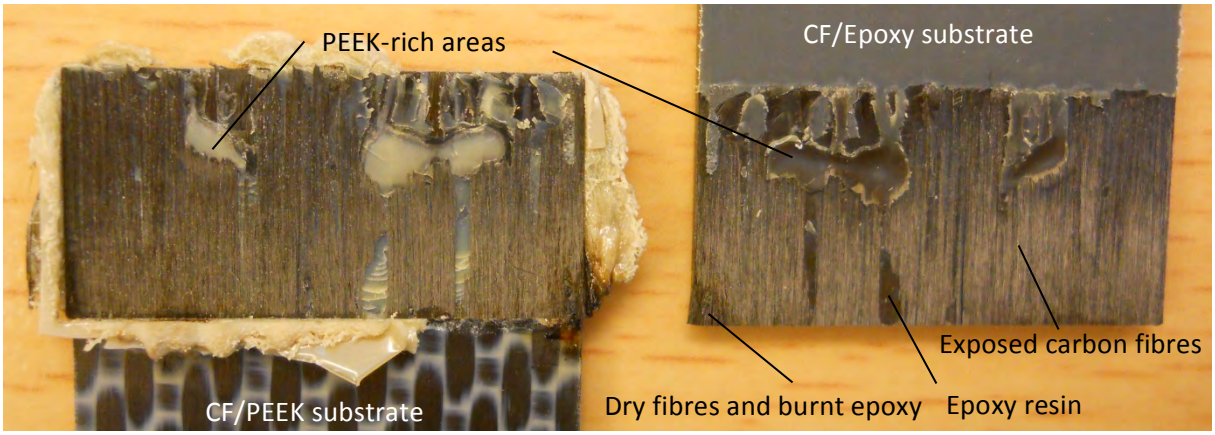

Figure 59: Fracture surface obtained after LSS test was performed of the weld formed by CF/Epoxy, co-cured with a UV-treated PEEK film, and CF/PEEK, ultrasonically welded using a PEEK ED. Interlaminar failure of the epoxy was the main failure type.

4.6. SHW: UD CF/PEEK layer [0/0]

4.6.1. Cross section analysis

As shown in Figure 60, where the cross section of the CF/Epoxy, co-cured with CF/PEEK UD layer, substrate is shown, before the welding there is good merging of these two materials. After the welding, their interface promotes what is believed to be the burning of the epoxy, and the not-complete melting of the energy director, as it can be appreciated in Figure 61.

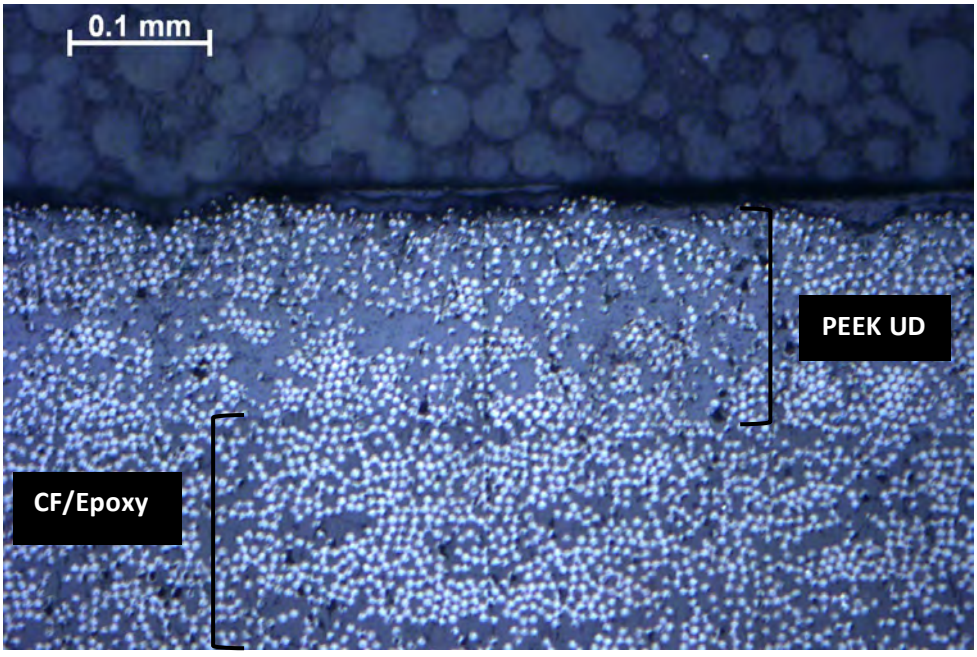

Figure 60: Zeiss optical microscope picture (x20 magnification) of the cross section of the substrate formed by CF/Epoxy with the co-cured layer of CF/PEEK UD. The colour difference between both can be appreciated, although there seems to be good merging and contact of the two matrices.

Figure 61 shows the cross section of the studied weld: CF/Epoxy co-cured with CF/PEEK UD layer [0/0] and ultrasonically welded to a CF/PEEK substrate using a PEEK ED. It reveals what the fracture surface had already predicted: Heat is concentrated between CF/PEEK UD layer and

CF/Epoxy, promoting a burnt area between these two materials across the whole interface, with an increase in the burnt area towards the edge of the weld. Heat is so focused between these two materials that there are some non-molten ED parts, which can be appreciated in the picture too. Some voids also appeared in the CF/PEEK substrate towards the edge of the weld.

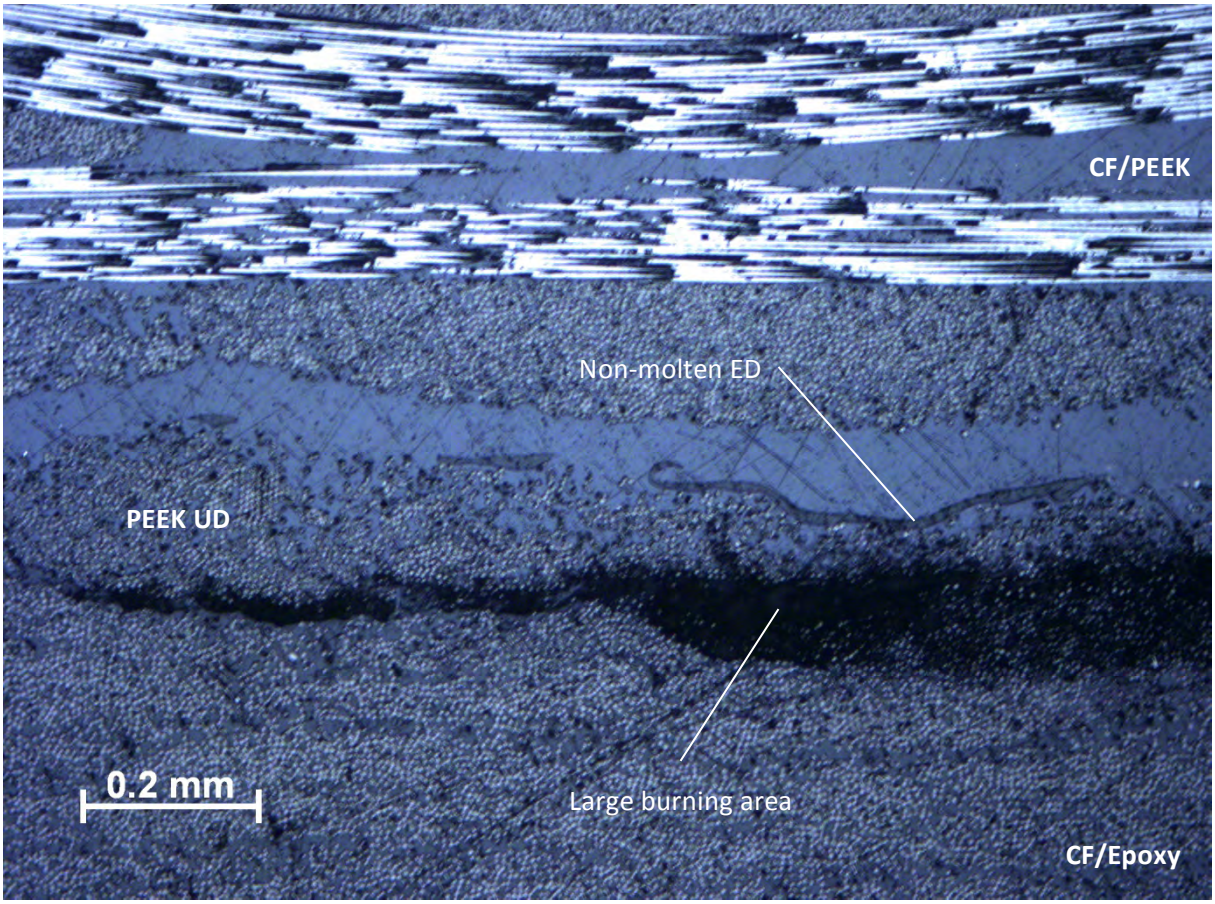

Figure 61: Zeiss optical microscope picture (x10 magnification) of the cross section of the weld formed by CF/Epoxy, co-cured with CF/PEEK UD prepreg layer [0/0], and CF/PEEK substrates, ultrasonically welded using a PEEK ED. The burnt area between CF/PEEK UD and CF/Epoxy, and the non-melted ED can be appreciated.

4.6.2. Fractography

The fracture surface obtained for the studied weld is shown in Figure 62. Failure occurred between the PEEK UD layer and CF/Epoxy, and between CF/PEEK UD and CF/PEEK, showing that there was not good connection between the PEEK prepreg layer and the substrates. This lack of rapport among the materials was reflected in the low LSS test result: 10.04 MPa. Dry exposed carbon fibres from the epoxy, with burnt epoxy resin, and CF/PEEK UD layer were also found on the edge of the weld; but the surface of the CF/Epoxy was also burnt in the centre of the weld, showing that mainly burning occurred between CF/PEEK UD and CF/Epoxy, showing that the first one did not act as a shield for epoxy degradation, and that heat was concentrated between these two materials.

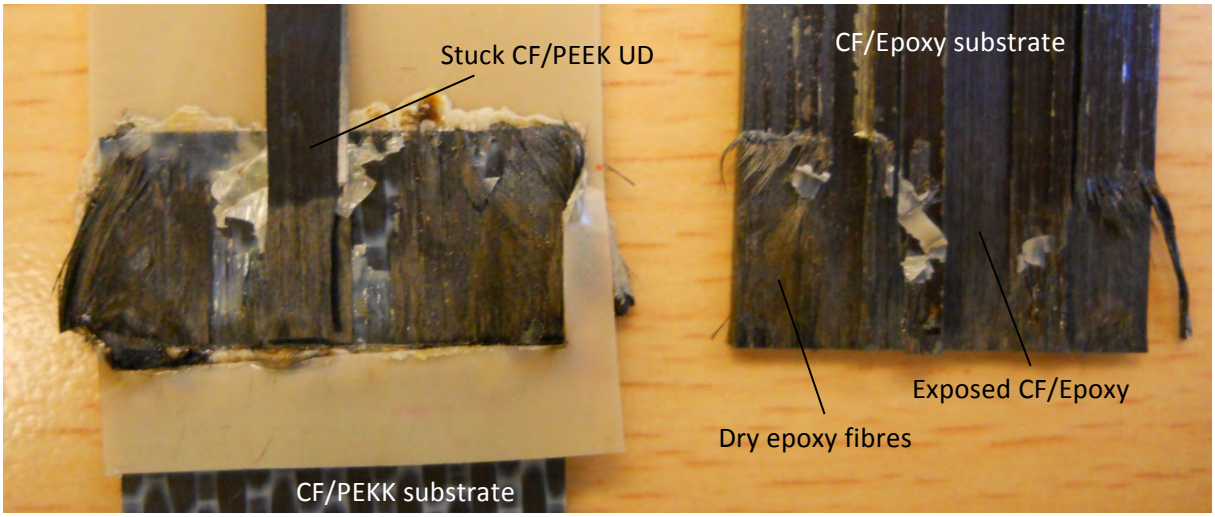

Figure 62: Fracture surface picture, after lap-shear test was performed of the ultrasonic weld formed by CF/Epoxy, co-cured with a CF/PEEK UD prepreg [0/0], and CF/PEEK, using a PEEK ED. Failure between the CF/PEEK UD layer and CF/Epoxy, and between CF/PEEK UD and CF/PEEK occurred. Dry carbon fibres and burnt epoxy resin can be also appreciated.

4.7. SHW: UD CF/PEEK LAYER [0/0] + PEEK FILM

4.7.1. Cross section analysis

Although this weld could be broken with the hands, it could be cut and embedded in resin for optical microscopy without separating the substrates. Figure 63 shows the cross section of the substrate formed by CF/Epoxy co-cured with a UD CF/PEEK prepreg layer [0/0] and a PEEK film on top of them. The PEEK film is not appreciated because it sank into the PEEK UD layer. A crack between the CF/Epoxy and the CF/PEEK UD layer merged with the PEEK film appeared in most of the interface, probably being one of the reasons for being able to break the weld with the hands. The part where the crack was smaller or inexistent had the same appearance as the interface of CF/PEEK UD and epoxy of the previous weld (section 4.6).

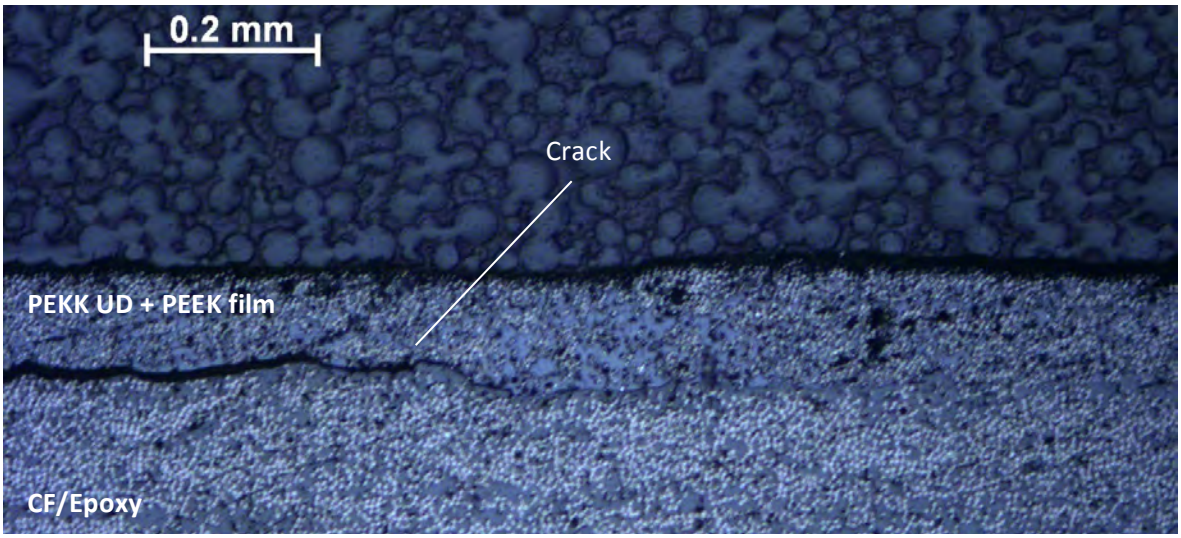

Figure 63: Zeiss optical microscope picture (x10 magnification) of the cross section of the substrate formed by CF/Epoxy substrate co-cured with a UD CF/PEEK prepreg layer [0/0] and a PEEK film on top. The PEEK film sank into the CF/PEEK UD layer, and a crack between them and the CF/Epoxy is observed in most of the interface.

In Figure 64, the cross section of the studied weld can be appreciated. A separation line between the CF/PEEK UD layer and CF/Epoxy can be appreciated and some voids can also be observed at this interface. In this case, heat seems to be more spread throughout the whole welding interface than in the previous weld (section 4.6), melting the PEEK ED and mixing it with the other PEEK matrices and film.

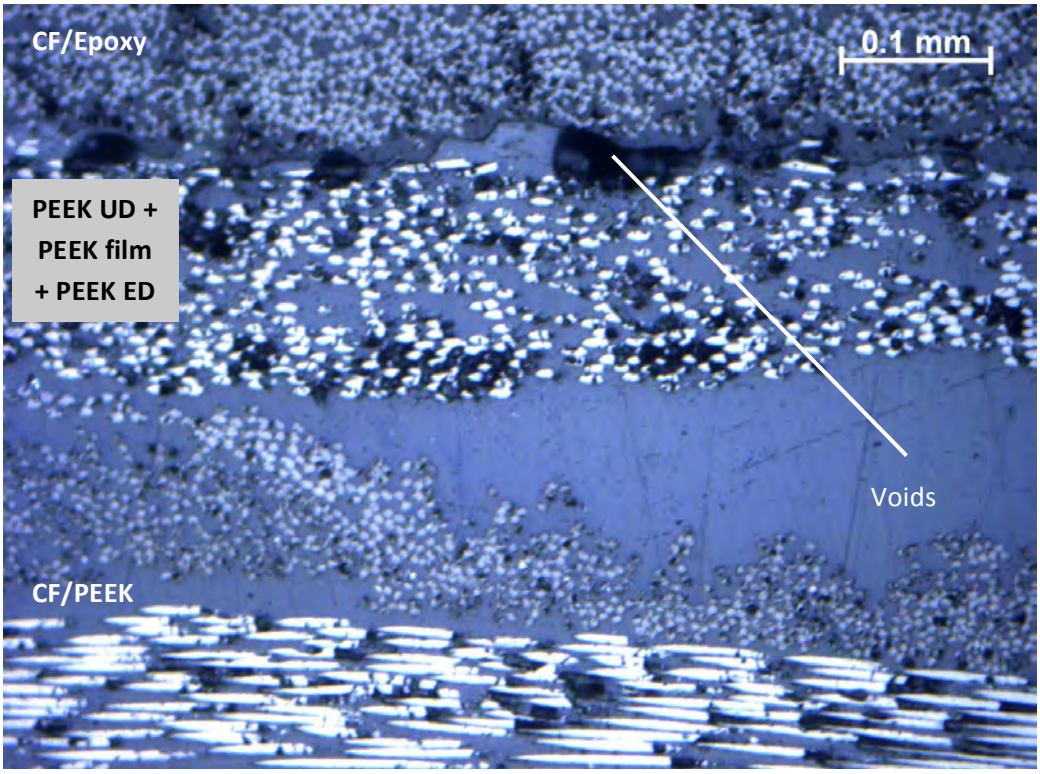

Figure 64: Zeiss optical microscope image (x20 magnification) of the interface of the weld formed by CF/Epoxy substrate, co-cured with a UD CF/PEEK prepreg layer [0/0] and a PEEK film on top of these two, and ultrasonically welded to CF/PEEK substrate using a PEEK ED. Separation between the CF/PEEK UD and the CF/Epoxy can be appreciated; also, voids appeared in this interface.

4.7.2. Fractography

Figure 65 shows the fracture surface of the studied weld. It reveals exposed dry carbon fibres, from the epoxy and the CF/PEEK UD layer, and burnt epoxy resin, especially at the edge of the weld, and burnt PEEK resin that outflowed from the interface. Main failure seems to have occurred between the CF/Epoxy and the CF/PEEK UD layer, remaining the carbon fibres of the last one stuck to the CF/PEEK substrate and exposing the dry and burnt carbon fibres from the epoxy.

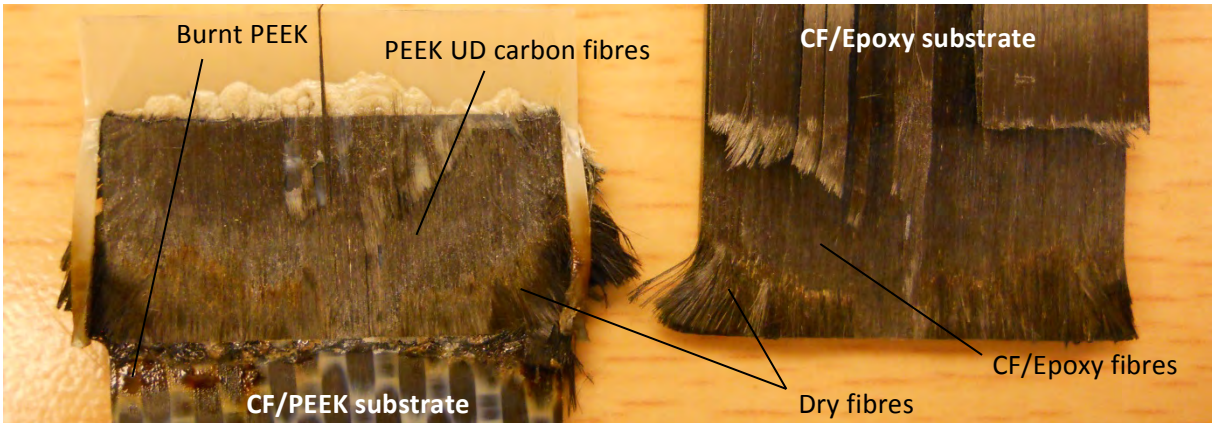

Figure 65: Fracture surface, after breaking it with the hands, of the weld formed by a CF/Epoxy substrate, co-cured with a UD CF/PEEK prepreg layer [0/0] and a PEEK film, and ultrasonically welded to CF/PEEK substrate using a PEEK ED. The fracture surface shows stuck fibres from the CF/PEEK UD layer on the CF/PEEK substrate, failure mainly between CF/Epoxy and CF/PEEK UD, and burnt fibres of these last two materials, especially close to the edge of the weld.

Although the compatibility of CF/PEEK substrate, the energy director and the PEEK UD seems to be improved by adding the PEEK film, the separation between the CF/Epoxy and the CF/PEEK UD layer and the epoxy burning that these co-cured films cannot avoid, revealed by the fracture surface, makes this weld fail.

4.8. COMPARATIVE EVALUATION

In this chapter, PEEK hybrid welds have been performed. As observed in the PEKK hybrid welds, treating the PEEK co-cured epoxy film enhances its adhesion towards the epoxy with respect to the non-treated film, which could not adhere after the water-jet cut of the panels.

In PEEK UV-O_3 and PEEK acetic acid + UV-O_3 welds, main failure was found in the internal layers of the epoxy, with dry carbon fibre exposure. They led to the highest LSS values of the PEEK hybrid welds, although not as high as expected for hybrid welds, an issue that will be studied in Chapter 6.

After analysing the other two weld types, SHW-PEEK-2 and SHW-PEEK-3, it seems that co-curing CF/Epoxy with a reinforced thermoplastic is not the most beneficial method for a successful weld, probably due to the high stiffness of the reinforced thermoplastic layer at the welding interface, leading to poor adhesion and low strength.

Chapter 5

Standard Hybrid Welding – PPS

In this chapter, CF/Epoxy to CF/PEEK hybrid welds will be studied.

5.1. PROCEDURE

Table 8 summarizes the total of welds performed, with the samples and energy directors explained in Chapter 2.

Sample reference	Bottom substrate	Top substrate	Thermoplastic coating	Observations
REF-PPS	CF/PPS (Ten Cate)	CF/PPS (Ten Cate)	-	Reference welds. Six welds performed: -5 samples for mechanical (LSS) testing. -1 sample for optical microscopy (OM).
SHW-PPS-1	CF/Epoxy (Hexcel 8552)	CF/PPS (Ten Cate)	PPS NT	Two welds performed, one for LSS testing and another one for OM.
SHW-PPS-2	CF/Epoxy (Hexcel 8552)	CF/PPS (Ten Cate)	PPS UV-O_3	Three welds performed, two for LSS testing and another one for OM [a].
SHW-PPS-3	CF/Epoxy (Hexcel 8552)	CF/PPS (Ten Cate)	PPS acetic acid	Two welds performed, one for LSS testing and another one for OM.

Table 8: PPS reference and hybrid welds.

[a] The reason why two welds were devoted for LSS testing for this treatment was to confirm the strength result for a study that will be carried in Chapter 6.

Table 9 collects the welding conditions and welder outputs for each welding combination:

Sample reference	Welding parameters			Average welding time (ms)	Average consumed power (%)	Average welding distance (mm)
	Force (N)	Amplitude	Travel (mm)			
REF-PPS [a]	1500	A9 (86.2 µm)	0.25	340	88	0.34
SHW-PPS-1				505	79	0.34
SHW-PPS-2				402	87	0.35
SHW-PPS-3				390	79	0.33

Table 9: Welding conditions and outputs for PPS welds.

5.2. MECHANICAL TESTING

Figure 66 shows a chart with the single-lap shear test results performed on the reference and the PPS hybrid welds.

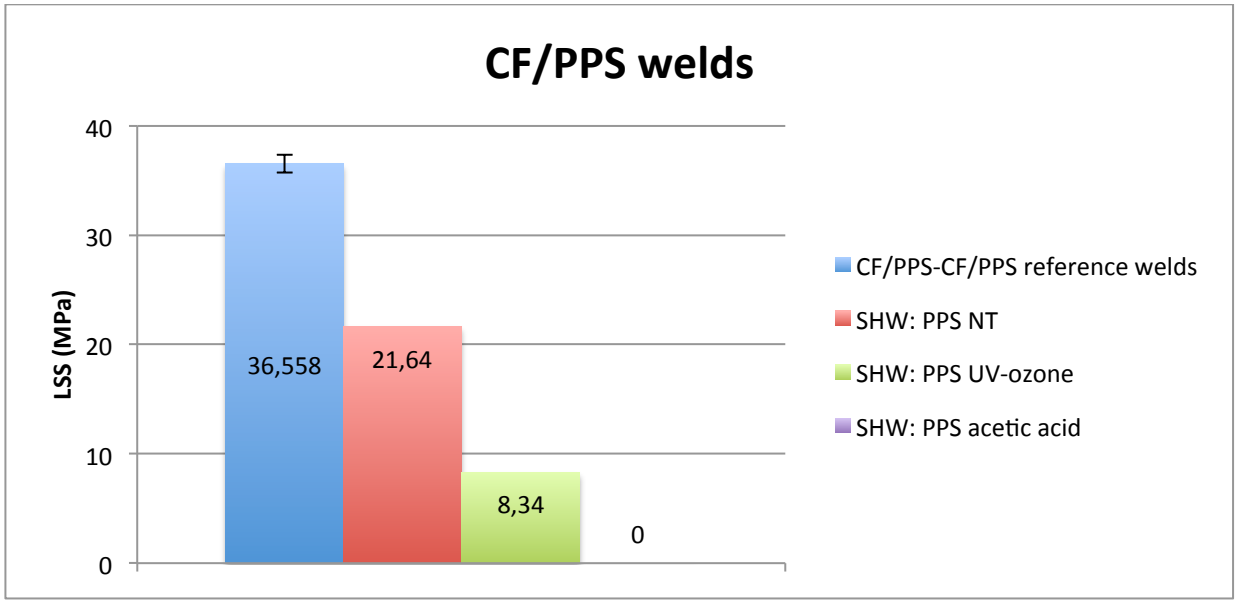

Figure 66: LSS values for PPS welds.

Five samples were tested for the reference welds, with a medium LSS value of 36.59 MPa and a standard deviation of 0.82. For PPS NT and PPS acetic acid, one sample per treatment was tested. This last one did not give any results when lap shear tested, so its strength was of 0 MPa. For PPS UV-O_3, two samples were tested, and 8.34 MPa was the mean lap shear stress obtained.

Once more, the obtained LSS results were lower than expected, as commented in Chapters 3 and 4.

The reference CF/PPS-CF/PPS weld and each PPS treatment results and characteristics, from higher to lower obtained strength, will be analysed separately below. As in the two previous chapters, analyses of the cross-sections and fracture surfaces will be mainly performed.

5.3. CF/PPS-CF/PPS REFERENCE WELD

5.3.1. Cross section analysis

Figure 67 shows an optical microscope image of PSS reference weld interface. As PEKK and PEEK reference welds, good merging of the PPS ED and substrates matrices is observed. In this case, more carbon-fibre diffusion towards the welding interface is observed.

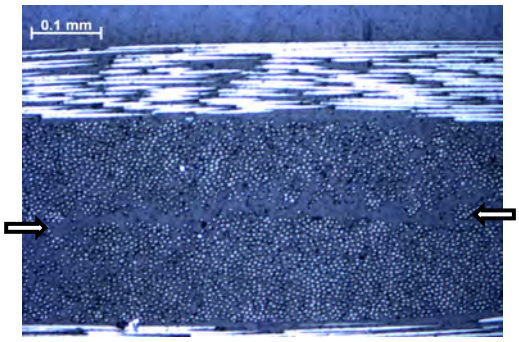

Figure 67: Zeiss optical microscope picture (x20 magnification) of CF/PPS-CF/PPS reference weld cross-section. Arrows point to the location of interface.

5.3.2. Fractography

Figure 68 shows the fracture surface of the CF/PPS-CF/PPS reference weld. It shows cohesive failure, nearly no fibre distortion on the edges, and small PPS-rich spots, as observed in practically all of the welds.

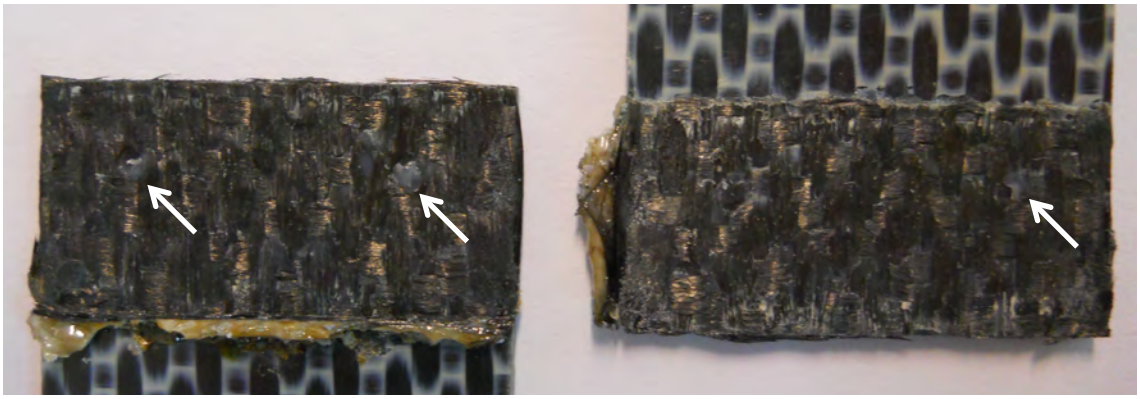

Figure 68: CF/PPS-CF/PPS reference weld fracture surface. White arrows point to PPS-rich spots.

5.4. SHW: PPS NT

5.4.1. Cross section analysis

Figure 69 shows the cross section of the sample composed of CF/Epoxy and the co-cured layer of non-treated PPS film. The adhesion of both materials is very good, with carbon fibres from the epoxy being diffused into the PPS film, providing also physical interlocking, or keying, between these dissimilar materials.

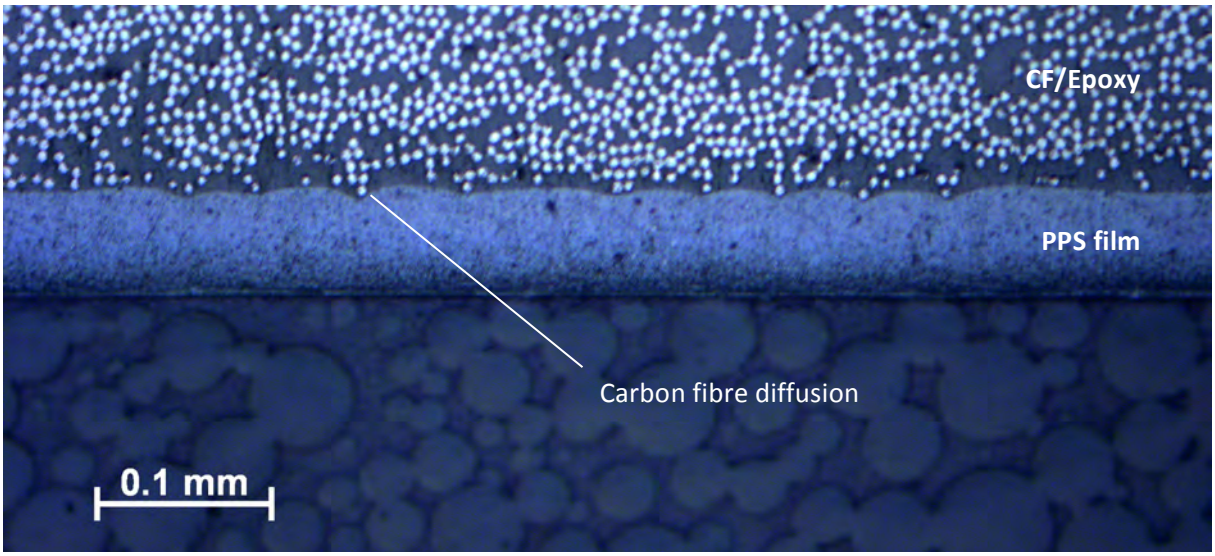

Figure 69: Zeiss microscope image (x20 magnification) of the cross section of CF/Epoxy, co-cured with non-treated PEKK, substrate. Good adhesion between the materials, as well as macro-interlocking or keying (epoxy carbon fibres diffusion into the thermoplastic film and merging of both resins), can be appreciated.

Figure 70 shows the weld of this substrate to the CF/PPS one. Some voids appeared on the CF/PPS substrate close to the edge of the weld; the rest of the interface was uniform, and good

adhesion and physical interlocking (keying) between the thermoplastic and thermoset materials was found. The lap-shear strength of this weld was on the order of the highest values obtained with this epoxy material (21.64 MPa), showing the feasibility of non-treated PPS for hybrid welding.

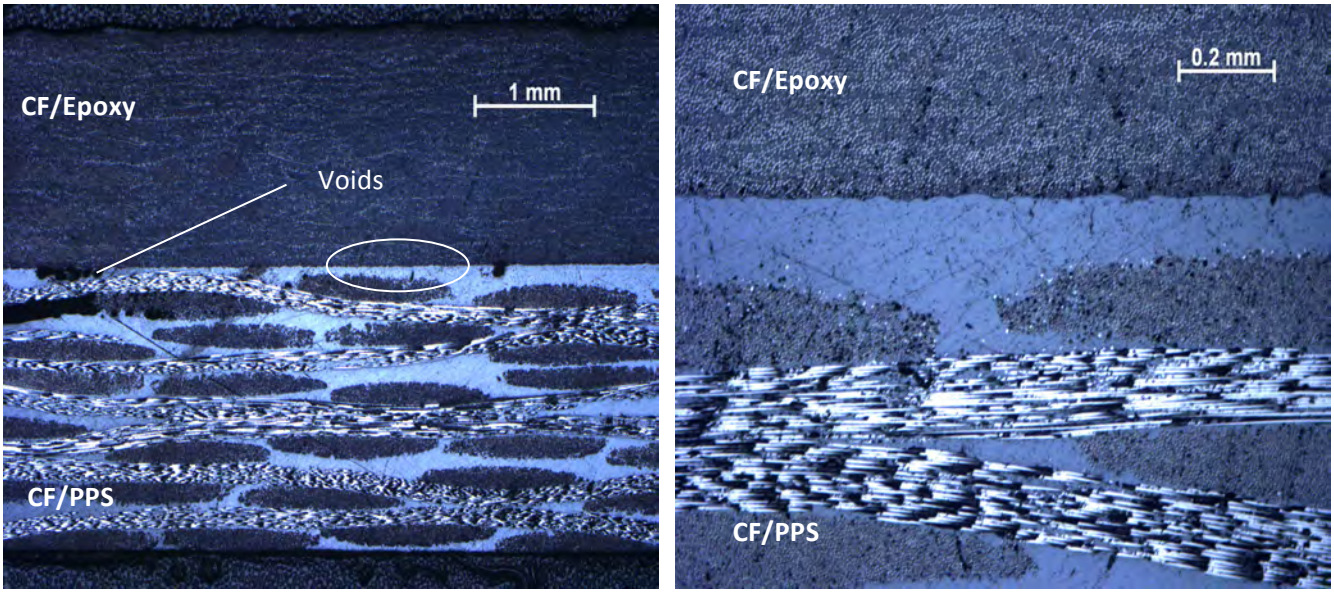

Figure 70: Zeiss microscope pictures (left: x2.5 magnification; right: x20 magnification) of the cross section of the ultrasonic weld formed by CF/Epoxy, co-cured woth non-treated PPS film, and CF/PPS substrates, using a PPS ED. Image on the right is a detail, using a higher magnfication, of the area enclosed in the white circle of image on the left. Voids on the thermoplastic substrate, close to the edge of the weld (left side of image on the left), can be appreciated.

5.4.2. Fractography

The fracture surface of the studied weld is shown in Figure 71. On the fracture surface of the CF/Epoxy substrate, three different things were observed: Interlaminar failure of the epoxy, exposure of the epoxy resin surface, with a scratched appearance, and bubbly mixture of PPS and epoxy on the edge and corner of the weld. On the CF/PPS surface, PPS rich areas, smaller than the ones found on PEKK and PEEK welds, were spotted; also, stuck epoxy carbon fibres, coinciding with the interlaminar failure zones of the epoxy, and brown (slightly burnt) PPS outflowing from the interface were found.

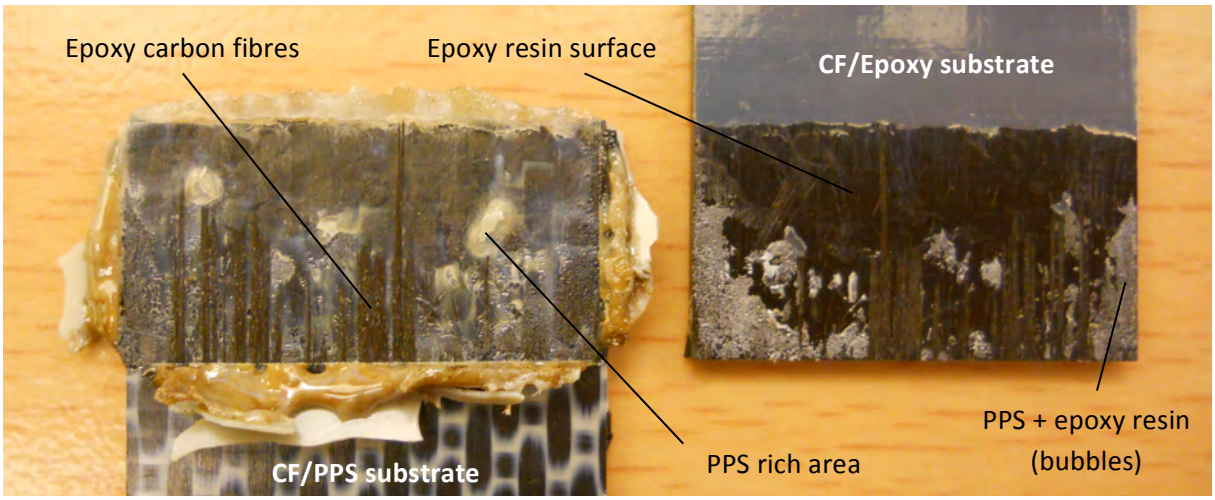

Figure 71: Fracture surface, after lap shear test was performed, of the weld formed by CF/Epoxy, co-cured with non-treated PPS, and CF/PPS, using a PPS ED. Interlaminar failure of the epoxy, epoxy resin surface exposure and bubbly

epoxy-PPS mixture are appreciated on the epoxy substrate; PPS rich areas and some stuck epoxy carbon fibres are observed on the PPS substrate fracture surface.

5.5. SHW: PPS UV-O_3

5.5.1. Cross section study

In Figure 72, the cross-section of the CF/Epoxy substrate, co-cured with PPS-UV film, was studied. It can be appreciated that the interface shows a keying of both materials stronger that for untreated PPS film, probably enhanced by the roughening that UV-light treatment produces of the films surface. Nevertheless, adhesion seems not to be optimum, due to the dividing line where the two materials meet, which is not due to colour difference of the two materials because of light incidence, but due to separation and not optimum entanglement between them.

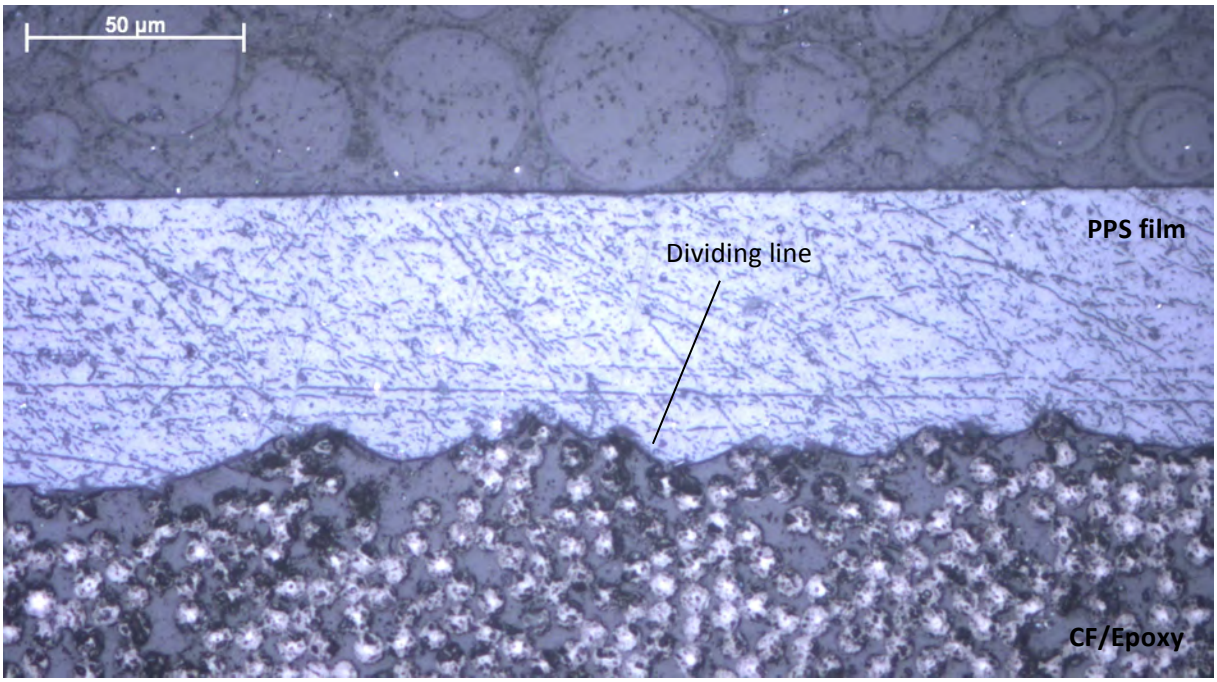

Figure 72: Zeiss microscope picture (x50 magnification) of the cross section of the sample formed by CF/Epoxy co-cured with PPS UV-treated film. Keying of both materials can be appreciated, as well as carbon fibre diffusion from the epoxy into the PPS, but a dividing line where the two materials meet is also observed.

Figure 73 shows the interface of the studied weld. A large crack growing near the edge of the weld towards the centre, and eventually stopping before reaching it, is observed, separating the PPS and the epoxy. This is due to the poor adhesion between the thermoplastic and the thermoset, Figure 74 shows two pictures of the main areas of this interface: The region where the crack starts to grow and where it eventually stops, close to the centre of the weld. Some voids are also observed near the crack in the thermoplastic substrate, and in both substrates at the crack-growth area, where the thermoplastic and the thermoset separate. Along the crack, epoxy is believed to be burnt.

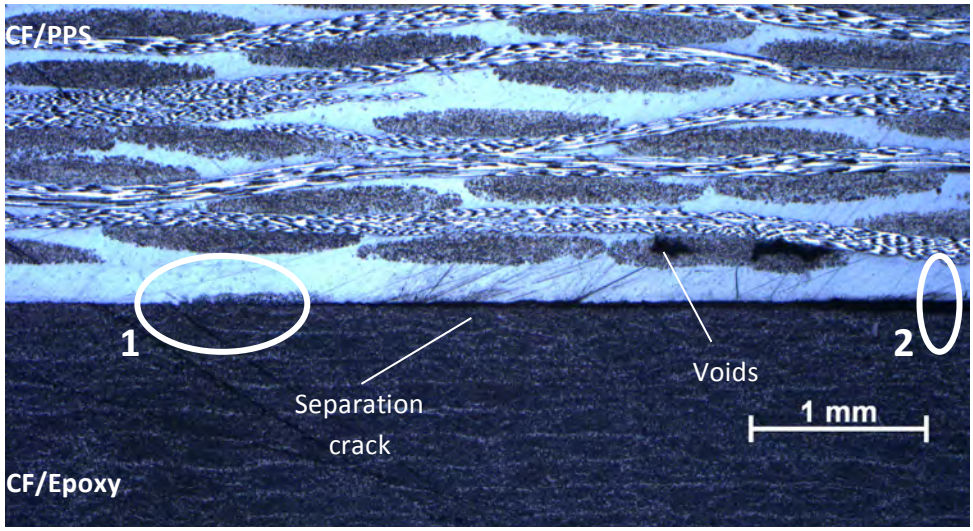

Figure 73: Zeiss microscope picture (x2.5 magnification) of the interface of the studied weld: CF/Epoxy, co-cured with UV-treated PPS, and CF/PPS substrates, using a PPS ED. The large crack and voids on the thermoplastic can be seen. The two circled areas, the beginning (1) and the end of the crack (2), are shown with more detail in the images below.

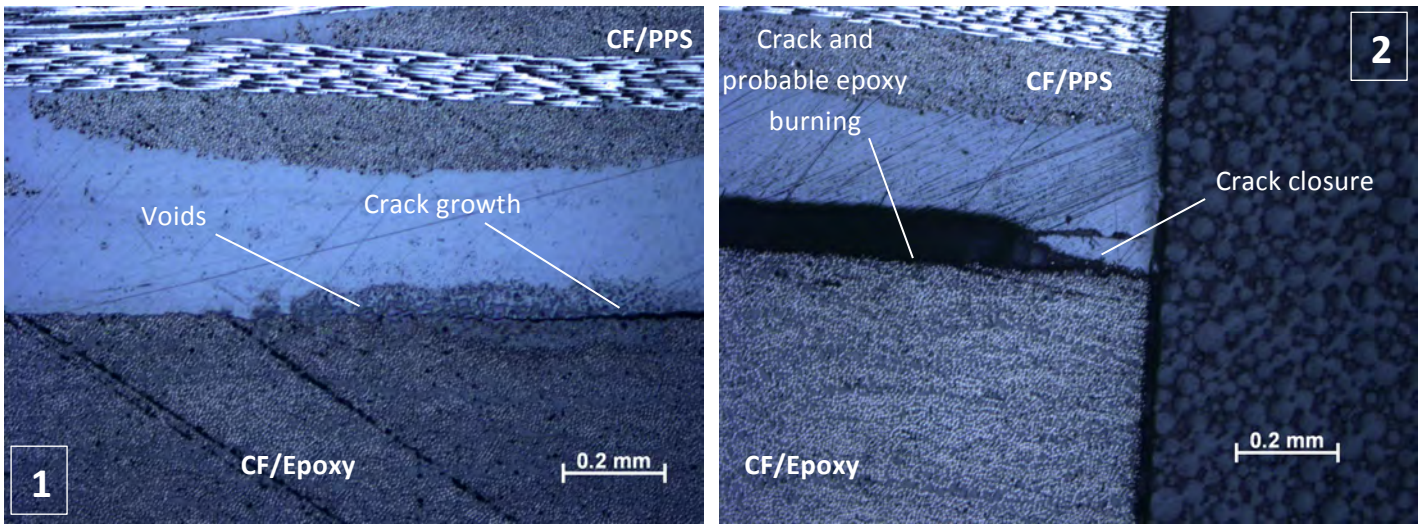

Figure 74: Zeiss microscope pictures (x10 magnification) of the beginning (left, 1) and end (right, 2) of the crack. In the beginning of the crack, voids and bubles were observed in the thermoplastic and thermoset substrates at the interface, where the thermosplastic and the thermoset separate and this last one starts degrading, probably burning. The end of the crack occurs near the center part of the weld.

5.5.2. Fractography

Figure 75 shows the fracture surface of the studied weld, after the LSS test was performed. On the CF/Epoxy substrate, a great area of exposed epoxy resin can be observed, reminding of the PEKK NT fracture surface, also with a low LSS result due to the lack of adhesion between the thermoset and the thermoplastic, as occurs in this case too. It has a dull, not-shiny appearance, which indicates that some kind of degradation occurred or that some part of the resin remained stuck to the other substrate; also, bubbly remains of PPS resin were observed on the edges of the interface. On the CF/PPS fracture surface, burnt PPS is observed in the fracture surface and outflowing from the weld; also, PPS-rich spots, as observed in the rest of the welds, can be appreciated.

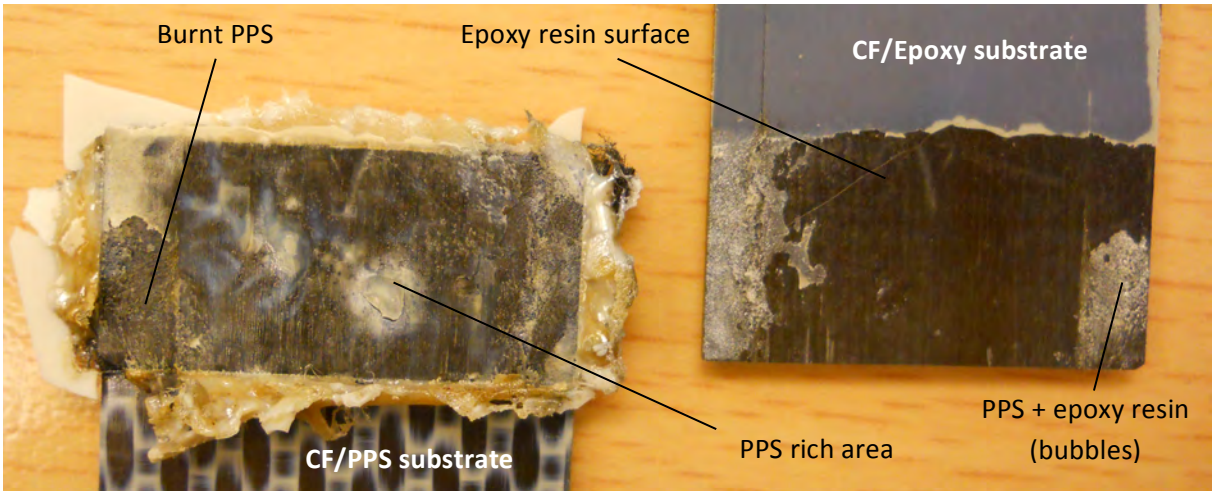

Figure 75: Fracture surface after lap-shear test was performed. On the CF/PEKK fracture surface, mainly not-shiny epoxy resin exposure is seen, with bubbly PPS film on the edges of the weld; on the CF/PPS substrate, PPS-rich spots and slightly burnt PPS resin at the interface and outflowing from the weld can be appreciated.

The mean LSS value (8.34 MPa), cross sections pictures and fracture surface made clear that treating PPS film with UV is not optimum. As already mentioned, an extra weld and lap shear test with this treatment were performed in order to confirm the results, which did check this incompatibility of the treatment for PPS ultrasonic welding, contrary to what happened with PEEK and PEKK, where UV enhances the adhesion and the strength of the weld. This, of course, relies on the fact that PEKK and PEEK have similar molecular structure, different to that of PPS. Further investigation to explain this behaviour, using FTIR among other tests, will bring more light to this difference (Chapter 6).

5.5.3. FTIR analysis

An FTIR analysis was tried on the exposed epoxy resin surface of the CF/Epoxy substrate, but the results obtained were not reliable, probably due to the rough surface of the exposed epoxy.

5.6. SHW: PPS ACETIC ACID

5.6.1. Cross section analysis

Figure 76 shows the cross section of the substrate formed by CF/Epoxy with the co-cured and treated thermoplastic film. Unlike what the inexistent LSS value revealed, and what shall be seen in the cross section of the weld, the thermoset seemed to have good merging, entanglement and adhesion with the PPS-acetic film.

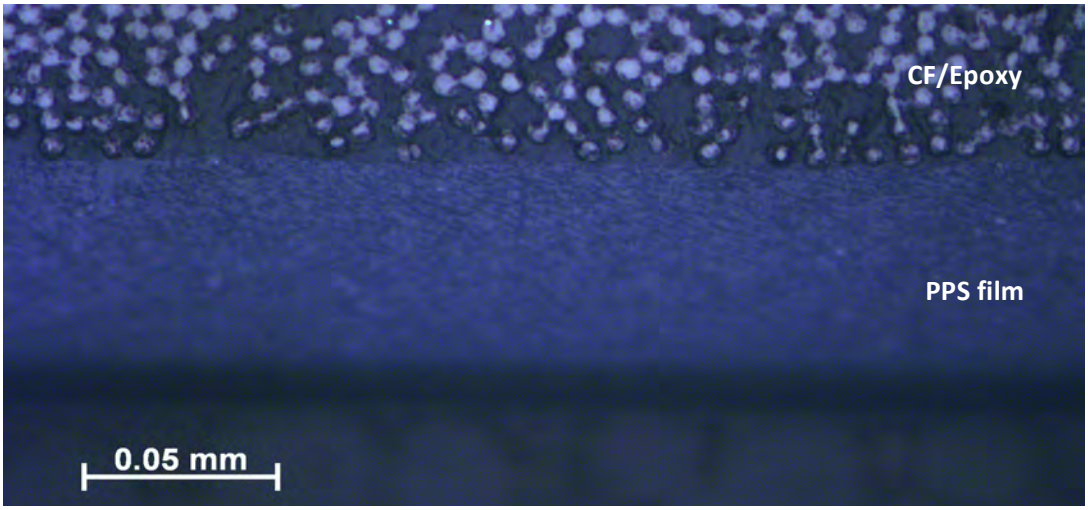

Figure 76: Zeiss microscope image (x50 magnification) of the cross-section of CF/Epoxy substrate, co-cured with PPS film treated with acetic acid. The adhesion between the thermoset and thermoplastic materials seems to be optimum, with merging of both materials at their interface.

The cross section of the weld, shown in Figure 77, revealed an actual gap or space between the epoxy and the PPS, confirming what observed in the fracture surface. It was filled with the embedding resin used for polishing, hence the bubbles that can be seen. PPS film, energy director and matrix of the reinforced thermoplastic substrate merged perfectly, but the lack of adhesion with the epoxy is the responsible of the failure of this weld.

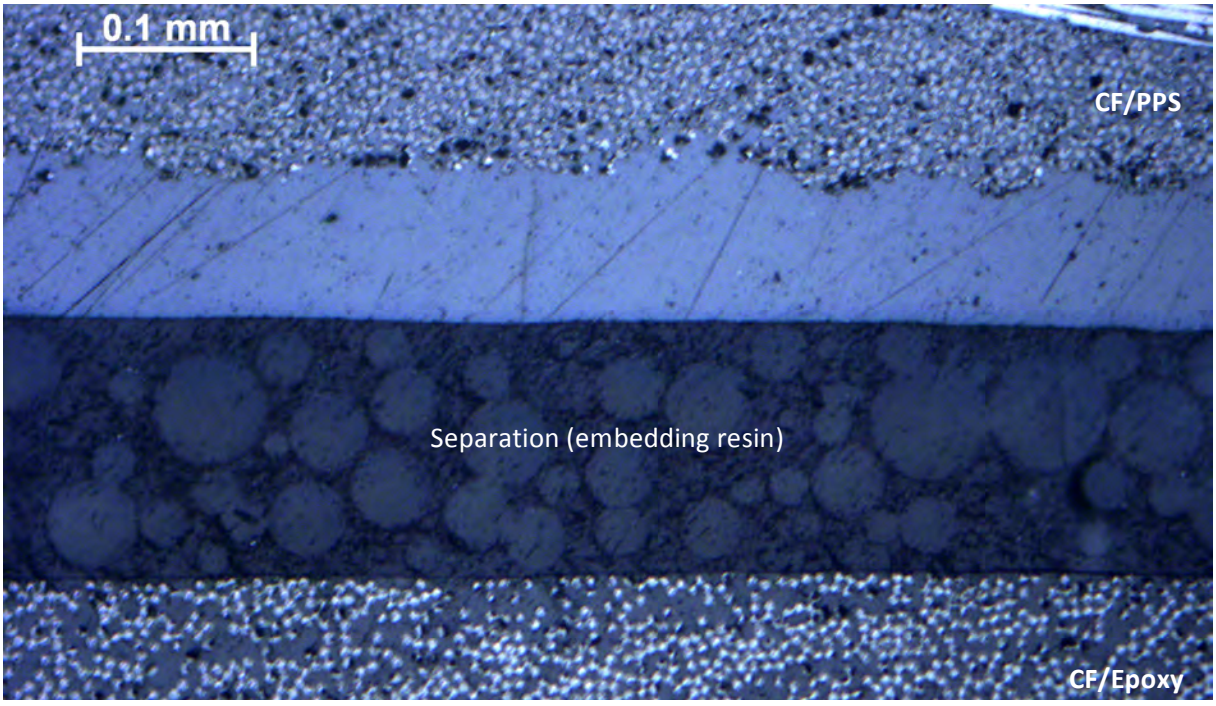

Figure 77: Zeiss microscope picture (x20 magnification) of the cross section of the weld formed by CF/PPS and CF/Epoxy, co-cured with PPS film treated with acetic acid, substrates. A large separation gap, filled with embedding resin, can be observed at the CF/Epoxy and PPS interface.

Although PPS-acetic and epoxy seemed to have good adhesion before the welding was performed, after it, it was demonstrated by mechanical testing and cross-section observation that this treatment is not beneficial for hybrid ultrasonic welding of PPS.

5.7. COMPARATIVE EVALUATION

This chapter has been devoted to the study of PPS hybrid welds. It has been acknowledged that treating the PPS film with UV and acetic acid is not beneficial for hybrid welding, due to the low LSS values and lack of adhesion between the thermoset and the thermoplastic found on post-welded cross-sections. Non-treated PPS film weld led to high LSS values, although not as high as expected due to failure in the epoxy, as it will be studied in the following chapter.

Chapter 6

SHW Additional Studies

In this chapter, the used Hexcel 8552 epoxy properties and the possible degradation of PPS when treated with UV will be studied.

6.1. Study of Hexcel 8552 epoxy degradation

As previously commented, the lap hear strength of the successful hybrid welds had a lower value than expected – according to the results obtained by P. Vizcaíno in the previous investigation carried out at this university, LSS values on the order of 30 MPa where obtained for epoxy-PEEK hybrid welds. Moreover, the fracture surfaces obtained after mechanical testing of the welds where better adhesion between the thermoset and the thermoplastic was found, show failure occurring in the thermoset, likely to be interlaminar failure. These two facts led to the idea that the epoxy was not performing as it should: When used (September 2014), the epoxy had already passed its expiration date: 12 months from manufacturing date, which for our prepreg was 31/05/2012, so it had been expired for one year and 4 months; according to the provider this should not have represented any problems. Nevertheless, more tests and study on the actual condition of the epoxy will be presented in this section.

To begin, a part of one the epoxy fracture surfaces of the successful welds (PEKK chloroform + amine, 1st formula) is shown in Figure 78, taken with the Zeiss SteREO Discovery V.8 microscope, able to capture fracture surfaces with an excellent resolution, available at the DASML of TU Delft. The numbers refer to the four areas of interest, where more focus was taken with the Scanning Electron Microscope (SEM), a potent, high-magnification device available at the DASML of TU Delft; the images of these areas taken with it are shown below (Figure 79). This fracture surface is a representative example of what was found in all of the rest: Mainly failure at the epoxy, exposing its shiny, dry carbon fibres (a step between the non-welded epoxy substrate part and the top resin exposed layer at the welding interface, and another one between these two areas and the exposed fibres can be appreciated), and some zones with a mixture of epoxy resin and thermoplastic. This image proves the interlaminar failure of the epoxy: the fracture occurs in the mainly epoxy substrate, by ripping-off its top resin and carbon fibres layer.

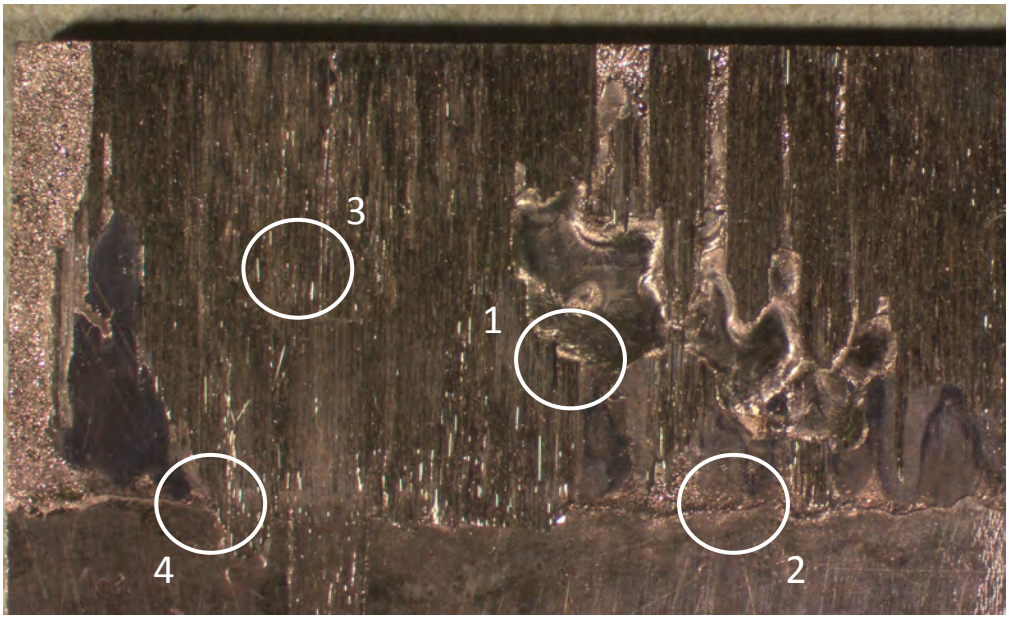

Figure 78: Zeiss SteREO Discovery V.8 microscope picture from PEKK chloroform-amine (1st formula) fracture surface. Four regions of interest were spotted.

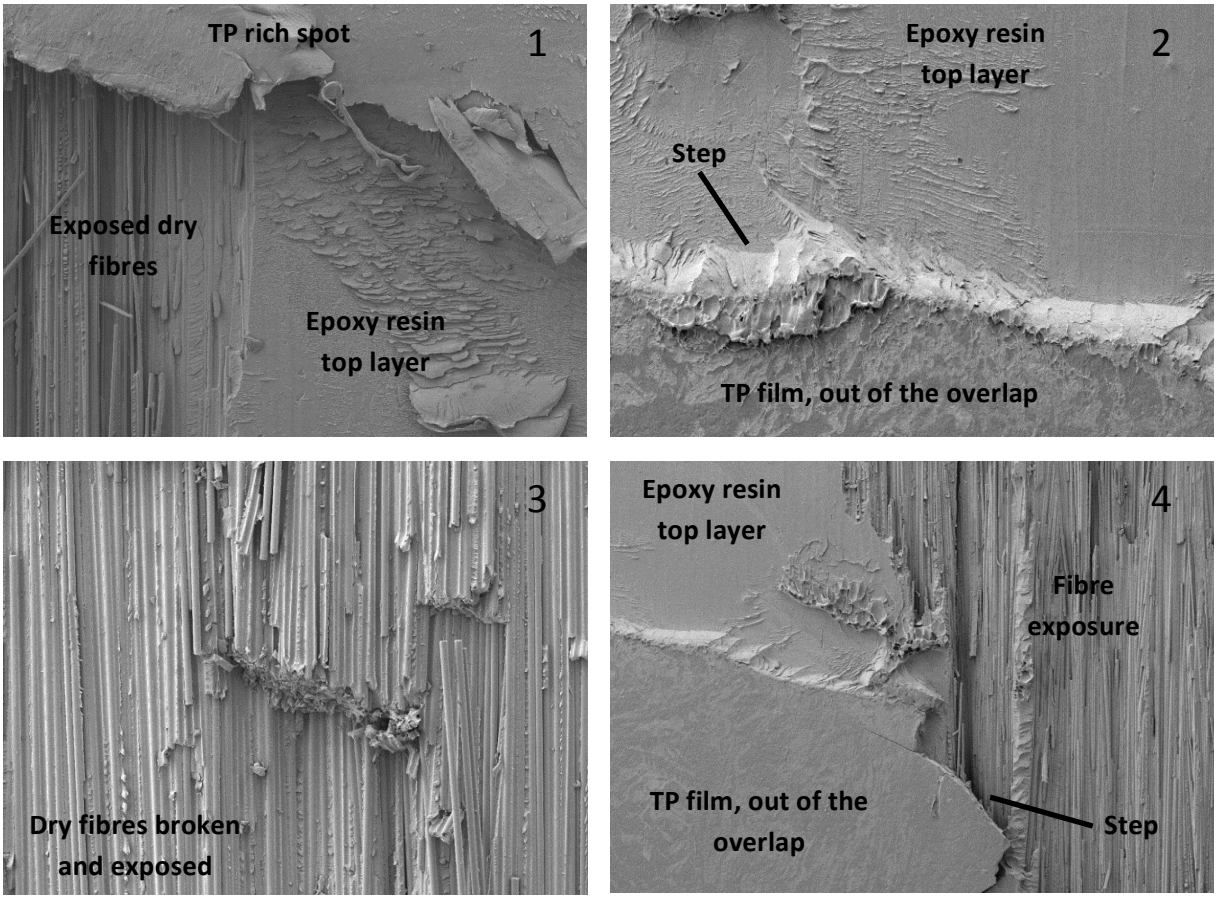

Figure 79: SEM microscope images of the four spotted areas of PEKK chloroform-amine (1st formula) fracture surface.

As can be observed in the SEM pictures, the exposed epoxy carbon fibres appear to be dry and not surrounded by resin, which led to the thought that failure in the sizing, the substance that binds the reinforcing fibres and the resin together, may be occurring. A Mode-I test was decided to be carried in order to check the interlaminar fracture toughness of our material and its G_{IC} value.

Mode-I test of Hexply 8552 CF-Epoxy

Mode-I test consists on the application of interlaminar tensile stress to a pre-cracked CF/Epoxy beam, measuring the energy necessary to cause and grow an interlaminar crack. The aim is to measure the Mode I interlaminar fracture toughness, G_{Ic}, of our material. The DCB (Double Cantilever Beam) method was used, following the ASTM D5528 standard. Samples of 150 mm long and 25 mm wide, and a thickness of 3-5 mm, in order to meet the standard prescribed dimensions, were manufactured in another autoclave cycle. In it, 22 layers of CF/Epoxy prepreg from the Hexply 8552 epoxy, of 300 x 300 mm^2 dimensions, were stacked one on top of the other, with the carbon fibres aligned in the same direction. A Teflon film with a thickness lower than 13 µm was inserted between prepreg layers 11 and 12 for half of the panel length, in order to provide the necessary pre-crack. Figure 80 shows a sketch of the autoclave panel to be cured. The curing cycle was the same one as in the other three autoclave processes: 110°C for 60 minutes, then 180°C for 120 minutes, 7 bars of pressure.

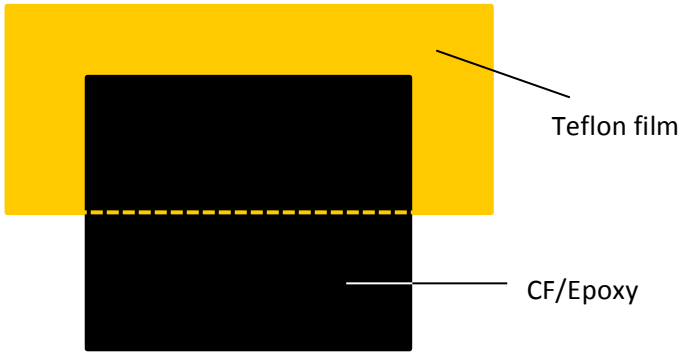

Figure 80: Sketch of the autoclave panel from which Mode-I samples were obtained.

Once the panel had been cured, it was taken to Van Nobelen Delft VB company to be water-jet cut. Five samples were obtained, with the specifications shown in Figure 81:

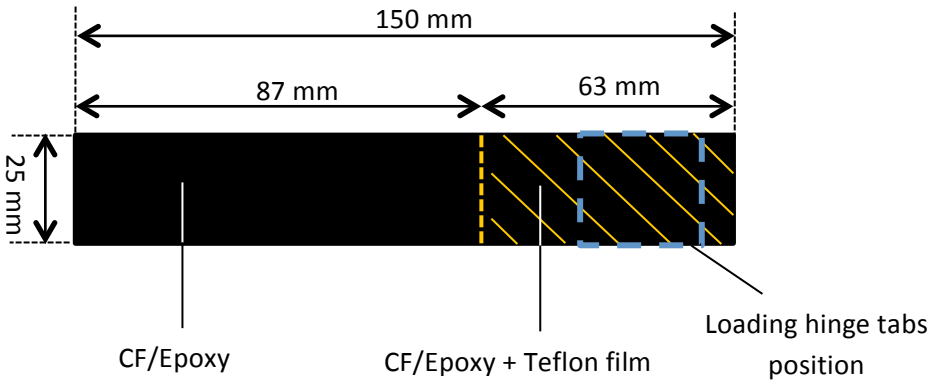

Figure 81: Sketch of Mode-I sample.

Then, loading hinge tabs were glued to the part; they will be screwed to the piano hinges, which were the devices chosen to apply the tension. Their position is shown in Figure 89, such that the load line is 50 mm from the end of the Teflon insert (a_0), as the standard specifies. The used adhesive for such purpose was Scotch-Weld 9323 B/A, composed of two mixing parts to which Glasparels 200/300 micron powder was added (1% of the adhesive's weight), in order to prevent the tabs from slipping while dried. Clamps were used to hold the tabs to the samples while adhesive was

being dried. It was dried for three days a room temperature, and then for 2 hours at 60°C in a Heraeus oven available at the DASML of TU Delft. Once they were dried, the side of the samples were coated with typewriter corrector fluid, in order to check the position of the crack growth. Figure 82 shows the final sample before being mounted on the testing machine.

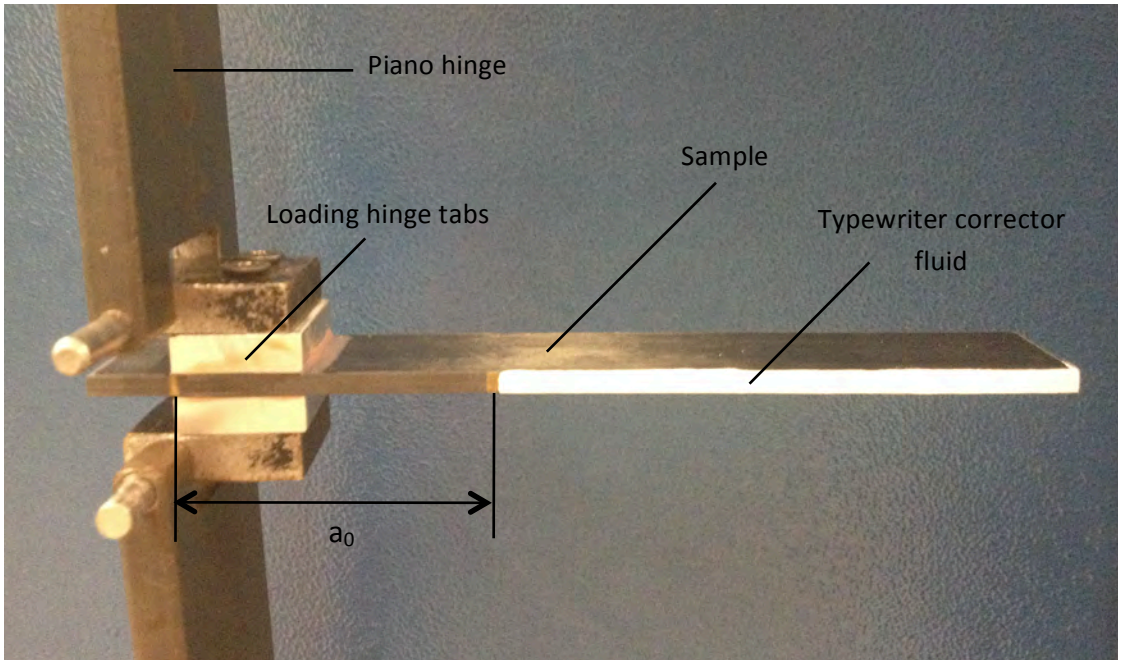

Figure 82: Mode-I test sample screwed to the pianos hinges through loading hinge tabs.

Adhesive measuring tapes where set on the typewriter corrector, at the bottom part of the samples side cross-section, so that the crack growth could be measured. Zwick 20 kN machine, available at the DASML of TU Delft, was used for the performance of the tests. An Optomotive camera was used to record and check with a higher magnification the growing of the crack. In the test, the specimen is pre-load to open the crack 5 mm, to remove the effects of possible trapped adhesive in the Teflon insert. Then, the sample is un-loaded back to the first position, and the tests starts. When the crack grows 55 mm from the end of the Teflon insert, the test is ended. The load speed was chosen to be 1 mm/min. Figure 83 shows a picture of the testing environment and apparatus:

Figure 83: Mode-I test environment and apparatus.

Five samples were tested, and graphs of the Load (P) vs. Load point deflection or vertical separation (δ) were obtained. Figure one shows one of them. To calculate G_{Ic}, the beam theory expression was used (Equation 1), with the Deviation from Linearity (NL) point, pointed out in the graph of Figure 84 with the green discontinuous lines.

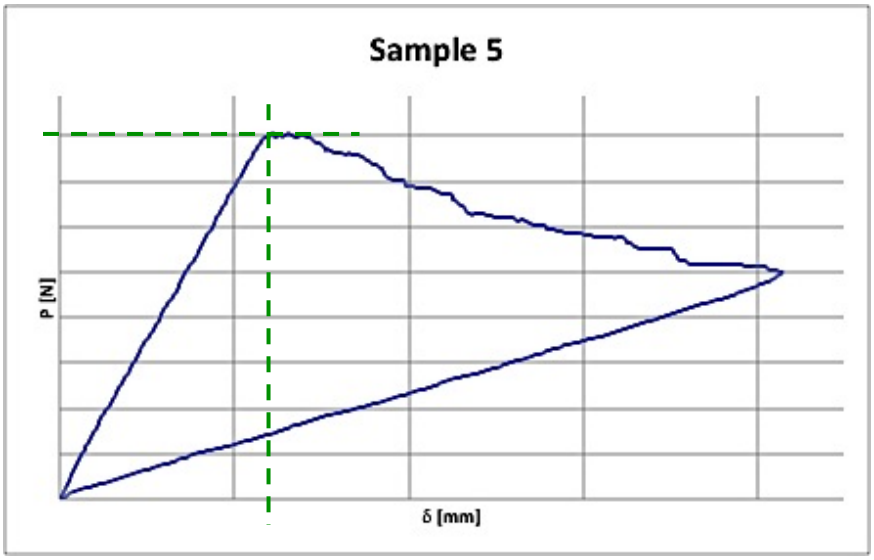

Figure 84: One of the Mode-I test obtained curves, which plots force as a function of load point deflection.

$$G_{Ic} = \frac{3P\delta}{2ba} \qquad (1)$$

In Equation 1, *P* and δ are, respectively, the load and load point deflection of the NL point, *b* is the specimen width and *a* is the delamination length, which is 55 mm because the specimen was pre-loaded and its pre-crack was opened 5 mm. Then, taking the mean of *P* and *δ* for the five tested samples, the G_{IC} for the expired Hexply 8552 epoxy material was: G_{IC}=0.291 kJ/m^2. The company did not provide a reference value in order to compare to it the obtained one. Nevertheless, for a Torayca T800H CF/Epoxy, with a similar curing cycle than our epoxy (180°C for 2 hours), had a G_{IC} of 0.43 kJ/m^2 [44], showing that the Mode-I interlaminar fracture toughness of our material was too low in comparison with similar aerospace epoxies.

A SEM observation of the Mode I fracture surface was done; Figure 85 shows a lower and a higher magnification (left and right, respectively) picture of this surface. In them, it can be appreciated that failure occurs mainly between the fibres and the epoxy matrix, the same failure observed in the fracture surfaces of the welds, as image number 3 of Figure 79 showed. It is thought that expiration degraded the sizing substance that binds the reinforcement and matrix together. Figure 86 shows a sketch of Mode-I fracture surface cross-section.

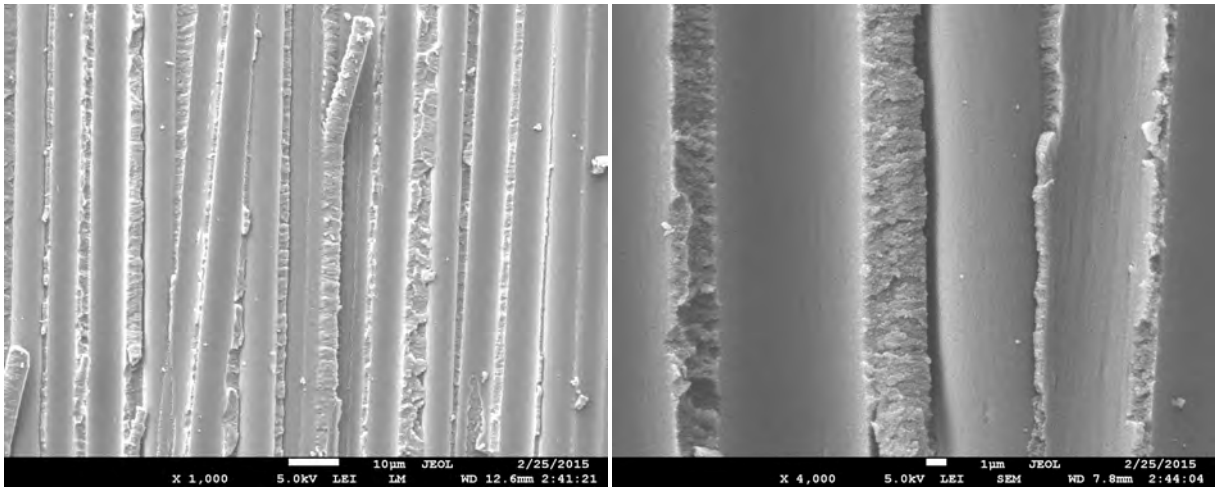

Figure 85: SEM microscope pictures (left: x1000 magnification, right: x4000 magnification) of the fracture surface of a Mode-I test sample.

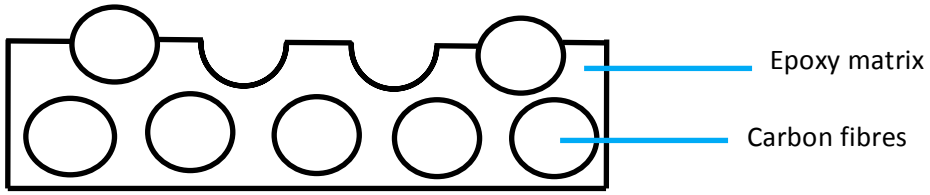

Figure 86: **Sketch of the cross-section of the fracture surface of Mode-I test sample. Failure between the fibres and the matrix was found.**

More matrix failure was expected, which would have increased value of G_{IC}, as Mode-I testing fracture surface for T800H epoxy shows in Figure 87, observed with SEM, where the fibres are clearly coated with epoxy matrix. This means that more matrix failure occurred, which explains the higher Mode-I fracture toughness value.

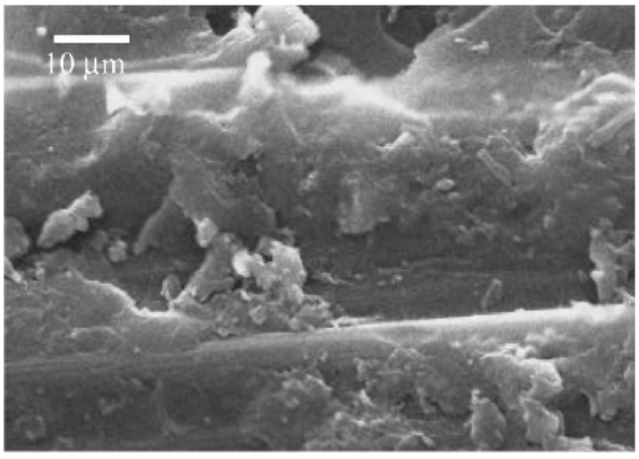

Figure 87: SEM picture (x1000 magnification) of Torayca T800H CF/Epoxy fracture surface after Mode-I testing was performed. It can be appreciated that the fibres are coated with epoxy matrix [43].

Once knowing the degradation of the epoxy due to expiration was a fact, three further tests were performed in order to check its effects on the glass transition temperature (TGA and DSC tests) and a study on the degradation of epoxy with temperature and time.

TGA

TGA – Thermal Gravimetric Analysis – is a technique where a sample of the studied material is subjected to an increase in temperature in order to check its degradation point, so that later DSC test can be performed taking this temperature as an approximate upper limit. A sample of the used CF/Epoxy was studied. Figure 88 shows the data obtained, a plot of the energy released or consumed (DTA), the percentage of mass (TG%) and the mass flow (DTG) as a function of temperature. The test was performed with the Pyris Diamond TG/DTA Thermogravimetric/Thermal analyser (Perkin Elmer), available at the DASML of TU Delft, and a cured CF/Epoxy sample, cut in a circle of 5 mm to fit in the test mould, was heated from room temperature to 350°C at 10°C/min.

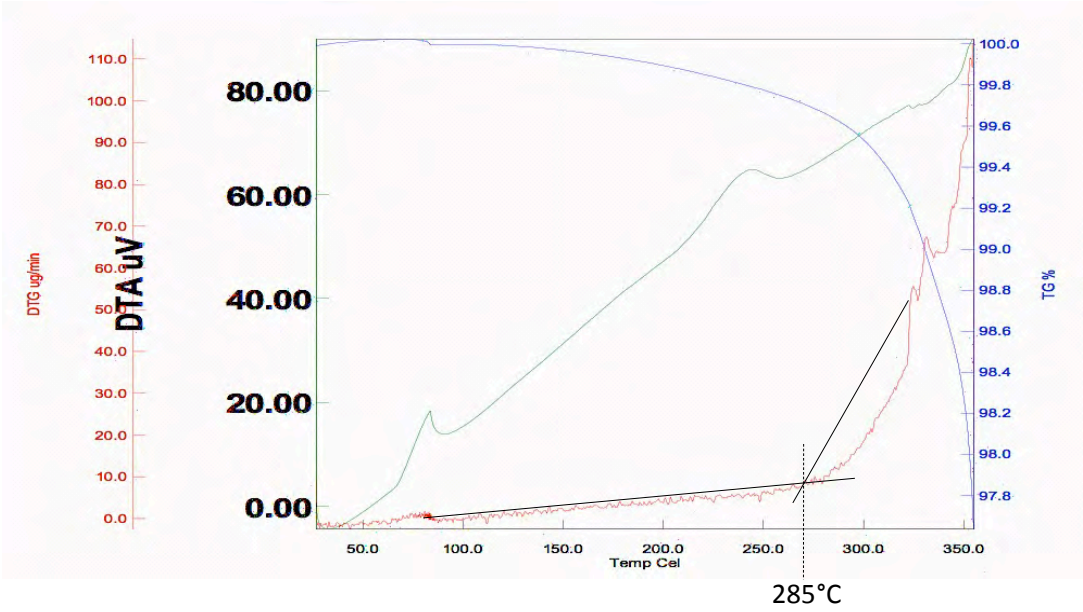

Figure 88: TGA results for Hexply 8852 CF/Epoxy. A degradation temperature of 285°C was found.

The degradation point or start of degradation, where there starts to be great material loss with increasing temperatures, can be obtained in two ways: One is the point where 2% mass loss has occurred, that is 98 % TG; another is the crossing point of the tangents of the mass flow curve (DTG). The second method was chosen, as it gave a lower temperature, therefore, more conservative. Then, it could be stated that the degradation point was, approximately, of 285°C.

DSC

DSC – Differential Scanning Calorimetry – is a technique that measures the heat a material requires to increase its temperature. To do so, the material is heated and cooled twice. A sample of cured CF/Epoxy was studied, with room temperature and 300°C (approximately the degradation temperature measured with the TGA) as the cycle temperature limits; a rate of 20°C/min was chosen. Saphire DSC Perkin Elmer scanner, available at the DASML of TU Delft, was used. A glass transition temperature accurate value can be better extracted from the second heating run, as in the first heating run cold crystallization occurs, where the polymer slightly increases its crystallinity as a reaction to increasing temperature (lower entropy), distorting the glass transition temperature value, so the T_g of the second heating run is a cleaner result [44], [45]. Figure 89 shows the results of this test:

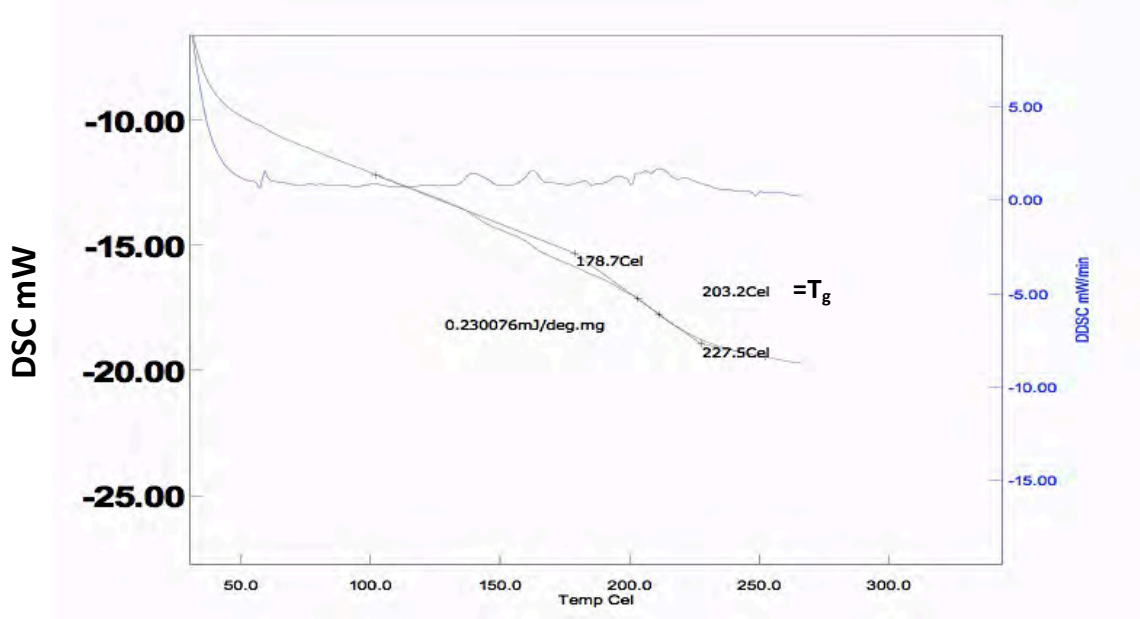

Figure 89: DSC results (2nd heating run) for Hexply 8852 CF/Epoxy. A glass transition temperature of 203.2°C was found.

As the Figure 89 indicates, the glass transition temperature is 203.2°C for our material.

Study on CF/Epoxy heating

In order to check how the used epoxy reacted to temperature held for different amounts of time, seven cured CF/Epoxy samples, of 25.4x101.6 mm^2 dimensions, were heated in the Nabertherm furnace available at the DASML of TU Delft. Table 10 summarizes the temperature and time at which each sample was treated. In the samples where a flat surface was found after heating (not completely delaminated), an FTIR measurement could be performed in order to check its degradation.

Sample ID	Temperature (°C)	Time (min)	Comments
CEH-01	180	4	FTIR test could be performed.
CEH-02	180	15	FTIR test could be performed.
CEH-03	220	4	FTIR test could be performed.
CEH-04	220	15	FTIR test could be performed.
CEH-05	320	4	Fully delaminated. FTIR test could not be performed.
CEH-06	320	15	Fully delaminated. FTIR test could not be performed.
CEH-07	300	4	The surface showed a slight curvature and some bumps that indicated some delamination had occurred, but FTIR test could be performed.

Table 10: CF/Epoxy heated samples information.

Figure 90 shows the two fully delaminated samples (CEH-05 and CEH-06), where most resin was burned away and swollen composites remain.

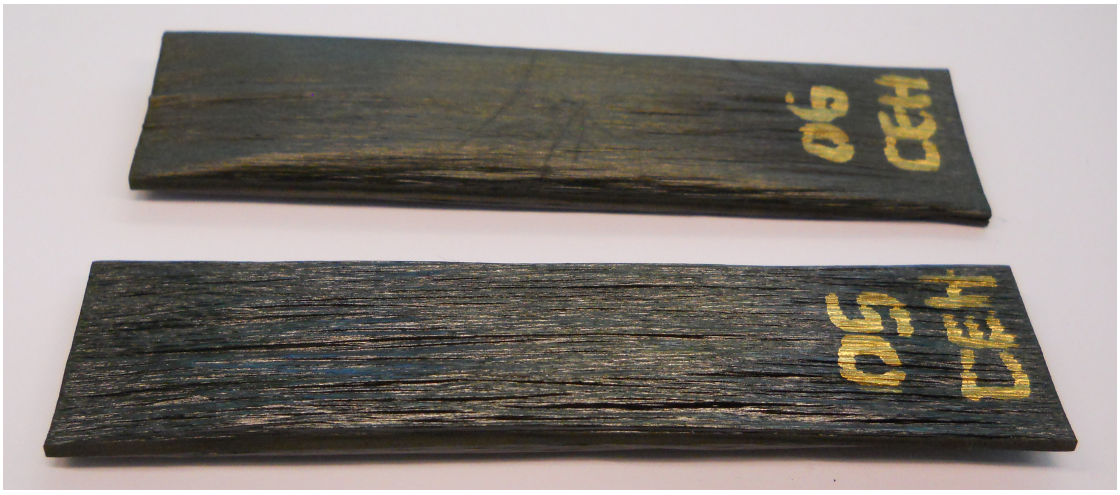

Figure 90: Delaminated CEH-05 and CEH-06 samples. They show swollen composites.

An FTIR analysis of the rest of the samples, compared to a reference non-heated CF/Epoxy sample. There were some areas of the spectra where important differences were found, shown in Figures 91, 92 and 93, which showed that degradation had occurred in all of the heated samples. Samples CEH-04 and CEH-07 had the same spectra, so only one of them is shown in the images for the sake of simplicity; the same was applied for samples CEH-02 and CEH-03.

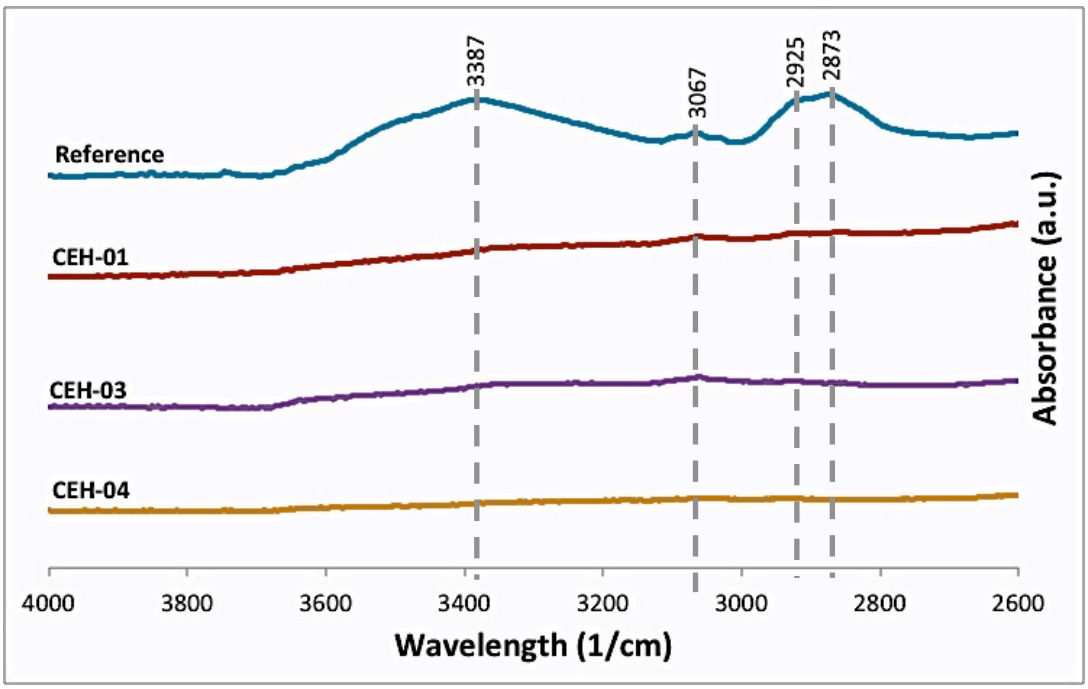

Figure 91: FTIR spectra, from 2600 to 4000 cm^{-1} wavelengths, of a reference CF/epoxy sample, and the heated specimens CEH-01, CEH-03 and CEH-04.

In Figure 91, spectra from 2600 to 4000 cm^{-1} wavelengths is represented. The four indicated peaks – at 3387, 3067, 2925 and 2873 cm^{-1} wavelengths – vanish for the three represented heated samples. The disappearance of the heated samples peaks at 2925 and 2873 cm^{-1} wavelengths, which belong to the CH_2 and CH_3 bonds, indicate damage to the epoxy backbone after the heating. The other two peaks, 3387 and 3067 cm^{-1} wavelengths, belong to the 0-H bond. In Figure 92, two peaks that were not in the reference non-heated sample appear: one at 1663 cm^{-1} wavelength, for sample CEH-01, and another peak at 1719 cm^{-1}, in samples 3 and 4. These peaks belong to the C=0 bond, meaning that the oxygen from the destroyed 0-H bond was rearranged in the heated samples to form a double bond with carbon, so oxidation is occurring. This behaviour may be a sign of oxidation, and consequent degradation.

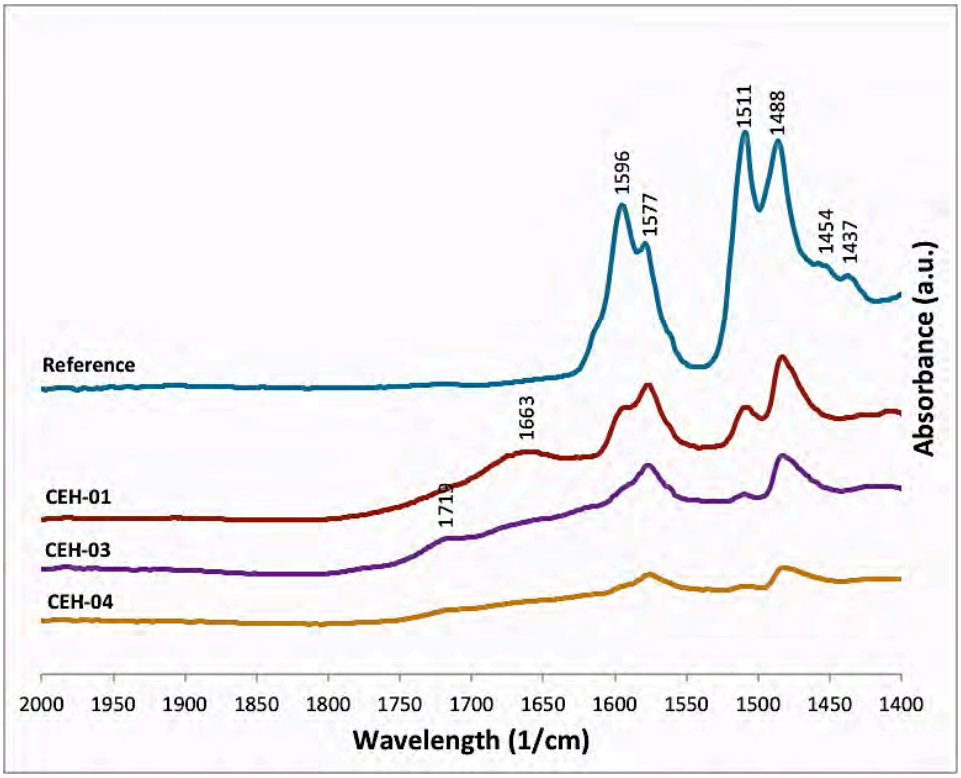

Figure 92: FTIR spectra, from 1400 to 2000 cm^{-1} wavelengths, of a reference CF/epoxy sample, and the heated specimens CEH-01, CEH-03 and CEH-04.

Moreover, in Figure 92, peaks at 1454 and 1437 cm^{-1} wavelengths, present in the reference CF/Epoxy sample, disappear for the heated ones. Peak pairs at 1596 and 1577 cm^{-1} wavelengths, and at 1511 and 1488 cm^{-1} wavelengths, respectively, shift peak intensity with the other peak in the pair for the heated samples, and 1596 and 1511 cm^{-1} ones gradually disappear from increasing temperature/time conditions. These peaks also belong to the C=0 bond region, and these changes happening in the oxygen bond region may also be a sign of oxidation and degradation of the heated samples.

In Figure 93, the indicated peaks – at 1041, 984, 816, 774 and 705 cm^{-1} wavelengths – present in the reference sample, vanish for the heated ones, belonging to the aromatic range of the C-H bond.

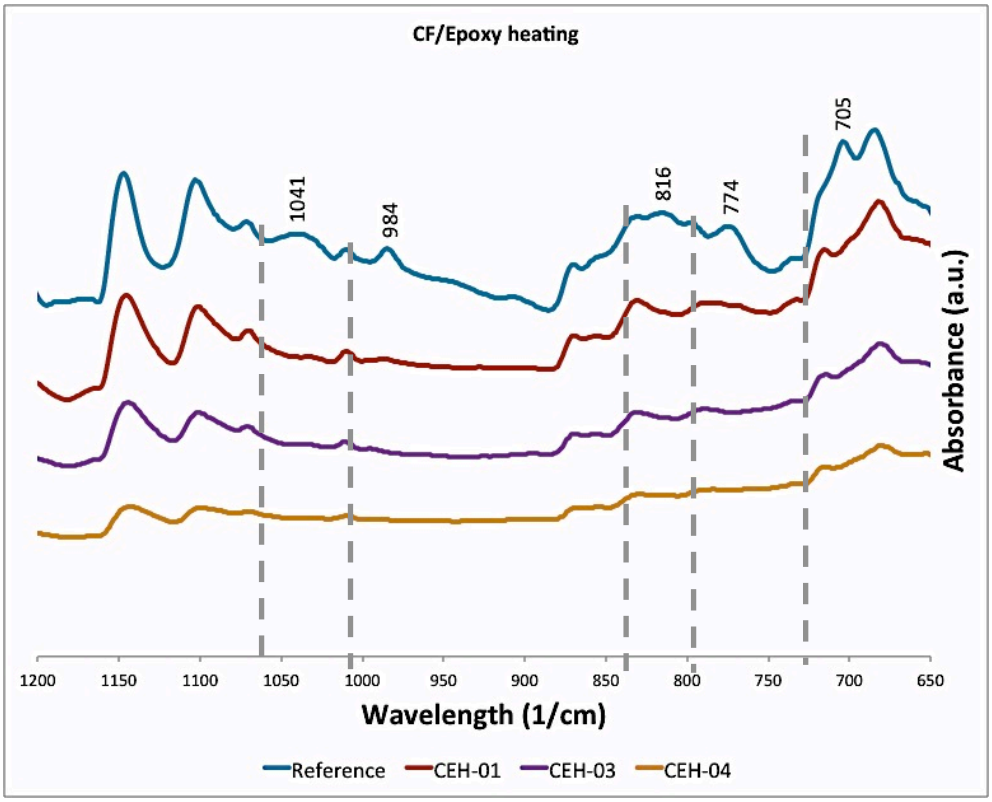

Figure 93: FTIR spectra, from 650 to 1200 cm^{-1} wavelengths, of a reference CF/epoxy sample, and the heated specimens CEH-01, CEH-03 and CEH-04.

The FTIR analysis shows that all the samples were degraded when heated at the oven, for different combinations of temperature and time.

6.2. PPS-UV study

The fact that PEKK and PEEK adhesion with epoxy is enhanced with the UV-ozone treatment, improving the LSS values of the welds, and that that the contrary effect happened when treating PPS film with UV light, raised the hypothesis of PPS degradation with UV-ozone treatments. The PPS film used in this study was the one available for this project, described in section 2.1.1.

TGA and DSC tests were carried out on non-treated and treated PPS – the same UV treatment than the one performed for the hybrid welds, 40 minutes of UV-light on one side of the film, 2 minutes on the other one –, but no significant difference was observed in the obtained graphs or glass transition temperature value. Then, another test was decided to be taken: Treating PPS films with UV light for different times – 5, 10, 15, 30, 45 and 60 minutes, respectively – and performing an FTIR analysis of the films, comparing them to a non-treated PPS film. There were two main areas of the spectra were differences could be observed, shown Figures 94 and 95. The rest of the spectra were the same for the treated and non-treated samples.

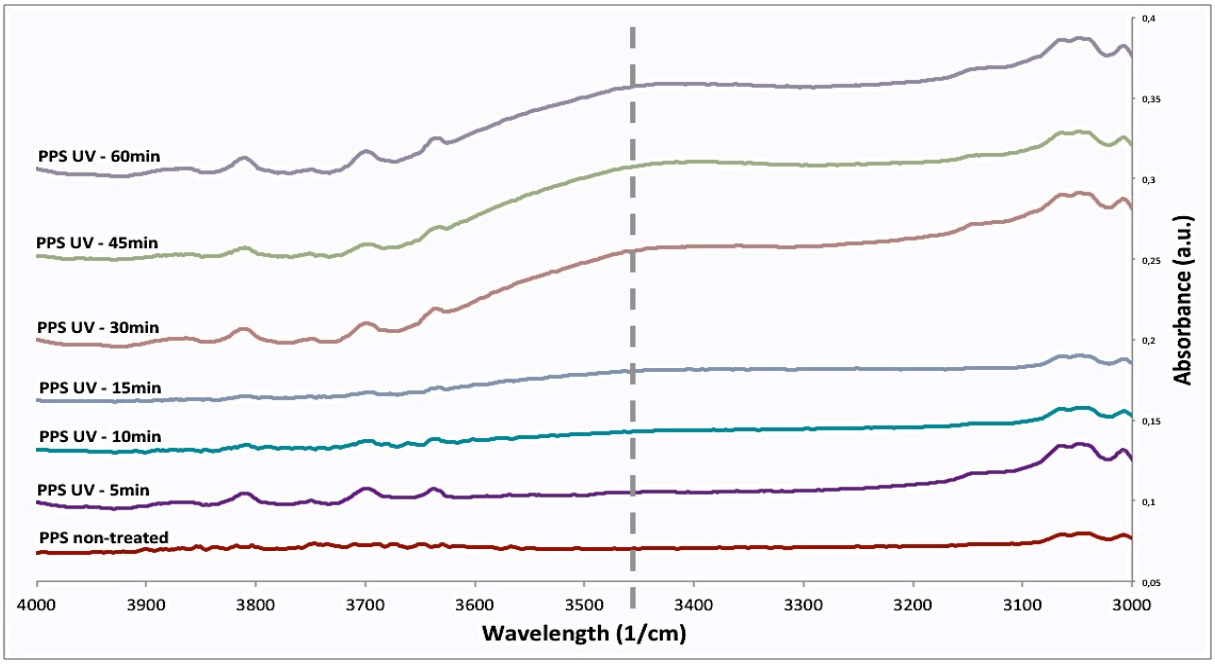

Figure 94: FTIR absorbance spectra from 3000 to 4000 cm^{-1} wavelengths for the non-treated and UV-treated PPS films. The graph shows that a peak at 3450 cm^{-1}, belonging to the O-H bond (3000 to 3600 cm^{-1}), is created with the UV treatment and increases its intensity for increasing UV-exposure times, shifting the baseline upwards.

In Figure 94, the absorbance spectra for the non-treated PPS film and the UV exposed ones, treated for different times. The most remarkable behaviour is the baseline change, shifting upwards, from the sample treated for 10 minutes to the one treated for 60, including also these two. This change occurs in the O-H bond part of the spectra – which covers from 3000 to 3600 cm^{-1} wavelengths –, increasing its intensity for increasing UV-exposure times, and gradually forming a peak at 3450 cm^{-1} (grey discontinuous line), also inducing an upward shift of the baseline. This seems to indicate that PPS starts absorbing water with increasing UV-exposure time, an interesting behaviour because PPS is known to absorb very little water.

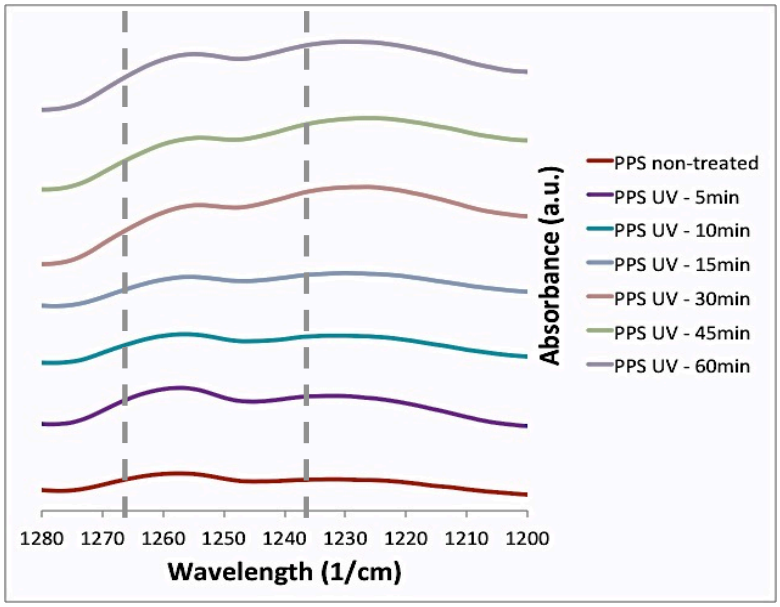

Figure 95: FTIR absorbance spectra from 1200 to 1280 cm^{-1} wavelengths for the non-treated and UV-treated PPS films. The graph shows that the peaks at 1260 and 1230 cm^{-1}, belonging to the C-O bond (1000 to 1300 cm^{-1}) shift their intensity and gradually increase, from the 15 minutes-treated film, with increasing UV-exposure time.

In Figure 95, which shows the C-O range, the peaks at 1260 and 1230 cm^{-1} wavelengths shift their intensity with increasing UV-exposure time: First, the 1260 cm^{-1} peak is higher than the 1230 cm^{-1} one, and from 15 minutes-treated film to the 60 minutes-treated one, including them, the peak intensity shifts, gradually increasing their intensity with UV-exposure.

These behaviours, observed in Figures 94 and 95, are originated by the ozone that is generated in the UV-treatment, as commented in Chapter 1: UV light is irradiated at different wavelengths, being absorbed by oxygen to form ozone, or by ozone/hydrocarbons to decompose the ozone/hydrocarbon substances. The formation and decomposition of ozone originates atomic oxygen, which acts as a strong oxidizer. That is the reason of changes in the bonds where oxygen takes part (O-H, C-O), keeping the rest of the bonds of the spectra unaltered; apart from the UV-ozone treatment, these changes indicate that possible oxidation and degradation of the PPS film is happening.

DSC analysis showed that the glass transition temperature was unchanged for the treated PPS films with respect to the treated one, suggesting that the overall crystallinity of the material does not change. Nevertheless, observations made with the Leica optical microscope, available at the DASML of TU Delft, of the 60 minutes-treated – the most limiting case because of having the highest UV-exposure time – and the non-treated films, show different crystal size and appearance in the two films – it is worth to remember that our material is semi-crystalline –, as well as other dissimilar features. Figures 96, 97, 98 and 99 show these observations.

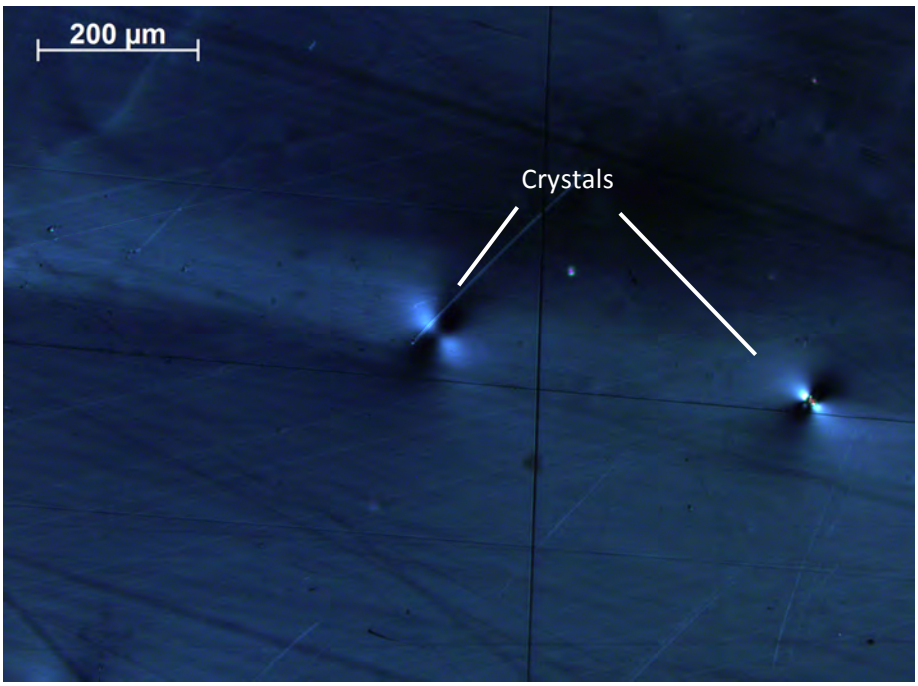

Figure 96: Leica microscope cross-polarized image (x10 magnification) of PPS non-treated film. Crystals surrounded by amorphous region can be appreciated.

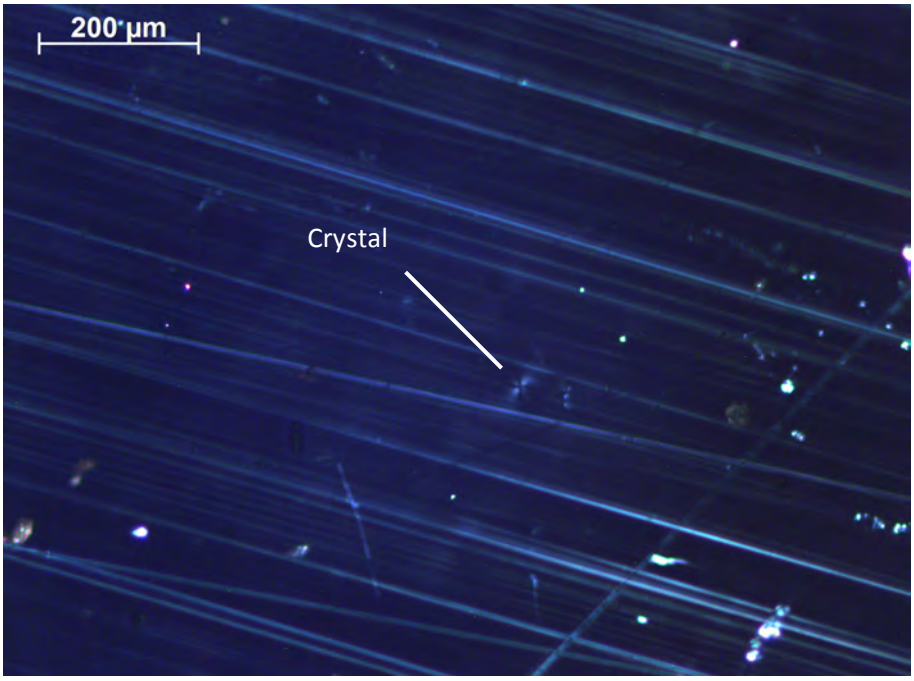

Figure 97: Leica microscope cross-polarized image (x10 magnification) of PPS UV-treated film (60 minutes). Smaller crystals and crystalline-lines can be observed.

Figures 96 and 97 show cross-polarized images of non-treated and 60 minutes-treated PPS films, respectively. The dark colour indicates amorphous regions, and the shiny flashes, the presence of a crystal. It can be appreciated that for non-treated PPS, crystals are bigger, and more quantity was observed, with a dark amorphous region surrounding them. For the treated analysed film, the size of the crystals decrease, and also straight shiny lights appear, into which the crystals seem to have merged and that also indicate directions of crystallinity. This proves that crystal size and morphology of PPS change with UV, remaining with the same overall crystallinity that give identical T_g value for the treated and non-treated films.

Figures 98 and 99 show the comparison of two optical microscope images taken with the reflection mode. It can be appreciated that film is decoloured in different areas when treating it with UV for 60 minutes, compared to the non-treated plain colour film. This appearance also suggests degradation and absorption of water (as Figure 94 indicated) are occurring.

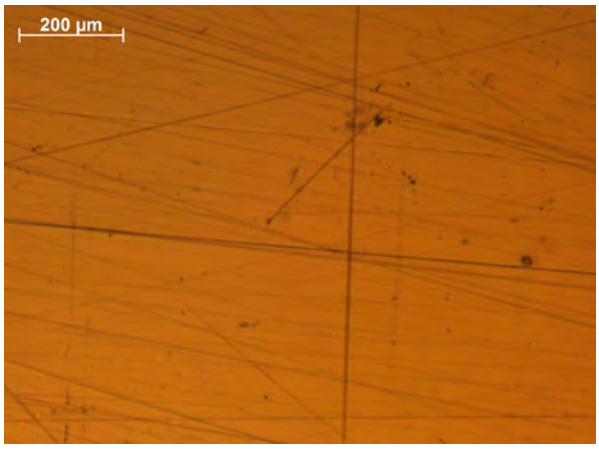

Figure 98: Leica microscope reflection-mode image (x10 magnification) of PPS non-treated film.

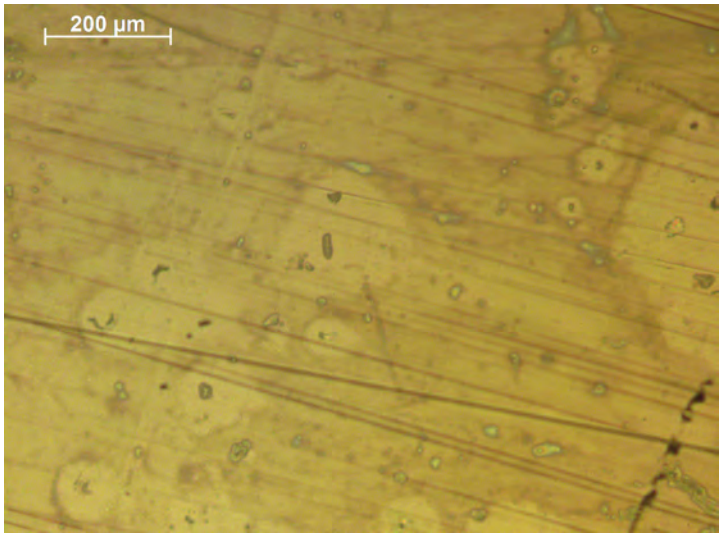

Figure 99: Leica microscope reflection-mode image (x10 magnification) of PPS UV-treated film (60 minutes). Decolouration of the film can be observed, which may indicate the presence of moisture.

Taking into account that FTIR obtains the infrared absorbance spectra from 550 to 4500 cm^{-1} wavelengths, a Raman analysis, performed with Renishaw inVia Raman microscope available at the DASML of TU Delft, was also done for these UV treated films and the non-treated one, which analyses the material absorbance from 0 to 550 cm^{-1} wavelengths, in order to check if there were additional peak alterations among the films for this range. No difference was observed among them for this range of the spectra.

Chapter 7

New experiments and SHW conclusions

7.1. NEW EXPERIMENTS

With the arrival of a new, fresh epoxy – Hexply M21, provided by Hexcel – one of the hybrid successful welds was decided to be repeated. As a reminder, the welds which provided a higher LSS value were the ones which used the following thermoplastic co-cured films: PEKK UV, PEKK 1st chloroform-amine formula, PEEK UV, PEEK acetic, and PPS NT. The weld formed by CF/Epoxy co-cured with PEKK UV-O_3 was decided to be repeated.

7.1.1. Part I

Materials

For the PEKK film, a new 40 µm-thick one, rough/mate on one side and shiny on the other, and provided by Arkema, was used. It was treated with the UV-ozone treatment used in the previous welds: 40 minutes of exposure on one side, 2 minutes on the other one. It was decided to apply the 40 minutes treatment to the rough face, as it will be the one in contact with the epoxy during the co-curing in the autoclave and the advantage of mechanical interlocking can be taken.

The Hexply M21 epoxy was available in prepreg form, with UD carbon reinforcement, in a roll of 300 mm wide and 11 metres long. Eleven layers of 150 x 300 mm^2, with the zero direction of the fibres aligned with the 165 mm side, were cut from the roll using a pair of scissors, and stacked one on top of the other with $[0]_{11}$ sequence. They presented some bubbles, and in order to remove them and possible air inside the stack, a vacuum bag was prepared and the 11 epoxy stacked layers were held under vacuum conditions for 30 minutes approximately. The UV treatment was performed on a 50 x 300 mm^2 PEKK film during this time. Figure 100 shows a sketch of the curing panel and the samples to be cut from it. Then, the autoclave vacuum bag was prepared in the same way as described in the processes of Chapter 2, with the PEKK film on top of the epoxy stack and an aluminium plate covered in red foil on top of them to assure a smooth surface. The autoclave cycle for this epoxy was: 2 hours at 180°C, 7 bars of pressure; Figure 101 shows the autoclave cycle for this epoxy.

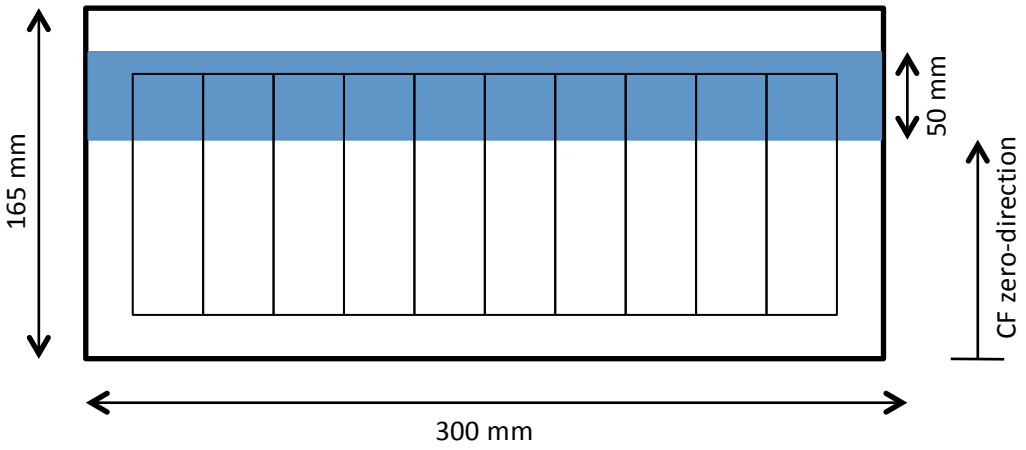

Figure 100: Sketch of the autoclave curing panel formed by Hexply M21 CF/Epoxy co-cured with a stripe of PEKK UV-treated film, and the samples that were cut from it afterwards.

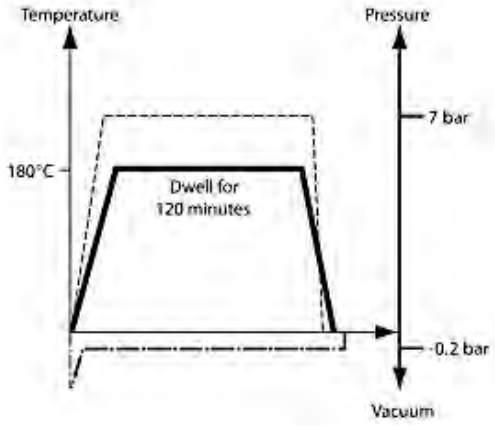

Figure 101: Hexply M21 CF/Epoxy curing cycle [41].

After the curing, it was observed that uneven resin outflow occurred, being higher on top part of the panel in the sketch that Figure 100 displays, and leaving a drier edge at the bottom part of the panel. This probably happened because the panel was not symmetric in the XY plane due to the presence of the thermoplastic co-cured film, an effect that may be probably enhanced by the aluminium panel on top; although it was very thin, this caused the thickness of the bottom part of the panel in sketch to be smaller. Luckily, this thickness difference did not affect the region of the panel where the samples were cut from. In the future, this problem can be avoided by the symmetric arrangement of the thermoplastic film on the panel in the XY plane, if its size is smaller than the CF/Epoxy panel. In the previous autoclave cycles, the thermoplastic film covered the whole panel, hence this problem was not encountered. The cured panel, with an approximate thickness of 2.4 mm, was cut with the diamond blade cutter, available at the DASML of TU Delft, in ten 25.4 x 101.6 mm^2 samples, as Figure 100 shows.

Energy directors were manufactures from the same Arkema film as the one used in the co-curing, re-consolidating them in the Joos Press following the same process as for PEKK EDs, described in Chapter 2, and obtaining 0.25 mm-thick energy directors.

Procedure

The samples were ultrasonically welded to CF/PEKK substrates. Table 11 summarizes the welds performed. PEKK reference samples are reminded in this section too.

Sample reference	Bottom substrate	Top substrate	Energy director	Thermoplastic coating	Observations
REF-PEKK	CF/PEKK (Ten Cate)	CF/PEKK (Ten Cate)	PEKK (Victrex)	-	Reference welds. Six welds performed: -5 samples for mechanical (LSS) testing. -1 sample for optical microscopy (OM).
NE1-PEKK-40	CF/Epoxy (Hexply M21)	CF/PEKK (Ten Cate)	PEKK (Arkema)	PEKK UV – 40 µm (Arkema)	Reference welds. Seven welds performed: -6 samples for mechanical (LSS) testing. -1 sample for optical microscopy (OM).

Table 11: Reference and New Experiments (I) welds.

As a new PEKK energy director was used, with a different type of resin, the optimum parameters for SHW-1PEKK-40 hybrid weld were determined by welding a CF/PEKK to another CF/PEKK substrate with 1500 N, A9 and 0.25 (100%) mm of travel, and checking in the obtained graph the optimum travel, which was 0.09 mm.

Table 12 collects the welding conditions and welder outputs for each weld type:

Sample reference	Welding parameters			Average welding time (ms)	Average consumed power (%)	Average welding distance (mm)
	Force (N)	Amplitude	Travel (mm)			
REF-PEKK [a]	1500	A9 (86.2 µm)	0.15	515	110	0.25
NE1-PEKK-40	1500	A9 (86.2 µm)	0.09	400	101	0.18

Table 12: Welding conditions and outputs for NE1-PEKK-40 and reference welds.

[a] It is worth to point out that these reference welds were the ones using the Victrex PEKK ED, used also as a reference for the welds in Chapter 3.

Mechanical Testing

The hybrid welds were lap-shear tested, and the results are shown in the chart of Figure 102.

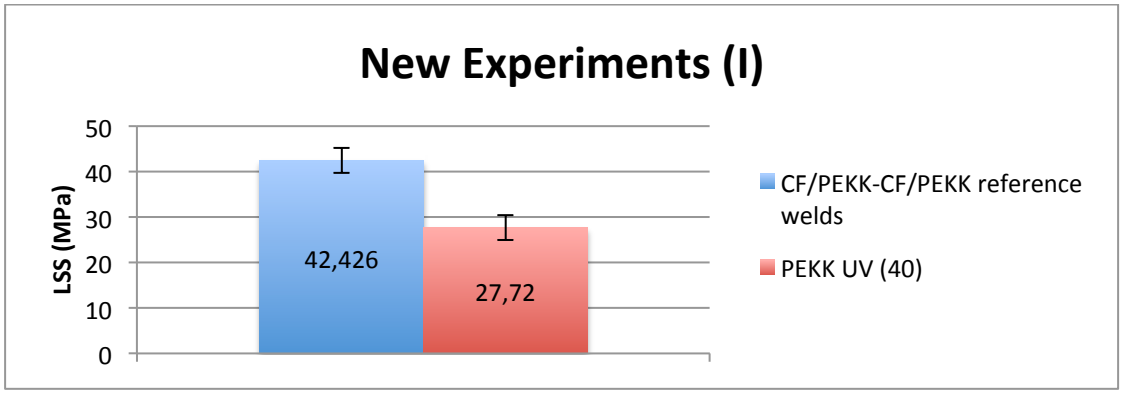

Figure 102: LSS values for New Experiments (I) welds.

As it can be appreciated, the mean LSS value (27.72 MPa) was higher than the value obtained with the other epoxy type (Chapter 3), which indicates that the strength of the joint is improved with the new fresh epoxy. The samples had a 2.77 scatter. Further fracture surface analysis will bring more light to this fact. One of the tested samples led to 31.04 MPa.

New experiments (I): PEKK UV 40 µm

- CROSS SECTION STUDY

Figure 103 shows the cross section of the CF/Epoxy substrate, co-cured with the 40 µm-thick PEKK UV film, before welding.

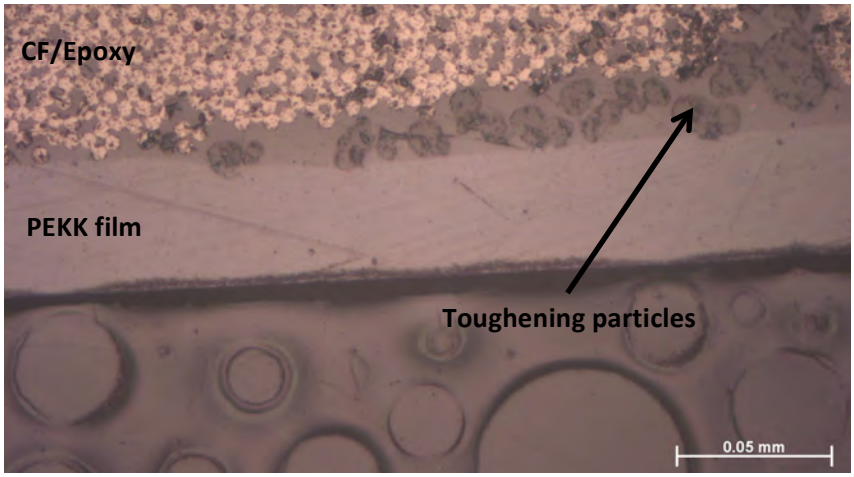

Figure 103: Zeiss microscope picture (x50 magnification) of the cross section of CF/Epoxy (Hexply M21) co-cured with PEKK UV (40 µm) – New Experiments I. Good merging of the epoxy resin and the thermoplastic can be appreciated. Toughening particles in the epoxy, shaped as bubbles, can be seen on the CF/Epoxy substrate.

Very good merging of the two materials can be appreciated. Epoxy toughening particles, in the shape of bubbles, can be appreciated at the interface with PEKK, as Figure 103 shows, and in the epoxy internal layer, as can be appreciated in Figure 104. At first they were thought to be voids, but the alternative of the toughening material is more strongly believed, also because voids have a black colour and these have a lighter one. These particles, probably composed by a thermoplastic such as PEEK or PEI, merge with the PEKK resin.

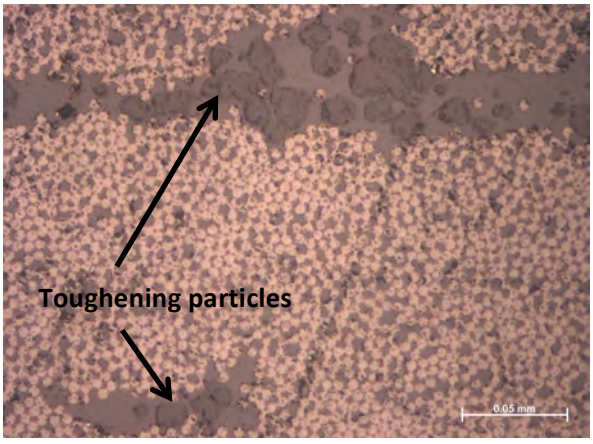

Figure 104: Zeiss microscope image (x50 magnification) of the internal layer of Hexply M21 CF/Epoxy, where toughening-material bubbles could be also spotted.

Figure 105 shows the cross section of the weld with CF/PEKK. It is interesting to see how the toughening material of the epoxy and the PEKK intermingle. Some voids were spotted in the PEKK-rich area of the interface along the weld cross section.

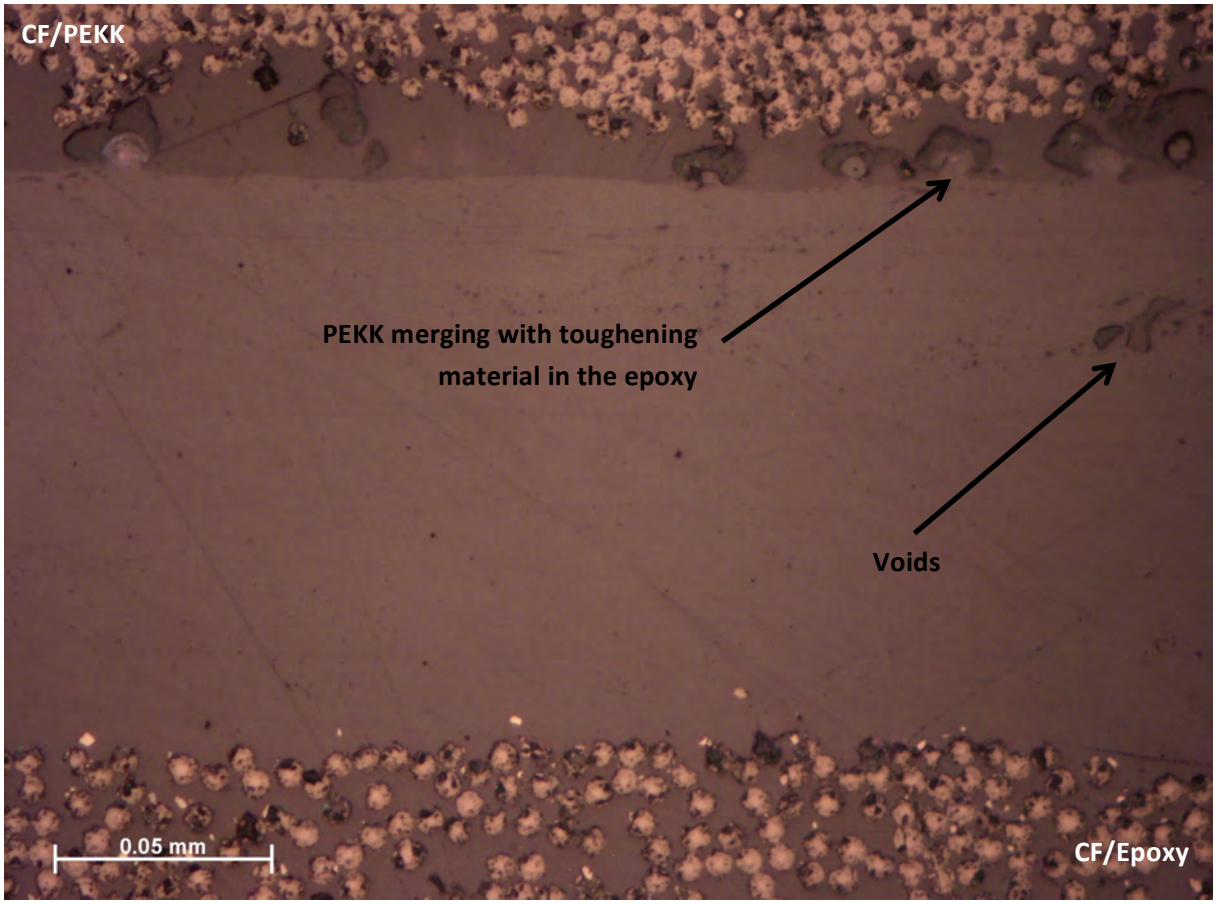

Figure 105: Zeiss microscope picture (x50 magnification) of the weld formed by CF/Epoxy co-cured with PEKK UV (40 µm) – New Experiments I. Some voids could be spotted in the PEKK-rich area of the interface.

- FRACTOGRAPHY

Figure 106 shows a camera picture of the fracture surface of the studied welding type. Cohesive failure is believe to be happening. On the CF/PEKK fracture surface, PEKK rich-spots can be appreciated. The CF/Epoxy surface shows a textured appearance, mainly covered with PEKK resin, but showing also some spots, which expose the CF/Epoxy. These spots coincide with the toughening particles at the interface, which suggest that the PEKK and the toughening material combination is not as string as the combination of the first one with the epoxy resin. Figure 107 shows a higher magnification image of this CF/Epoxy surface, taken with the Zeiss SteREO Discovery V.8 microscope.

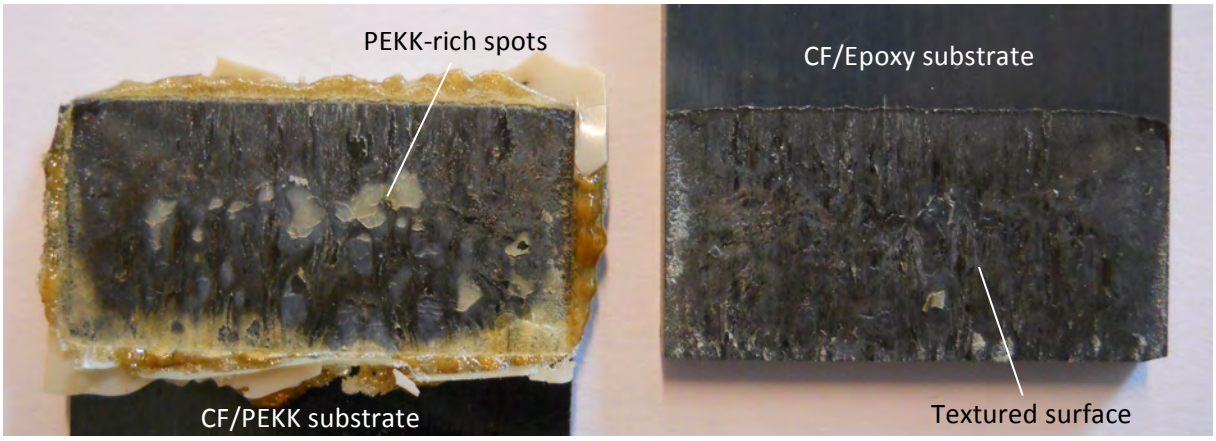

Figure 106: Fracture surface of NE1-PEKK-40 weld. PEKK-rich spots can be appreciated on the CF/PEKK fracture surface; cohesive failure and textured surface are seen on the CF/Epoxy one.

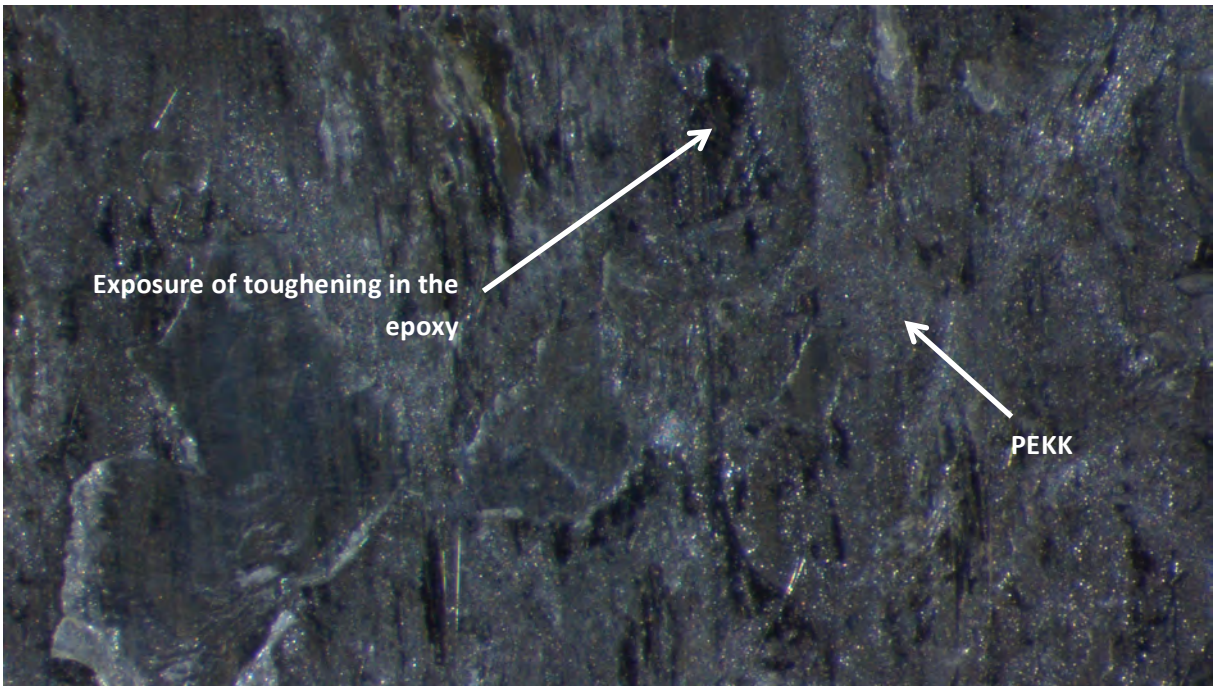

Figure 107: Zeiss SteREO microscope picture of CF/Epoxy fracture surface. Mainly, PEKK can be found, which shows that cohesive failure is the fracture type of this weld. Spots or small areas of CF/Epoxy are also exposed, coinciding the part if the interface where the epoxy toughening particles are in contact with the PEKK resin.

Induced Degradation Experiment

With a spare sample of CF/Epoxy co-cured with PEKK UV (40 µm), an additional experiment was carried out. In order to prove that short welding times, achieved with a combination of high amplitude-force parameters, avoid the degradation of the epoxy, a hybrid weld using low amplitude and force was performed. Table 13 summarizes the welds performed.

Sample reference	Bottom substrate	Top substrate	Energy director	Thermoplastic coating	Observations
ID-PEKK-40	CF/Epoxy (Hexply M21)	CF/PEKK (Ten Cate)	PEKK (Arkema)	PEKK UV – 40 µm (Arkema)	Reference welds. Six welds performed: -5 samples for mechanical (LSS) testing. -1 sample for optical microscopy (OM).

Table 13: Induced-degradation weld.

Table 14 collects the welding conditions and welder outputs for each weld type:

Sample reference	Welding parameters			Average welding time (ms)	Average consumed power (%)	Average welding distance (mm)
	Force (N)	Amplitude	Travel (mm)			
ID-PEKK-40	300	A1 (51.8 µm)	0.09	3524	36	0.12

Table 14: Welding conditions and outputs for ID-PEKK-40 weld.

The welding had to be stopped before it finished due to the large smoke coming out of it. It can be appreciated that a small power consumption and large welding timed were achieved with the low amplitude-force combination. The weld could be broken with the hands, and its fracture surface is shown in Figure 108:

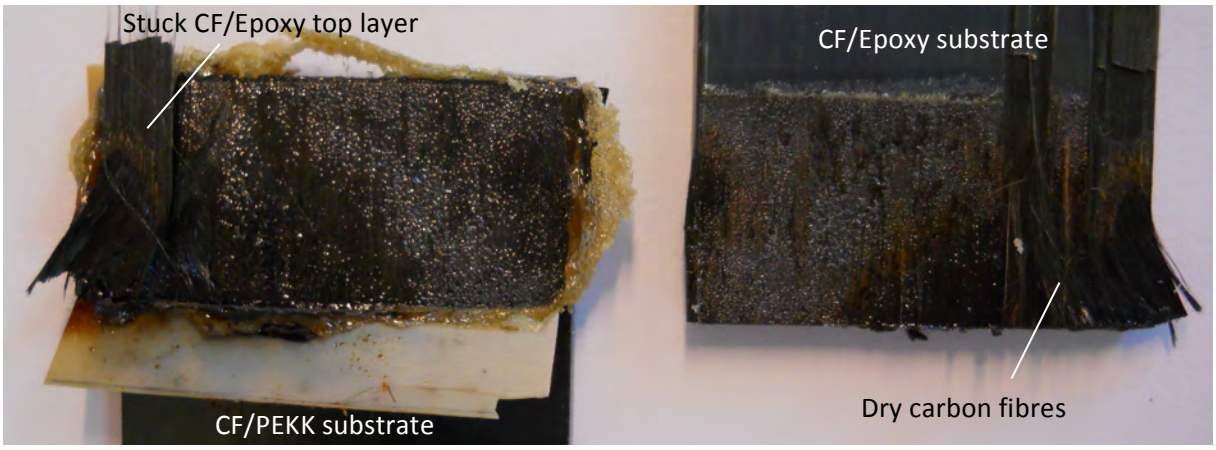

Figure 108: Induced-degradation weld fracture surface. High-intensity burning of the epoxy and PEKK resins, with exposure of dry carbon fibres and delamination on the CF/Epoxy substrate is appreciated.

The fracture surface image shows that epoxy and PEKK resins are greatly burned at the interface, the epoxy being degraded. Delamination of the CF/Epoxy also occurs, with a part of its top layer remaining attached to the CF/PEKK substrate. The experiment showed that a low amplitude-force combination for the welding parameters leads to high welding time that degrade the epoxy and destroy the hybrid weld.

Conclusions

In this first part of the new experiments, the PEKK UV-O_3 hybrid weld was repeated using a new and fresh CF/Epoxy (Hexply M21) and a 40 µm-thick PEKK film. The welds show to achieve a higher LSS value than the one performed in Chapter 3, with cohesive failure as the main failure type. Bubbles of toughening material, probably of thermoplastic, were found at all the epoxy layers, mixing with the PEKK at the interface.

An additional experiment, where a CF/Epoxy sample co-cured with PEKK UV-O_3 was ultrasonically welded to a CF/PEKK substrate, was carried out: Low amplitude-force parameters were selected in order to seek and prove epoxy degradation. A very large welding time was achieved, resulting in burnt and degraded epoxy with the result of an ineffective weld.

7.1.2. Part II

The same type of hybrid weld – CF/PEKK co-cured with PEKK UV-O_3 treated film ultrasonic welded to CF/PEKK – was decided to be repeated, using 40 and 100 µm-thick co-cured PEKK films.

Materials

Arkema PEKK films were used for the co-curing with the epoxy, a 40 and 100 µm-thick, both rough/mate on one side and shiny on the other. They were treated with the same UV-O_3 procedure as in the first part of the new experiments.

The same Hexply M21 epoxy prepeg was used. Eleven layers of 250 x 300 mm^2, with the zero direction of the fibres aligned with the 250 mm side, were cut and stacked ($[0]_{11}$ sequence). The vacuum process prior to autoclave curing was performed, but this time for 5 layers first, and 6 layers afterwards, in order to enhance the ejection of voids between the layers and their compactness. The UV-O_3 treatment was performed on two 50 x 300 mm^2 PEKK films, 40 and 100 µm-thick respectively. A sketch of the curing panel and the samples to be cut from it is shown in Figure 109. The same vacuum bag layup as before and in Chapter 2 was used. Nevertheless, this time no aluminium plate was placed on top of the stack, and the thermoplastic films were placed below the layers of epoxy prepeg, so that the welding surface was smooth. The other panel surface will have a weave or textured pattern induced by the layup blankets on top of it. The same autoclave cycle as in the first part was used (2 hours at 180°C, 7 bars of pressure).

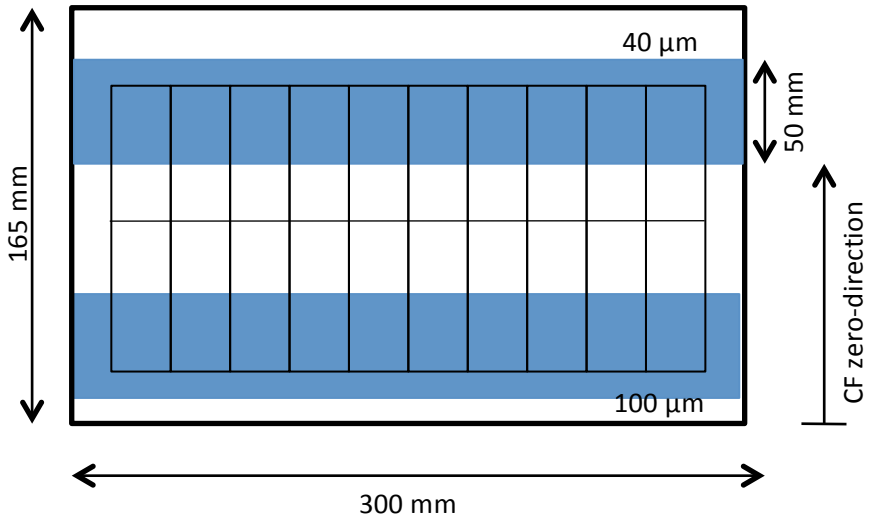

Figure 109: Sketch of the autoclave panel for the second part of the new experiments.

The cured panel had a thickness of 2.4 mm approximately. No uneven resin flow or dry edges, as well as lower resin outflow, were seen in this panel, meaning that the panel layup of this second part implies a better curing approach. Although the thickness of the thermoplastics films was on the top and bottom parts of the panel in Figure 109, not using the top aluminium plate certainly made this asymmetry unimportant. The panel was also cut at the DASML with the diamond blade cutter, this time in twenty 25.4 x 101.6 mm^2 samples. The same 0.25 mm-thick PEKK energy directors, provided by Arkema, were used.

Procedure

Table 15 collects the two types of new hybrid welds, as well as the reference PEKK welds.

Sample reference	Bottom substrate	Top substrate	Energy director	Thermoplastic coating	Observations
REF-PEKK	CF/PEKK (Ten Cate)	CF/PEKK (Ten Cate)	PEKK (Victrex)	-	Reference welds. Six welds performed: -5 samples for mechanical (LSS) testing. -1 sample for optical microscopy (OM).
NE2-PEKK-40	CF/Epoxy (Hexply M21)	CF/PEKK (Ten Cate)	PEKK (Arkema)	PEKK UV – 40 µm (Arkema)	Reference welds. Six welds performed: -5 samples for mechanical (LSS) testing. -1 sample for optical microscopy (OM).
NE2-PEKK-100	CF/Epoxy (Hexply M21)	CF/PEKK (Ten Cate)	PEKK (Arkema)	PEKK UV – 100 µm (Arkema)	Reference welds. Six welds performed: -5 samples for mechanical (LSS) testing. -1 sample for optical microscopy (OM).

Table 15: Reference and New Experiments (II) welds.

In Table 16, the welding conditions and welder outputs for each weld type are summarized:

Sample reference	Welding parameters			Average welding time (ms)	Average consumed power (%)	Average welding distance (mm)
	Force (N)	Amplitude	Travel (mm)			
REF-PEKK	1500	A9 (86.2 µm)	0.15	515	110	0.25
NE2-PEKK-40	1500	A9 (86.2 µm)	0.09	370	102	0.16
NE2-PEKK-100	1500	A9 (86.2 µm)	0.09	350	106	0.15

Table 16: Welding conditions and outputs for MMHW and reference welds.

Both welding times were very short, a clear advantage for the avoidance of epoxy degradation. It is interesting to check that, for the 40 µm welds, the same type as in the first part of the new experiments, the average welding time was 30 ms lower than in the previous case. It is believed that this difference might be caused by the richer content of resin of the samples that resulted from the new panel layup in the autoclave curing.

Mechanical Testing

The chart of Figure 110 shows the LSS results for the two types of welds of this second part.

NE2-PEKK-40 samples had a mean LSS of 34.74 MPa, a high and very positive value for the case of a hybrid weld, and a standard deviation of 2.73. One of its welds led to an LSS value of 37.36 MPa.

LSS tests of NE2-PEKK-100 samples resulted in a mean lap-shear stress of 28.61 MPa, and a standard deviation of 6.85. It is interesting to check that for the weld type with a thicker thermoplastic interface, the strength was lower and the results had a larger scatter.

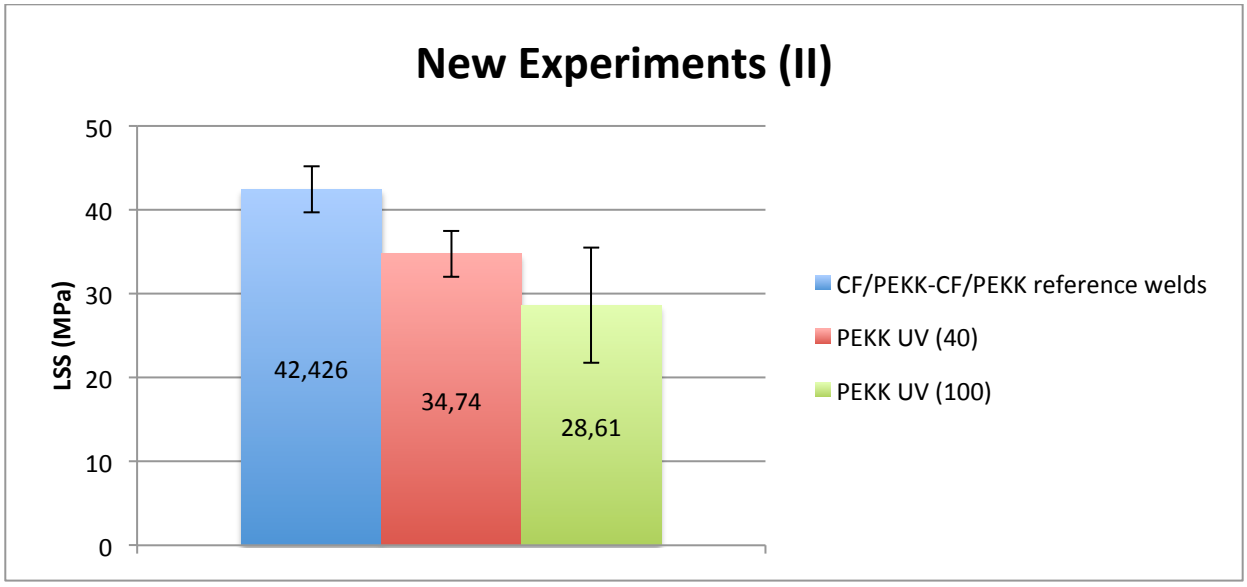

Figure 110: LSS values for New Experiments (II) welds.

New experiments (II): PEKK UV 40 µm

- CROSS SECTION STUDY

Figure 111 shows the cross-section of the CF/Epoxy co-cured with 40 µm-thick PEKK UV substrate, which has the same appearance as the same substrate of NE1-PEKK-40 weld. Good merging of the thermoset with the thermoplastic material, and the toughening epoxy particles can be appreciated.

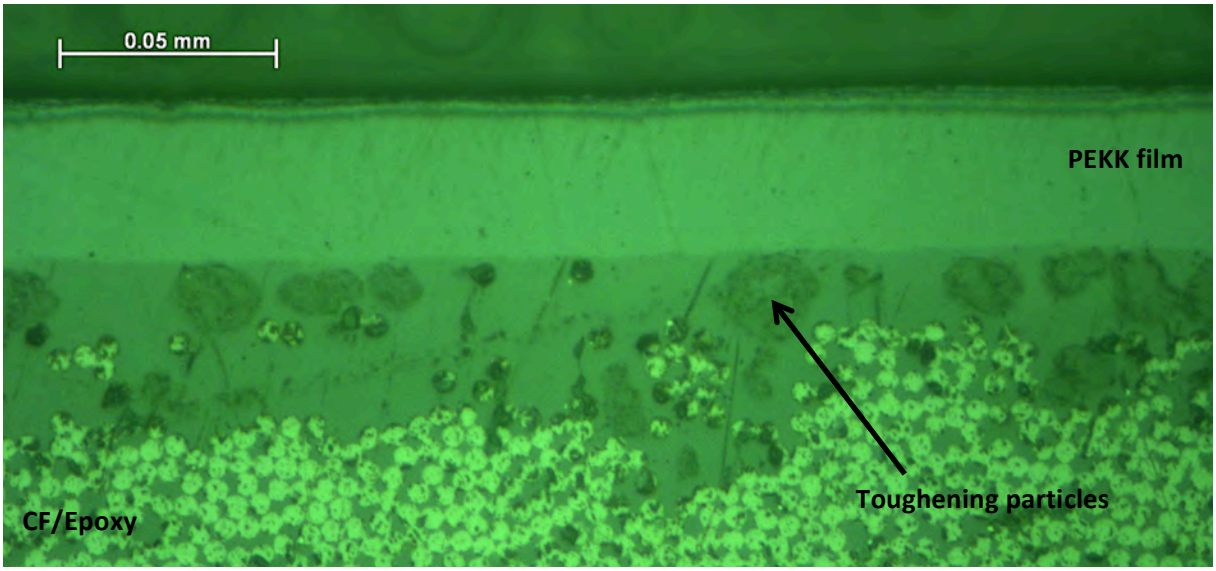

Figure 111: Zeiss optical microscope picture (x50 magnification) of the CF/Epoxy, co-cured with 40 µm-thick PEKK UV film (New Experiments II). Good merging between the epoxy and the PEKK film, as well as toughening particles in the epoxy, can be seen.

Figure 112 shows the cross section of the studied weld NE2-PEKK-40. Good merging and compatibility among the materials can be appreciated. There were some areas with a line between the PEKK ED and the PEKK matrix from the substrate, showing that at those points they did not

optimally merge, but they are believed to be local unimportant defects. Some voids appeared at the PEKK interface across the cross section.

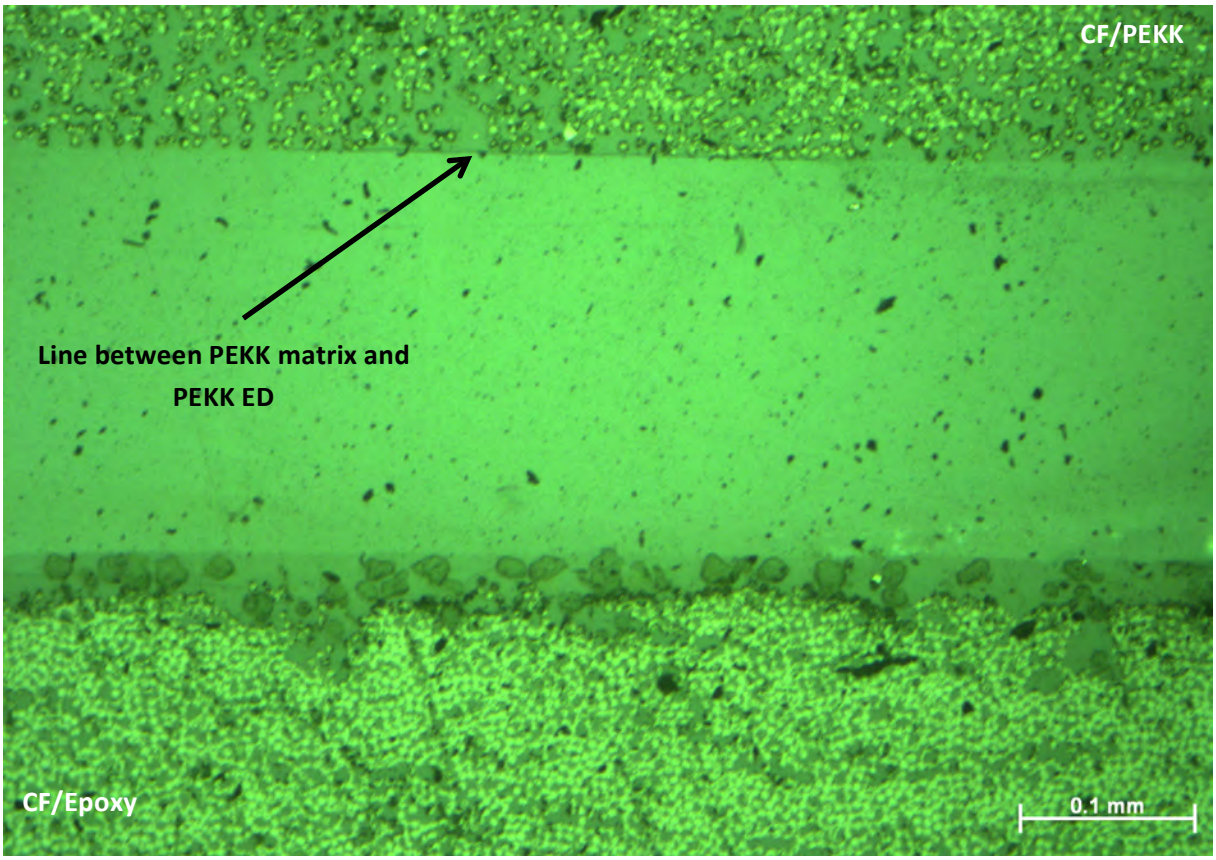

Figure 112: Zeiss optical microscope image (x50 magnification) of NE2-PEKK-40 weld. Good merging and compatibility among the materials can be appreciated. There were some areas with a line between the PEKK matrix and ED.

- FRACTOGRAPHY

Figure 113 shows the fracture surface of the studied weld. Cohesive failure is the main fracture type. On the CF/PEK surface, PEKK-rich spots can be seen. CF/Epoxy surface shows to be mainly covered by PEKK, with some spots or cavities that expose the epoxy. They coincide with the areas where PEKK and the toughening material from the epoxy were in contact, showing that their compatibility was not as good as the epoxy-PEKK one. There are also a few narrow lines of interlaminar failure of the epoxy, with stuck carbon fibres from it on the CF/PEKK substrate, due to the strong joint between PEKK and epoxy resins, not to epoxy degraded properties, as what happened with Hexply 8552 one.

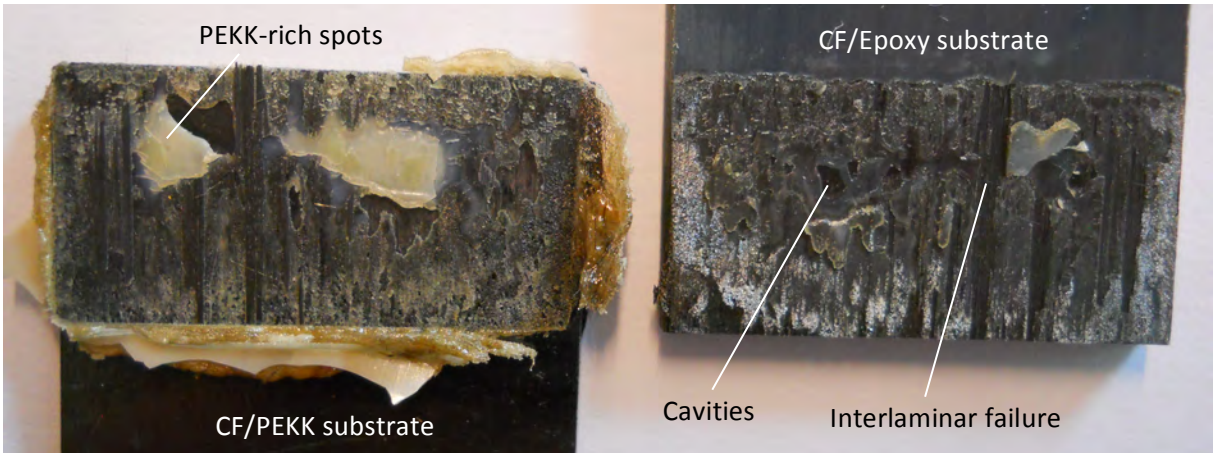

Figure 113: Fracture surface of NE2-PEKK-40. Cohesive failure is the main failure type, with cavities and slight interlaminar failure on the CF/Epoxy substrate, and PEKK-rich spots on the CF/PEKK one.

New experiments (II): PEKK UV 100 µm

- CROSS SECTION STUDY

Figure 114 shows the cross section of the substrate formed by CF/Epoxy co-cured with 100 µm-thick PEKK UV-O_3 film. As with the thinner co-cured film, epoxy and treated PEKK show an excellent adhesion.

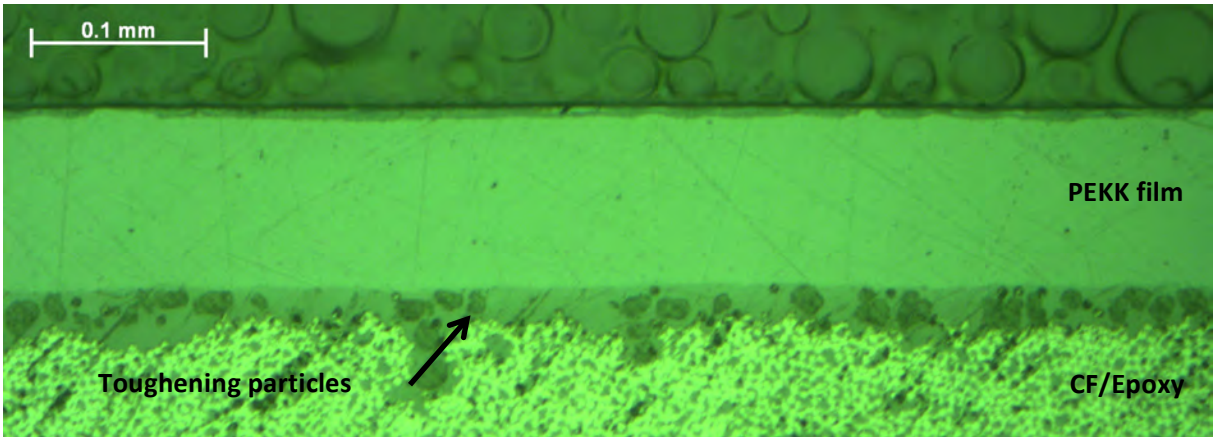

Figure 114: Zeiss optical microscope picture (x20 magnification) of CF/Epoxy, co-cured with 100 µm-thick PEKK UV, substrate. Good merging of the thermoset and thermoplastic materials, as well as the toughening particles of the epoxy, can be appreciated.

Figure 115 shows the cross section of NE2-PEKK-100 weld. In this case, there was a large area with a separation between the ED and the PEKK matrix, bigger than in NE2-PEKK-40 weld, which may explain the lower LSS value and larger scatter obtained, compared to the previous weld. A part of the interface showed also separation between the ED and the co-cured PEKK film, but it was an isolated and local defect.

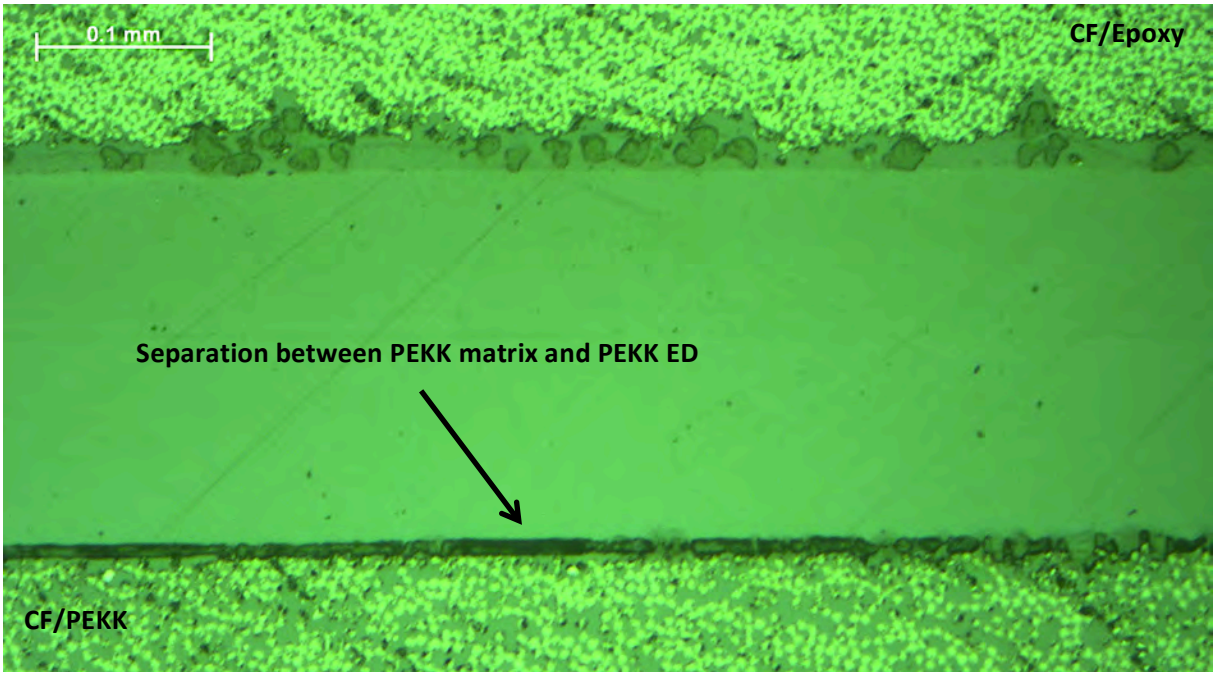

Figure 115: Zeiss microscope picture (x20 magnification) of NE2-PEKK-100 weld. Separation between the PEKK ED and matrix is observed in a large area of the cross section.

- FRACTOGRAPHY

Figure 116 shows the fracture surface of the studied weld. Cohesive failure, with a very rich area of thermoplastic covering both substrates, can be appreciated. On the CF/Epoxy substrate, there are some areas where the top layer of epoxy resin is believed to be exposed. The cavities induced by the epoxy toughening particles do not appear in this fracture surface due to the thicker thermoplastic layer found on each substrate, nevertheless, some could be spotted close to one of the edges of the weld, near the areas where the epoxy was exposed.

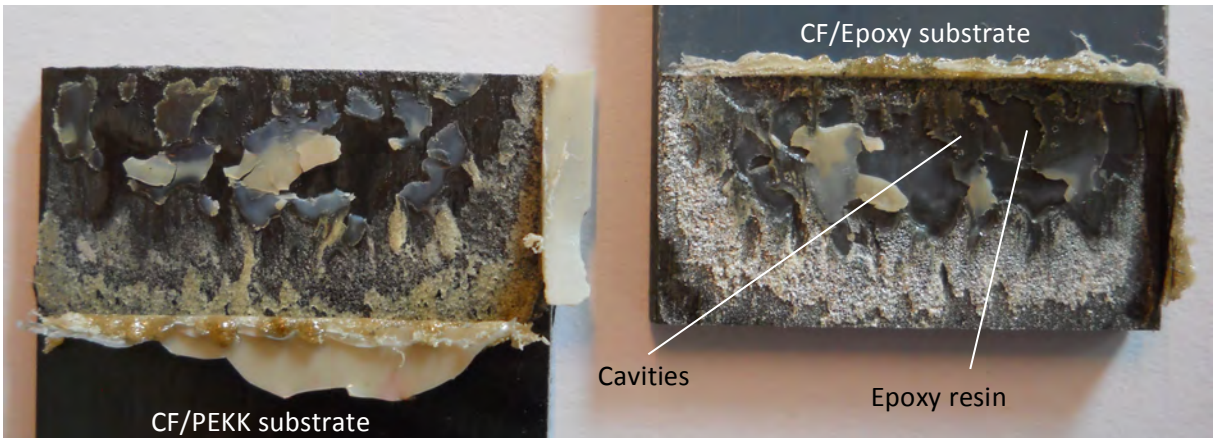

Figure 116: Fracture surface of the NE2-PEKK-100 weld. Cohesive failure, with a thick layer of thermoplastic on each substrate, can be spotted. Toughening-material cavities and exposure of the epoxy resin can be appreciated near one of the edges of the CF/Epoxy substrate.

Conclusions

PEKK UV hybrid weld was repeated, using 40 and 100 µm-thick co-cured films and a new panel layup for the autoclave co-curing. For the 40 µm-thick co-cured film, the mean LSS was the

highest obtained for a hybrid weld in this thesis: 34.74 MPa; their scatter was also low. The improvement in the LSS value and characteristics of the weld with respect to NE1-PEKK-40 ones, may rely on the new panel layup for the curing in the autoclave, which ensures optimum flow of epoxy resin during the process. NE2-PEKK-40 led also to a lower average welding time, and its fracture surface had also small areas with interlaminar failure of the epoxy, showing that for these samples, the compatibility of the epoxy and the PEKK resin was better. The main failure type of the welds was cohesive failure.

In the case of the 100 µm-thick co-cured film, the LSS value was lower (28.61 MPa), and the scatter was high. The welds led also to cohesive failure, with richer thermoplastic fracture surfaces.

7.2. STANDARD HYBRID WELDING CONCLUSIONS

In this first part of the thesis results, indirect or hybrid welding was performed. CF/Epoxy substrates where co-cured to a treated or not treated thermoplastic film and welded to a CF/TP substrate using a 0.25 mm-thick energy director. The thermoplastic materials used were PEKK, PEEK and PPS, and each weld will use the same type for the co-cured film, the energy director and the matrix of the thermoplastic substrate. The following ideas could be concluded:

Some of the welds presented a good adhered thermoplastic film co-cured with the thermoset substrate before welding, but after the ultrasonic process the weld turned out to be unsuccessful. These are the cases of the welds were PEKK chloroform-amine (2^{nd} formula), CF/PEEK UD [0/0] and PPS acetic films were used. This fact is of paramount importance for this investigation: Adhesion of a thermoplastic treated (or non-treated) film should always be checked with the performance of a weld for the check of suitability of the assembly because, as in the cases just mentioned, sometimes the high welding temperatures, pressure and vibrations may interact with the substances of the treatment, causing burning or detachment at the interface.

The CF/Epoxy available for this investigation and used for the welds was expired and degraded. Several analyses were performed to confirm this issue: Mode-I testing, FTIR analysis, and CF/Epoxy heating at different times and temperatures, and all the tests checked the degradation in the properties of the epoxy. Interlaminar failure, with corrupted properties of the sizing substance that binds the reinforcing fibres and the epoxy resin together, was found in the fracture surface of the Mode-I tested sample, inducing a low G_{Ic} value. The degraded epoxy was the cause of the interlaminar failure that was also found in most of the fracture surfaces of the welds after mechanical testing, which gave a lower LSS value than expected (on the order of 30 MPa). This also meant that the strength achieved at the interface was higher than the interlaminar strength of the epoxy. Despite the lower LSS values, it could be perfectly assessed and studied the suitability of the treatments, being able to determine with the LSS value and the cross-section observation the welds with better adhesion and characteristics. These were the ones that used the following co-cured films: PEKK UV, PEKK 1^{st} chloroform-amine formula, PEEK UV, PEEK acetic, and PPS NT.

The fact that PEEK and PEKK improved their adhesion and LSS of the welds with UV treatment, and that the opposite effect happened for PPS was investigated. FTIR tests and optical microscope observation analyses were performed on non-treated and treated PPS films for different UV-exposure times. It could be concluded that the overall crystallinity of the semi-crystalline polymer did not change, as confirmed by DSC analysis, but the local crystallinity, size and morphology did, as

well as de-colouring of the film which, which pose the fact that degradation of the films was occurring with UV-exposure. FTIR analyses also suggest the oxidation and degradation of the films with this treatment.

PEEK UV hybrid welds were repeated with a fresh CF/Epoxy, Hexply M21. After optimizing the panel layup for curing in the autoclave, a mean LSS value of 34.74 MPa, and low scatter, was achieved with a 40 µm-thick co-cured PEKK UV film. This result constitutes a positive end result for this thesis hybrid welding, showing that with the right epoxy and treatment, which enhances the adhesion between the thermoplastic and the thermoset, optimum joint strengths can be achieved. Due to the high force-amplitude combination of welding parameters, the epoxy was not degraded during the welding even though a very thin thermoplastic film was used, in the case of PEKK (it is worth to remember that the co-cured thermoplastic film shields the epoxy from degradation), another positive fact of this welds.

The same welding type was performed with a 100 µm-thick PEKK UV film, but its LSS values revealed a lower strength and higher scatter in the results than for the 40 µm-thick co-cured film.

Part II: Other Types of Welds

This second part of the thesis experiments and results will be devoted to three studies:

- Multi-Material Hybrid Welding: In this chapter, hybrid welds combining different thermoplastic materials will be performed.
- Direct welding, where no co-cured thermoplastic layer will be used. A study of epoxy degradation and the welding of laser-treated epoxy samples will be performed.
- Thermoset to Thermoset Welding, together with the study of the use of the energy director for ultrasonic welding, related to the thickness of the co-cured thermoplastic layer on the thermoset substrate.

Chapter 8

Multi-Material Hybrid Welding

The standard hybrid welding procedure uses the same thermoplastic matrix for the reinforced thermoplastic substrate, the co-cured layer in the thermoset substrate and the energy director. In this chapter, another approach will be studied: Multi-Material Hybrid Welding (MMHW). In it, a carbon-fibre reinforced epoxy substrate will be coated with a PEI layer and ultrasonic welded to a carbon-fibre reinforced PEEK substrate. Two types energy directors will be used: a PEEK ED and a PEI ED, in order to study if the use of one is preferable or more beneficial for the welding properties. In this assembly, the compatibility between epoxy and PEI, and between PEI and PEEK will be studied. Figure 117 shows a sketch of the hybrid welding combinations that will be performed:

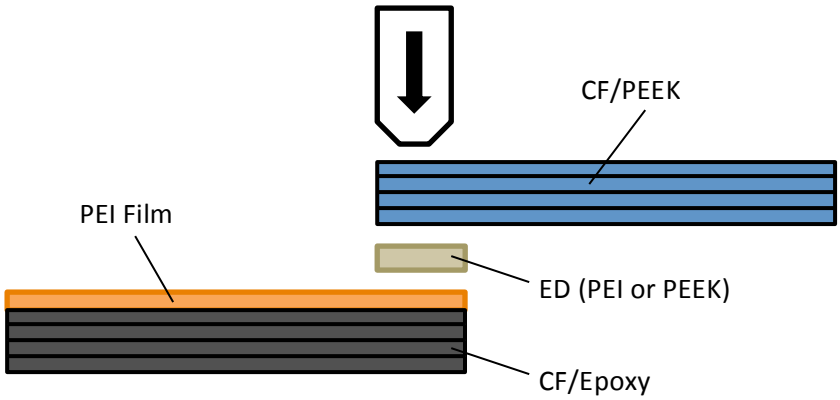

Figure 117: Sketch of the ultrasonic hybrid welding combination. A CF/Epoxy substrate co-cured with a PEI film welded to a CF/PEEK substrate, using a PEI or PEEK ED.

But why this combination of materials? The main answer is for the creation of a strong physical connection between the epoxy and PEI molecules that not only relies on adhesion: A semi-interpenetrating network (SIPN). This type of the called “micro-molecular interlocking”, as explained in Chapter 1, consists in the formation of one or more networks or branched polymers: some of the linear or branched macromolecules must penetrate in a molecular scale in at least one the networks. The linear macromolecules correspond to the thermoplastic chains, and the network into which they penetrate, is thermoset molecular structure. The branched or linear polymers can be separated from the polymer network without breaking the chemical bonds because they are polymer blends. This type of entanglement and mingling between PEI and epoxy has been proved to be able to occur [45], [49], what cannot be achieved with the three thermoplastics used in the ‘Standard Hybrid Welding’ (PEEK, PEKK and PPS).

8.1. MATERIALS

In this chapter, the following materials, whose manufacturing was explained in Chapter 2, were used:

- CF/PEEK, 25.4 x 101.6 mm^2 samples, to be used as the other welding substrates.
- PEEK and PEI 26 x 26 mm^2 energy directors.
- CF/Epoxy 25.4 x 101.6 mm^2 samples of Hexply 8552 epoxy, co-cured with a 0.045-0.05 mm-thick PEI film. As previously mentioned, two panels from two different autoclave processes were obtained. An issue with the samples of the first panel was observed: The top surface of the stacks, the one that was in contact with the bleeder blanket, remained with the blanket textile pattern after curing, so the PEI surface of the first stack and one of the surfaces of the second stack had not-smooth face. The other face of the stacks and substrates was smooth, because the aluminium plate and layers below had a flat surface. The textile pattern had led to a surface were sunk and not-sunk areas of PEI into the epoxy could be appreciated. In order to gather more information about the interface between the thermoset and thermoplastic material, the cross section of this co-cured stack was observed with optical microscopy. To do so, two parts of the stack were cut using a diamond blade cutter, embedded in resin and polished with the Rotopol-2 Struers machine, in order to observe the sunk and un-sunk areas. The observations were performed with Leica and Zeiss optical microscopes, all devices available at the DASML of TU Delft. Three different areas could be observed:

1. A totally detached PEI film.
2. Attached and entangled PEI with a slight colour difference between the two materials.
3. Attached and entangled PEI with little colour difference between PEI and epoxy.

Figure 118 shows a sketch of the PEI-Epoxy cross-section, identifying the three different regions and their interfaces. Figures 119 to 113 show the Zeiss microscope pictures for them.

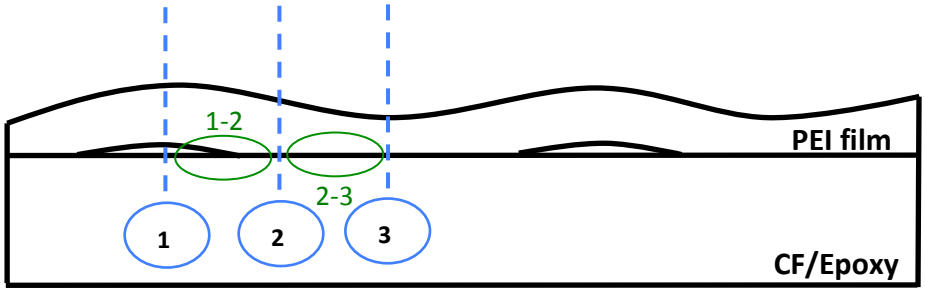

Figure 118: Sketch of the PEI-Epoxy cross-section. Three regions of interest, and their interfaces, were spotted.

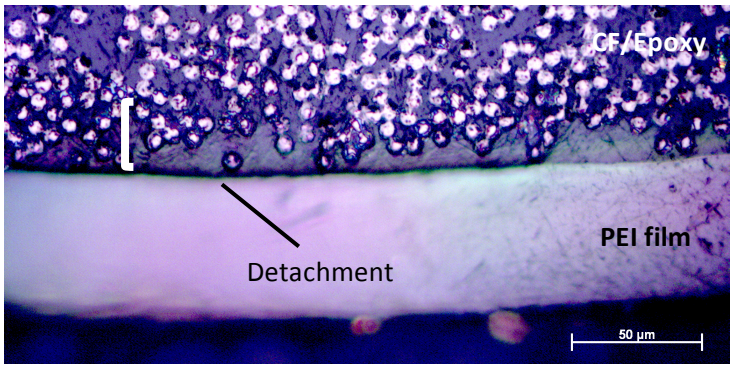

Figure 119: Zeiss optical microscope picture (x50 magnification) of region 1, where completely a detached PEI layer can be observed: there is an actual space between the epoxy and the PEI film.

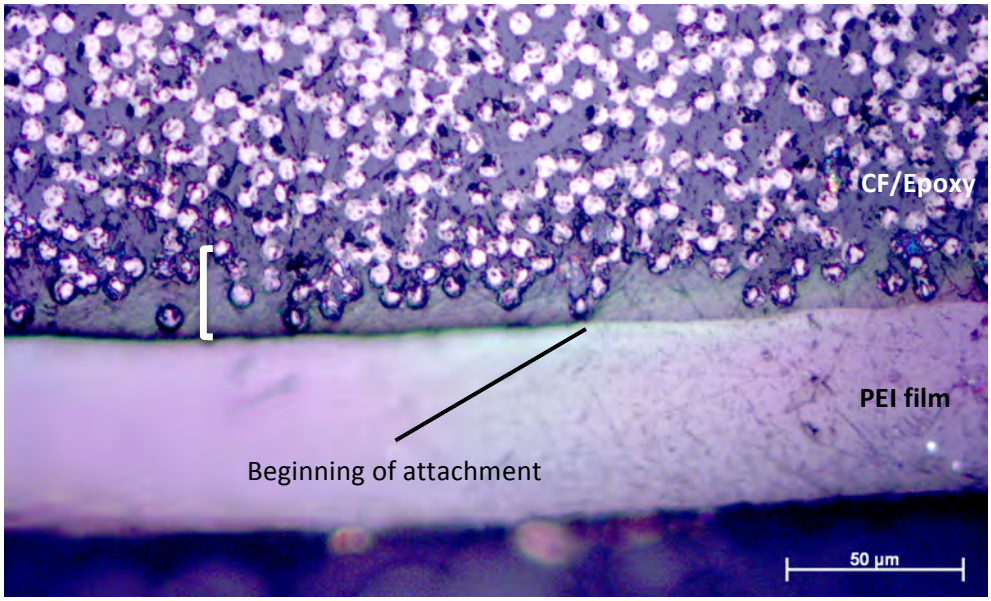

Figure 120: Zeiss optical microscope picture (x50 magnification) of the interface between regions 1-2. The transition from the detached PEI film gradually becoming attached to the epoxy can be appreciated.

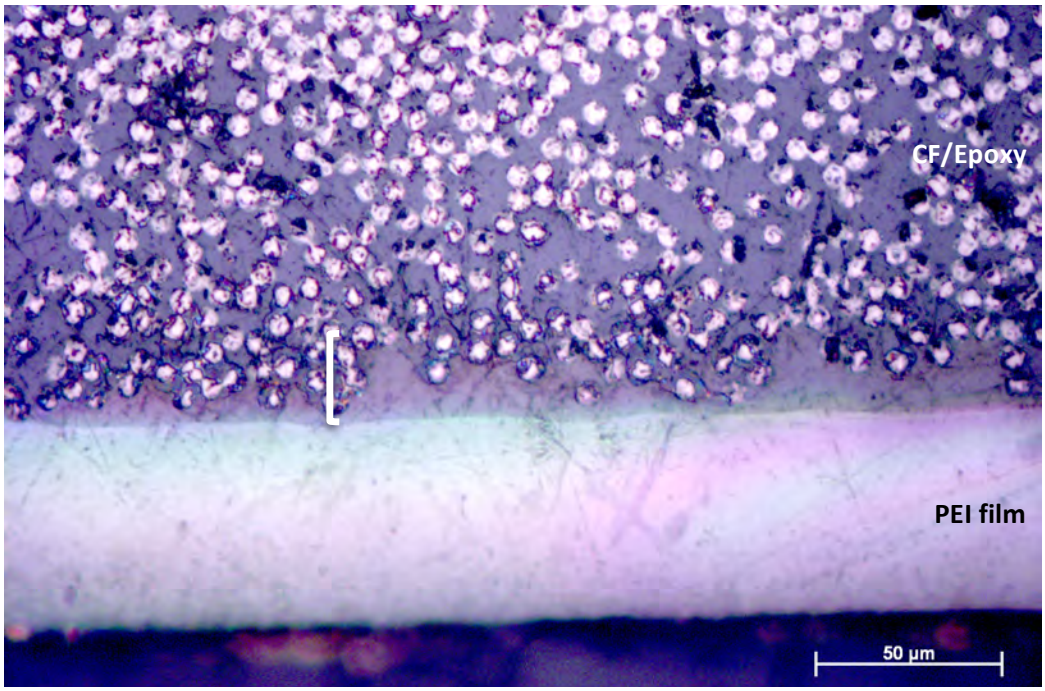

Figure 121: Zeiss optical microscope picture (x50 magnification) of region 2. It can be seen that, despite of the colour difference between the epoxy and the PEI film, they are completely attached. It can also be appreciated the glowing and rainbow-colour flashes characteristic of the PEI film.

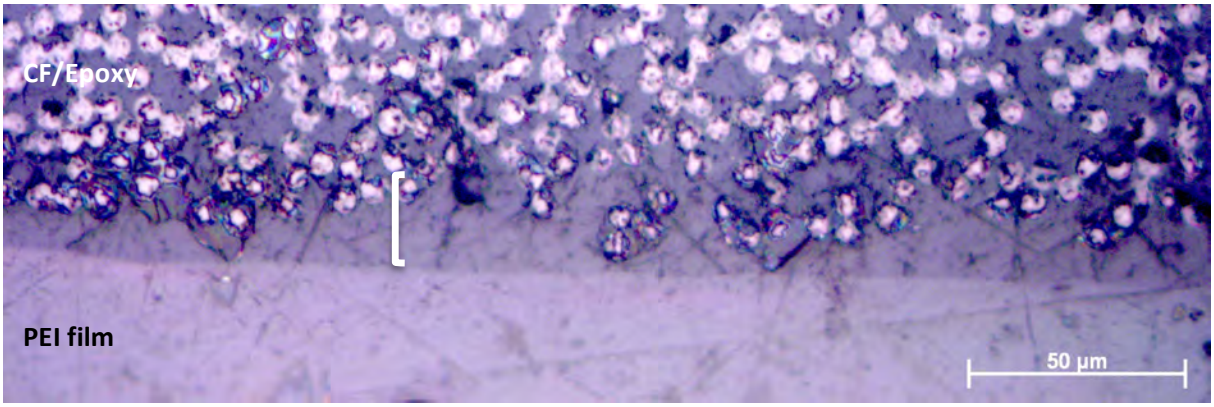

Figure 122: Zeiss optical microscope picture (x50 magnification) of the interface between regions 2-3. The gradual merging of the colours from the left side of the image (region 2) to the right part (region 3) can be appreciated.

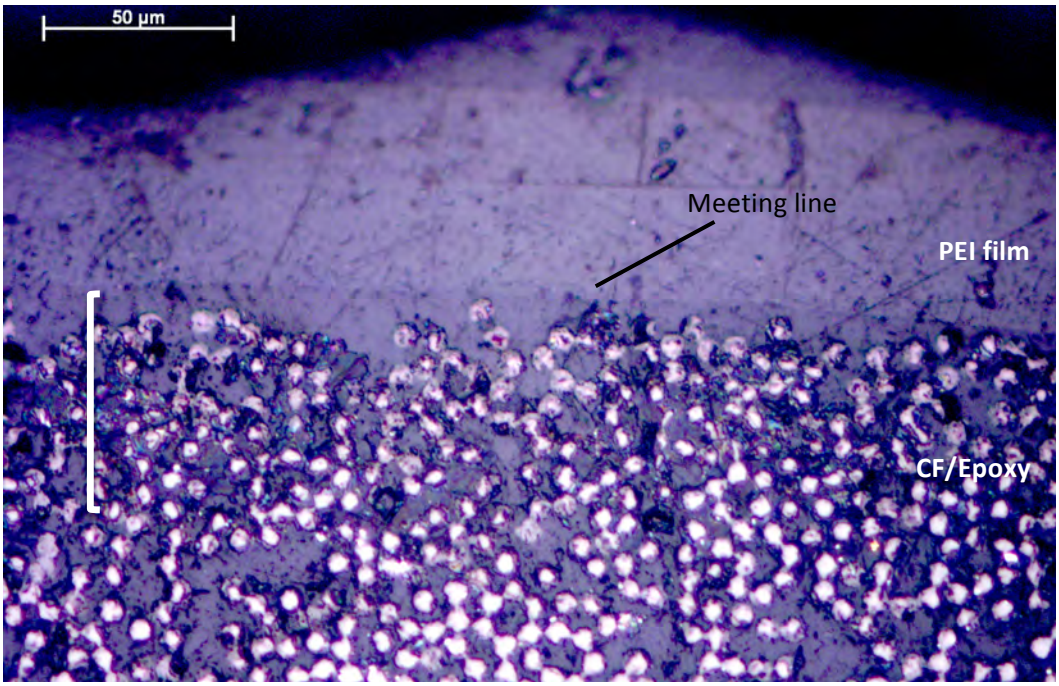

Figure 123: Zeiss optical microscope picture (x50 magnification) of region 3. More uniform colour between the PEI and the epoxy can be appreciated, as well as perfect contact between the epoxy and the PEI film, but the line were the two materials meet can still be appreciated.

In all of the images, white brackets were place to indicate an interesting region: This part between the epoxy and the PEI film shows a different shining of the carbon fibres, with colours like the characteristic glowing of the PEI film. This may be due just to reflectance of the nearby PEI film. Nevertheless, a different colour of the resin in this region from the rest of the thermoset substrate can be appreciated, especially in regions 2 and 3. This suggests the possibility of the presence of a diffusion layer or intermingling of the thermoset and the thermoplastic: A SIPN. Then, the different shining of the carbon fibres in that region can be due to the presence of PEI around them. It is interesting to see that this layer also appears in the detached film of region 1, also its effects are not so evident; a hypothesis is that this phenomenon started to occur in this region before the two substances eventually separated. It is worth to remember that SIPNs are polymer blends, and that the two substances forming them can be separated without breaking chemical bonds.

This irregular profile of the surface that was intended to be devoted to welding, led to the manufacture of another PEI-Epoxy panel, placing an aluminium plate on top during the curing to assure a smooth surface, as explained in Chapter 2. A sample of this new panel, the one used for the welds of this chapter, was embedded in resin and observed with the optical microscope. Figure 124 shows its cross-section:

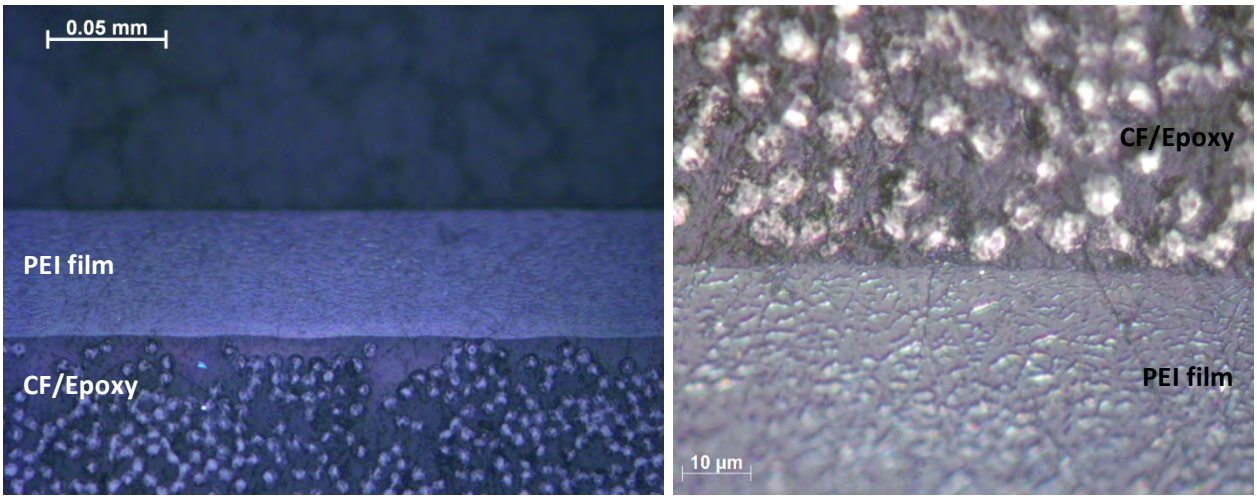

Figure 124: Pictures of the cross-section of the stack from the CF/Epoxy and PEI co-curing repetition, taken with Zeiss (left, x50 magnification) and Leica (right, x100 magnification) microscopes. A colour difference between both resins can be observed, but no separation at the interface is noticed.

In order to gather more information, and to assure the PEI film was totally adhered to the epoxy, a SEM – Scanning Electron Microscope, available at the DASML of TU Delft – observation of the interface between the thermoplastic and thermoset materials was performed (see Figures 125 and 126).

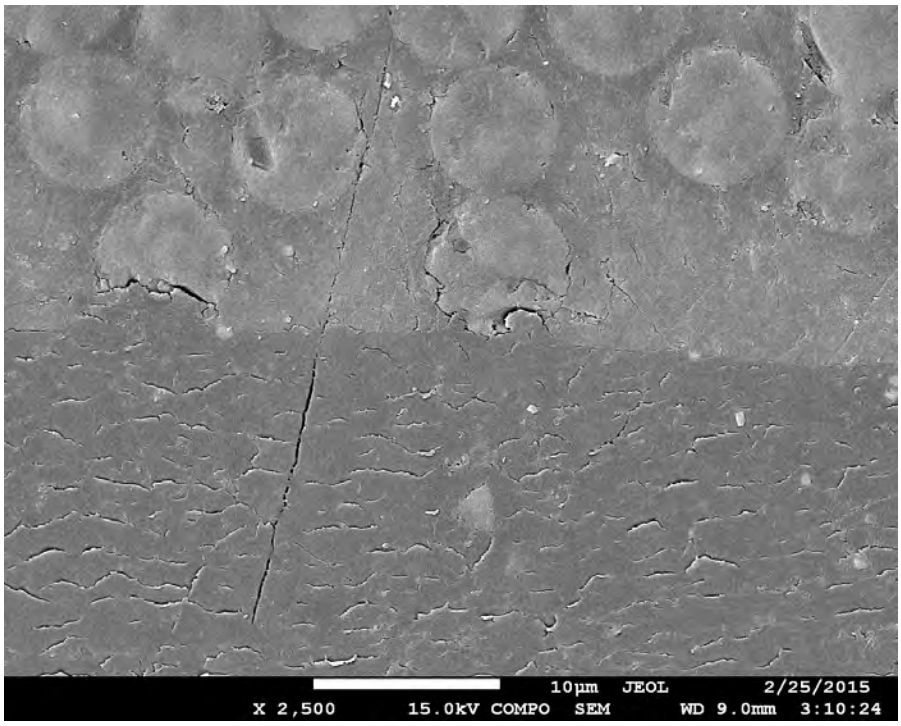

Figure 125: SEM picture (x2500 magnification) of the interface between the epoxy and the PEI film. Perfect adhesion between the epoxy and the thermoplastic layer can be appreciated.

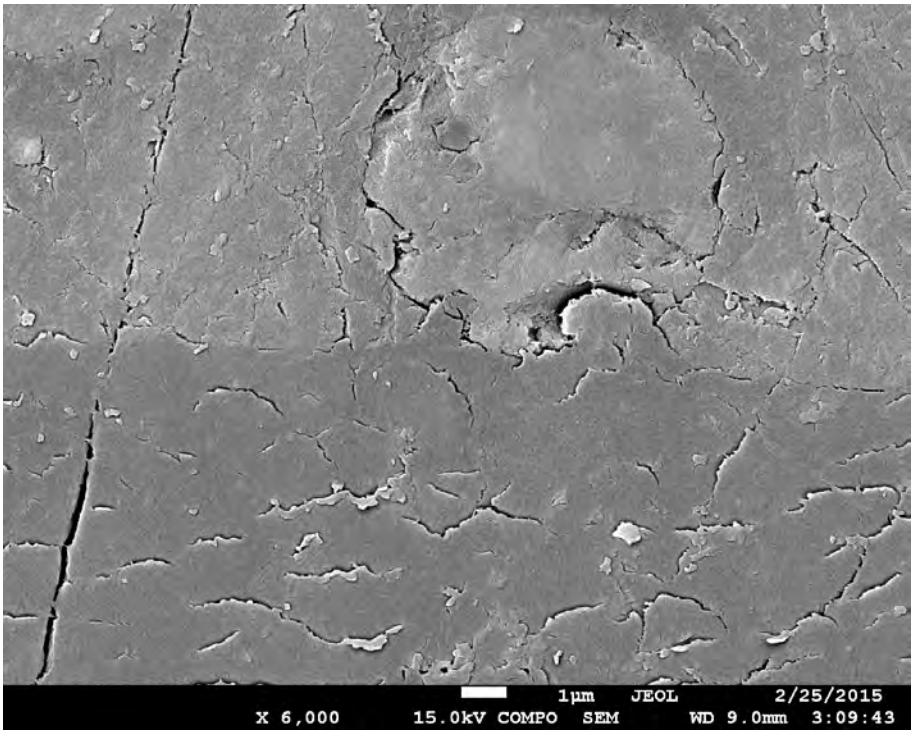

Figure 126: SEM microscope image with a higher magnification (x6000) of the PEI-epoxy interface. Here the characteristic wrinkles of the PEI film can be better appreciated, and also the continuous transition from the epoxy to the thermoplastic film, with perfect merging and adhesion of the two materials. The fact that the interface is not a straight line shows the mechanical interlocking and keying of the two materials.

With the SEM images, it was checked that the last co-cured panel had a perfect adhesion of the thermoset and thermoplastic films, so the 25.4 x 101.6 mm^2 samples obtained from it were the ones used for the welds of this chapter. In Figure 126, it is interesting to check that the epoxy resin is bi-colour. This may indicate the presence of a diffusion layer or SIPN between them, with PEI penetrating into the epoxy, but this hypothesis cannot be confirmed with the optical or SEM microscopes.

Further optical microscopy after the SEM was performed, with the sample still coated with the golden particles, which gave it a red colour and enhanced the optical microscope observation of the PEI wrinkles (see Figure 127).

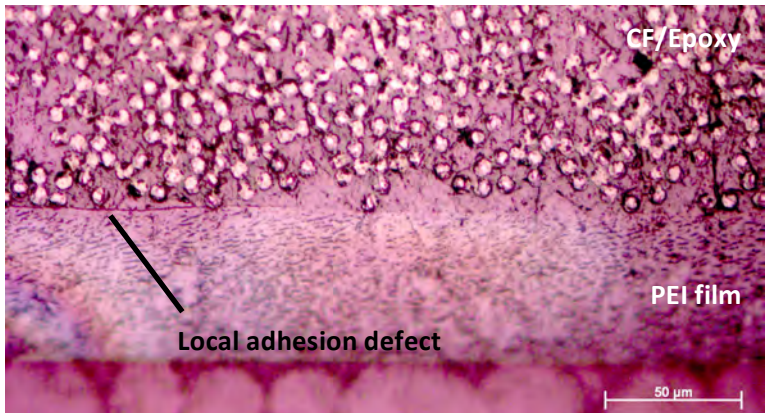

Figure 127: Zeiss optical microscope picture (x50 magnification) of the PEI-epoxy interface. In it, a line between the epoxy and the thermoplastic film can be appreciated, but it was an occasional isolated local defect. The rest of the interface was as the centre and right part of the image: Perfectly adhered, with good merging of both materials.

One of the most concerning observations that could be made was that the CF/Epoxy-PEI substrate did not show a clear SIPN or diffusion layer prior to welding. Optical microscope and SEM images suggest there is an intermingling interface between them, but none of these techniques could actually confirm it.

One of the hypotheses of the inability to confirm the existence of a SIPN, was the possible limitations of the methods used to observe them: Optical microscopy and SEM. In the literature, L. J. Vandi, M. Hou *et al.* were able to observe SIPN with optical microscopy, but in that case they were working with non-reinforced A-stage resins [35]. The presence of the carbon fibres in the used prepeg may be making difficult to appreciate this interface layer. In another investigation, where an aerospace epoxy prepreg was co-cured with a PEI layer using different curing cycles, the formation of a SIPN could be observed too, but in this case AFM technique was used to observe this diffusion layer [36]. Also, M. Hou, in another article [3], claimed to have been able to see the SIPN between CF/Epoxy prepreg co-cured with a thermoplastic with a Scanning Electron Microscopy.

An additional possible reason for the inability to clearly see a SIPN is, precisely the fact of epoxy expiration, as proposed by R. Van Moorleghem: When epoxy prepreg (B-stage) expires, it cures (C-stage), a transformation that deducts the potential of the co-curing process – a fact that might also have affected the adhesion of the welds in Chapters 3, 4 and 5, as it will be highlighted in the conclusions of Chapter 11. As M. T. Heitzmann *et al.* explain in their investigation [36]: "In prepregs, however, the epoxy resin is in a partially-cured pre-polymer stage (B-stage). This consequently means that the resin of a prepreg has a higher molecular weight and, as such, is less likely to diffuse into the thermoplastic". If the epoxy cures when expired, it increases even more its molecular weight, making it more difficult for the epoxy resin to diffuse.

It is worth to mention that it is believed that the curing temperature in relation to the glass transition temperature of PPS may have constituted a drawback: As confirmed in an investigation carried out by B. Lestriez *et al.* [46], diffusion of the thermoplastic into the thermoset in enhanced if, for the curing temperature of the epoxy, the thermoplastic is in a glassy state (beyond its glass transition temperature). The fact that the curing temperature of the epoxy (180°C) is below the glass transition temperature of PEI (216°C), so that the thermoplastic is not in a glassy state, represents a drawback for diffusion and the formation of SIPN.

8.2. PROCEDURE

Two types of ultrasonic welding were performed: the first type used a PEI ED (which will be called 'MMHW-1'), and the second one, a PEEK ED ('MMHW2').

Table 17 summarizes the welds performed with the samples and energy directors explained in Chapter 2.

Sample reference	Bottom substrate	Top substrate	Energy director	Thermoplastic coating	Observations
REF-PEEK	CF/PEEK (Ten Cate)	CF/PEEK (Ten Cate)	PEEK	-	Reference welds. Six welds performed: -5 samples for mechanical (LSS) testing. -1 sample for optical microscopy (OM).
REF-PEI	CF/PEEK (Ten	CF/PEEK (Ten	PEI	-	Reference welds. Six welds performed:

	Cate)	Cate)			-5 samples for mechanical (LSS) testing. -1 sample for optical microscopy (OM).
MMHW-1	CF/Epoxy (Hexcel 8552)	CF/PEEK (Ten Cate)	PEEK	PEI	Three welds performed, one for LSS testing and another two for OM.
MMHW-2	CF/Epoxy (Hexcel 8552)	CF/PEEK (Ten Cate)	PEI		Three welds performed, one for LSS testing and another two for OM.

Table 17: MMHW and reference welds.

For MMHW-1, the chosen welding parameters were the optimum ones of CF/PEEK to CF/PEEK ultrasonic welding using a PEEK ED (REF-PEEK), already explained in Chapter 2: 2000N, A6, 0.15 mm of travel. Two welds were performed with these parameters: One for LSS testing and another one for optical microscopy.

For MMHW-2, the same force and amplitude parameters were used. In order to determine the optimum travel for these materials, the same process as described in Chapter 2 was followed, but this time using a PEI ED with CF/PEEK substrates as the reference weld (REF-PEI): A preliminary weld using 100% travel was performed, finding an optimum travel of 0.19 mm. Then, the parameters for MMHW-2 and its reference weld were: 2000 N of force, 73.4 µm of amplitude (A6) and 0.19 mm of travel. Two welds were performed with these parameters: One for LSS testing and another one for optical microscopy.

The lower force parameters combination ('B' in Chapter 2), with the same travel for each weld type as the high-force set, was also tried. One weld per welding type was performed with these parameters and devoted to optical microscopy.

In Table 18, the welding conditions and welder outputs for each welding combination are collected:

Sample reference	Welding parameters			Average welding time (ms)	Average consumed power (%)	Average welding distance (mm)
	Force (N)	Amplitude	Travel (mm)			
REF-PEEK	2000	A6 (73.4 µm)	0.15	500	79	0.23
REF-PEI	2000	A6 (73.4 µm)	0.19	500	80	0.25
MMHW-1	2000	A6 (73.4 µm)	0.15	492	85	0.22
	1500	A9 (86.2 µm)	0.15	439	97	0.22
MMHW-2	2000	A6 (73.4 µm)	0.19	493	86	0.24
	1500	A9 (86.2 µm)	0.19	467	91	0.26

Table 18: Welding conditions and outputs for MMHW and reference welds.

8.3. MECHANICAL TESTING

The results for the single-lap shear tests performed on the reference welds and the two welding types (using the higher-force parameters) are shown in the chart of Figure 128.

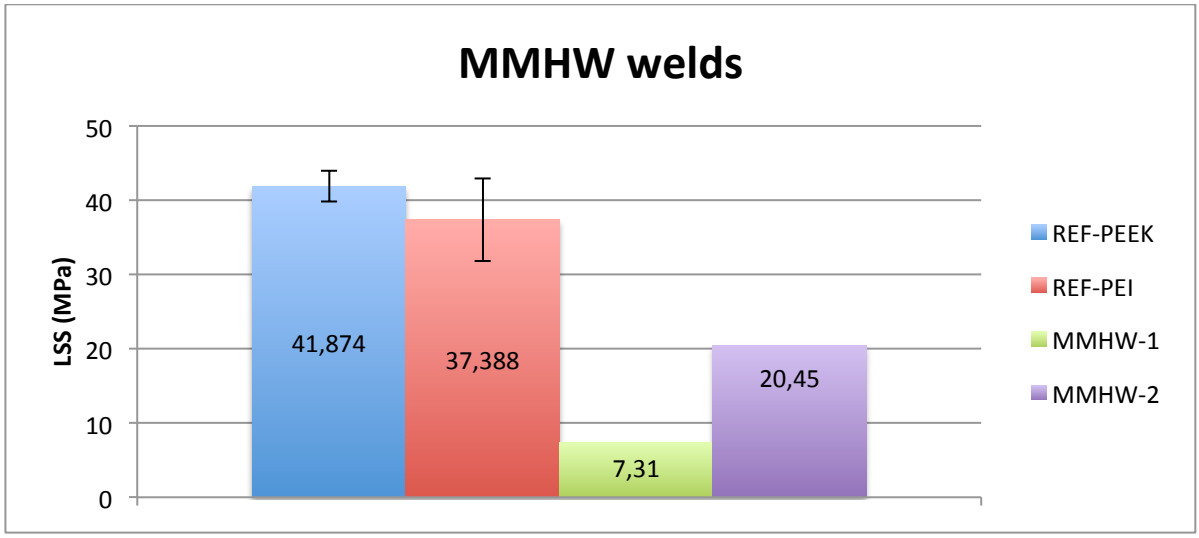

Figure 128: LSS values for MMHW welds.

Five samples were tested for the reference welds, with a medium LSS value of 42.43 MPa and a standard deviation of 6.30. For PEKK hybrid welds, one sample per treatment was tested.

From the results presented, it could be appreciated that treating chemically the PEKK co-cured film prior to welding, greatly improved the mechanical behaviour of the weld, specially for UV-O_3 and chloroform + amine (1st formula) treatments. Nevertheless, these lap-shear results were found to be lower than expected. According to ultrasonic hybrid welds performed with CF/PEEK and using another epoxy (Hexply 913), with a co-cured layer of PEEK treated with UV-O_3 for 5 minutes, performed by Pablo Vizcaino, strengths up to 30 MPa can be achieved in this type of hybrid joints [28]. Observation of the fracture surface and cross-section of the samples will bring more light to the reason of this drop in the lap-shear strength.

Hereinafter, the reference CF/PEKK-CF/PEKK weld and each PEKK treatment results and characteristics, from higher LSS obtained to lower, will be analysed separately. Cross-section and fracture surface studies will be mainly performed. An FTIR test could be carried out in PEKK NT weld, where flat epoxy fracture surfaces were found and reliable measurements were obtained.

8.4. CF/PEEK-CF/PEEK (PEEK ED) REFERENCE WELD

Cross-section and fractography analyses for this reference weld were already presented in Chapter 4, section 4.4.

8.5. CF/PEEK-CF/PEEK (PEI ED) REFERENCE WELD

8.5.1. Cross section analysis

Figure 129 shows an optical microscope picture of this cross section. Merging of the two thermoplastic resins at the interface can be appreciated, the PEI one with a darker colour than the PEEK matrix.

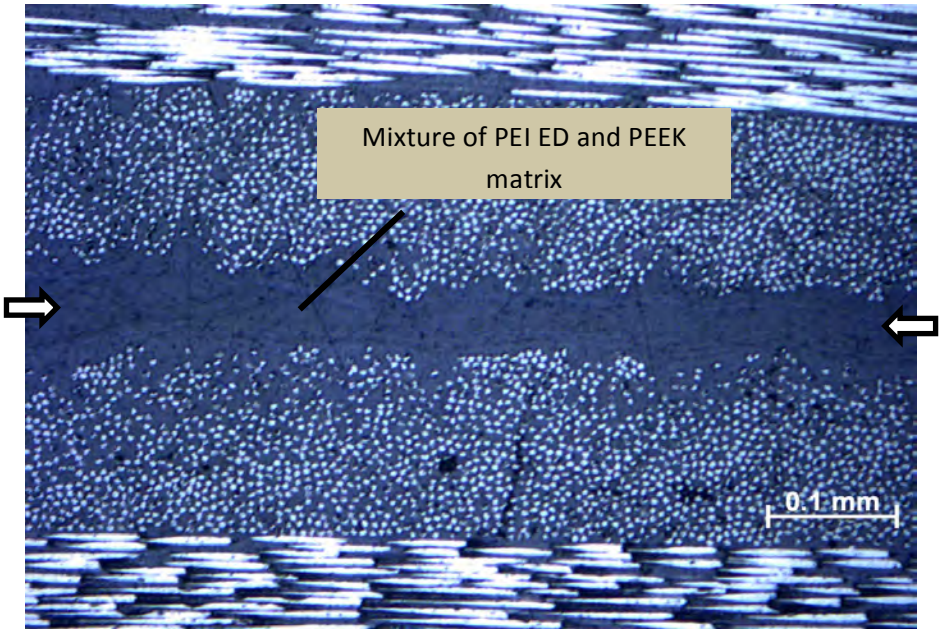

Figure 129: Zeiss optical microscope picture, with a x20 magnification, of CF/PEEK to CF/PEEK (PEEK ED), using 2000 N, A6, 0.19 mm-travel parameters. The arrows point to the welding interface. It can be appreciated the colour difference of the two thermoplastics, and their mixture at the welding interface.

8.5.2. Fractography

The fracture surface of studied reference weld is shown in Figure 130. Cohesive failure can be appreciated, together with some carbon fibre exposure. In one of the edges, slight burning occurs.

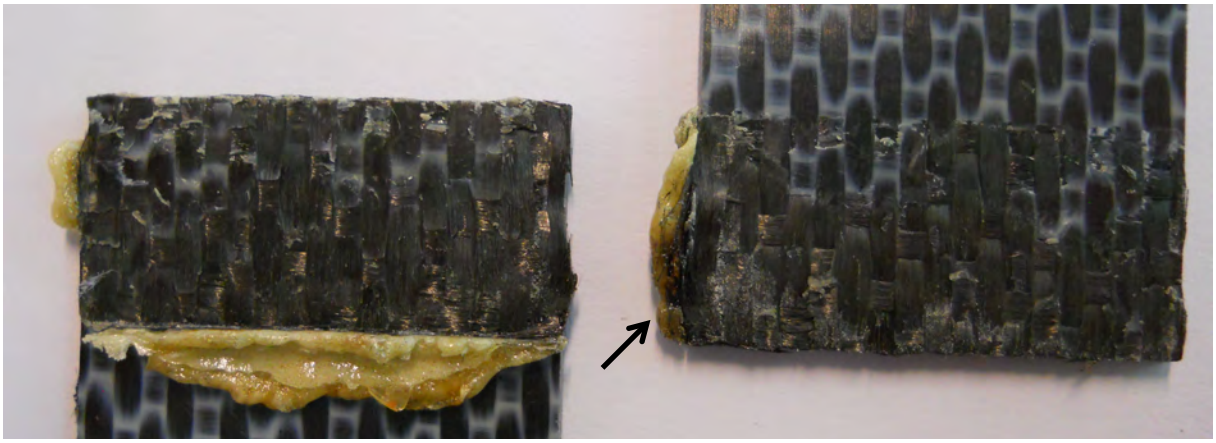

Figure 130: CF/PEEK to CF/PEEK, using a PEI ED, ultrasonic-weld fracture surface. The black arrow points to the slightly burned edge.

8.6. MMHW-1 (PEEK ED) – 2000 N, A6 PARAMETERS

8.6.1. Cross section analysis

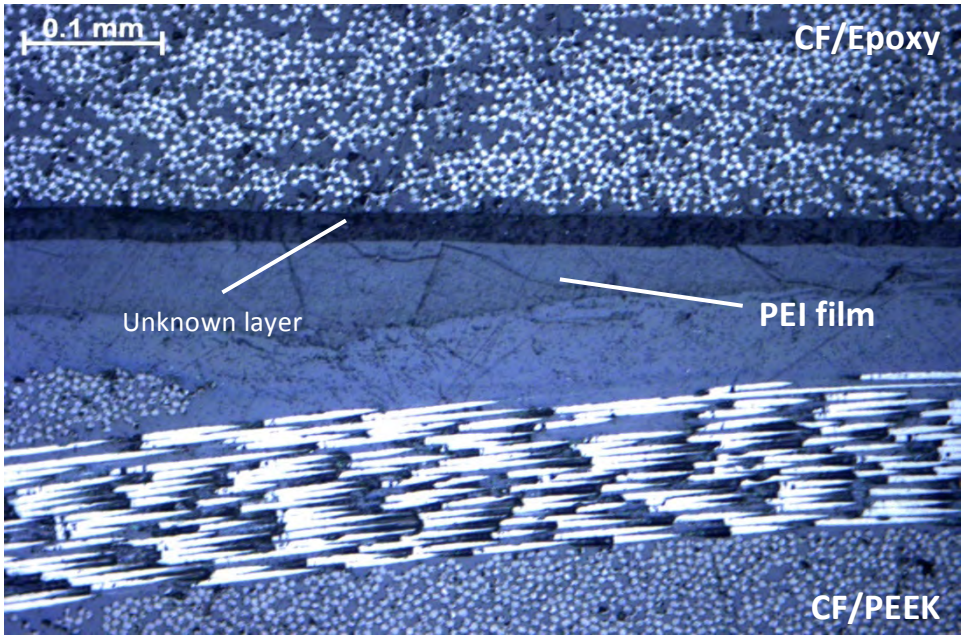

Figure 131: Zeiss optical microscope picture, with x20 magnification, of MMHW-1 weld (2000 N, A6). The PEI film can be seen to have mixed with the PEEK resins. A dark layer between the epoxy and the PEI film is also observed.

As can be appreciated in Figure 131, a dark layer between the epoxy and the PEI film was found. Its provenance was unknown, because such layer did not appear in the cross-section of the CF/Epoxy co-cured with PEI substrate, prior to welding. Was it an interface layer (SIPN) between the epoxy resin and the PEI film? Perhaps embedding resin? Another part of this cross section revealed more information:

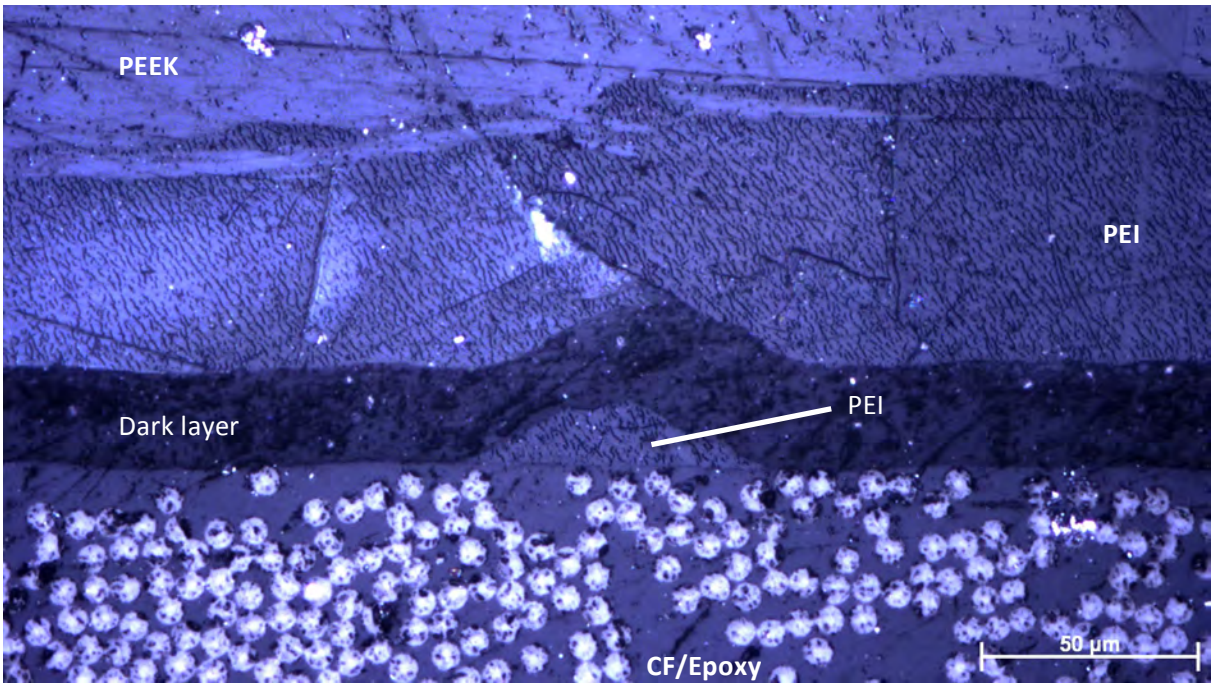

Figure 132: Zeiss optical microscope picture (x50 magnification) of a detail of MMHW-1 weld (2000 N, A6) cross-section. In it, the dark layer between the PEI film and the epoxy resin seems to be an actual separation between these materials, one of the hypotheses discussed. Also, the wrinkles of the PEI surface and its shiny reflections can be appreciated in this image.

Figure 132 shows another part of the interface: In it, PEEK resin on top, PEI film (characterized by its wrinkles and shiny reflections), the dark layer and CF/Epoxy can be appreciated. A PEI peak, still attached to the epoxy and below the dark layer, led to the idea that the dark layer is actually a separation between the PEI film and the epoxy, after the welding and embedding were performed. Figure 133 shows a sketch of this separation hypothesis:

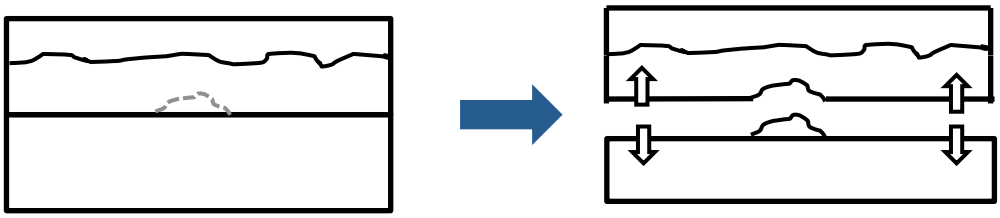

Figure 133: Sketch of the gap-formation hypothesis between the thermoset and the PEI film. It most likely formed after the welding and during the embedding-in-resin process.

Nevertheless, observations of this weld interface performed with the Scanning Electron Microscope (SEM) show that the substance of the dark layer is not embedding resin (there is a clear separation between them, and between the embedding resin and the weld), and that it is not a gap, so that the hypothesis of a separation between epoxy and PEI can be discarded (see Figure 134). An actual gap between the CF/PEEK substrate and the PEEK ED can be appreciated, probably corresponding to the thermoplastic-rich spots found on the fracture surfaces of the weld. Previously to observing the sample with the SEM, it was coated with a thin gold layer, in order to improve the conductivity and observation of the sample with this high-definition and augmentation microscope.

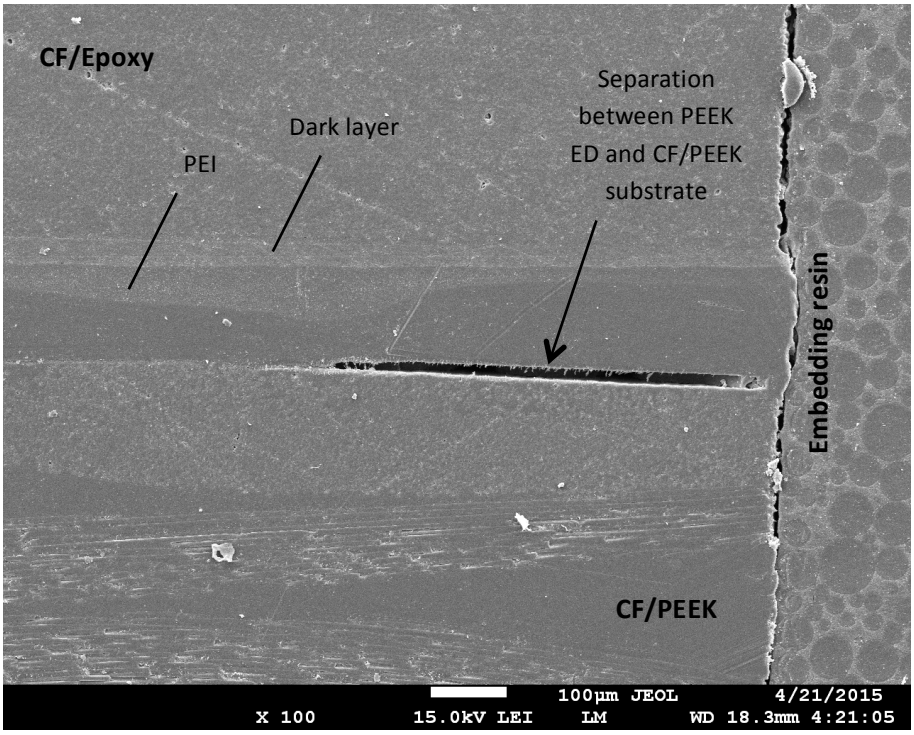

Figure 134: SEM image (x100 magnification) of MMHW-1 weld (2000 N, A6) cross-section. In it, a clear separation between the embedding resin and the dark-layer material can be appreciated, as well as their texture differences. Also, an actual separation (local defect) between the CF/PEEK substrate and the PEEK ED can be seen. These facts made clear that the hypothesis of a separation between the epoxy and the PEI film, being filled by embedding resin could be totally discarded.

Apart from the conclusions that the SEM observation led to, another idea came to mind: From what observed in the PPS-acetic weld, where there was actual separation, filled by bubbly embedding resin, between the thermoplastic co-cured film and the epoxy after the welding was performed, the LSS of that weld gave no results, which is logical because the adhesion of the thermoplastic and the thermoset turned out to be inexistent. In this case, however, the LSS value was one of the highest values obtained with this resin (22.11 MPa), which does not match the idea of not a good adhesion between the epoxy and the PEI.

Combining what acknowledged in the images obtained with both microscopes, the high LSS value for this weld, and the connection or continuation between this dark layer and the PEI and epoxy adjacent ones, the hypothesis of the dark layer being an actual diffusion interface (SIPN) between the epoxy and the PEI stands as the principal one. An interesting fact is that this layer was created or enhanced after the welding was performed.

Closer observation of the PEI and interphase layer substance surfaces was done also the SEM microscope, in order to gather more information about their differences. As can be seen in Figure 135, PEI film presents long and diagonal wrinkles in its surface; the interphase substance presents these PEI wrinkles, combined with rounded cracks or holes.

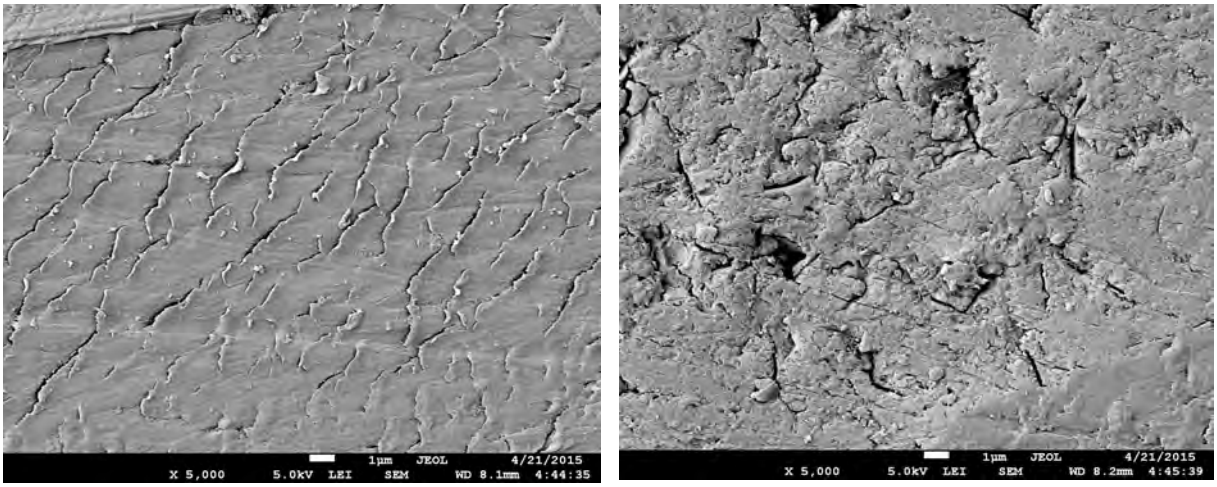

Figure 135: SEM pictures (x5000 magnification) of two surfaces: PEI film (left) and the dark layer substance (right). While PEI presents diagonal and long wrinkles on its surface, the other substance presents a combination of the PEI type of wrinkles and rounded cracks or holes.

According to this interface hypothesis, the PEI peak observed in Figure 132, still attached to the CF/Epoxy, would just be a part of the PEI that did not formed this intermingling with epoxy and simply remained attached to it.

8.6.2. Fractography

Figure 136 shows the fracture surface of the studied weld. Mainly, interlaminar failure of the epoxy can be spotted on the CF/Epoxy substrate surface, with stuck carbon fibres from it on the CF/PEEK substrate. On the thermoset substrate, a thermoplastic-rich area and a line of TP bubbles on the right edge can be also appreciated, as well as some narrow areas with exposure of the epoxy-resin top surface.

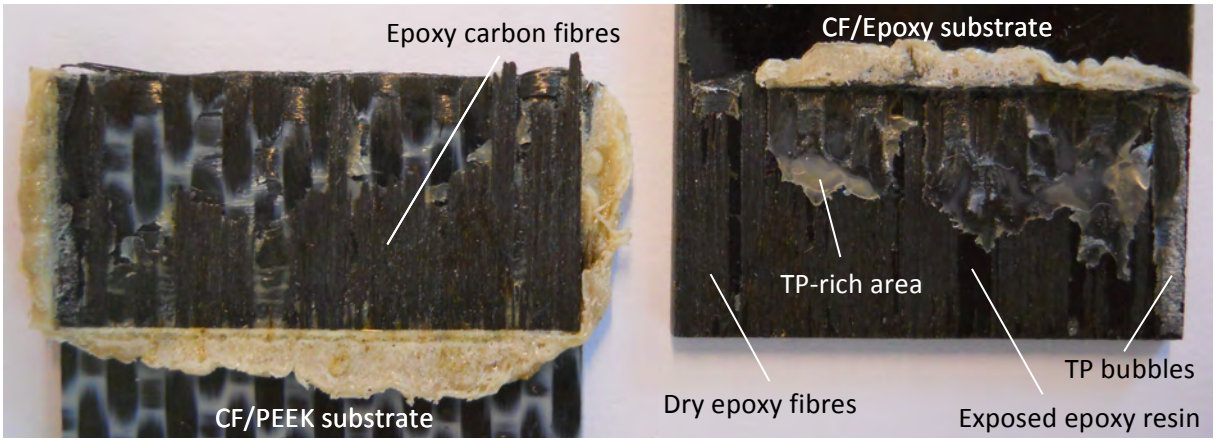

Figure 136: Fracture surface of MMHW-1 weld (higher-force parameters), using a PEEK ED. Interlaminar failure of the epoxy, with dry fibre exposure, TP bubbles on the right edge and a thermoplastic-rich area can be spotted on the CF/Epoxy substrate.

8.7. MMHW-1 (PEEK ED) – 1500 N, A9 PARAMETERS

8.7.1. Cross section analysis

Figures 137 and 138 show the cross section of this weld. It was very interesting to check that, with the new parameters, separation between the carbon fibres and the epoxy resin, and between the epoxy and the PEI, occurs at the centre of the weld. A possible reason may be the higher vibration amplitude and lower force, which does not hold as close as before the higher-shaken interface. It is also remarkable the lack of the diffusion layer found for the same weld using higher-force lower-amplitude parameters.

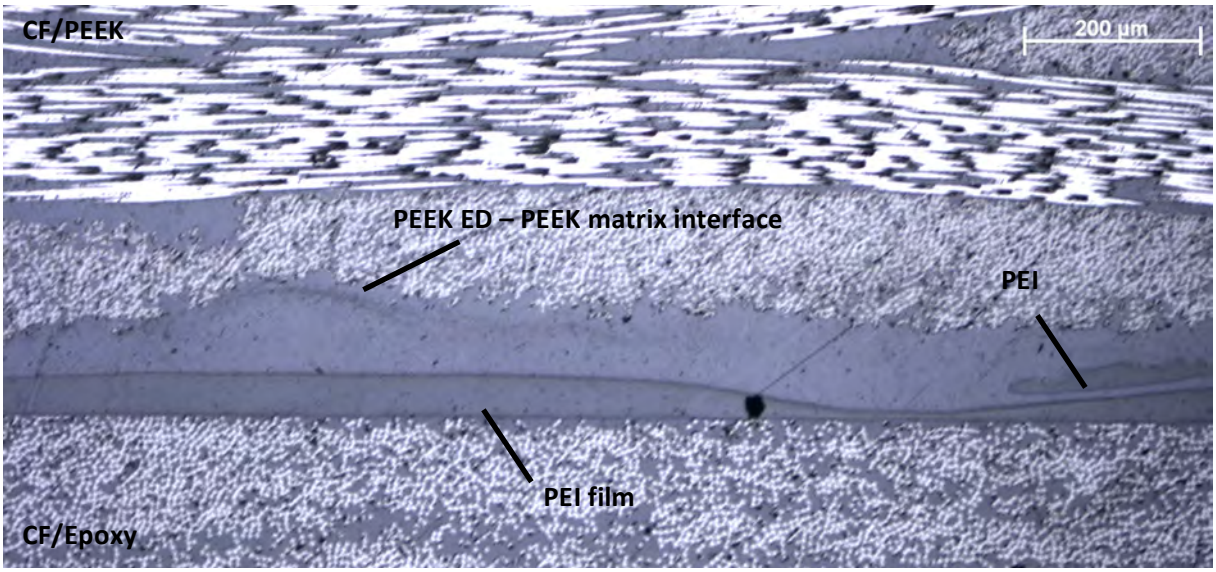

Figure 137: Zeiss optical microscope picture (x10 magnification) of the cross-section of MMHW-1 weld (1500 N, A9). With the new parameters, no interface region was observed. An interface between the PEEK ED and the PEEK matrix of the substrate can be observed in a part of this cross-section. There was good merging of the PEI and PEEK resins.

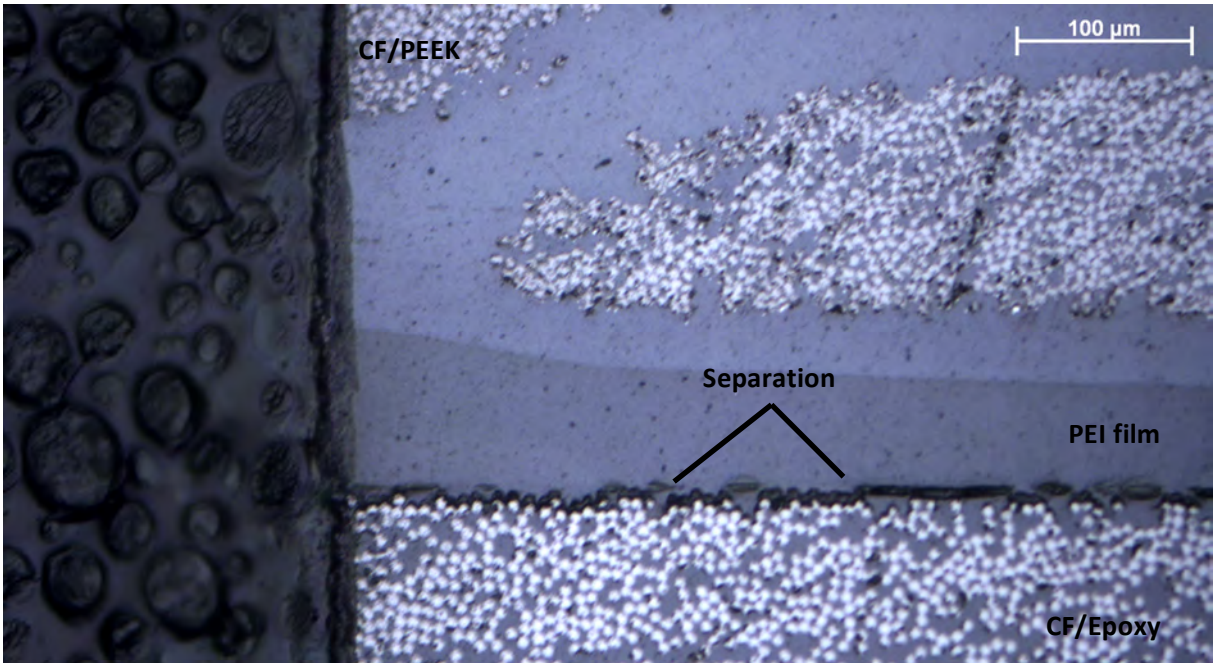

Figure 138: Zeiss microscope image (x20 magnification) of the cross-section centre of MMHW-1 weld (1500 N, A9). Separation between the carbon fibres of the epoxy substrate and the epoxy resin, and between the epoxy and the PEI film can be appreciated in this part of the cross-section.

8.8. MMHW-2 (PEI ED) – 2000 N, A6 PARAMETERS

8.8.1. Cross section analysis

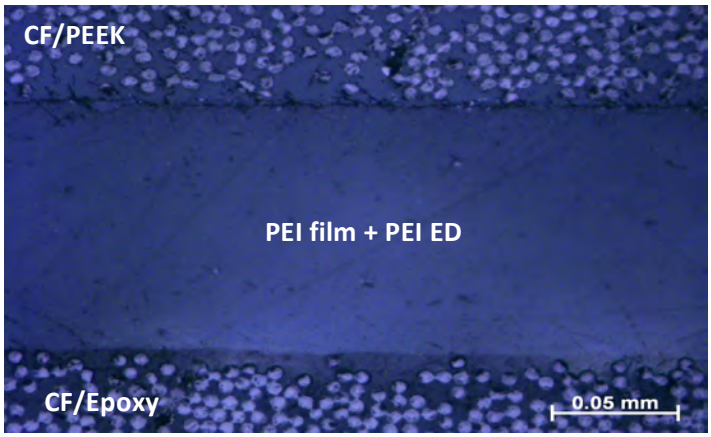

Figure 139: Zeiss optical microscope picture, with x50 magnification, of MMHW-2 weld (2000 N, A6). The welding interface shows to be very uniform, with a good compatibility between the epoxy and the PEI. The interface between PEI and PEEK seems show little cracks

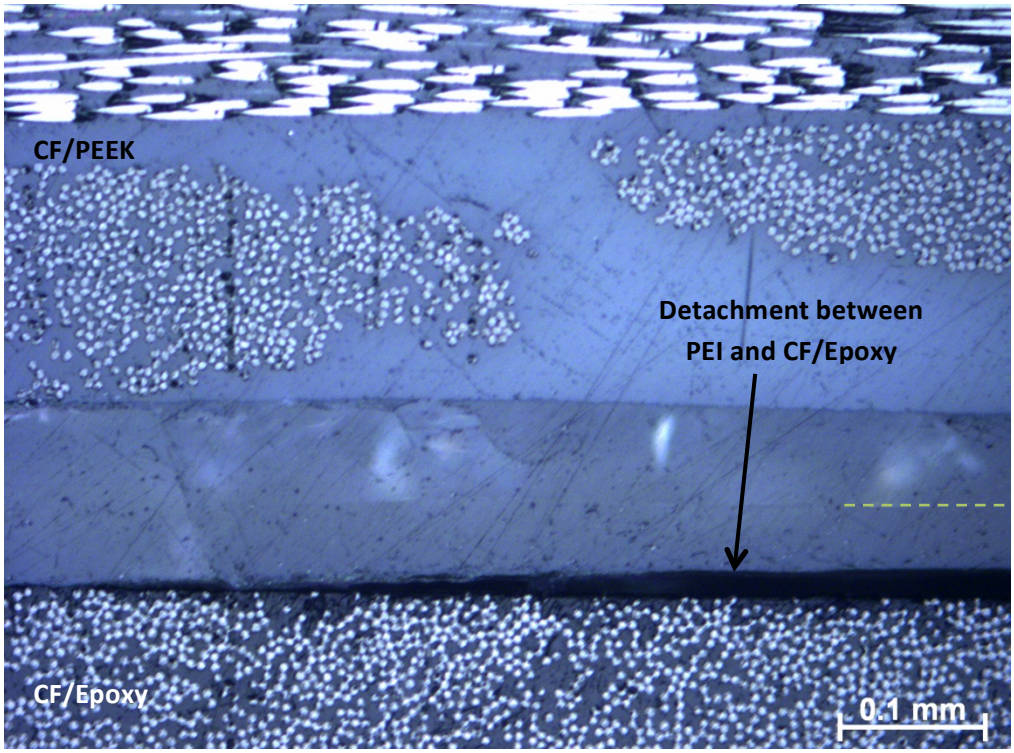

Figure 140: Detail of the detached area between PEI and CF/Epoxy of MMHW-2 weld (2000 N, A6). Picture taken with Zeiss optical microscope, x20 magnification. The purpose of the green discontinuous line is explained below.

Figures 139 and 140 showed the cross section of this weld. MMHW-2 interface appears to be more uniform, although there were some areas where the PEI film had detached from the epoxy, which showed a slight burning in that region, probably due to its attraction to merge with the PEI ED rather than to remained stuck to the epoxy. Also, some little cracks were seen at some areas of the interface between the PEI and PEEK resins, so not so well merging was observed between these two thermoplastics as in the reference weld formed by CF/PEEK substrates, using a PEI ED. Nevertheless, its LSS value was high, so a solid joint was achieved.

One fact that did not match the interface hypothesis is that this transition layer between epoxy and PEI was not found in this weld *a priori*, which should have appeared in this case too. A possible reason may be the light reflectance: As this interface used other materials, with different surface colours, the interface may not be so evident or easy to notice. Observing carefully Figure 140, it can be appreciated that the reflections, characteristic of the PEI material, are cut or stop towards the middle part of the "PEI" layer of the interface, the height where the reflections stop indicated by a green discontinuous line. This may mean the existence of an interface layer there. A SEM observation of this interface was done in order to closer look to this weld cross-section:

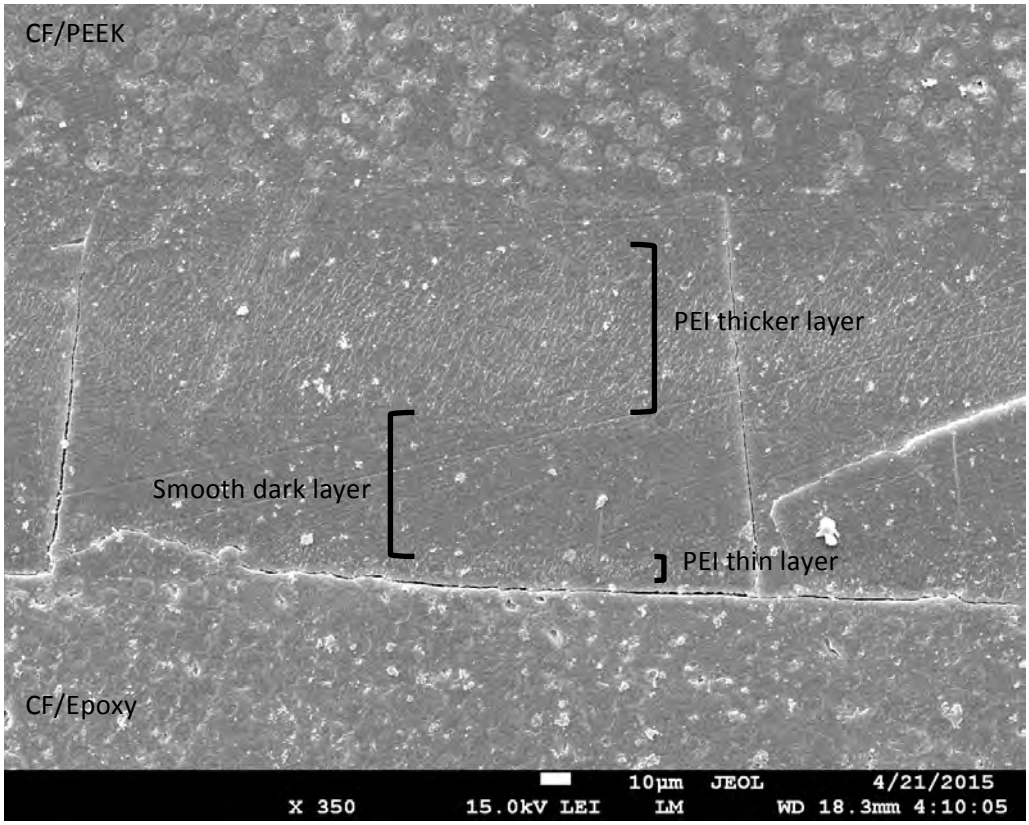

Figure 141: SEM image (x350 magnification) of the cross section of MMHW-2 weld (2000 N, A6). In it, a thin wrinkled PEI layer close to the epoxy, below a darker smooth area can be appreciated. On top of these last one, a thicker PEI region is found, which merges with the PEEK resin on top.

Figure 141 shows one of the SEM pictures of the studied weld cross-section. Some cracks appeared, due to the brittleness of PEI film. It can be appreciated that, just above the epoxy, there is a thin layer of PEI, characterized by its wrinkles, and above it, a smooth darker region. On top of this smooth zone there is a thick layer of PEI with its characteristic wrinkled surface, which then merges with the PEEK resin. This smooth dark layer between the epoxy-PEI and the thick PEI layer is most likely the diffusion interface seen in the other weld. In this case it was not so easily seen, because of the different materials light reflectance, and also because maybe in this case, the PEI film was led to merge with the PEI ED during the fast welding time rather than to form the interface layer with the epoxy, hence the thin PEI layer close to the epoxy interface (like the PEI peak found in the cross section of MMHW-1, 2000 N A6 parameters). This confirms the lack of reflections in this zone, previously commented.

There were also some regions of the weld cross-section where the characteristic wrinkles of the PEI layer were found all over the interface, so that there was no formation of the interface layer in those regions. This fact, together with the difficulty to spot it, show this interface region is not as strong as the one found in MMHW-1 (higher-force parameters). Figure 142 shows an optical microscope picture of this mentioned area.

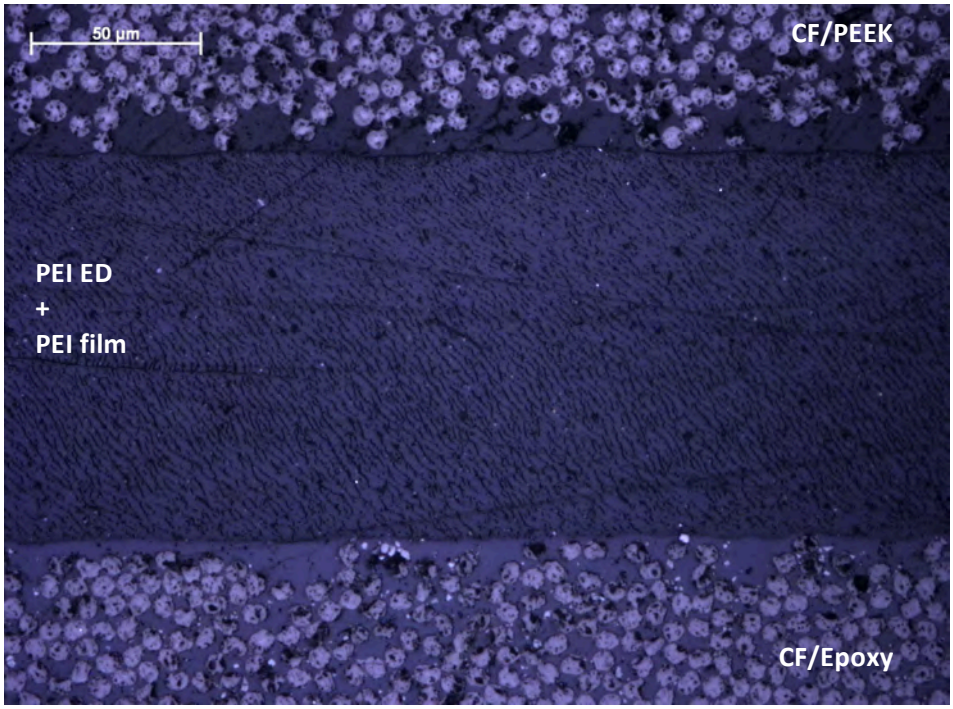

Figure 142: Zeiss optical microscope picture (x50 magnification) of MMHW-2 weld (2000 N, A6). This area of the cross section shows that the wrinkly PEI covers the whole interface, with no diffusion layer between the epoxy and the PEI.

8.8.2. Fractography

The fracture surface of this weld, shown in Figure 143, is very similar to the one of the MMHW-1 (Figure 136), with interlaminar failure of the epoxy and stuck carbon fibres from it on the CF/PEEK substrate. Nevertheless, in this case, a wider area of exposed epoxy fibres and a narrower thermoplastic-rich one can be appreciated on the CF/Epoxy surface. Thermoplastic bubbles on the right CF/Epoxy edge can be also appreciated too, but no exposed epoxy resin surface could be spotted here.

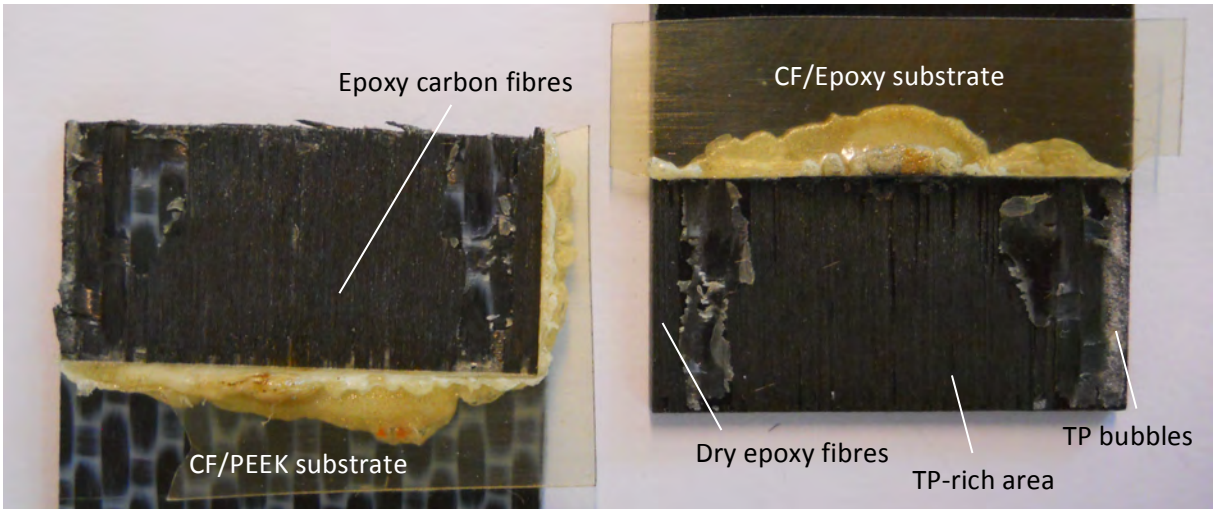

Figure 143: Fracture surface of MMHW-2 weld (higher-force parameters), using a PEI ED. Here as well, interlaminar failure of the epoxy, TP bubbles on the right edge and a thermoplastic-rich area can be spotted on the CF/Epoxy substrate.

8.9. MMHW-2 (PEI ED) – 1500 N, A9 PARAMETERS

8.9.1. Cross section analysis

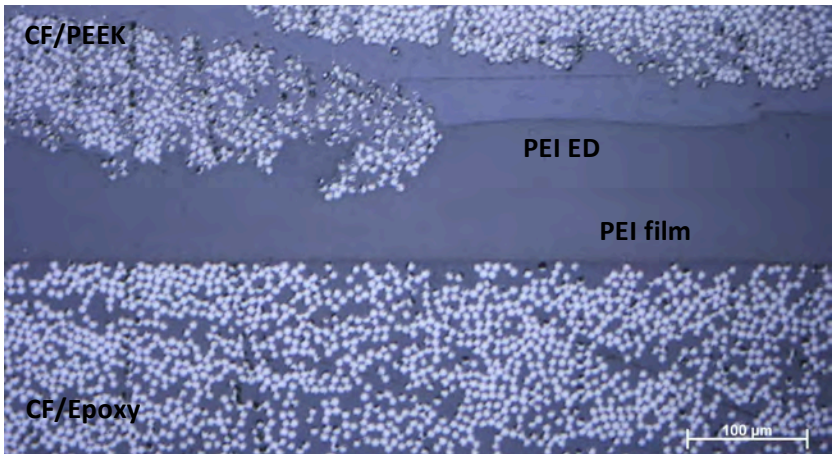

Figure 144: Zeiss microscope picture (x20 magnification) of the cross-section of MMHW-2 weld (1500 N, A9). Very good merging between PEI and PEEK was observed. A slight colour difference between PEI film and PEI energy director could be observed.

Figure 144 shows the cross section of the studied weld. In MMHW-2 weld with the lower-force higher-amplitude parameters, more intermingling between PEEK and PEI resins was observed, the first one penetrating into the PEEK substrate and even mixing with its carbon fibres. A slight colour difference between the PEI film and the PEI ED can be appreciated if looked carefully.

It is worth to mention that voids were found at the edge of the cross-section of the four types of welds, where the energy director is squeezed-out from the welding interface. They appear on the thermoplastic part, and they are due to the lack of pressure from the substrates in the area where the ED is squeezed out.

8.10. CONCLUSIONS

Ultrasonic welds of carbon fibre reinforced epoxy and PEEK substrates have been performed. The CFR thermoset co-cured with a PEI film and welded to the CF/PEEK substrates using either a PEEK or a PEI energy director. The quality of the welds was studied with LSS testing and optical microscope observation of their cross section.

One of the goals of this investigation was to prove the compatibility of PEEK and PEI. The average LSS value of 37.39 MPa, obtained for five tested samples of CF/PEEK substrates welded with a PEI ED, showed that the ultrasonic weld of these materials produces a strong joint. Optical microscope pictures of the cross section of these welds confirmed the feasibility of this combination of thermoplastics.

Another goal was to show the compatibility of PEI and epoxy. After setting a suitable autoclave lay-up for the co-cure of these two materials, it could be checked with cross-section observation that the PEI film effectively attached to the CF/Epoxy. Further investigation in the improvement of the compatibility and adhesion of PEI film and carbon fibre epoxy can be done. Previous experiments have shown the improvement of the adhesion between PEEK and PEKK with

epoxy when these thermoplastic films are treated with UV light. PEI, PEEK and PEKK have a similar molecular structure and, as this investigation has shown, PEI and PEEK have an extremely good compatibility. It is believed that treating the PEI film with UV-light may improve its compatibility with the epoxy.

The existence of a SIPN at the CF/Epoxy-PEI could not be confirmed. Optical microscope and SEM images suggest there is an intermingling interface between them, but none of these techniques could actually prove it. Hypotheses for the inability to clearly see a SIPN were the limitations of the used equipment, the presence of the carbon fibres that difficult this observation, epoxy expiration, or the curing temperature of the epoxy in relation to PEI's T_g.

Finally, for the welding with high-force parameters (2000 N, A6), the LSS strength values for both types – the one which used a PEEK energy director and the other one that used a PEI ED – were on the order of 22 MPa, among the highest ones obtained in other experiments with this epoxy that, as previously commented, was expired and did not obtained as high LSS values as expected due to interlaminar failure of the epoxy. These lap-shear values and the cross section observation confirmed that both types of welds produced an effective joint. In the weld where a PEEK energy director was used (MMHW-1), a layer between PEI and Epoxy appeared, which is believed to be a diffusion layer between these materials. The weld that used a PEI ED (MMHW-2) had some areas where the PEI film had detached. There was the trace of what seemed a diffusion layer between epoxy and PEI in some areas of the cross-section.

The welds with lower-force higher-amplitude parameters (1500N, A9) showed different interfaces: For MMHW-1 (PEEK ED) weld, the layer between epoxy and PEI did not appear and detachments at the epoxy contact-weld part where observed; for MMHW-2 (PEEK ED), there was better merging of PEEK and PEI resins. It is believed that the first set of parameters benefits MMHW-1, and that this second set works better for MMHW-2, due to the different materials involved in the interface, which count with dissimilar properties and stiffness.

Chapter 9

Direct Welding

This chapter will be devoted to the study of the welds that did not use a thermoplastic co-cured layer with the epoxy, which shields the epoxy from degradation due to the heat developed at the welding interface and enables to achieve an effective and strong weld of thermoset to thermoplastic materials. Here, epoxy degradation when direct welding and mechanical interlocking between laser-treated epoxy and thermoplastic will be studied.

9.1. STUDY OF EPOXY DEGRADATION

Direct welding of CF/Epoxy (no co-cured thermoplastic film) with a CF/PEKK substrate, using a PEKK energy director was performed. This thermoplastic material was chosen because it was the one that lead to higher welding times – compared to PEEK and PPS – therefore representing a conservative check of epoxy degradation. Two CF/Epoxy substrates were used: one of Hexply 8552 epoxy (expired) and another one of Hexply M21 (fresh). Degradation was studied by visual inspection and FTIR analysis.

9.1.1. Procedure

Table 19 summarizes the materials and welds performed for this study:

Sample reference	Bottom substrate	Top substrate	Energy director	Observations
SED-1	CF/Epoxy (Hexply 8552)	CF/PEKK (Ten Cate)	PEKK (Victrex)	One weld performed for FTIR analysis.
SED-2	CF/Epoxy (Hexply M21)	CF/PEKK (Ten Cate)	PEKK (Arkema)	Two welds performed. One of them analysed with FTIR.

Table 19: Welds of the epoxy study degradation.

Table 20 collects the welding conditions and welder outputs for each weld:

Sample reference	Welding parameters			Welding time (ms)	Consumed power (%)	Welding distance (mm)
	Force (N)	Amplitude	Travel (mm)			
SED-1	2000	A6 (73.4 µm)	0.17	210	62	0.20
SED-2	2000	A6 (73.4 µm)	0.09	450	104	0.16

Table 20: Welding conditions and outputs for the study of epoxy degradation.

It is very interesting to check that, for Hexply M21 epoxy, the welding time was higher (450 ms) for direct welding than for the hybrid welds performed with it in Chapter 7 (350-400 ms). The opposite happens with Hexply 8552 epoxy, whose welding time is 100-200 ms lower than the one obtained for its hybrid welds.

9.1.2. FTIR analysis

Both welds could be separated with the hands, a fact that shows the benefit of co-curing the thermoset with a thermoplastic film to achieve a stronger and effective weld. FTIR analyses were performed on both and compared to non-welded CF/Epoxy samples of each type, in order to check that no degradation occurred.

Hexply 8552 CF/Epoxy

A completely clean CF/Epoxy surface was obtained, with no burning or visible degradation, just as the surface of a non-welded CF/Epoxy sample.

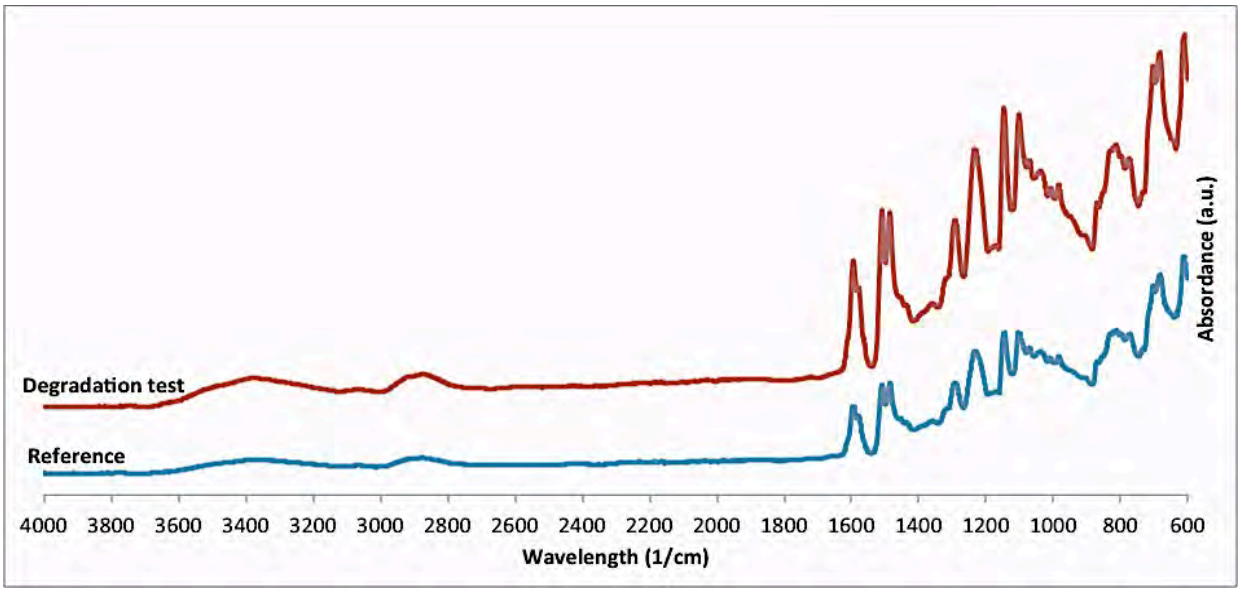

Figure 145: FTIR spectra (from 600 to 4000 cm^{-1} wavelength) for the welded and the reference Hexply 8552 CF/Epoxies. No difference is observed between them, which confirms no degradation occurred.

As it can be appreciated in Figure 145, the spectra of the reference and the welded sample are identical, showing that no degradation occurred and confirming what observed by visual inspection.

Hexply M21 CF/Epoxy

The epoxy surface obtained after the welding showed slight degradation on the edge, as Figure 146 shows. This is the results of the higher welding time obtained in the direct welding of this epoxy.

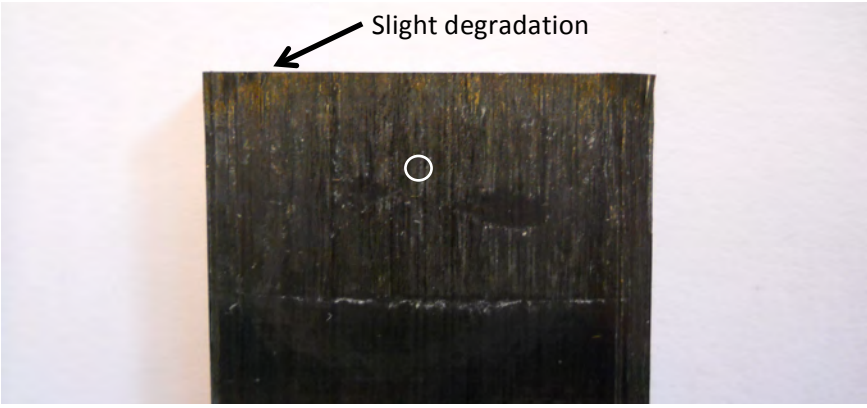

Figure 146: Hexply M21 CF/Epoxy substrate after welding. Slight degradation on the top edge can be appreciated.

An FTIR analysis (see Figure 147) was performed on the circled and centred part of Figure 146.

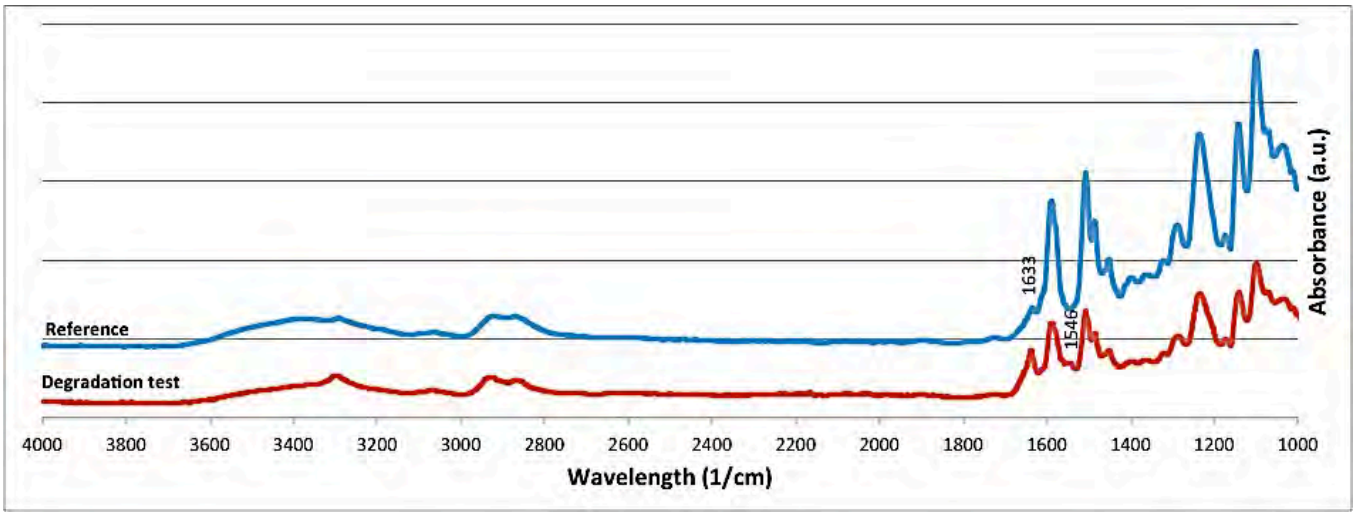

Figure 147: FTIR spectra (from 100 to 4000 cm^{-1} wavelength) for the welded and the reference Hexply M21 CF/Epoxies. Few differences are observed, with both spectra being practically identical.

Both spectra show the same peaks, with the only differences being a slight change of curve between 3400 and 3600 cm^{-1} wavelengths (which can be due to moisture), an increase in the peak at 1663 cm^{-1} wavelength and a peak appearing at 1546 cm^{-1} wavelength for the welded sample, with respect to the reference one. These last two may be indicating that slight degradation is occurring, but the magnitude and quantity of the differences in both spectra is so small, that it can be conservatively stated that no degradation is occurring. Moreover, the welds performed with this epoxy were coated with a thermoplastic layer that shields the epoxy from degradation, and had a lower welding time.

Even though the epoxy was not co-cured with a thermoplastic, therefore not having the protection it implies, the short welding time achieved with the high force-amplitude combinations avoid its degradation.

9.2. LASER TREATMENT

In this section, the improvement of adhesion between thermoset and thermoplastics in direct welding will be studied: The thermoset composite substrate will be treated with UV-laser and different conditions, with different levels of fibre exposure, and later the substrate will be ultrasonic welded to a thermoplastic reinforced substrate, using a thermoplastic energy director of the same material as the thermoplastic matrix. The aim of the laser treatment is to seek for mechanical interlocking between the thermoset and the thermoplastic materials, that is, keying of these two materials (macro-interlocking). As checked in section 9.1, direct welding of untreated epoxy produced a weld that could be separated with the hands, so this strength is sought to be improved by the enhancement of mechanical interlocking when laser-treating the epoxy. Laser treatments have showed to greatly improve the strength of adhesion-bonded samples [27], and now it will be tried for ultrasonic welding of thermosets to thermoplastic composites. Figure 148 illustrates this idea.

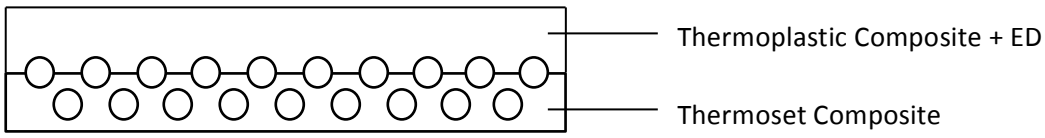

Figure 148: Mechanical interlocking between thermoplastic composite and thermoset-laser-treated composite after ultrasonic welding.

One of the experiments of P. Vizcaínos investigation, where CF/Epoxy substrates were grit blasted prior to direct welding, showed that increasing the roughness of the thermoset substrate surface greatly improves the lap-shear strength of direct welds: 10.1 MPa of LSS mean value compared to the 4.3 MPa of non-treated epoxy substrate [28].

The laser treatment was performed at the Technical University of Braunschweig, Germany, by Dr. Fabian Fischer, head of the Department of Adhesive Bonding and Composite Technologies at the Institute of Joining and Welding. The rest of the experiments and procedures were carried out at the Technical University of Delft.

9.2.1. UV-Laser Treatment

Dr. F. Fischer applied UV-laser treatment to Hexply 8552 CF/Epoxy 25.4 x 101.6 mm^2 cured samples. This method, performed with an excimer laser, is a cleaning technique for carbon fibre reinforced polymers (CFRPs). By regulating the intensity, the process can be controlled from the removal the surface contaminant and the remaining bulk material unchanged, to the exposure of the underlying fibres through resin removal. The UV-laser performs photoablation, a process that removes material by breaking molecular or atomic bonds rather than by bulk heating of the composite, so they can remove CFRP material without producing a Heat Affected Zone (HAZ).

There were three different conditions of UV-laser treatment applied to the CF/Epoxy samples; each type of condition was applied to four CF/Epoxy samples:

-P1: Removal of just a few µm of the matrix.
-P2: 50% excavation of the fibres.
-P3: 100% excavation of the fibres.

The surfaces of three samples, each one with a different type of condition, were observed with the SEM (see Figure 149).

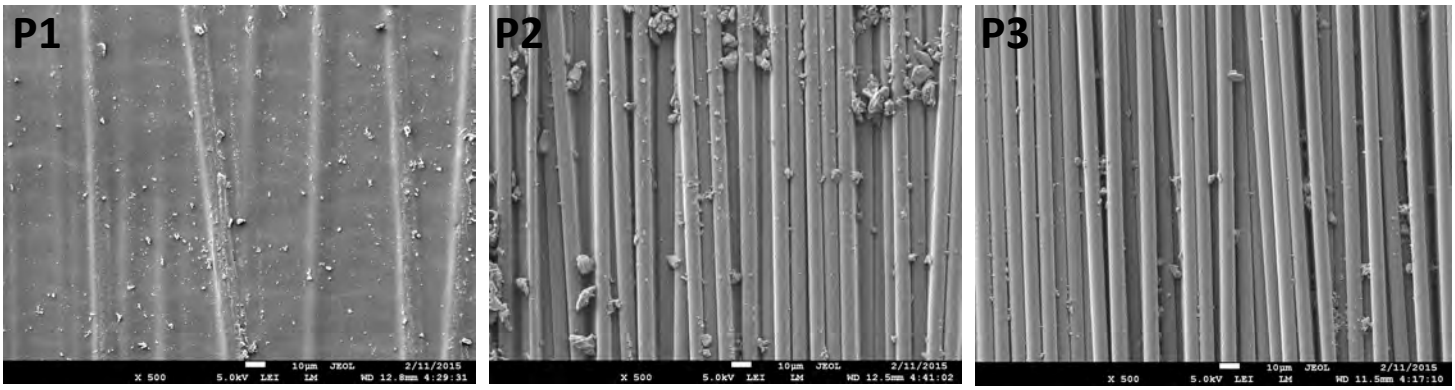

Figure 149: SEM pictures of the surfaces of CF/Epoxy samples treated with P1 (left), P2 (centre) and P3 (right) conditions.

It can be appreciated the gradual resin removal: from the first treatment P1, where a part of the matrix is being removed and fibres can be seen, but are still covered with resin, to treatment P2, where the fibres are exposed, but some resin can still be observed between them, and finally to treatment P3, where the carbon fibres are completely exposed with practically no matrix between them.

9.2.2. Procedure

The UV-laser treated CF/Epoxy samples were ultrasonically welded to the CF/PEEK samples, using a PEEK ED. Also, a CF/PEEK substrate was direct welded to a Hexply 8552 CF/Epoxy one, in order to compare the welding outputs and check if effective joining was achieved when not treating the epoxy substrate.

Table 21 summarizes the materials and welds performed for this study:

Sample reference	Bottom substrate	Top substrate	Epoxy treatment	Observations
REF-NT	CF/Epoxy (Hexply 8552)	CF/PEEK (Ten Cate)	-	One weld performed.
LT-P1	CF/Epoxy (Hexply 8552)	CF/PEEK (Ten Cate)	Laser P1 conditions	Two welds performed [a].
LT-P2	CF/Epoxy (Hexply 8552)	CF/PEEK (Ten Cate)	Laser P2 conditions	One weld performed.
LT-P3	CF/Epoxy (Hexply 8552)	CF/PEEK (Ten Cate)	Laser P3 conditions	One weld performed.

Table 21: Laser treatment reference and hybrid welds.

[a] The first welding of the P1 treatment could be broken simply using the hands, so it was repeated; it was also decided not to perform LSS tests to any of the welds.

In Table 22, the welding conditions and welder outputs for each weld are collected:

Sample reference	Welding parameters			Welding time (ms)	Consumed power (%)	Welding distance (mm)
	Force (N)	Amplitude	Travel (mm)			
REF-NT	2000	A6 (73.4 µm)	0.15	668	83	0.23
LT-P1				883	91	0.24
LT-P2				782	89	0.24
LT-P3				747	84	0.24

Table 22: Welding conditions and outputs for laser-treatment and reference welds.

It can be appreciated that welding time decreases with increasing excavation of the fibres. As previously commented, no LSS tests were performed on these welds. Cross-section analysis was the selected technique to study the interfaces.

9.2.3. Reference weld (Not Treated epoxy)

This reference weld could be broken simply with the hands, showing that no effective weld was actually developed. No cross section analysis could be performed.

9.2.4. P1 conditions

Cross section analysis

For P1 conditions, Figure 150 shows optical microscope pictures at different magnifications. The CF/Epoxy laminate was severely damage, with the formation of large transverse cracks during welding.

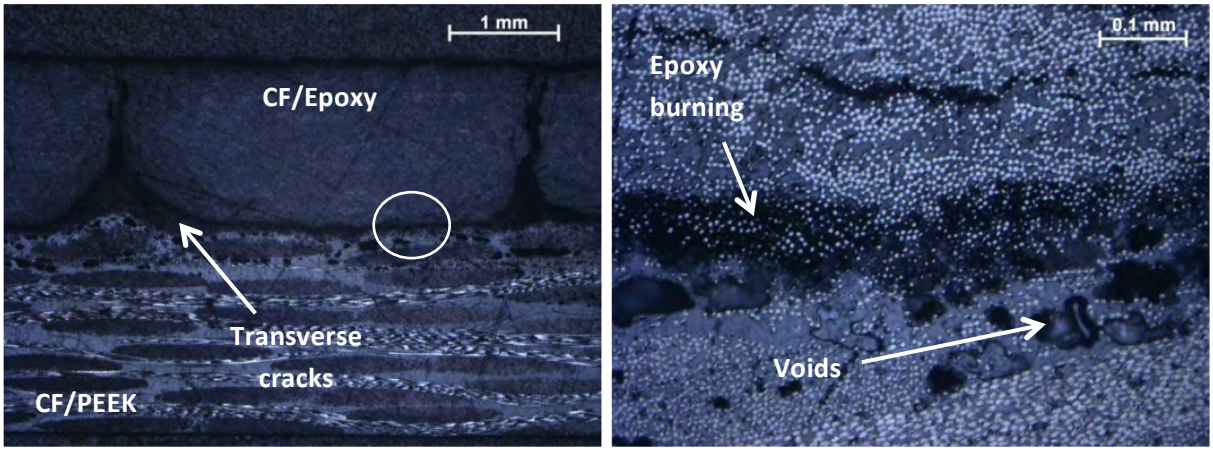

Figure 150: Optical microscope pictures of P1 conditions weld. Left picture shows an image of the centre of the cross-section (x2.5 magnification); transverse cracks across the epoxy substrate can be appreciated. Picture on the right represents a detail of that part of the cross section, the area inside the circle on the left image; voids in the CF/PEEK substrate and burning of the epoxy appear at the interface (x20 magnification).

Voids, transverse cracks in the thermoset laminate and what is believed to be burning of the epoxy resin can be observed at the interface of the entire cross-section: Voids tend to appear in the CF/PEEK part of the interface, and the burning and longitudinal cracks occur in the resin of the CF/Epoxy at the interface. At the edges of the cross-section, these effects are enhanced. Also, large

transverse cracks appear, growing from the welding interface through the thickness of the CF/Epoxy substrate, which were created during the welding.

The reason of these defects may be the large temperature concentration at the interface: For this low excavation of the fibres, it is believed that the thermoplastic from the ED and the TPC matrix cannot flow between the epoxy fibres, so the heat is concentrated in burning of the epoxy resin, and also in melting a wider thickness of the thermoplastic substrate, the reason why the voids appear so far from the welding interface. This heat burns the epoxy and eventually even breaks it. As the epoxy seems to be thermally degraded during the welding process, which generates heat that increases the temperature at the welding interface, decomposition voids appear at the first layer of the CF/PEEK laminate because not enough pressure can be applied due to the crumbling into pieces of the adhered epoxy.

It is worth to remember that these voids did not appear when welding CF/PEEK to CF/PEEK using a PEEK ED (Figure 52 of Chapter 4), using the same welding parameters (only a few at the edge of the cross section, due to the contact with the air oxygen). This made clear that the voids in the centre and along the cross-section when welding CF/PEEK to CF/Epoxy treated with P1 laser conditions, are not a common behaviour of the thermoplastic, but of this specific materials and parameters combination.

Fractography

The first sample of P1 treatment that was welded could be hand-broken, as mentioned previously, so the weld was repeated in order to be able to study the cross-section, as already done. Nevertheless, the fracture surface of this first weld was visually inspected: on the CF/Epoxy welding surface, epoxy resin burning on the edge and centre of the overlap area and delamination failure were found. Moreover, a large burned transversal crack was also spotted at the cross section of this epoxy sample. On the CF/PEEK welding surface, burnt and not-burnt fibres from the epoxy remained attached. Figure 151 shows a picture of these fracture surfaces:

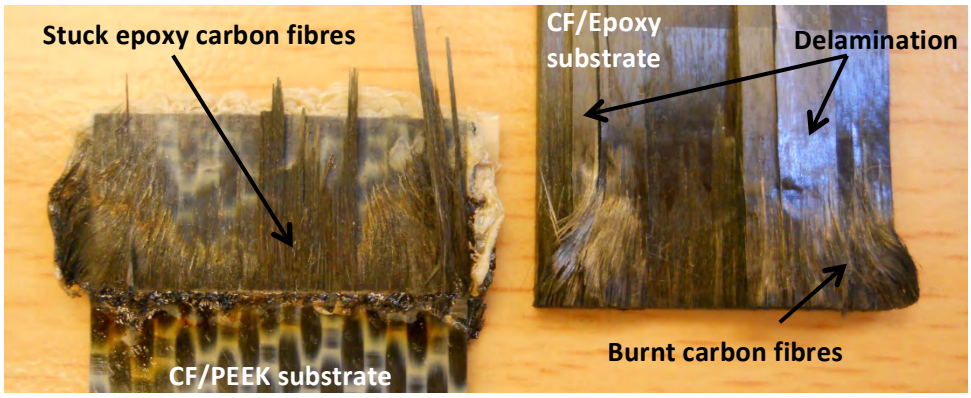

Figure 151: Fracture surface of hand-broken P1-treatment weld. Stuck epoxy carbon fibres can be observed in the CF/PEEK surface; on the CF/Epoxy surface, delamination and burnt carbon fibres are appreciated.

9.2.5. P2 conditions

Cross section analysis

Optical microscope pictures, using different magnifications, were taken for P2 weld cross-section. Three regions, with different interface characteristics, could be identified in the studied part of the cross section. Figure 152 shows a scheme of the location of these regions (R1, R2 and R3):

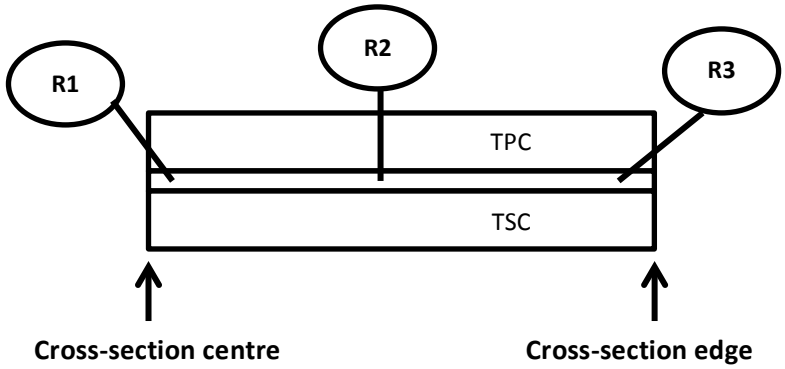

Figure 152: Scheme of treatment P2 cross-section observable regions (R1, R2 and R3).

Diffusion of the carbon fibres from the epoxy substrate across the interface and towards the CF/PEEK substrate is clearly observed in the three regions, achieving partial mechanical interlocking between the thermoplastic and the thermoset.

Region R1 is characterized by a gap between the thermoplastic and the thermoset resins. The diffused carbon fibres from the epoxy into the thermoplastic substrate and the gap pattern lead to the hypothesis that the thermoplastic resin could reach the thermoset at some point of the welding process but, due to the high vibrations, the two materials eventually separated in this region. Figure 153 shows two optical microscope images of this area of the joint:

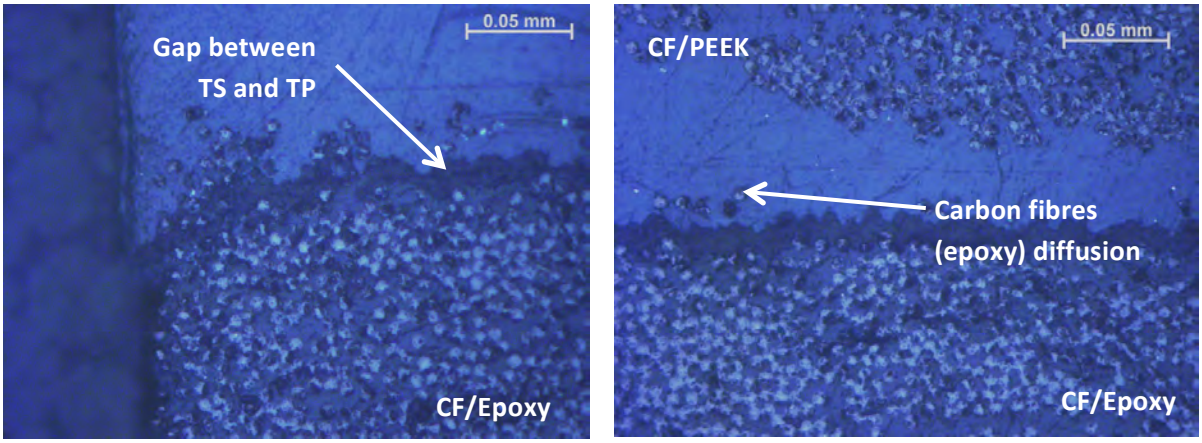

Figure 153: Optical microscope images of region R1, both with x50 magnification, where the gap between the thermoset and the thermoplastic matrices can be observed. Carbon fibres flow from the CF/Epoxy substrate are also pointed out.

Region R2 shows the optimum type of interface for this welding materials and conditions: the thermoplastic matrix completely wets the thermoset, without the appearance of voids, cracks or burning areas at the interface. Figure 154 shows an optical microscope picture of this area:

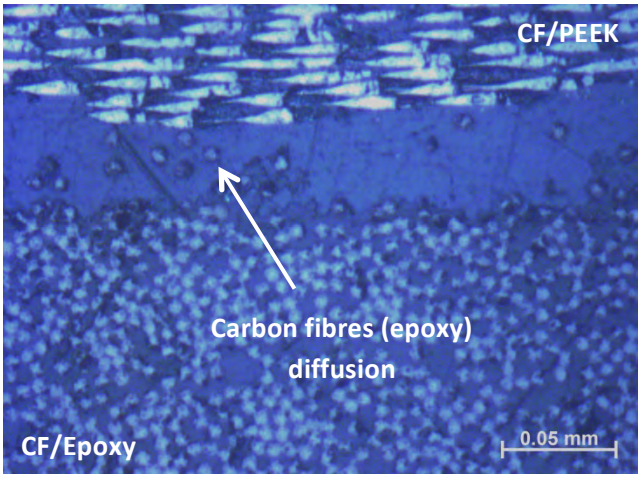

Figure 154: Optical microscope image of region R2, with x50 magnification. The thermoplastic matrix wets all the carbon fibres and resin interface of the thermoset substrate. Diffusion of carbon fibres from the CF/Epoxy substrate can also be observed.

Region R3 is characterized by, what is believed to be, burning of the thermoset resin, longitudinal cracks on the thermoset substrate and voids on the thermoplastic substrate near the interface, the same characteristics as the ones observed in P1-treatment weld (see Figures 155 and 156). Also, what seem to be thermoset resin drops diffuse across the interface into the thermoplastic substrate, an effect that probably occurred in the P1-treatment weld, but that was difficult to see due to the believed large burning occurring (these drops were probably also burnt). In regions R1 and R2, there is also diffusion of epoxy drops, but not as large and as many as in R3. These drops may indicate that the degradation of the epoxy and the believed burning occurring in this region separated the welding interface here.

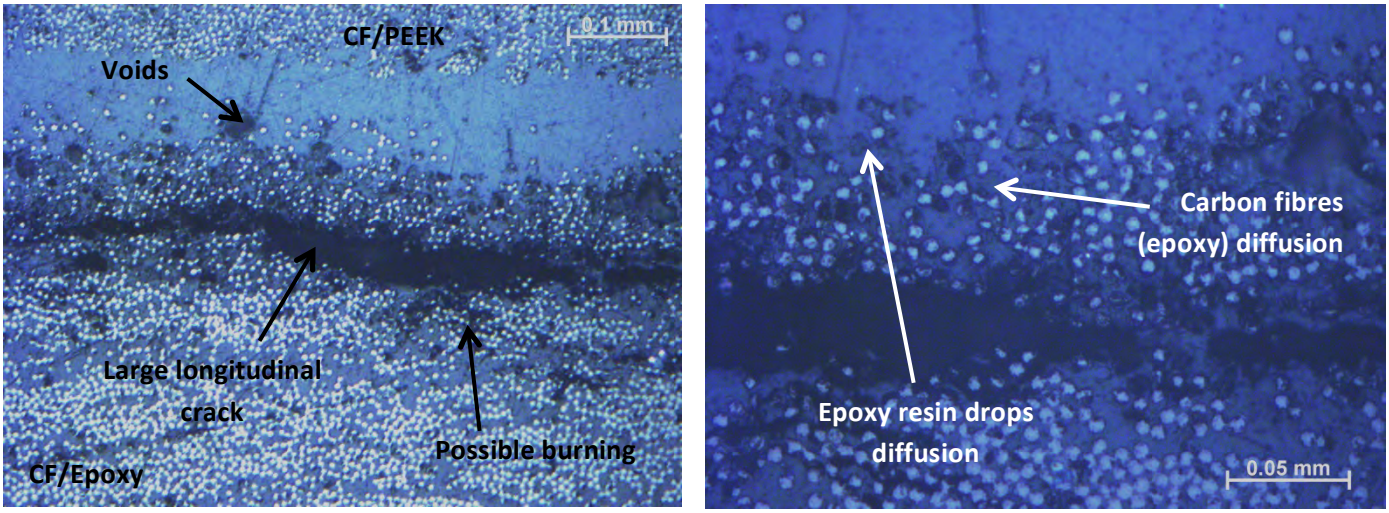

Figure 155: Optical microscope images of region R3 of the P2-treatment weld. Picture on the left has x20 magnification, and picture on the right, x50. In both of them, likely burning and large longitudinal cracks near the interface in the CF/Epoxy substrate can be observed. Diffusion of epoxy carbon fibres and resin drops across the interface is also noticeable.

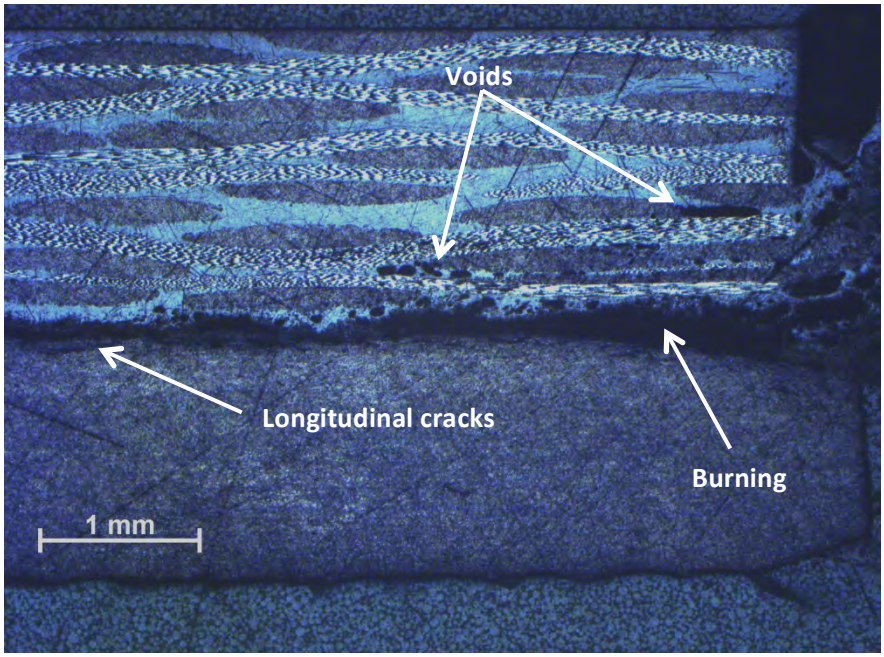

Figure 156: Optical microscope image, with a x2.5 magnification, of the edge of the weld. Voids on the thermoplastic substrate, and burning and longitudinal cracks on the thermoset one are enhanced at this part of the cross-section.

The difference in the three regions relies in the fact that pressure is not uniform across the interface, so that the optimum pressure and thermoplastic flow is achieved in region R2.

9.2.6. P3 conditions

For P3-conditions weld, the optical microscope pictures are shown in Figure 157.

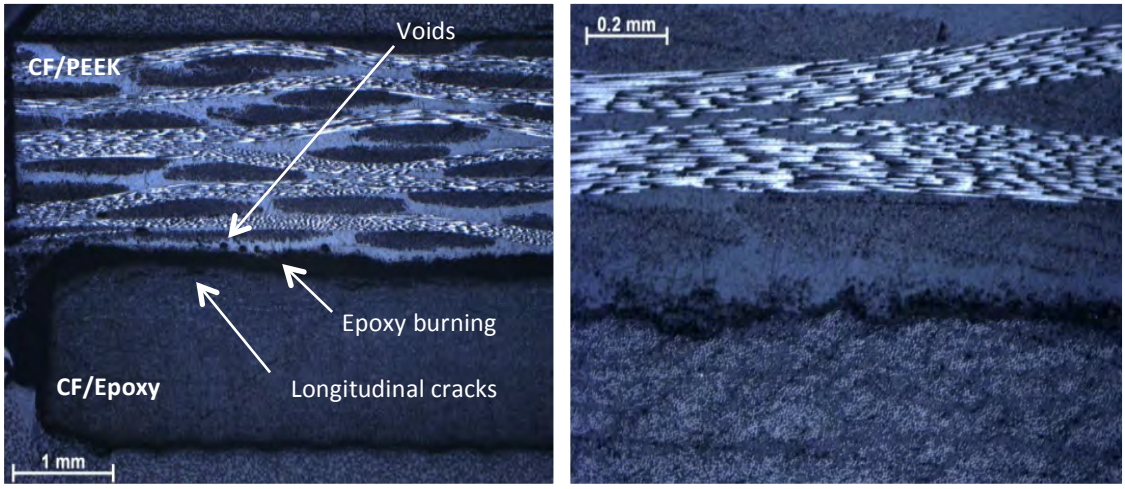

Figure 157: Optical microscope images of P3 conditions weld. Picture on the left shows the edge of the weld (x2.5 magnification), where some cracks and burning on the epoxy, and voids on the thermoplastic substrates, can be appreciated; picture on the right shows a closer view of the centre of the cross-section (x10 magnification).

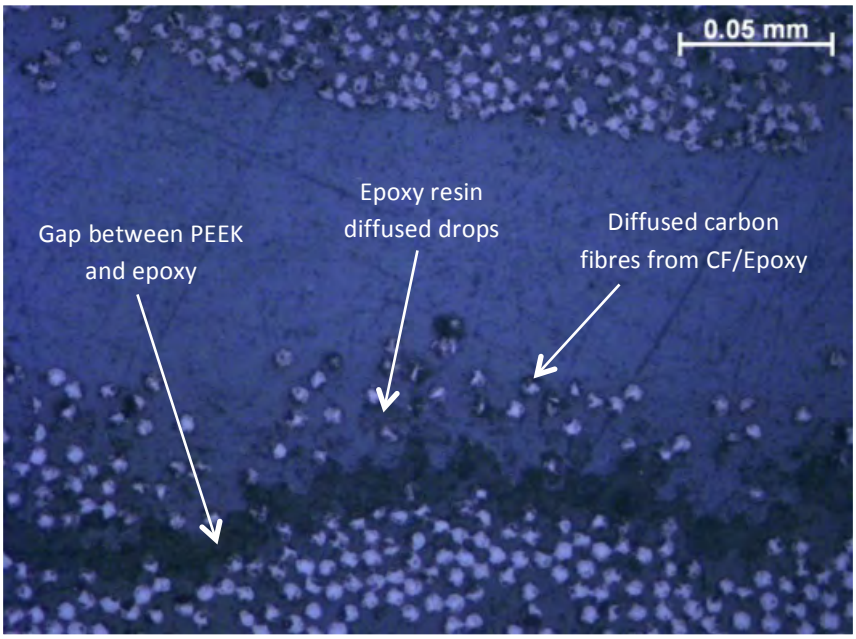

Figure 158: Optical microscope image of the interface at the centre of the P2 welding cross-section (x50 magnification). The relevant characteristics of this weld, which are observed through the whole interface, can be appreciated: the gap between the thermoplastic and the thermoset substrates, and the resin drops and carbon fibres from the CF/Epoxy substrate that diffused across the gap and merged with the thermoplastic matrix.

In Figure 158, a similar interface as the one observed in region R1 of P2-weld can be appreciated: There is a gap between the thermoset and thermoplastic resins, which occurs throughout the whole interface. The presence of some drops of epoxy travelling across this gap into the thermoplastic substrate, which seem to burn towards the edge of the cross section, and carbon fibres, as well as the gap pattern indicate that the materials were merged during the welding and separated due to the large vibrations. The epoxy at the lower part of the gap is also believed to be burnt towards the edge of the cross section, where also voids on the CF/PEEK and cracks on CF/Epoxy substrates appear close to the interface. The resin drops and carbon fibres that diffused across the gap and merged with the thermoplastic matrix are achieving the sought mechanical interlocking phenomenon between the thermoset and the thermoplastic.

9.2.7. Conclusions

Ultrasonic welds of carbon fibre reinforced epoxy and PEEK substrates have been performed. The CFR thermoset was UV-laser treated with different conditions and intensities. The quality of the welds was studied with optical microscope observations of their cross section.

In view of the cross-section pictures, P1 conditions can be immediately discarded, due to the large burning areas, voids and cracks that appear after welding. Comparing the other two types of conditions, P2 are the ones which provide a less degraded epoxy resin across the interface and enable the formation of a mechanical interlocking (macro-interlocking) between the thermoset and the thermoplastic. The study of the cross-section revealed a not-uniform interface due to different pressure profile across it, being able to identify three different regions. Region R1 seemed to have the characteristics of the P3-weld interface, with a gap between the thermoplastic and thermoset resins; region R3 resembled the interface of P1-treatment weld, with a large burning area and

longitudinal cracks in the epoxy substrate, and voids in the PEEK one. Region R2 showed no burning of the epoxy, no voids appearing in the PEEK substrate, full wetting of the CF/Epoxy fibres and resin interface by the thermoplastic matrix, and diffusion of small drops of epoxy resin and carbon fibres across the interface, the optimum characteristics.

The high obtained welding times, combined with the fact that the epoxy has no thermoplastic co-cured layer acting as a protective shield against the heat generated in the welding process, are the reason of the large burning areas of the CF/Epoxy substrate at the interface. Another fact that is worth to pay attention to is the decrease of the welding time with fibre exposure. The reason is that the welding process is travel-controlled, setting 0.15 mm of sonotrode travel as the target value, and it is easier/faster for the thermoplastic matrix to flow through the more exposed epoxy fibres than to overcome the obstacle of the epoxy resin interface, which cannot re-melt. In the case of hybrid welding, for example, times are shorter due to the fact the CF/Epoxy is coated with a layer of thermoplastic which is able to quickly melt and flow, achieving the desired travel value faster than if the epoxy is not coated of the thermoplastic has to penetrate through the exposed fibres.

Moreover, the strength of the welds seems to be low. In view of these results, P2 conditions give the best cross section, but a further treatment should be applied to, first, enhance the adhesion (micro-interlocking) of the thermoset to the thermoplastic to improve the strength value, and second, to increase the flow velocity of the thermoplastic, such that the wetting occurs faster and at all the regions of the interface. Otherwise, indirect or hybrid welding is a good answer for thermoset to thermoplastic welding.

Nevertheless, although the strength of welds P2 and P3 could not be measured, it was greater than the lack of adhesion experienced in direct welding of CF/PEEK to non-treated CF/Epoxy, which produced no effective weld. It was demonstrated that macro-molecular interlocking, by exposing the thermoset fibres, can certainly improve the adhesion and strength of the weld.

Chapter 10

Thermoset to Thermoset Welding

Although in hybrid welding, the co-curing of the thermoplastic film with the thermoset substrate protected it from degradation and adds more thermoplastic resin to the interface, still an energy director is needed to proceed with the ultrasonic welding. In this chapter, welding without energy director with thick thermoplastic co-cured film, will be tried. This will be done together with another type of materials combination: Welding of thermosets to thermosets. This technique may give more freedom for the manufacture of the parts, not constraining them to be cured together (as in the co-curing and co-bonding processes).

Bearing in mind that direct welding of thermosets is not possible – because their resin cannot be re-melted when welded – different methods are being investigated. Particularly, in this paper the following technique is implemented: Ultrasonic welding of thermoset to thermoset substrates, using a co-cured thermoplastic layer on both parts, which enables the performance of this fusion bonding technique and shields the thermoset from degradation during this process, as commented previously. Two type of welds will be performed: the first type, which will be called "TS-PVB-1", will be performed with an ED and a thinner layer of thermoplastic film co-cured with the thermoset, and the second one, "TS-PVB-2" will use a thicker layer of thermoplastic and no ED. Welding of thermosets to thermosets was one of the experiments performed by P. Vizcaíno in the investigation carried at TU Delft, and 90% of the LSS the thermoset adhesive joints was achieved by ultrasonic welding, using a thick co-cured TP layer (0.25 mm) and energy directors of the same material [28].

Although these experiments will not use a thermoplastic composite substrate, they can be regarded as a type of hybrid welding. All the materials used in this part of the investigation were provided by Professor Alfonso Maffezzoli, from the Innovation Engineering Department at Salento University, Italy.

10.1. MATERIALS

Two cured panels of thermoset with co-cured layer of thermoplastic were provided by Prof. Alfonso Maffezzoli, both with 305 x 310 mm^2 dimensions. The epoxy was carbon-fibre reinforced, with glass-fibre reinforcement lines arranged as a mesh. The thermoplastic film co-cured was of PVB (Polyvinyl butyral) material. One of the samples used a 250 µm-thick layer of PVB – the one which will not use an ED when ultrasonic welded – and the other sample had a 45 µm-thick layer of PVB – the one which will use an ED. Two PVB separate films were also provided, 250 µm and 45 µm thick, respectively.

The two cured epoxy panels were taken to Van Nobelen Delft VB company to be water-jet cut into 25.4 x 101.6 mm^2 samples; 14 samples were obtained from each panel. For the energy

directors on the second type of welding, 26 x 26 mm^2 EDs were cut with a pair of scicssors from the 0.25 mm-thick PVB film.

Figure 159 shows the reinforcement pattern of the 305 x 310 mm^2 samples

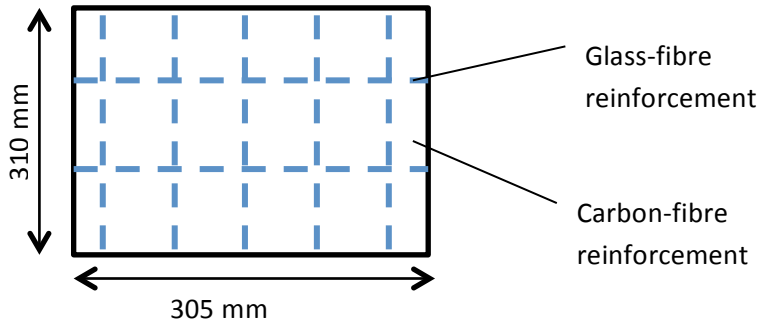

Figure 159: Reinforcement pattern (glass and carbon fibres) of the cured epoxy + PVB panels, with 305 x 310 mm^2 dimensions.

10.2. PROCEDURE

Figure 160 illustrates the two types of welds that are going to be performed:

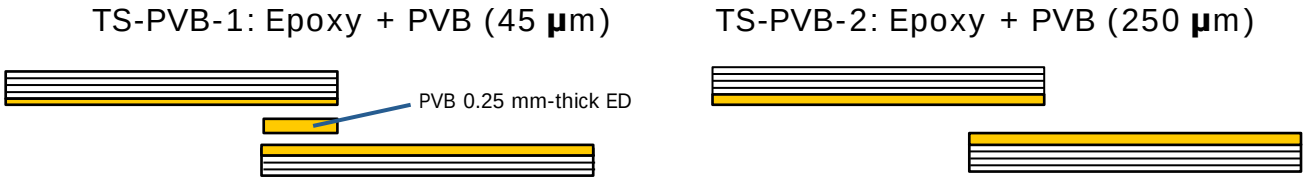

Figure 160: The two types of welding that will be performed: TS-PVB-1 (left) uses the 45 µm PVB film co-cured with the reinforced epoxy and a 0.25 mm-thick ED; TS-PVB-2 (right) uses no ED and the thickness of the co-cured PVB film is 250 µm.

Table 23 summarizes the materials and welds performed for this study:

Sample reference	Bottom substrate	Top substrate	Co-cured TP thickness (µm)	Energy director	Observations
TS-PVB-1	CF/Epoxy	CF/Epoxy	45	0.25 mm-thick PVB	Six welds performed: -Five for LSS testing. -One for OM.
TS-PVB-2	CF/Epoxy	CF/Epoxy	250	-	Six welds performed: -Five for LSS testing. -One for OM.

Table 23: TS-TS welds.

Table 24 collects the welding conditions and welder outputs for each weld:

Sample reference	Welding parameters			Average Welding time (ms)	Average Consumed power (%)	Average Welding distance (mm)
	Force (N)	Amplitude	Travel (mm)			
TS-PVB-1	1500	A9 (86.2 µm)	0.25 [a]	300	90	0.30
TS-PVB-2	1500	A9 (86.2 µm)	0.25 [a]	220	96	0.34

Table 24: Welding conditions and outputs for TS-TS welds.

[a] This travel is the total thickness of the ED in TS-PVB-1, and the thickness of each of the co-cured PVB films in TS-PVB-2.

It is interesting to study the Power and Displacement vs. Time curves, since two different approaches of ultrasonic welding are being studied (see Figures 161 and 162).

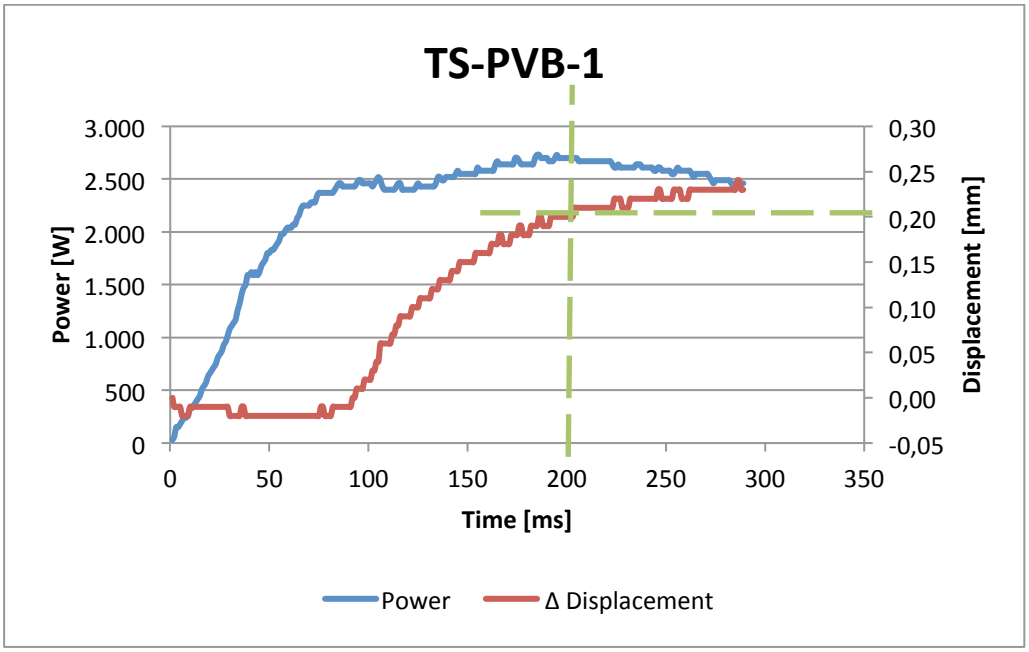

Figure 161: Power, Displacement vs. Time curves for one of the TS-PVB-1 samples. They resemble the curves obtained for ultrasonic welding of thermoplastic to thermoplastic reinforced substrates using a flat ED. The green discontinuous lines purpose will be explained hereinafter.

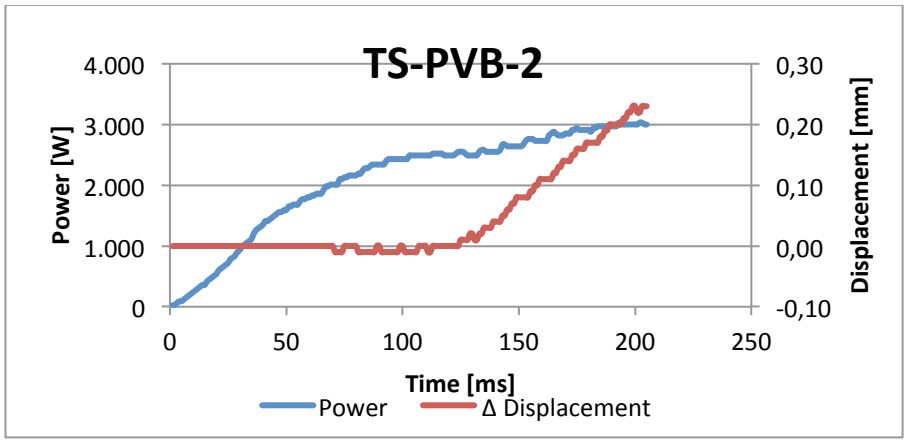

Figure 162: Power, Displacement vs. Time curves for one of the TS-PVB-2 samples. Here, the power continuously increases with time from the beginning of the welding process, and that seems to be reaching a plateau towards the end of the welding process; displacement of the sonotrode remains constant at the beginning of the process and then starts increasing with constant slope, coinciding with a change in slope in the power curve.

It is worth to mention that two other welds, which turned out not to be successful, were tried:

- One with two 45 µm-substrates and no ED, using 0.04 mm travel (the thickness of each co-cured PVB films) and the same force-amplitude parameters as in the previous cases. The weld

produced could be broken with the hands and the substrates were burnt, which explained the smoke that came out during the process.

- Another using two 250 µm-substrates, no ED and 0.30 mm travel (higher than TS-PVB-2 travel) and the same force-amplitude parameters as in the previous cases. It was discarded because the fracture surface obtained after performing a lap-shear test revealed a less cohesive failure and more fibre breakage than for TS-PVB-2 samples.

To characterize the interface, single-lap shear tests of the welds and optical-microscope observation of the joint cross section were done.

10.3. MECHANICAL TESTING

- For TS-PVB-1 welding (45 µm) samples, the results for the lap shear strength (LSS) are shown in Table 25:

Sample reference	LSS (MPa)	Average LSS (MPa)	Standard deviation	Coefficient of Variance (%)
TS-PVB-1-1	27.38	24.30	2.51	10.33
TS-PVB-1-2	2.11			
TS-PVB-1-3	21.31			
TS-PVB-1-4	26.09			
TS-PVB-1-5	22.41			

Table 25: TS-PVB-1 LSS test results.

There was some scatter in the results, leading to a coefficient of variance of 10% (an acceptable value would be below 6%).

The second sample had an extremely low strength (2.11 MPa): It failed. For the calculation of the average and the standard deviation, it was not taken into account, because it led to unrealistic results with large scatter. Another weld could not be done because there was no material left.

The cause that led this sample to fail was degradation. Its welding time was 545 ms, much higher than the average welding time of the other four samples.

Looking its the Power and Displacement vs. Time curves (Figure 153), a ceiling in the sonotrode displacement was found, which occurs for high travel values. This confirms that the value of the travel selected for this type of welding was a little bit higher than the optimum, which would be around 0.20 mm (in Figure 161, this would coincide with the power plateau and the change of slope in the displacement curve, indicated with green discontinuous lines in the figure). As the travel control value was a little bit higher, close to the region where a displacement ceiling can be reached, the process will finish when this value is achieved; for the rest of the samples it finished before, but for this failed one, the welding time was much longer, the PVB was squeezed from the interface and the sample was degraded. This kind of arbitrary degradation failures are more prone to occur for welds whose control travel is higher than the optimum value. For the weld of thermoset to thermoset substrates, achieving a ceiling value in the sonotrode displacement is logical: when all the thermoplastic of the interface is compressed and squeezed out, as the thermoset resin cannot re-melt after being cured, the sonotrode cannot displace further. The addition of the ED can be regarded too as an increment in room for sonotrode displacement when thermosets are involved in

the welding, apart from their lower stiffness that makes them concentrate the heat at the interface, of course. Although the total thickness of the thermoplastic at the interface is higher than 0.25 mm (approximately the ceiling value reached), because it also accounts with the co-cured thermoplastic films of the epoxy substrates, compression of thermoplastic also occurs in the force value build-up (1500 N), which is not recorded in Figure 163 plot.

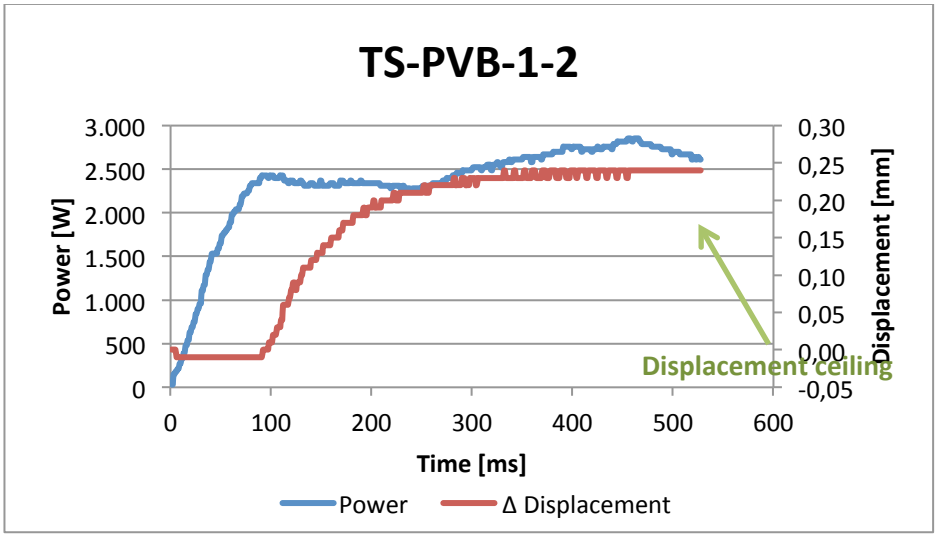

Figure 163: Power, Displacement vs. Time curves for the failed TS-PVB-1-2 sample. A ceiling in the sonotrode displacement, can be appreciated.

- For TS-PVB-2 welding (250 µm) samples, the results for the lap shear strength (LSS) are shown in Table 26:

Sample reference	LSS (MPa)	Average LSS (MPa)	Standard deviation	Coefficient of Variance (%)
TS-PVB-2-1	29.24	27.91	1.09	3.91
TS-PVB-2-2	28.87			
TS-PVB-2-3	26.96			
TS-PVB-2-4	26.38			
TS-PVB-2-5	28.12			

Table 26: TS-PVB-2 LSS test results.

These samples had low scatter and the average strength was higher than for TS-PVB-1 welding type.

10.4. TS-PVB-1-2 (FAILED)

7.2.1. Fractography

Figure 164 shows the fracture surface of the failed weld. The PVB that was squeezed out the interface during the welding had a dark brown colour, unlike the other samples, due to the burning. The fracture surface of the interface shows dry fibres, and little trace of PVB resin, so it is a mixture of cohesive and substrate failure. It seems that almost of the PVB was squeezed out during the welding, so the weld could not effectively be achieved.

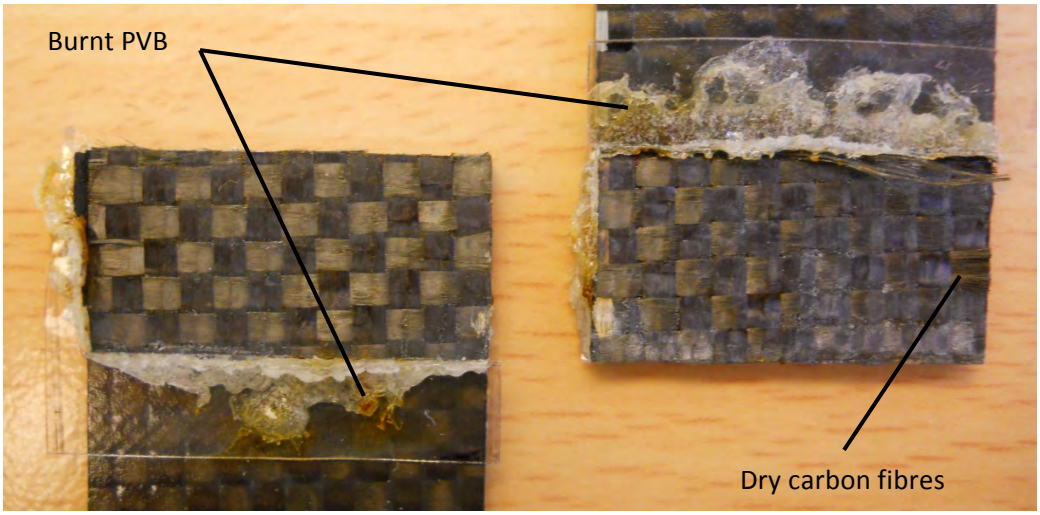

Figure 164: TS-PVB-1-2 failed sample fracture surface picture. Burnt PVB and dry carbon fibres can be appreciated.

Figure 165 displays two SEM images of TS-PVB-1-2 fracture surface, the failed sample of this type of welding. Exposed fibres from the thermoset and little remaining of the PVB film can be observed.

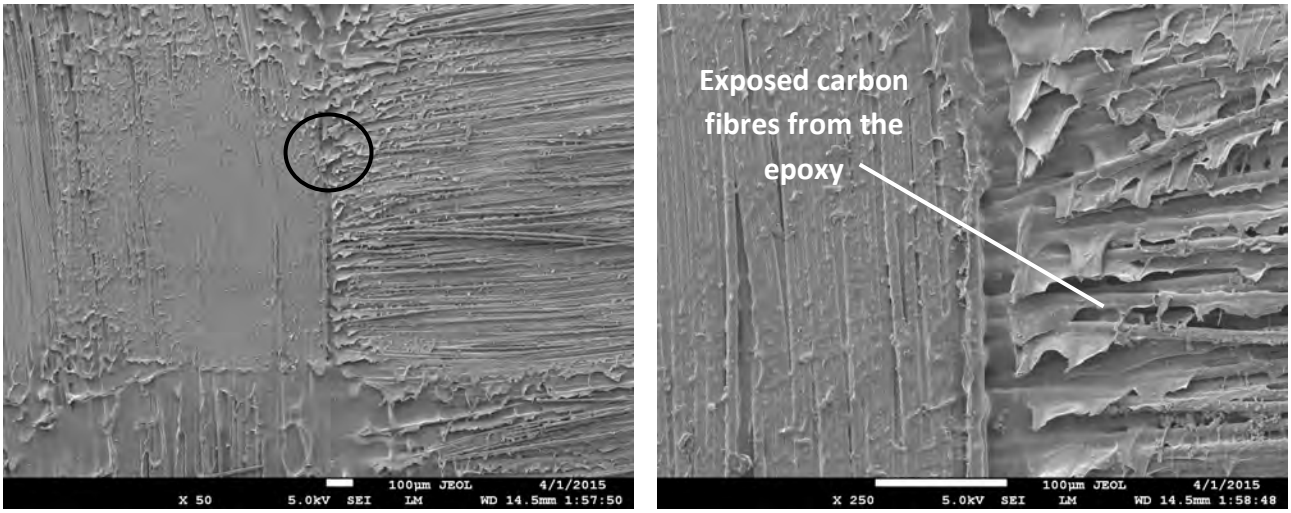

Figure 165: *SEM pictures of failed TS-PVB-1-2 sample fracture surface, (left has x50 magnification, right one has x500 magnification). Image on the right corresponds to the circled detailed on the left picture. Little remains of PVB can be seen, and fibres from the epoxy substrate are highly exposed.*

10.5. TS-PVB-1 (45 µm)

10.5.1. Fractography

The other four samples of TS-PVB-1 weld, which did not fail, had cohesive failure type, the breakage occurred in the thermoplastic at the interface, and remains of PVB are observed on both fracture faces of the substrates (see Figure 166).

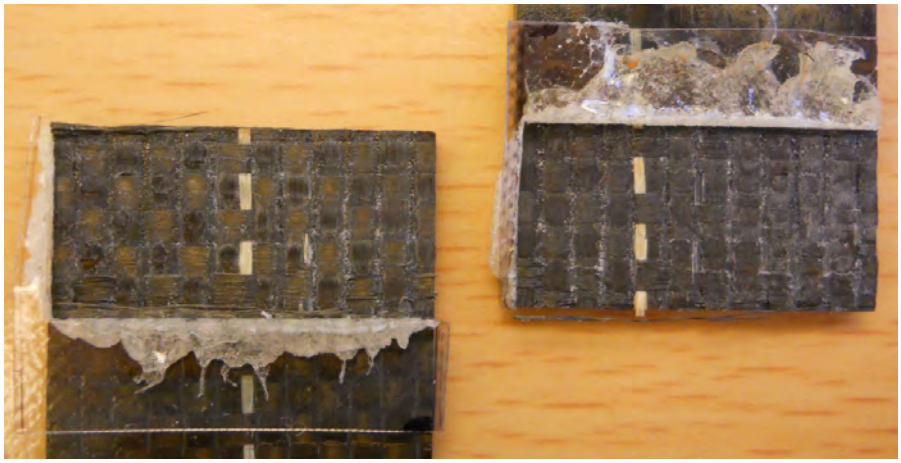

Figure 166: Non-failed TS-PVB-1 sample. Remains of PVB resin at the interface can be appreciated, which led to cohesive failure and high LSS values.

Figures 167 shows SEM pictures of the fracture surface of TS-PVB-1-5, an un-failed sample of this type of welding. Remains of PVB that cover the fibres can be clearly seen, showing cohesive failure of the sample and the difference with the failed sample fracture surface.

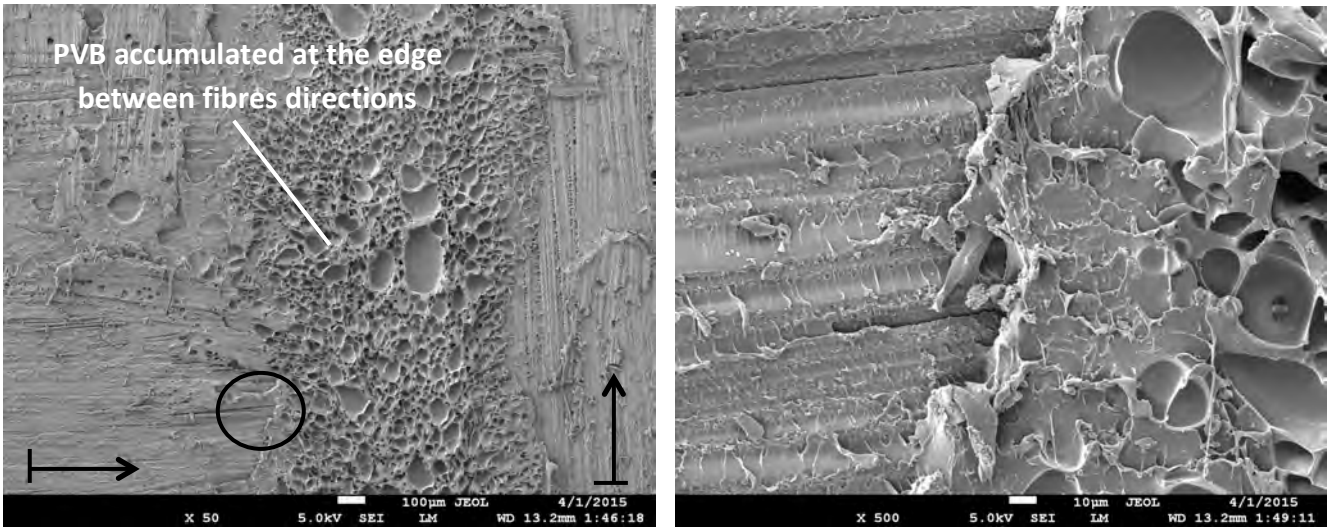

Figure 167: SEM pictures of TS-PVB-1-5, non-failed sample, fracture surface (left has x50 magnification, right one has x500 magnification). Image on the right corresponds to the circled detailed on the left picture. There are remains of PVB all over the surface, covering the fibres of the epoxy substrates, and especially a higher amount of this thermoplastic can be appreciated on the edges where the two directions of the epoxy reinforcement meet (recall that the epoxy had a weave carbon and glass reinforcement). Black arrows on the left image indicate fibre direction.

10.5.2. Cross section analysis

Figure 168 shows the cross section for this weld:

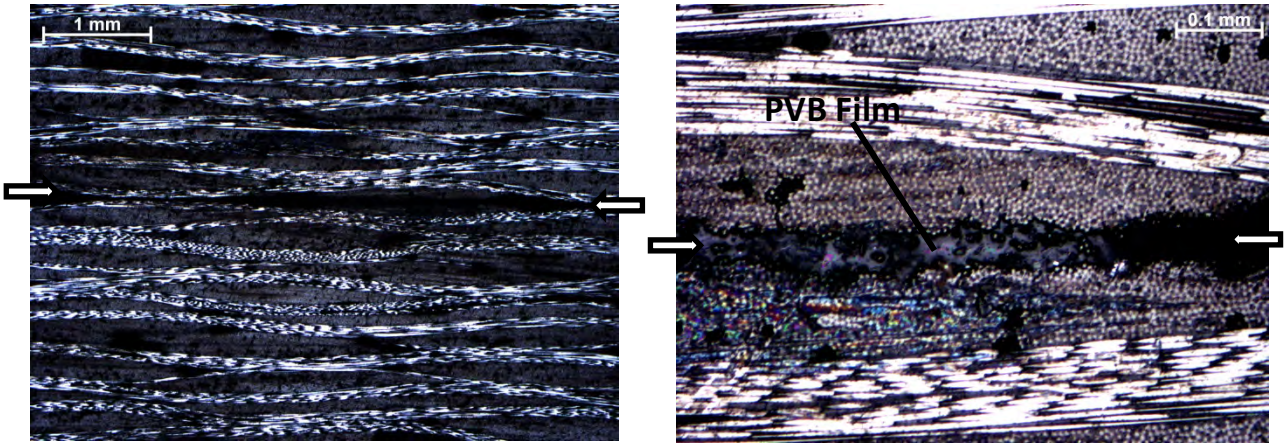

Figure 168: TS-PVB-1 cross-section pictures, x2.5 (left) and x20 (right) magnifications. Picture on the right shows remains of PVB film that the polishing did not removed. Blue arrows show the location of the welding interface.

Due to the polishing, the PVB film was removed from the interface, and a large gap between both substrates of the two welding types can be observed. Some remains of the PVB film can be appreciated on the right image of Figure 168.

In order to check that the PVB was removed during the polishing procedure, a 45 µm and 250 µm-thick PVB pieces were submerged in ethanol. Both of the films dissolved, the thinner one doing it immediately. This proves the hypothesis of the PVB film being dissolved during the polishing process, where ethanol is used in the ultrasonic cleaning between polishing steps and as a lubricant for the fine polishing cloths.

10.6. TS-PVB-2 (250 µm)

10.6.1. Fractography

The failure type was quite interesting: it had cohesive failure at the interface and interlaminar failure (delamination) in both substrates. Figure 169 shows a picture of these failure types:

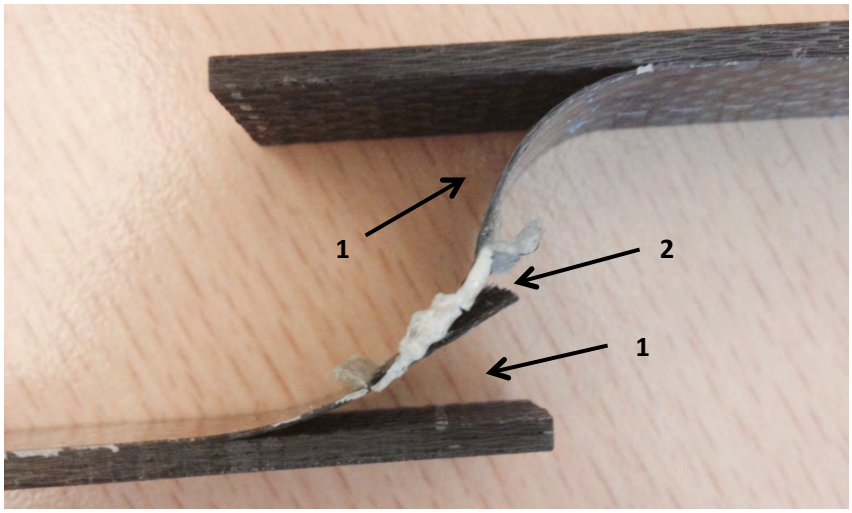

Figure 169: Fracture surfaces of TS-PVB-2 sample. Two failure types can be identified: (1) Interlaminar failure in both substrates, where the first layer of each substrate is teared out, and (2) cohesive failure at the weld interface.

This type of fracture suggests that the strength achieved at the interface approaches the interlaminar strength of the thermoset.

10.6.2. Cross section analysis

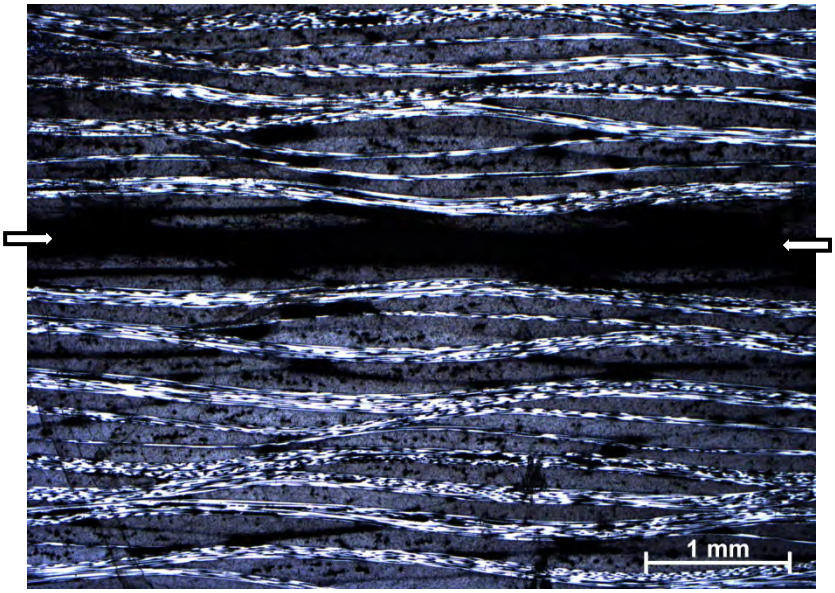

Figure 170: TS-PVB-2 cross-section picture, x2.5 magnification. Blue arrows show the location of the welding interface. The gap between the substrates, filled with PVB before the polishing, is wider than in TS-PVB-1. There was no trace of the thermoplastic film.

In spite of the gap where the PVB was before ethanol from the polishing dissolved it, it can be appreciated in Figure 170 that the separation in TS-PVB-2 weld (corresponding to the PVB interface) was much thicker than the one for TS-PVB-1, indicating that this interface was much more thermoplastic-rich. This fact may be the responsible for the higher LSS value and lower scatter of this samples with respect to TS-PVB-1.

10.7. CONCLUSIONS

Ultrasonic welds of glass and carbon reinforced thermoset substrates were done. The substrates had a PVB film co-cured. Two types of welding were performed: ultrasonic welding of 45 µm-thick PVB film co-cured samples using a flat PVB 0.25 mm-thick ED (TS-PVB-1), and ultrasonic welding of 250 µm-thick PVB film co-cured samples using no ED (TS-PVB-2).

The strength achieved with both types of welds shows the feasibility of welding thermoset to thermoset substrates. TS-PVB-2, where no energy director was used and whose interface was thermoplastic-richer, LSS results showed a higher average strength and less scatter. Moreover, its type of fracture, a combination of interlaminar substrate failure and cohesive failure at the interface, suggests that the strength achieved in the weld approaches the interlaminar strength of the thermoset substrates. Also, its welding interface was thicker. These characteristics determine that the best type of welding was TS-PVB-2, and the peculiarity of not using an ED for ultrasonic welding also shows the possibility of performing these kind of welding when there is a thick-enough layer of thermoplastic at the interface (0.5 mm in the case of TS-PVB-2). The power-travel as a function of time curve was slightly different from the ones obtained with a flat energy director, but the power

plateau was still found. This fact means that although the initial shape of the power curve is different, the process can be controlled and monitor to achieve an optimum weld (end of the power plateau) in the same way as with the flat energy director.

The travel selected for TS-PVB-1 was 0.05 mm higher than the optimum one; it is believed that by reducing it to the optimum value, arbitrary failures like sample TS-PVB-1-2 can be avoided. Nevertheless, it was interesting to check that a displacement ceiling can be achieved for this type of welding, which for welding of thermoset to thermoset can be though to be logical: For a high travel demand, once all the thermoplastic ED has been squeezed out from the interface, the thermoset resin cannot be melted to continue with the travel of the sonotrode – thermosets cannot be re-processed or re-melted once cured – so the welder achieves a displacement ceiling.

CONCLUSIONS AND FUTURE WORK

Chapter 11

Conclusions and future work

11.1. CONCLUSIONS

Travel-controlled ultrasonic welding of thermoset to thermoplastic composites has been studied. This joining technique counts with short welding times that avoid the degradation of the thermoset substrate, which cannot re-melt once cured. There were two main lines of investigation in this thesis:

I. The improvement in direct welding, where the thermoset substrate was laser-treated by Dr. Fabian Fischer at Braunchsweig Univeristy (Germany), and direct welded to a CF/PEEK substrate using a PEEK energy director – previously, the welding parameters used were checked by visual inspection and FTIR analysis to produce no degradation on the CF/Epoxy when direct welded. Three types of laser treatment were applied: One where only a few µm of the epoxy matrix were removed, and two others with different intensities of fibre excavation. The welds were studied with cross-section observation. The treatment with lower fibre excavation proved to be the most successful one of the three, leading to an interface were the thermoplastic resin could successfully penetrate into the thermoset substrate, clamping its carbon fibres, showing the improvement with respect to a non-treated CF/Epoxy (the direct weld for the check of epoxy degradation with the welding parameters produced no effective joint).

In this part, epoxy degradation when direct welding was also studied by visual inspection and FTIR analyses. With the high force-amplitude combination for the welding parameters, the welding times achieved were very low and epoxy was not degraded even when not co-curing with a thermoplastic film, which shields it from degradation.

II. The study of hybrid or indirect welding of thermoset and thermoplastic composites, where the carbon-fibre reinforced epoxy substrate was co-cured with a thermoplastic film and later welded to a carbon-fibre reinforced thermoplastic substrate, in particular, seeking for an improvement in the

adhesion between these dissimilar materials (micro-interlocking). Two approaches have been studied regarding this topic:

- 'Standard Hybrid Welding', where PEKK, PEEK and PPS thermoplastics have been used. The same thermoplastic material type was chosen for the reinforced-thermoset co-cured film, the flat energy director used for the performance of the ultrasonic weld, and the matrix thermoplastic reinforced substrate. The thermoplastic co-cured films were non-treated and treated with different procedures. After the welding and analysis of results, it could be concluded that the optimum welds were the ones that used PEKK UV, PEKK 1st chloroform-amine formula, PEEK UV, PEEK acetic, and PPS NT thermoplastic films, with LSS values on the order of 20-23 MPa.

It could be checked that PEKK and PEEK improved their LSS, and therefore their adhesion with the epoxy, when treated with UV-ozone. PPS on the contrary, showed poor adhesion after welding. A study was performed and it is believed that PPS oxidises and degrades when UV-treated.

The LSS strength values were not as high as expected (on the order of 30 MPa). It was checked that the used Hexply 8552 epoxy, which was already expired when used, was also degraded, as confirmed by a Mode-I test and other studies. This was the reason of the lower LSS values. Nevertheless, the strength attained in the welds and the cross-section observation where sufficient to determine the success of the mentioned welds in the 'Standard Hybrid Welding' section, and the new combination of materials in the 'Hybrid Welding Combination' part.

With the arrival of a new CF/Epoxy prepeg, Hexply M21, one of the successful hybrid welds, the one which used PEKK treated with UV-O_3 as the co-cured film was repeated. After optimizing the panel layup for the co-curing in the autoclave, a high and positive mean LSS value of 34.74 MPa was attained, with one of the samples even achieving 37.36 MPa. Despite the thickness of the TP co-cured film was 40 µm (very thin), no epoxy degradation occurred and the strongest welds of this thesis were achieved. These results confirmed the feasibility of achieving an optimum and strong weld when using the right epoxy and treating the thermoplastic to improve its adhesion with epoxy (in the case of PEKK). Other welds performed with a thicker thermoplastic layer, 100 µm, has a lower mean LSS value (28.61 MPa) and larger scatter than with the thin co-cured layer.

- 'Multi-material Hybrid Welding', where the Hexply 8552 CF/Epoxy was co-cured with a PEI film, and later welded to a CF/PEEK, using both PEI and PEEK energy directors. Two sets of force-amplitude welding parameters were used: 2000N-A6 and 1500N-A9. For the weld where the PEEK energy director was used, the first set of parameters was more beneficial, with the creation/enhancement of a diffusion layer between the epoxy and the PEI film. The other weld type, where a PEI ED was placed, showed better merging between the PEEK and PEI resins with the second set of parameters. The welds performed with the first set of parameters for the two welding types where mechanically tested, and a LSS value of 22 MPa was obtained for this new combination of materials.

An additional type of experiment, where the use of the energy director with respect to the thickness of the co-cured film, was studied. Thermoset to thermoset welding was performed in this case, using a weave CF/Epoxy provided by Prof. Alfonso Maffezzoli from Salento University (Italy) where the substrates were co-cured with a thin and a thick layer of PVB thermoplastic. Although the welds did no use a reinforced thermoplastic substrate, these experiments were regarded as a type of hybrid welding. The samples with the thin thermoplastic co-cured layer were welded using an energy

director. The travel selected was slightly higher than the optimum one, which may be responsible for more scatter in the samples LSS. However, because of this over-travel, one of the samples showed a displacement ceiling in the welding curves, which matches the reality of thermosets being unable to re-melt: Once the thermoplastic has been squeezed out from the interface, the sonotrode cannot travel any further, which can be regarded as one of the reasons for the addition of the ED when thermosets take part on the welding. The welds with the thick co-cured thermoplastic film used no energy director showed to have higher LSS value and less scatter, and demonstrated the feasibility of ultrasonic welding without energy director and controlling the process to produce an optimum weld in the same way as with the flat energy director in between.

11.2. FUTURE WORK

Regarding the results and conclusions after the studies developed in this thesis, the following future work proposals are suggested:

i. Repeating the welds which used PEKK 1st chloroform-amine formula, PEEK acetic, and PPS NT thermoplastic films from the 'Standard Hybrid Welding' part, and the two types of welds in the 'Multi-Material Hybrid Welding' chapter, using both sets of parameters, with a fresh epoxy, test them mechanically (LSS) and check the weld cross-section with SEM and optical microscopy.

Apart from obtained higher and more reliable LSS values, the expiration of the epoxy may have altered the capacity of the resin to form SIPN with PEI, in the case of the Multi-Material Hybrid Welding, and perhaps also interfered with the development of optimum adhesion between the thermoset and the thermoplastic in the standard hybrid welds.

ii. Check with other techniques, such as Atomic Force Microscopy or nano-indentation, if SIPN were actually developed between the co-cured epoxy and the PEI. Repeat the co-curing with a non-expired epoxy prepeg and observe the interface with SEM and optical microscopy too.

For points i and ii, an epoxy prepeg whose curing cycle is beyond the glass transition temperature of PEI is recommended, at which temperatures the thermoplastic is in a glassy state that promotes diffusion and the formation of SIPNs between the epoxy and PEI.

iii. Perform the same study about UV-ozone treatment effects on PEEK and PEEK films, as the one done with PPS, in order to gather more information about the effects of this treatment on the other two thermoplastic films.

iv. Another way in which the adhesion of the thermoplastic film can be tested is by the performance of peel-tests. Art chemists perform these tests on canvas-canvas and canvas-wood samples, joined with adhesives such as BEVA, which is from where this test idea came from.

v. As PEEK and PEI have a similar molecular structure – both are polyethers – and perfectly compatible for welding, as it has been demonstrated, treating PEI with UV prior to co-curing with the epoxy, to check whether its entanglement with the epoxy improves.

vi. Repeat laser treatment P2 (50% excavation of the fibres) with a fresh epoxy and perform LSS tests.

Appendix

- **TECHNICAL/LEGAL REGULATING FRAME**

No legal or technical constraints affected the investigation and experiments carried out in this thesis, from its beginning on the 1st of September, 2014, to its ending on the 1st of July, 2015.

- **SOCIO-ECONOMIC BACKGROUND**

An estimated number of 1500 hours were devoted to the fulfilment of the thesis.

All the machines and materials used in the completion of this investigation were available at the 'Delft Aerospace Structures and Materials Lab', in the Aerospace Engineering faculty of the Technical University of Delft. No information about the material prices, labour or equipment costs are provided by this university, so a general budget cannot be calculated nor estimated.

References

[1] "The Dream of Composites", M. Walz, R&D Magazine, 2006.

[2] "Analytical characterization of CFRP laser treated by excimer laser radiation", S. Kreling, F. Fischer, R. Delmdahl, F. Gäbler and K. Dilger, Lasers in Manufacturing Conference 2013.

[3] "Thermoplastic Adhesive for Thermosetting Composites", M. Hou, University of Queensland, Australia, 2012.

[4] "Hybrid Welding of Thermoset and Thermoplastic Composites", P. Vizcaíno Rubio, BSc Thesis. Supervisors: Irene Fernández Villegas (TU Delft), José Manuel Torralba Castelló (UC3M).

[5] "Ultrasonic Welding of PEEK Graphite APC-2 Composites", A. Benatar and T. G. Gutowski.

[6] "Adhesion of polymers", F. Awaja, M. Gilbert, G. Kelly, B. Fox, P. J. Pigram.

[7] "Putting it together – science and technology of composite materials". Australian Academy of Science, November 2000.

[8] "Manufacturing processes for advanced composites", F.C. Campbell, 2004.

[9] "Fundamentals of Composite Manufacturing: Materials, Methods, and Applications", A. Brent Strong, Second Edition.

[10] "Fundamentals of Modern Manufacturing 2/e", John Wiley & Sons, Inc. M. P. Groover, 2002.

[11] IUPAC (International Union of Pure and Applied Chemistry) Compendium of Chemical Terminology Gold Book.

[12] "Thermoplastics and Thermoplastic Composites", Michael Biron, November 2012.

[13] "Handbook of Thermoset Plastics", Sidney W. Goodman, Second Edition.

[14] "Handbook of Plastics Joining: A practical guide", PDL staff.

[15] "Composite Materials for Aircraft Structures", Second Edition, Baker, Alan A. Baker, Donald W. Kelly.

[16] "Advances in fusion bonding techniques for joining thermoplastic matrix composites: a review", C. Ageorges, L. Ye, M. Hou.

[17] "Adhesive bonding of composites", Michael J. Hoke. Abaris Training Inc. Reno, Nevada.

[18] "NDT of Kissing Bond in Aeronautical Structures", P. Noël Marty, N. Desaï and J. Andersson.

[19] "Virtual Chembook", C. E. Ophardt, 2003.

[20] "Using excimer lasers to clean CFRP prior to adhesive bonding", F. Fischer, S. Kreling, F. Gäbler and R. Delmdahl.

[21] "Ultraviolet-ozone surface treatment", Three Bond Technical News.

[22] "Atmospheric-Pressure Plasma and UV-Laser radiation – A comparison for surface pre-treatment of CFRP", F. Fischer, D. Blass, S. Kreling and K. Dilger, 16th European Conference on Composite Materials (ECCM16), Seville (Spain), June 2014.

[23] "Process and performance evaluation of ultrasonic, induction and resistance welding of advanced thermoplastic composites", I. F. Villegas, L. Moser, A. Yousefpour, P. Mitschang and H. E. N. Bersee.

[24] "Ultrasonic Welding of PEEK Graphite APC-2 Composites", A. Benatar and T. G. Gutowski.

[25] "An Experimental Investigation into Resistance and Induction Welding for Aerospace Structures: A Comparison", T. J. Ahmed, D. Stavrov and H. E. N. Bersee.

[26] "A study on the induction heating of carbon fibre reinforced thermoplastic composites", H. Kim, S. Yarlagadda, J.W. Gillespie Jr., N.B. Shevchenko and B.K. Fink.

[27] “Fusion bonding/welding of thermoplastic composites”, A. Yousefpour, M. Hojjati and J.P. Immarigeon.
[28] “Strength development versus process data in ultrasonic welding of thermoplastic composites with flat energy directors and its application to the definition of optimum processing parameters”, I. F. Villegas.
[29] “Ultrasonic Welding Of Advanced Thermoplastic Composites: An Investigation On Energy Directing Surfaces”, I. F. Villegas, D. Stavrov and H. E. N. Bersee.
[30] “In situ monitoring of ultrasonic welding of thermoplastic composites through power and displacement data”, I. F. Villegas.
[31] “Combined Processing: Advanced Composites Processing”, Mario Danzi, Zurich, 2012.
[32] “Joining techniques for high performance thermoplastic compositions”, Roderic C. Don, John W. Gillespie Jr. and Steven H. MacKnight; Patent No. 5,643,390; 1st July 1997, The University of Delaware, Newark.
[33] “Interpenetrating Polymer Networks: An Overview”, L. H. Sperling, Lehigh University, Bethlehem.
[34] “A review on interpenetrating polymer network”, M. Shivashankar and B. K. Mandal, VIT-University, Tamilnadu, India, 2012.
[35] “Interface Diffusion and Morphology of Aerospace Grade Epoxy co-cured with Thermoplastic Polymers”, L. J. Vandi, M. Hou, M. Veidt, R. Truss, M. Heitzmann and R.Paton, Australia.
[36] “Morphology of an Interface between Polyetherimide and Epoxy Prepreg”, M. T. Heitzmann, M. Hou, M. Veidt, L. J. Vandi and Rowan Paton.
[37] “PEKK Thermoplastic Polymer. Technical Data Sheet”, Cytec Engineered materials.
[38] “PEEK Biomaterials Handbook”, Steven M. Kurtz.
[39] “Polyether Imide (PEI) Typical Properties Generic PEI - Carbon Fibre”, Prospector.
[40] “What is PPS?”, Chevron Phillips Chemical.
[41] “Hexply Prepreg Technology”, Hexcel.
[42] “How to Perform an Adhesive Lap Joint Shear Strength Test - ASTM D1002”, ADMET.
[43] “Mode-I Interlaminar Fracture Toughness in Unidirectional Carbon-fibre/Epoxy Composites”, M. Barikani, H. Saidpour, M. Sezen, 2002.
[44] “Methods of Measuring the T_g of Lyophilized Protein-Excipient Formulations”, Kevin Menard, Perkin Elmer.
[45] “DSC as Problem Solving Tool: Measurement of Percent Crystallinity of Thermoplastics”, W.J. Sichina, Perkin Elmer.
[46] “Gradient Interphase between Reactive Epoxy and Glassy Thermoplastic from Dissolution Process, Reaction Kinetics, and Phase SeparationThermodynamics”, B. Lestriez, J. P. Chapel, and J. F. Gérard, 2000.